DISS. ETH NO. 17977

TOPOLOGICAL STRINGS, MATRIX MODELS, AND NONPERTURBATIVE EFFECTS

A dissertation submitted to

ETH ZURICH

for the degree of

Doctor of Sciences

presented by

MARLENE JULIA WEISS

Dipl. Phys., ETH Zurich

Date of birth 18.08.1980

citizen of Germany

accepted on the recommendation of

Jürg Fröhlich

Marcos Mariño

2008

Acknowledgements

First of all, I would like to thank my supervisor Marcos Mariño for his continuous support and guidance throughout all stages of this work, for teaching me countless things on string theory, for many animated discussions, and also for organizing great graduate students' seminars at CERN. I am similarly indebted to my second advisor Jürg Fröhlich for all his support, many insightful comments, and for tirelessly insisting on clear, rigorous statements. One could hardly wish for two more committed and inspiring thesis advisors.

I also wish to thank Thomas Grimm, Ricardo Schiappa and especially Albrecht Klemm for pleasant collaborations in which I had the honour to participate. Furthermore, I take the opportunity to thank my teachers in Zurich, Paris and Lausanne, in particular Dietmar Salamon, Misha Shaposhnikov, Michael Spira, Gian-Michele Graf, Jean-Pierre Rivoal and Eduard Zehnder. They have very much shaped my view on physics and mathematics. All the members of the ITP at ETH Zurich, as well as my students, have contributed to making my weekly visits very delightful, and I thank them for creating such a friendly atmosphere.

It has been a great pleasure to share office with James Bedford, Johanna Knapp and Are Raklev. Johanna gets extra thanks for countless mostly non-physics discussions, hilarious sarcastic comments on many occasions, and for competent Linux support. Thanks for the latter also to the worldwide Ubuntu community. I also thank the adorable staff at CERN, especially Nanie Perrin and Suzy Vascotto.

I am grateful to many people I met at CERN, in Zurich and at conferences, among others Murad Alim, Luis Álvarez-Gaumé, François Arléo, Matthias Blau, Vincent Bouchard, Ilka Brunner, Frederik Denef, Ron Donagi, Alexander Flossdorf, François Gelis, Gero von Gersdorff, Alessandra Gnecchi, Chris Herzog, Gabi Honecker, Max Kreuzer, Wolfgang Lerche, Tristan Maillard, Sara Pasquetti, Emanuel Scheidegger, Cornelius Schmidt-Colinet, Joan Simón, Stefan Stieberger, Andy Strominger, David Tong and Aleksi Vuorinen, for very enjoyable encounters, and to some of the above also for interesting discussions on physics. I am especially indebted to James Bedford for help with the manuscript and to Emanuel Scheidegger for sharing his knowledge on Gromov-Witten theory and related topics. Mauro Papinutto's and Kevin Schnelli's skiing, climbing and italian lessons and friendship are gratefully acknowledged, and I thank Babis Anastasiou for providing greek food, fun company, and putting up with my grammar obsession.

I thank Yannis, Henri, Thérèse Burnier and family for all their support and advice, and for introducing me to windsurfing.

Without my friends Stephan Debrunner, Elisabeth Furtwängler, Nora Graser, Andrea Harbach, Barbara Loisch, David Noth, Stefan Schwarz and Daniel Weiller, I would not be the person I am today, and I thank them for everything.

Last but by no means least, I am grateful to my parents and sisters, who were always there.

Kurzfassung

Diese Dissertation befasst sich mit topologischer Stringtheorie und ihrer Beziehung zu Matrixmodellen und Instantoneffekten. Topologische Stringtheorie ist ein Sektor der Stringtheorie. Sie wird konstruiert, indem in einem $\mathcal{N} = (2, 2)$ supersymmetrischen Sigmamodell auf dem Worldsheet durch den sogenannten topologischen Twist die Lorentzströme neu definiert werden, bevor es an zweidimensionale Gravitation gekoppelt wird. Das Ergebnis ist eine Stringtheorie mit metrikunabhängigen Observablen. Da der topologische Twist auf zwei konsistente Weisen definiert werden kann, gibt es zwei topologische Stringtheorien, das A- und das B-Modell, die mittels Mirrorsymmetrie zueinander äquivalent sind. Ihre Amplituden entsprechen effektiven Ladungen in der Typ IIA beziehungsweise IIB Theorie, kompaktifiziert auf der Calabi-Yau-Mannigfaltigkeit, in die das Sigmamodell das Worldsheet abbildet. Vom mathematischen Standpunkt aus beschreiben sie die Gromov-Witten-Invarianten des betreffenden Calabi-Yaus.

Das B-Modell zeigt die sogenannte holomorphe Anomalie, die sich durch rekursive Differentialgleichungen ausdrücken lässt, die die B-Modell-Amplituden erfüllen. Die durch diese Gleichungen beschriebene Nicht-Holomorphizität der Amplituden steht in enger Beziehung zu ihrer Modularität. Ein Resultat dieser Arbeit ist eine Methode, die holomorphen Anomaliegleichungen effizient zu integrieren, wobei die modulare Struktur der Amplituden genutzt wird.

Ein weiterer Aspekt der topologischen Amplituden ist ihre Bedeutung in Verbindung mit der Dualität zwischen heterotischer und Typ II-Stringtheorie. Wir berechnen die topologischen Amplituden auf der heterotischen Seite für eine grosse Klasse von vorgeschlagenen Paaren von heterotischen und Typ II-Theorien. In einem Teil der Fälle sind die Gromov-Witten-Invarianten der betreffenden Calabi-Yau-Mannigfaltigkeit bekannt und stimmen mit unseren Ergebnissen überein, was einen weiteren präzisen Test der Dualität darstellt.

Gegenstand des zweiten Teils dieser Arbeit ist die Verbindung zwischen topologischer String-Theorie, Matrixmodellen und Instantoneffekten. Es wird seit einigen Jahren vermutet, dass das topologische B-Modell in vielen Fällen äquivalent zu einem Matrixmodell ist. Andererseits besteht eine klassische Beziehung zwischen dem asymptotischen Verhalten der Störungsreihe und der Zustandssumme der Instantonübergänge. Wir zeigen, dass diese Beziehung auch für Matrixmodelle gilt. Mittels der Dualität zwischen Matrixmodellen und topologischen Strings können wir aus der Instanton-Zustandssumme im Matrixmodell auch Vorhersagen für das asymptotische Verhalten topologischer Stringtheorien machen, unter Umgehung der zugehörigen Instantonamplitude innerhalb der Stringtheorie. Wir testen unsere Vorhersagen für eine Reihe von Matrixmodellen und topologischen Stringtheorien und finden in allen Fällen hervorragende Übereinstimmung. Die Matrix-Formulierung des B-Modells liefert so eine mögliche nicht-perturbative Erweiterung, die mit *perturbativen* Methoden überprüfbar ist.

Abschliessend zeigen wir, dass Lösungen von Matrixmodellen, die die Eigenwerte auf Gebiete um mehrere Extrema des Potentials verteilen, sogenannte Multi-Cut-Modelle, sich mithilfe eines Multi-Instanton-Formalismus aus den Single-Cut-Modellen heraus beschreiben lassen.

Abstract

This thesis is about topological string theory and its relation with matrix models and instanton effects. Topological string theory is a sector of string theory. It is constructed by redefining the Lorentz currents on the worldsheet of an $\mathcal{N} = (2, 2)$ supersymmetric Sigma model by means of a so-called topological twist, before coupling it to two-dimensional gravitation. The result is a string theory with metric-independent observables. As the topological twist can be defined in two consistent ways, there are two topological string theories, the A model and the B model, equivalent to one another by mirror symmetry. Their amplitudes correspond to effective charges in the type IIA and IIB theories, respectively, compactified on the Calabi-Yau manifold which is the target of the Sigma model. In mathematical terms, the topological string describes the Gromov-Witten invariants of that Calabi-Yau manifold. The B-model exhibits a so-called holomorphic anomaly. This can be expressed in recursively defined differential equations which are satisfied by the amplitudes. The deviation of the amplitudes from being holomorphic, as described by the differential equations, is closely related to their modularity. A key result of this thesis is a method for integrating the anomaly equations efficiently by exploiting the modular structure of the amplitudes.

Another important aspect of the topological amplitudes is their role in the duality between heterotic and type II string theory. On the heterotic side, we calculate the topological amplitudes for a large class of conjectured pairs of heterotic and type II theories. In some of these examples, the Gromov-Witten invariants of the appropriate Calabi-Yau manifolds are known and agree with our calculations. This provides further data in favor of heterotic-type II duality.

Furthermore, we explore the connections between topological string theory, matrix models and instanton effects. In recent years it has been conjectured that the topological B model is equivalent to a matrix model. On the other hand, there is a classical relationship between the asymptotic behavior of the perturbation series and the instanton corrections to the partition sum. We use this relationship to make predictions concerning the asymptotic behavior of the perturbation series based on the partition sum. By means of the duality between matrix models and topological strings, we are then also able to make predictions for the asymptotic behavior of topological string theories, avoiding the corresponding instanton amplitude within string theory. These predictions are tested for some matrix models and topological string theories. In all cases tested we find precise agreement. In this way, the matrix formulation of the B model leads to a possible nonperturbative extension which can be tested with *perturbative* methods.

Finally, we show that solutions of matrix models which distribute the eigenvalues over regions around several extrema of the potential (multi-cut models) can be described in terms of the single-cut models by means of a multi-instanton formalism.

Contents

Part I

INTRODUCTION

Motivation

The search for a unified theory of particle physics and gravitation has occupied theoretical physicists since the early days of quantum mechanics and general relativity at the beginning of the last century, and is likely to continue for a long time to come. This is due to the very different nature of general relativity and quantum physics. In order to be unified with the standard model of particle physics, we surely need a quantum theory of gravity. However, general relativity defies quantization. A simple argument for this comes from dimensional analysis. Since the gravitational coupling G_N is of dimension mass^{-2}, the one-graviton correction to the zero-graviton amplitude is of order $\frac{\Lambda^2}{M^2_{\text{Planck}}}$. Accordingly, the gravitational interaction grows weaker at low energy, but diverges at high energy. We therefore need either a nontrivial UV fixed point or new physics at the Planck scale to soften the divergence. One way to "smear out" the divergence is offered by string theory: if the graviton is generated by a vibrating string, the graviton-fermion vertex is not a point, but a one-dimensional object, and the divergence coming from coincident graviton vertices is softened.

The idea to introduce strings as the fundamental building blocks of particle physics came out of the observation that seeing particles as vibrational modes of strings could explain the Regge behaviour of resonances arising in strong interactions, and at the same time remove UV divergences. String theory was thus proposed in the late 1960s as a theory of strong interactions. However, experimental data from SLAC soon disposed of this idea, since it confirmed the competing parton model of hadrons as composite objects that ultimately led to QCD. Still, research in string theory continued, and it eventually emerged as a candidate for a theory unifying the four fundamental forces. With the advent of string dualities during the 1990s, it became clear that the various versions of the theory are all connected to each other and are nothing but descriptions of one theory in different regimes. Accordingly there was hope that string theory would ultimately lead to a *unique* description of nature, with the standard model with all its masses and charges as the only possible solution.

It is by now far from clear whether this will ever happen. It seems rather that one has to get used to the idea of a landscape of string vacua, among which ours may be entropically or anthropically favoured but by no means unique. Even though there has been some progress in making string theory a consistent, testable theory of nature with research on topics such as flux compactifications, orientifolds, and metastable supersymmetry breaking (see e.g. [1] and [2] for reviews), and there may even be some hope of seeing traces of it at the LHC in the near future [3], string theory still has to find its place in our picture of the world.

It is thus all the more important to understand the many fundamental aspects of string theory that still remain unclear, rather than look for the standard model within the zillions of vacua as for a needle in a gargantuan haystack. At the same time, this approach can push progress in both physics and mathematics as indeed it has done over the last 30 years.

On the physics side, one of the most dramatic developments has been triggered by the AdS-CFT conjecture due to Maldacena [4], a concrete realization of the general idea of gauge/string correspondence due to 't Hooft [5]. In mathematics, string theory has made important contributions to various fields such as algebraic topology, differential geometry and representation theory.

One particularly fruitful area where new findings have emerged is topological string theory [6, 7, 8], the main focus of this thesis. There are several ways to look at the topological string. It serves as a toy model of string theory, useful for studying fundamental properties of more general string theories in a simplified setting. Indeed, this aspect has led to deep insights about string dualities, the gauge/string correspondence, and nonperturbative effects. Furthermore, since it captures and organizes topological information about the target space, topological string theory can be seen as a mathematical construction which is interesting in its own right. As such, it has been a source of new developments in enumerative geometry and algebraic topology. Finally,

it is intimately related to physical amplitudes of type II string theory, and this connection has led to many new insights not only about string theory, but also about supersymmetric gauge theories and black holes.

Chapter 1

Topological Strings

This chapter contains a brief review of the topics most relevant to this thesis, focusing on the topological string. For more detailed surveys, see e.g. [9, 10, 11, 12].

1.1 String Perturbation theory

In the following, we will briefly sketch the main ideas on which perturbative string theory is based. For a textbook treatment, see [13, 14, 15].

In relativistic quantum field theory, particles are generated by fields in four-dimensional space-time. A moving particle can therefore be seen as a map from a one-dimensional worldline to four-dimensional Minkowski space, and its classical action is equal to the length of this worldline,

$$S(\gamma) = \int |\dot{\gamma}| \mathrm{d}t. \tag{1.1.1}$$

String theory merely adds one dimension to this picture, generating particles by fields living on one-dimensional strings sweeping out a two-dimensional worldsheet Σ. The classical action of the bosonic string is the surface of the worldsheet, analogously to (1.1.1),

$$S(\Sigma) = \frac{1}{4\pi\alpha'} \int \sqrt{h} h^{\alpha\beta} g_{\mu\nu}(X) \partial_\alpha X^\mu \partial_\beta X^\nu \mathrm{d}\sigma \mathrm{d}\tau. \tag{1.1.2}$$

In the above action, the string tension appears as a new parameter α'. The perturbative expansion is therefore always twofold, in α' and in the string coupling g_s. String theory is thus constructed as a two-dimensional conformal field theory on the worldsheet, mapped to a higher-dimensional target. In order to include fermions in the picture, one has to incorporate supersymmetry, a symmetry relating bosonic and fermionic degrees of freedom. The requirement of anomaly cancellation upon quantization of the above action restricts the target space to be 26 dimensional for bosonic strings, or 10-dimensional for superstrings. The supposedly "physical" string theory comes in five versions, called type I, heterotic with symmetry group $SO(32)$, heterotic with symmetry group $E_8 \times E_8$, type IIA and type IIB. They are related by various dualities, as shown in Fig. 1.1. Since at least at low energies, our world certainly appears four-dimensional, the extra dimensions have to be compactified. This can be done preserving supersymmetry if the compactification space is a complex Kähler manifold of vanishing first Chern class, a so-called Calabi-Yau space.

Thus, from the algebraic point of view string theory is a two-dimensional conformal field theory on the world-sheet coupled to two-dimensional gravity, mapped to a target space. If the correlation functions of the conformal field theory in question do not depend on the worldsheet metric, we call it topological and the resulting string theory *topological string theory*. We will here take the target to be a Calabi-Yau manifold. There are essentially two ways to construct such a topological field theory. Either one starts with a theory whose action does not contain

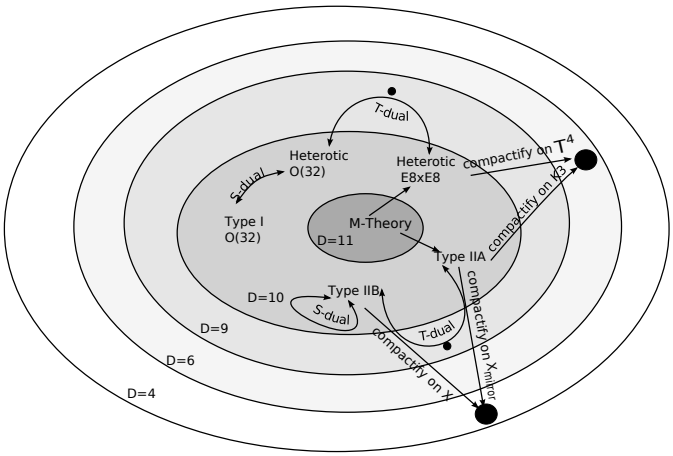

Figure 1.1: The web of string dualities

the metric at all, therefore metric independence of correlation functions is trivial. One example for such a theory is Chern-Simons theory. The other option is to construct the theory in such a way that even though the metric does appear in the action, the metric dependence drops out of physical quantities such as correlation functions. Theories of this type are called *cohomological field theories*, for reasons which will be explained below.

1.2 Twisting $\mathcal{N} = 2$ theories

One way to obtain a topological field theory is to take a two-dimensional $\mathcal{N} = (2, 2)$ superconformal field theory, here a sigma model, and redefine its symmetry currents in a specific way called twisting. Let us start with some basic facts about theories with $\mathcal{N} = (2, 2)$ supersymmetry[1].

1.2.1 Supersymmetry and Superspace

A supersymmetry transformation is a transformation of the form

$$\begin{aligned} \delta X^\mu =& \bar{\epsilon}\psi^\mu \\ \delta\psi^\mu =& \rho^\alpha \partial_\alpha X^\mu \epsilon, \end{aligned} \tag{1.2.3}$$

where

$$\epsilon = \begin{pmatrix} \epsilon_- \\ \epsilon_+ \end{pmatrix} \tag{1.2.4}$$

is an infinitesimal constant Majorana spinor. A convenient way to make supersymmetries manifest is the superfield formalism. In addition to the world-sheet coordinates σ^α, we introduce four fermionic coordinates $\theta_\pm, \bar{\theta}_\pm$. $\theta_\pm$ and $\bar{\theta}_\pm$ are anticommuting Grassmann coordinates forming a Majorana spinor. Note that since

$$\{\theta_A, \theta_B\} = 0, \tag{1.2.5}$$

the anticommuting variables square to zero. This motivates the rules of Grassmannian integration

$$\int \mathrm{d}\theta\ 1 = 0, \qquad \int \mathrm{d}\theta\ \theta = 1. \tag{1.2.6}$$

We can now organize the bosonic and fermionic fields of the theory into "superfields" Φ with a finite expansion in θ, since $\theta_\pm^2 = 0$,

$$\Phi(x^\mu, \theta, \bar{\theta}) = \phi(y^\pm) + \theta^\alpha \psi_\alpha(y^\pm) + \theta^+\theta^- F(y^\pm), \tag{1.2.7}$$

[1]For a review of $\mathcal{N} = 2$ special geometry, see section 2.1

where $y^{\pm} = x^{\pm} - \mathrm{i}\theta^{\pm}\bar{\theta}^{\pm}$. An important property of supersymmetric theories in general is the *localization* of certain correlation functions. If both the action and the inserted operators $\mathcal{O}$ are invariant under some supersymmetry transformation generated by $\mathcal{Q}$, the path integral $\int \mathrm{e}^{-S}\mathcal{O}$ reduces to a sum over local contributions from the fixed points of $\mathcal{Q}$ [16]. The reason for this simplification is that for all other configurations, one can introduce coordinates in which $\mathcal{Q}$ acts by shifting one of the fermionic coordinates in the integration measure. Since the integrand is invariant under the transformation, the coordinate does not appear and the integral vanishes by (1.2.6) .

In the following we will consider a non-linear sigma model defined by an action of the form

$$\int \mathrm{d}^2z\mathrm{d}^2\theta K(\Phi, \bar{\Phi}), \tag{1.2.8}$$

where $K(\Phi, \bar{\Phi})$ is the Kähler potential, giving rise to the Kähler metric

$$g_{ij} = \partial_i \partial_{\bar{j}} K. \tag{1.2.9}$$

Note that the action (1.2.8) involves an integral over both ordinary and Grassmanian coordinates. The sigma model describes maps φ from a Riemann surface Σ, the worldsheet, into a target manifold X with a metric g. Locally, the maps φ are described by configurations of bosonic fields ϕ^i. If we denote by K, $\overline{K}$ the canonical and the anticanonical bundle on Σ, fermion fields $\psi^i_{\pm}$ on Σ transform as sections of $K^{\frac{1}{2}} \times \varphi^*(TX)$ and $\overline{K}^{\frac{1}{2}} \times \varphi^*(TX)$ respectively, where $\varphi^*(TX)$ is the pullback of the tangent bundle on X.

In terms of component fields, the action (1.2.8) reads

$$\mathcal{S} = t \int \mathrm{d}^2z \left(g_{i\bar{j}} \partial^\mu \phi^i \partial_\mu \bar{\phi^j} - g_{i\bar{j}} \bar{\psi}^{\bar{j}}_- \left(D_0 + D_1\right) \psi^i_- + g_{i\bar{j}} \bar{\psi}^{\bar{j}}_+ \left(D_0 - D_1\right) \psi^i_+ - R_{i\bar{j}k\bar{\ell}} \psi^i_+ \psi^k_- \bar{\psi}^{\bar{j}}_- \bar{\psi}^{\bar{\ell}}_+ \right), \tag{1.2.10}$$

where D_μ are covariant derivatives

$$D_\mu \psi^i_{\pm} = \partial_\mu \psi^i_{\pm} + \partial_\mu \phi^j \Gamma^i_{jk} \psi^k_{\pm}, \tag{1.2.11}$$

and we have eliminated the auxiliary fields $F, \bar{F}$ using their equations of motion. We also have introduced the parameter t as a coupling constant. The Christoffel symbols Γ^i_{jk} and Riemannian curvature R are defined with respect to the Kähler metric. Symmetries of superspace are generated by operators that leave the measure of integration invariant and we can organize the generators of $U(1)$-Lorentz symmetry together with the operators generating fermionic coordinate shifts into the combinations

$$\begin{aligned} \mathcal{Q}_{\pm} &= \frac{\partial}{\partial\theta^{\pm}} + \mathrm{i}\bar{\theta}^{\pm}\partial_{\pm} \\ \overline{\mathcal{Q}}_{\pm} &= -\frac{\partial}{\partial\bar{\theta}^{\pm}} - \mathrm{i}\theta^{\pm}\partial_{\pm} \\ D_{\pm} &= \frac{\partial}{\partial\theta^{\pm}} - \mathrm{i}\bar{\theta}^{\pm}\partial_{\pm} \\ \bar{D}_{\pm} &= -\frac{\partial}{\partial\bar{\theta}^{\pm}} + \mathrm{i}\theta^{\pm}\partial_{\pm}. \end{aligned} \tag{1.2.12}$$

The conserved charges $Q_{\pm}, \overline{Q}_{\pm}$ acting on a superfield Φ generate the supersymmetry transformation

$$\delta\Phi = \epsilon_+ \mathcal{Q}_- - \epsilon_- \mathcal{Q}_+ - \bar{\epsilon}_+ \overline{\mathcal{Q}}_- + \bar{\epsilon}_- \overline{\mathcal{Q}}_+. \tag{1.2.13}$$

An (anti-)chiral superfield is defined as a field Φ satisfying $D_{\pm}\Phi = 0$ ($\bar{D}_{\pm}\Phi = 0$). There are two more $U(1)$ symmetry groups compatible with superfields of fixed chirality, generated by left-and

rightmoving currents F_L, F_R. They combine into vector and axial R-symmetry currents $F_V,\ F_A$ defined as

$$F_V = F_R + F_L, \qquad F_A = F_R - F_L \tag{1.2.14}$$

and act on the superfields as

$$\begin{aligned} \mathrm{e}^{\mathrm{i}\alpha F_V}\mathcal{F}(x^\mu,\theta^\pm,\bar\theta^\pm) =& \mathrm{e}^{\mathrm{i}\alpha q_V}\mathcal{F}(x^\mu,\mathrm{e}^{-\mathrm{i}\alpha}\theta^\pm,\mathrm{e}^{\mathrm{i}\alpha}\bar\theta^\pm) \\ \mathrm{e}^{\mathrm{i}\beta F_A}\mathcal{F}(x^\mu,\theta^\pm,\bar\theta^\pm) =& \mathrm{e}^{\mathrm{i}\beta q_A}\mathcal{F}(x^\mu,\mathrm{e}^{-\mathrm{i}\beta}\theta^\pm,\mathrm{e}^{\mathrm{i}\beta}\bar\theta^\pm). \end{aligned} \tag{1.2.15}$$

Note that these are internal currents acting only on the Grassmann variables $\theta, \bar\theta$. We obtain the following (anti-)commutation relations for the $\mathcal{N}=2$ supersymmetry algebra:

$$\begin{aligned} \{Q_\pm, \overline{Q}_\pm\} &= H \pm P, \\ \{J, Q_\pm\} &= \pm\frac{1}{2}Q_\pm, \qquad \{J, \overline{Q}_\pm\} \quad = \pm\frac{1}{2}\overline{Q}_\pm, \\ \{F_V, Q_\pm\} &= \pm\frac{1}{2}Q_\pm, \qquad \{F_V, \overline{Q}_\pm\} \quad = \pm\frac{1}{2}\overline{Q}_\pm, \\ \{F_A, Q_\pm\} &= \pm\frac{1}{2}Q_\pm, \qquad \{F_A, \overline{Q}_\pm\} \quad = \mp\frac{1}{2}\overline{Q}_\pm, \end{aligned} \tag{1.2.16}$$

and all other combinations vanish.

1.2.2 Twisting

So far, we have been considering flat worldsheets. However, in order to couple to 2d gravity we'll need to sum over worldsheets of arbitrary geometry. All it takes to formulate the theory on a curved worldsheet is to endow the surface with a spin structure such that spinors on the surface are well-defined objects. In order for supersymmetry of the action to be preserved, we would need a covariantly constant spinor ϵ in our definition of the supersymmetry transformation. However, such an object does not exist on a general Riemann surface! The way out is to *define* a new generator of Lorentz symmetry by either

$$J_A = J - F_V \quad (\mathrm{A-twist}) \tag{1.2.17}$$

or

$$J_B = J + F_A \quad (\mathrm{B-twist}). \tag{1.2.18}$$

Note at this point already that if one changes the sign of F_R, F_V gets replaced by $-F_A$ and vice versa, thus exchanging the A- with the B-twist. This is what happens under mirror symmetry, one of the central ingredients of (topological) string theory.

From the supersymmetry algebra (1.2.16), one sees that in both cases a new scalar supercharge, also called *topological charge*, can be defined:

$$\begin{aligned} \mathcal{Q}_A &\equiv \mathcal{Q}_+ + \overline{\mathcal{Q}}_- \quad (\mathrm{A-twist}), \\ \mathcal{Q}_B &\equiv \overline{\mathcal{Q}}_+ + \overline{\mathcal{Q}}_- \quad (\mathrm{B-twist}). \end{aligned} \tag{1.2.19}$$

It also follows from the supersymmetry algebra that the new topological charge is nilpotent and the Hamiltonian and momentum are $\mathcal{Q}$-exact:

$$\begin{aligned} \mathcal{Q}_A^2 = 0, \qquad & H_A = \frac{1}{2}\{\mathcal{Q}_A, \overline{\mathcal{Q}}_+ + \mathcal{Q}_-\}, \qquad P_A = \frac{1}{2}\{\mathcal{Q}_A, \overline{\mathcal{Q}}_+ - \mathcal{Q}_-\}, \\ \mathcal{Q}_B^2 = 0, \qquad & H_B = \frac{1}{2}\{\mathcal{Q}_B, \mathcal{Q}_+ + \mathcal{Q}_-\}, \qquad P_B = \frac{1}{2}\{\mathcal{Q}_B, \mathcal{Q}_+ - \mathcal{Q}_-\}. \end{aligned} \tag{1.2.20}$$

The effect of this twist, as we will see in a moment, is to make all physical observables metric independent! The new, twisted sigma models turn out to be topological quantum field theories.

They are of the cohomological type[2] mentioned above, by definition quantum field theories with a scalar symmetry $\mathcal{Q}$ acting on the fields in such a way that the correlation functions are metric independent. The physical observables are the $\mathcal{Q}$-invariant operators. Since $\mathcal{Q}$-exact operators have vanishing correlation functions, they decouple from the theory and one can restrict the set of observables to the cohomology of $\mathcal{Q}$;

$$\mathcal{O} = \frac{\mathrm{Ker}\mathcal{Q}}{\mathrm{Im}\mathcal{Q}}. \tag{1.2.21}$$

For both the A- and the B-model, one can indeed show that not only Hamiltonian and momentum, but the complete energy-momentum tensor is $\mathcal{Q}_{A/B}$-exact. This immediately implies topological invariance, as for any set of $\mathcal{Q}$-invariant operators $\{\mathcal{O}_i\}$ and $T_{\mu\nu} = \{\mathcal{Q}, G_{\mu\nu}\}$ for some tensor $G_{\mu\nu}$,

$$\begin{aligned}\frac{\delta}{\delta g^{\mu\nu}}\langle \mathcal{O}_1 \cdots \mathcal{O}_n\rangle &= \langle \mathcal{O}_1 \cdots \mathcal{O}_n T_{\mu\nu}\rangle = \langle \mathcal{O}_1 \cdots \mathcal{O}_n \{Q, G_{\mu\nu}\}\rangle \\ &= \pm\langle Q\mathcal{O}_1 \cdots \mathcal{O}_n G_{\mu\nu}\rangle + \langle \mathcal{O}_1 \cdots \mathcal{O}_n G_{\mu\nu} Q\rangle = 0,\end{aligned} \tag{1.2.22}$$

since $\mathcal{Q}$ annihilates the vacuum.

1.2.3 The A-model

Let us now have a closer look at the physical implications of the A-twist. In order to make the new spin manifest, we rename the component fields of Φ

$$\begin{aligned}\chi^i &:= \psi^i_+, \qquad & \chi^{\bar{i}} &:= \overline{\psi}^{\bar{i}}_- \\ \rho^{\bar{i}}_z &:= \overline{\psi}^{\bar{i}}_+, \qquad & \rho^i_{\bar{z}} &:= \psi^i_-.\end{aligned} \tag{1.2.23}$$

The $\mathcal{Q}_A$ charge acts as

$$\begin{aligned}&\{\mathcal{Q}_A, \phi^i\} = \chi^i, && \{\mathcal{Q}_A, \bar{\phi}^i\} = \chi^{\bar{i}}, \\ &\{\mathcal{Q}_A, \rho^i_{\bar{z}}\} = 2\partial_{\bar{z}}\phi^i - \Gamma^i_{jk}\rho^j_{\bar{z}}\chi^k, && \{\mathcal{Q}_A, \rho^{\bar{i}}_z\} = 2\partial_z\bar{\phi}^{\bar{i}} - \Gamma^{\bar{i}}_{\bar{j}\bar{k}}\rho^{\bar{k}}_z\chi^{\bar{j}}, \\ &\{\mathcal{Q}_A, \chi^i\} = 0.\end{aligned} \tag{1.2.24}$$

After integrating over the Grassmann variables, the action (1.2.10) reads in the new variables

$$\mathcal{S}_A = t\int \mathrm{d}^2 z \left(\frac{1}{2} g_{i\bar{j}}\partial_z\phi^i\partial_{\bar{z}}\bar{\phi}^j - g_{i\bar{j}}\rho^{\bar{j}}_z D_{\bar{z}}\chi^{\mathrm{i}} - g_{i\bar{j}}\rho^i_{\bar{z}} D_z\chi^{\bar{j}} + R_{i\bar{j}k\bar{\ell}}\rho^i_{\bar{z}}\chi^j\rho^{\bar{k}}_z\chi^{\bar{\ell}}\right). \tag{1.2.25}$$

Next, we need to show that the energy-momentum tensor is $\mathcal{Q}$-exact, such that the theory really is cohomological. It turns out that the action (1.2.25) is *almost* $\mathcal{Q}$-exact. Introducing the operator

$$V_A = g_{i\bar{j}}\left(\rho^{\bar{j}}_z\partial_{\bar{z}}\phi^i + \partial_z\phi^{\bar{j}}\rho^i_{\bar{z}}\right), \tag{1.2.26}$$

we find that $\mathcal{S}_A$ can be written as

$$\mathcal{S}_A = t\int_{\Sigma_g}\{\mathcal{Q}_A, V_A\} + t\int_{\Sigma_g}\mathrm{d}^2 z g_{i\bar{j}}\left(\partial_z\phi^i\partial_{\bar{z}}\bar{\phi}^j - \partial_{\bar{z}}\phi^i\partial_z\bar{\phi}^j\right). \tag{1.2.27}$$

However, the extra bosonic term is nothing else than the pullback of the Kähler class $\omega = \mathrm{i}g_{i\bar{j}}dz^i\wedge d\bar{z}^{\bar{j}}$ to the worldsheet Σ_g! We can therefore write

$$\mathcal{S}_A = t\int_{\Sigma_g}\{\mathcal{Q}_A, V_A\} + t\int_{\Sigma_g}\varphi^*\omega = t\int_{\Sigma_g}\{\mathcal{Q}_A, V_A\} + t\int_{\varphi(\Sigma_g)}\omega. \tag{1.2.28}$$

[2] also called "Witten type"

Now, since the Kähler class is a closed form, its integral only depends on the homology class β of $\varphi(\Sigma_g)$, not on the worldsheet metric. So this term simply contributes a prefactor

$$\mathrm{e}^{-t\int_{\varphi(\Sigma_g)}\omega} \equiv \mathrm{e}^{-t\beta\cdot\omega}, \tag{1.2.29}$$

and we have shown that the A-model is indeed topological. As discussed above, the observables in a cohomological field theory are the elements of the $\mathcal{Q}$-cohomology. In the A-model, the most general local operator satisfying the requirement of metric independence is

$$\mathcal{O}_K = K_{i_1\cdots i_p\bar{j}_1\cdots\bar{j}_q}\chi^{i_1}\cdots\chi^{i_p}\chi^{\bar{j}_1}\cdots\chi^{\bar{j}_q}, \tag{1.2.30}$$

where $K_{i_1\cdots i_p\bar{j}_1\cdots\bar{j}_q}$ is a (p,q)–form on X. One can show that

$$\{\mathcal{Q}_A, \mathcal{O}_K\} = -\mathcal{O}_{\mathrm{d}K}, \tag{1.2.31}$$

where d is the ordinary exterior derivative, so the BRST-cohomology of the A-model on X, with BRST-operator $\mathcal{Q}_A$, is in direct correspondence with the de Rham cohomology of the target manifold X, and $\mathcal{Q}_A$ can be interpreted as the de Rham differential on X. Note also that after extracting the prefactor, the action S_A is $\mathcal{Q}_A$-exact. This implies that for any correlation function, we find

$$\partial_t\langle\mathcal{O}\rangle = -\langle\mathcal{O}\partial_t\mathcal{S}_A\rangle = \pm\langle\{\mathcal{Q}_A, \mathcal{O}V_A\}\rangle = 0, \tag{1.2.32}$$

and therefore the correlator is independent of t. This means in particular that the semi-classical approximation $t\to\infty$ is *exact*. Hence, the only contributions to the path integral

$$\langle\mathcal{O}\rangle = \int \mathcal{D}\phi\mathcal{D}\psi\mathcal{D}\chi\ \mathcal{O}\ \mathrm{e}^{-\mathcal{S}_A} \tag{1.2.33}$$

come from configurations extremizing the action, that is, instanton configurations. Because of the localization principle introduced above, these are precisely those that are fixed points of $\mathcal{Q}_A$. From the variation of the fields under $\mathcal{Q}_A$ (1.2.24), one can deduce that the fixed points of $\mathcal{Q}_A$ have to satisfy $\chi^i = 0$ and

$$\partial_{\bar{z}}\phi = 0, \tag{1.2.34}$$

therefore the worldsheet instantons of the A-model are nothing else than holomorphic maps $\phi : \Sigma \to X$. This can also be seen when rewriting the bosonic part of the action as

$$\begin{aligned} S_b &= \int_\Sigma g_{i\bar{j}}\left(\partial_z\phi^i\partial_{\bar{z}}\bar{\phi}^{\bar{j}} + \partial_{\bar{z}}\phi^i\partial_z\bar{\phi}^{\bar{j}}\right) \\ &= 2\int_\Sigma g_{i\bar{j}}\left(\partial_{\bar{z}}\phi^i\partial_z\bar{\phi}^{\bar{j}}\right) + \beta\cdot\omega \geq \omega\cdot\beta. \end{aligned} \tag{1.2.35}$$

Since the action is bounded from below and the minimum is reached if and only if the map ϕ is holomorphic, this is the dominant contribution in the semiclassical approximation, and therefore –as we have just seen– the only relevant one.

The action being $\mathcal{Q}_A$-exact up to the term $-\int_{\varphi(\Sigma_g)}\omega$, by the same argument as above physical observables don't depend on *anything* appearing only in V_A. The only relevant structure is the Kähler form that appears in the extra term. However, the moduli space of the target contains not only the Kähler moduli parametrizing the Kähler form, but also complex structure moduli to which the A-model is blind. Therefore, it is "half-topological" with respect to the target space. We will see shortly that the B-model depends on the other half of the moduli.

The classical R-symmetries $U(1)_V$ and $U(1)_A$ survive the twisting procedure and lead to a selection rule for a correlation function to be non-vanishing. Consider a correlation function of the form

$$\langle\mathcal{O}_1\cdots\mathcal{O}_s\rangle. \tag{1.2.36}$$

As we have seen above, each of the inserted operators is given by a differential form in $H^{p,q}(X)$. The vector and axial charges of such an operator are $q_V = q - p$ and $q_A = q + p$. While the vacuum is invariant under $U(1)_V$ and thus the total vector charge of the inserted operators has to vanish, there is an anomaly in the axial R-symmetry which the inserted operators have to compensate. The mismatch in zero modes is given by the index of the fermion kinetic operators which can be shown to be

$$2\int_{\Sigma_g} \varphi^*(c_1(X)) + 2\dim(X)(1-g). \tag{1.2.37}$$

We therefore find the selection rule

$$\sum_{i=1}^{s} p_i = \sum_{i=1}^{s} q_i = \int_{\Sigma_g} \varphi^*(c_1(X)) + \dim(X)(1-g). \tag{1.2.38}$$

This is an important result! It implies that if the target has vanishing first Chern class, the only truly nontrivial correlation functions appear at $g = 0$. At $g = 1$, the only quantity satisfying (1.2.38) is the partition function itself, and at higher genus $g > 1$ all correlation functions vanish. To put it otherwise, there are no holomorphic maps from a generic Riemann surface Σ_g to a target X unless X has non-vanishing first Chern class or $g \leq 1$.

1.2.4 The B-model

Now what happens if instead of choosing the A-twist, we go for the B-twist? Following [6], we rename the fields as follows:

$$\begin{aligned} \rho^i_z &= \psi^i_+, & \rho^i_{\bar{z}} &= \psi^i_- \\ \eta^{\bar{i}} &= \overline{\psi}^{\bar{i}}_+ + \overline{\psi}^{\bar{i}}_-, & \theta_i &= g_{i\bar{j}}\left(\overline{\psi}^j_+ - \overline{\psi}^j_-\right). \end{aligned} \tag{1.2.39}$$

We now have another field content. There's still a scalar, commuting map $\phi : \Sigma_g \to X$, but in addition two Grassmannian fields η, θ, scalars on the world-sheet, and a Grassmannian one-form ρ. The action of the $\mathcal{Q}_B$-transformation is now

$$\begin{aligned} \{\mathcal{Q}_B, \phi^i\} &= 0, & \{\mathcal{Q}_B, \theta_i\} &= 0, \\ \{\mathcal{Q}_B, \bar{\phi}^i\} &= \eta^{\bar{i}}, & \{\mathcal{Q}_B, \eta^{\bar{i}}\} &= 0, \\ \{\mathcal{Q}_B, \rho^i_z\} &= \partial_z \phi^i, & \{\mathcal{Q}_B, \rho^i_{\bar{z}}\} &= \partial_{\bar{z}} \phi^i. \end{aligned} \tag{1.2.40}$$

We thus immediately see that the only $\mathcal{Q}_B$-fixed point is

$$\partial_z \phi^i = \partial_{\bar{z}} \phi^i = 0. \tag{1.2.41}$$

According to the localization principle, the only contributions to B-model observables come from constant maps. The observables in this model now take the form

$$\mathcal{O}_W = W^{J_1 \cdots J_q}_{\bar{I}_1 \cdots \bar{I}_p} \eta^{\bar{I}_1} \cdots \eta^{\bar{I}_p} \theta_{J_1} \cdots \theta_{J_q}. \tag{1.2.42}$$

Note that these are not (p, q)–forms as in the A-model case, but rather $(0, p)$–forms taking values in $\bigwedge^q (T^{(1,0)})(X)$, i.e. elements of $\Omega^{0,p}(X, \bigwedge^q T^{(0,1)}X)$. Similarly to the A-model case, one can show that [16]

$$\{\mathcal{Q}_B, \mathcal{O}_W\} = -\mathcal{O}_{\bar{\partial} W}. \tag{1.2.43}$$

Hence, $\mathcal{O}_W$ as an element of the BRST-cohomology of the B-model corresponds directly to an element of the Dolbeault cohomology $H^p_{\bar{\partial}}(X, \bigwedge^q TX)$ [3].

[3] For a very brief description of cohomology theories, see appendix C.2.

Consider now the correlation function

$$\langle \mathcal{O}_1 \cdots \mathcal{O}_k \rangle = \int \mathrm{e}^{-S} \mathcal{O}_1 \cdots \mathcal{O}_k, \tag{1.2.44}$$

with $\mathcal{O}_i$ corresponding to an element of $H^{p_i}_{\bar\partial}(X, \bigwedge^{q_i} TX)$, having vector and axial charge $q_V = q_i - p_i$, $q_A = q_i + p_i$. As in the A-model case, we find a selection rule from the fact that the $U(1)$ vector R-symmetry is non-anomalous, namely

$$\sum_i (p_i - q_i) = 0, \tag{1.2.45}$$

while the $U(1)$ axial R-symmetry has an anomaly. The zero mode mismatch to be compensated by the inserted operators $\mathcal{O}_1 \cdots \mathcal{O}_k$ is

$$2\dim(X)(g-1), \tag{1.2.46}$$

so that we get the selection rule

$$\sum_i p_i = \sum_i q_i = \dim(X)(1-g) \tag{1.2.47}$$

As in the A-model, the only nontrivial correlation functions occur at $g = 0$, whereas at $g = 1$ only the partition function itself is non-vanishing. However, since we only have to sum over constant maps, computation of correlation functions reduces to an integral of forms over the target X itself. How do we compute such a correlation function? After all, the product of operators in the integrand corresponds to a form in $H^p_{\bar\partial}(X, \bigwedge^q TX)$. In order to integrate this object over X, we somehow need to map it into an ordinary (p,p)–form in a canonical way.

At this point, we need to make another assumption about the target space. While the A-model could be defined on any Kähler manifold, the B-model is most conveniently defined for a Calabi-Yau target. In this case, there is a holomorphic, nowhere vanishing section $\Omega_{I_1 \cdots I_d}$ of the canonical bundle $\Omega^{(d,0)}(X)$[4]. The prescription to compute correlation functions is then to use the invertible map

$$\begin{aligned} \Omega^p_{\bar\partial}(X, \bigwedge^q TX) &\to \Omega^{d-q,p}(X) \\ W^{J_1 \cdots J_q}_{\bar I_1 \cdots \bar I_p} &\to \Omega_{I_1, \cdots I_q I_{q+1} \cdots I_d} W^{I_1 \cdots I_q}_{\bar I_1 \cdots \bar I_p} \end{aligned} \tag{1.2.48}$$

to map $W \in H^d_{\bar\partial}(X, \bigwedge^d TX)$ to a $(0,d)$–form contracting the holomorphic indices with those of Ω, and then multiply by the $(d,0)$–form Ω to obtain a (d,d)-form that can be integrated over X.

It turns out that the full information about the B-model at genus 0 can be encoded in a single function called the *prepotential*. It only depends on the complex structure moduli and can be computed by purely classical methods from $\mathcal{N} = 2$ special geometry, as will be explained in section 2.1.

A-model versus B-model

Summarizing, we have seen that even before coupling to gravity the A-model contains interesting geometric information that is comparatively hard to compute, while the B-model is much simpler, but also less interesting at first sight. Both models are completely trivial at worldsheet genera higher than one. In the next section, we will explain how the extension to higher genus is achieved via coupling to gravity, and how mirror symmetry connects the two models, allowing one to compute A-model geometric information with B-model technology.

[4] In particular, this implies that the canonical line bundle is trivial, therefore $c_1(X) = 0$ and we recover the standard Calabi-Yau definition.

1.3 Coupling to Gravity: Topological Strings

In order to couple a two-dimensional quantum field theory to gravity, one essentially has to integrate over the space of all possible worldsheet metrics. Naively, one might assume that in the special case of a topological theory, this should have no effect on the observables, since they are independent of the worldsheet metric. This is not so. The most obvious reason for this is that the volume of the gauge group of all possible metric configurations is infinite, so just performing the path integral over all metrics and dividing by this volume is not a well-defined operation. Furthermore, we have to be careful with the loitering anomalies. However, help with the problem of coupling to gravity comes from an unexpected side: the bosonic string. All the ingredients we have introduced above have their analogous counterparts in bosonic string theory, as is summarized in table 1.1. The topological charge $\mathcal{Q}$ plays the role of the BRST-operator $\mathcal{Q}_{BRST}$, and the operator

$$G_{\mu\nu} \equiv \frac{\delta V_{A/B}}{\delta g^{\mu\nu}} \tag{1.3.49}$$

is associated with the antighost $b(z)$. It is a very fortunate coincidence that the ghost number anomalies of the two theories precisely agree if the target is a Calabi-Yau threefold, and therefore the critical dimension of the topological string is precisely the one we will be most interested in in order to study the connection to the superstring. For a more detailed comparison between

Property	Topological String	Bosonic String
$\exists$ nilpotent operator	$\mathcal{Q}_{A/B}$	BRST-operator $\mathcal{Q}_{BRST}$
energy-momentum tensor exact	$T(z) = \{\mathcal{Q}, G_{\mu\nu}\}$	$T(z) = \{\mathcal{Q}, b(z)\}$
antighost field	$G_{\mu\nu}$	$b(z)$
ghost number anomaly	$2\ d(X)(g-1)$	$6g-6$

Table 1.1: Comparison bosonic/topological string

bosonic and topological string theory, see [17].

We thus couple the topological sigma model to gravity just as in the case of the bosonic string [13, 14], defining a free energy

$$F_g = \int_{\mathcal{M}_g} \langle \prod_{k=1}^{6g-6} (G, \mu_k) \rangle, \tag{1.3.50}$$

where the antighost fields have to be included in the integral over the metric moduli space in order to cancel the axial charge anomaly, and μ_k are Beltrami differentials. It can be shown that the F_g so defined still depend only on the Kähler moduli for the A-model, and only on the complex structure moduli for the B-model. However, note that F_g as defined above is not a function on (half) the moduli space of a Calabi-Yau, but a *section* of a bundle over it, as will be made explicit in section 2.1.

1.3.1 Topological amplitudes in type II compactifications

As we have already mentioned, there is a beautiful story about the connection between topological strings and the more "physical" type II theories, started by the ground-breaking papers [18, 19, 20]. It turns out that the A- and B-model topological string on a given target Calabi-Yau are deeply related to the four-dimensional effective action of type IIA and type IIB theory respectively, compactified on that same Calabi-Yau. In the following, we will briefly summarize how this comes about, and how this connection has led to startling new developments both in string theory and in mathematics.

Take a type II theory in ten dimensions. After compactification on a generic Calabi-Yau manifold, the resulting theory has $\mathcal{N} = 2$ supersymmetry (see [13] for more details on superstring

	IIA	IIB
$h^{1,1}$ Kähler	vector	hyper
$h^{2,1}$ complex structure	hyper	vector

Table 1.2: Organization of the moduli into vector- and hypermultiplets for IIA and IIB theory

	IIA	IIB
$\mathscr{M}_H$-corrections	λ	λ and α'
$\mathscr{M}_V$-corrections	α'	exact

Table 1.3: Corrections to hyper- and vectormultiplet moduli space

compactifications, and section 2.1 for a more detailed review of $\mathcal{N} = 2$ special geometry). The moduli space of the compactified theory can be organized into multiplets as follows.

For IIA theory, the massless ten-dimensional fields are $g_{MN}, b_{MN}, \phi, c_M$ and c_{MNP}. After Kaluza-Klein decomposition, their four-dimensional components are the metric $g_{\mu\nu}$, dilaton ϕ, axion field a and a massless vector c_μ. The remaining components are decomposed under the forms of the Calabi-Yau; the single $(3,0)$ and $(0,3)$ forms each give rise to one scalar from c_{ijk} and $c_{\bar{i}\bar{j}\bar{k}}$, the $h^{1,1}$ harmonic one-forms split off two scalars from $g_{i\bar{j}}$ and $b_{i\bar{j}}$, and one gets a vector from $c_{\mu i\bar{j}}$. For each of the $h^{2,1}$ harmonic $(2,1)$-forms, there are four scalars from $g_{ij}, g_{\bar{i}\bar{j}}, c_{ij\bar{k}}$ and $c_{\bar{i}\bar{j}k}$. The model-independent fields form the bosonic content of the supergravity multiplet (graviton $g_{\mu\nu}$ and graviphoton c_μ) and one hypermultiplet (ϕ, a, c_{ijk} and $c_{\bar{i}\bar{j}\bar{k}}$). Of the remaining fields, the vector and two scalars for each $(1,1)$-form fall into a vector multiplet and the four scalars from each $(2,1)$-form organize into a hypermultiplet. All in all, there is therefore one supergravity multiplet, $h^{(1,1)}$ vector multiplets and $h^{(2,1)}+1$ hypermultiplets. For IIB theory, the only difference is that the massless ten-dimensional fields are c, c_{MN} and c_{MNPQ}, such that now the $(2,1)$-forms lead to two scalars and a vector (from $c_{\mu ij\bar{k}}$), while the $(1,1)$-forms only produce scalars, and we get $h^{(2,1)}$ vector multiplets and $h^{(1,1)}+1$ hypermultiplets. Summarizing, the moduli of the Calabi-Yau manifold are organized into multiplets as shown in table 1.2. A crucial observation is that the dilaton ϕ sits in both type IIA and IIB theory in a hypermultiplet. Since the moduli space factorizes *exactly* into $\mathscr{M} = \mathscr{M}_V \times \mathscr{M}_H$ due to supersymmetry [21], only the part of moduli space containing the dilaton gets higher genus corrections in the string coupling $\lambda = \mathrm{e}^{\phi}$. Similarly, the α'-expansion in the string length has to vanish in the large radius limit and should therefore only affect the part of moduli space sensitive to volume, namely the one containing the Kähler moduli. This situation is summarized in table 1.3.

In compactifications of superstring theories on Calabi-Yau spaces, conifold singularities in the moduli space generically appear at the classical level. In 1995, Strominger showed that these singularities could be resolved by the appearance of massless black holes due to nonperturbative effects in the full quantum theory [22]. A crucial postulate for this mechanism to work is that the above absence of couplings between vector and hypermultiplets even holds nonperturbatively.

As a consequence, the couplings appearing in the four-dimensional effective action of type II theories are subject to strong non-renormalization theorems. In particular, one can show that the self-dual part of the four-dimensional effective action is *exactly* determined by the topological string amplitudes and does not receive any further quantum corrections. More precisely, the effective action of both type II theories contains an F-term

$$S_F \sim \int \mathrm{d}^4x \mathrm{d}^4\theta \; F_g(t_i)\mathcal{W}^{2g} = \int \mathrm{d}^4x \; F_g(t_i) R_+^2 T_+^{2g-2} + \cdots , \tag{1.3.51}$$

where $\mathcal{W}$ is the supergravity multiplet in superfield notation, R is the Riemann tensor, T the graviphoton field strength, and $F_g(t_i)$ is the topological string free energy. For type IIA, $F_g(t_i)$ is

the A-model free energy, depending on the Kähler moduli t_i, whereas for type IIB the statement holds with respect to the B-model free energy and complex structure moduli.

In chapter 3, we will explain this in more detail and use heterotic-type II duality to compute the $F_g(t_i)$ for a large class of models.

1.3.2 The A-model topological string and Gromov-Witten invariants

As we have explained in section 1.2.3, the A-model localizes on fixed points of $\mathcal{Q}$ and is constant on the homology classes of the map φ, and therefore the integral over the moduli space $\mathcal{M}_g$ reduces to a sum over homology classes

$$F_g(t) = \sum_\beta N_{g,\beta} Q^\beta, \tag{1.3.52}$$

which we can reorganize into a generating function

$$F(t, g_s) = \sum_g F_g(t) g_s^{2g-2}. \tag{1.3.53}$$

Here, $N_{g,\beta}$ are the Gromov-Witten invariants of the Calabi-Yau X, "counting" the number of embeddings of a Riemann surface of genus g in the two-homology class β. Precisely what is meant by "counting" in this context has only become clear with the work of Gopakumar and Vafa [23, 24], who uncovered the hidden integrality structure in the rational Gromov-Witten invariants. We will here summarize the main ideas; for more details about both mathematical and physical aspects, we refer the reader to [12].

Recall that in the previous section, we saw that compactification of type II theory on a Calabi-Yau manifold generates higher-derivative F-terms in the effective action that are given by topological string amplitudes. These terms actually have a target space interpretation as resulting from integrating out hidden degrees of freedom [23].

If we give a constant vacuum expectation value g_s to the self-dual part of the graviphoton field T, the F-term appearing in (1.3.51) reads

$$F(t, g_s) R_+^2. \tag{1.3.54}$$

The computation of such a term is then analogous to the Schwinger computation for integrating out a charged scalar field coupled to a constant background field strength,

$$S = \int \mathcal{D}\phi \mathrm{e}^{-\int |(\partial_\mu - \mathrm{e}A_\mu)\phi|^2 + m^2|\phi|^2}. \tag{1.3.55}$$

This standard computation involves the determinant of the operator in the exponent, and the result is the famous Schwinger formula

$$S = \int \frac{ds}{s} \frac{\mathrm{Tr}(-1)^F \mathrm{e}^{-sm^2} \mathrm{e}^{-2se\sigma_L F}}{(2\sin(seF/2))^2}, \tag{1.3.56}$$

where $F = 2(\sigma_L + \sigma_R)$ is the total fermion number.

The particles we have to take into account when performing a similar computation in string theory are BPS states. They turn out to be obtained from D2 branes, bound to D0-branes and wrapped around two-cycles in the Calabi-Yau X, and their mass is given by the central charge of the bound state. For the D2-brane, the central charge is the area of the wrapped two-cycle. If this two-cycle is in the homology class β, its area is given by $t \cdot \beta$, where t_i are the Kähler moduli. Here, we have decomposed β with respect to a basis $\{S_i\}$ of $H_2(X, \mathbb{Z})$ such that

$$\beta = \sum_i \beta_i S_i, \qquad \beta \cdot t = \sum_i \beta_i t_i, \tag{1.3.57}$$

and we also write in the following

$$Q_i = \mathrm{e}^{-t_i},\ Q^\beta = \mathrm{e}^{-t\cdot\beta}. \tag{1.3.58}$$

The full mass of the bound state is shifted by $2\pi\mathrm{i}$ for each D0-brane (this can be understood from the lift to M-theory where this shift is nothing but the momentum of the M2 brane along the eleventh dimension compactified on a circle). For the trace in (1.3.56), we change basis from σ_L to

$$I_g = \left[\left(\frac{1}{2}\right) + 2(0)\right]^{\otimes g}. \tag{1.3.59}$$

The $\{I_g\}$ form a basis for $SU(2)$-representations with integer coefficients, i.e.

$$\sum_{g=0}^{\infty} n_\beta^g I_g = \sum_{j_L} n_\beta^{j_L}[j_L], \tag{1.3.60}$$

and one finds

$$\mathrm{Tr}_{I_g}(-1)^F \mathrm{e}^{-2\tau\sigma_L g_s} = (-1)^g \left(2\sinh\left(\frac{\tau g_s}{2}\right)\right)^{2g}, \tag{1.3.61}$$

where we have absorbed F in the coupling g_s. Finally, we have to sum over all possible BPS states, parametrized by the number of D-branes d, $SU(2)_L$-representations I_g and homology classes β. After performing the integral, we obtain

$$F(g_s, t) = \sum_{g=0}^{\infty}\sum_{\beta}\sum_{d\geq 1} n_\beta^g \frac{1}{d}\left(2\sinh\left(\frac{dg_s}{2}\right)\right)^{2g-2} Q^{d\beta}, \tag{1.3.62}$$

where n_β^g are the integer Gopakumar-Vafa invariants, labeled by genus g and homology class β.

This integrality structure finally uncovers the enumerative meaning of the Gromov-Witten invariants. The reason why this structure is hidden in the original Gromov-Witten invariants is that even though the latter do count maps at genus g in a fixed homology class, these maps are not primitive maps in one-to-one correspondence with BPS states, but receive weighted contributions from maps at lower-genus and lower homology class destroying integrality. These two effects are known as *multicovering* and *bubbling*: given one holomorphic map from a genus g Riemann surface into X, one can construct an infinity of similar maps either composing it with a d-multiple cover of $\mathbb{P}_1$ leading to a map in homology class $d\beta$, or by letting the genus g surface "bubble" into a higher-genus surface by gluing a small genus h surface to it. All these derived maps contribute with a non-integer weight to the Gromov-Witten invariants, whereas the Gopakumar-Vafa invariants only count primitive maps, in direct correspondence with BPS states.

The above can be summarized in the so-called Gopakumar-Vafa conjecture stating that all n_β^g are indeed integers for all Calabi-Yau threefolds. There is a bold generalization of this conjecture due to Pandharipande for more general non-singular threefolds. Both conjectures, even though well-motivated physically, remain unproved at the time of writing but for some special cases. There is another class of invariants closely related to the Gromov-Witten and Gopakumar-Vafa invariants introduced above, namely the Donaldson-Thomas invariants. Again, a conjecture motivated by the duality of Chern-Simons theory with the A-model and proved for the special case of toric Calabi-Yaus states their equivalence with Gromov-Witten invariants [25, 26, 27]. In a nutshell, S-duality of the type II theories implies that A-model worldsheet instantons, encoded in Gromov-Witten and Gopakumar-Vafa invariants, capture B-model D-brane instantons, encoded in Donaldson-Thomas invariants. Thus, the latter can be seen as S-dual partners of Gromov-Witten invariants [28]. The story of Gromov-Witten, Gopakumar-Vafa and Donaldson-Thomas invariants is a beautiful example where mathematical puzzles can be understood from a string point of view.

It is instructive to expand (1.3.62) in g_s. One finds the following form for $F_g(t)$:

$$F_g(t) = \sum_\beta \left(\frac{|B_{2g}| n_\beta^0}{2g(2g-2)!} + \frac{2(-1)^g n_\beta^2}{(2g-2)!} + \cdots - \frac{g-2}{12} n_\beta^{g-1} + n_\beta^g \right) \mathrm{Li}_{3-2g}\left(Q^\beta\right). \tag{1.3.63}$$

From this expression, one can read off that e.g. at genus 0, each BPS state (counted by n_β^0) contributes

$$\mathrm{Li}_3(Q^\beta) = \sum_d \frac{Q^d}{d^3}, \tag{1.3.64}$$

i.e. the weight of the multicovering solutions is $\frac{1}{d^3}$.

The appearance of the polylogarithm was already predicted from heterotic-type II duality in [29]. In chapter 3, we will use heterotic-type II duality to compute Gopakumar-Vafa invariants for a large class of models.

The proposed duality between the A-model and Chern-Simons theory [27] has been used in [30, 31] to derive a method to compute all-genus A-model amplitudes for any non-compact toric Calabi-Yau threefold.

1.3.3 The B-model topological string

As we have seen above, the B-model localizes on constant maps and is therefore generally much simpler to compute with than the A-model. However, as we will see below, the two models are related by mirror symmetry and are therefore completely equivalent, so it is often convenient to compute the geometric content of the A-model on the B-model side and map to the A-model at the end, as we will do many times in the following chapters.

The B-model has some beautiful properties that have not only shed light on many surprising connections between string theory and mathematics, but also allow one to compute the topological amplitudes in a comparatively simple way. We will briefly summarize some of them:

- The holomorphic anomaly.
  As we have mentioned in section 1.2, $\mathcal{Q}_B$-exact operators should in principle decouple completely from the theory. However, as will be explained in detail in section 2.2, the argument for the decoupling fails after coupling to gravity because the moduli space of Riemann surfaces Σ_g has a boundary, and it is precisely this boundary which keeps some deformations from decoupling even though they are $\mathcal{Q}_B$-exact. As a consequence, B-model amplitudes are almost, but not quite holomorphic in the complex structure moduli, and this effect can be quantified in a set of differential equations for the $F_g(t, \bar{t})$ called holomorphic anomaly equations. In chapter 2, we will develop an efficient method to integrate these to obtain the amplitudes F_g of the B-model. This method relies heavily on the interplay between holomorphicity and *modularity* properties of F_g, as stated most clearly in [73]. We explain this in more detail in section 2.1.

- Connection to matrix models.
  In [32], Dijkgraaf and Vafa have proposed a duality between the B-model topological string on some specific Calabi-Yau targets and a matrix model. Building on the matrix model technologies constructed in [33], this connection has recently been developed into a general formalism for computing B-model amplitudes and generalized to a much larger class of targets including those with interesting mirror geometry in [34, 35, 36]. This will be explained in more detail in section 4.2. See chapter 5 for applications.

- Picard-Fuchs equations.
  The Picard-Fuchs equations are differential equations for the periods of the target space. Their system of solutions allows one to determine the mirror map and the prepotential, which completely determines the B-model at genus 0, see also section 2.1.

1.3.4 Mirror Symmetry

The statement of mirror symmetry is that the A-model on one Calabi-Yau is completely equivalent to the B-model on another Calabi-Yau, called "mirror".

At the algebraic level, mirror symmetry changes the sign of the right-moving $U(1)$ current F_R. The result is that the spaces $H^{p,q}(X)$ and $H^{d-p,q}(X_{\text{mirror}})$ get identified, that is, the Kähler moduli space of one Calabi-Yau is completely equivalent to the complex structure moduli space of its mirror, or again equivalently: the A-model on X becomes the B-model on X_{mirror}. This extends to the full string theory, such that type IIA compactified on X is equal to type IIB compactified on X_{mirror}.

Unfortunately, a detailed introduction to mirror symmetry and its many applications in mathematics and physics is beyond the scope of this thesis. We therefore refer the reader to the book [12].

1.4 Topological strings and heterotic-type II duality

Heterotic and type IIA theory are among the best-connected knots in the web of string dualities (see also Fig. 1.1), and hence at the heart of many fundamental results about string theory and supersymmetric gauge theories. Apart from their relations to the other realizations of superstring theory, they are tied together by the fact that after compactification on suitable pairs of manifolds, they yield identical low-energy theories. This has first been proposed for compactification of the heterotic string on $\mathbb{T}^4$ and the type II theory on $K3$ [37], where $K3$ is a compact Calabi-Yau twofold, namely, the only Calabi-Yau twofold that is not the four-torus[5]. After further compactification to four dimensions on $\mathbb{T}^2$, these theories have $\mathcal{N} = 4$ supersymmetry. Furthermore, there is by now overwhelming evidence that heterotic strings compactified on $K3 \times \mathbb{T}^2$ are dual to type IIA compactified on a suitable $K3$-fibration [39, 40], both yielding four-dimensional theories with $\mathcal{N} = 2$ supersymmetry.

A crucial observation is that the dilaton, governing the expansion in the string coupling, sits in a hypermultiplet in type IIA and in a vectormultiplet in heterotic theory. This is what makes heterotic-type II duality so appealing. According to the (perturbative and even nonperturbative) decoupling of vector- and hypermultiplet moduli mentioned in section 1.3.1, it implies that both the vector multiplet prepotential F_0 on the type II side and the hypermultiplet superpotential on the heterotic side are exact at tree-level, while they get nonperturbative quantum corrections on the respective other sides. Thus, using the duality we can compute the exact quantum moduli space classically! In particular, worldsheet instantons on the type IIA side, accessible to a classical computation, determine space-time instanton effects on the heterotic side and vice versa [39].

The non-renormalisation argument can be extended to g-loop level, such that the couplings F_g appearing in the type II effective action (1.3.51) should be generated at g-loop level only and not receive further quantum corrections, which is why they correspond *exactly* to the topological string amplitudes, as we have mentioned above. On the heterotic side, even though the F_g are not protected by supersymmetry since the dilaton sits here in a vectormultiplet, general arguments imply that they arise at one-loop level only [20]. It turns out that the F_g are given by a one-loop integral over the heterotic gauge lattice of the form studied by Borcherds [41], and can be computed with his technique of lattice reduction (see also appendix A.1). Computations of this type have first been performed in [29] and later also in the articles [42, 43] presented in this thesis. A particularly nice aspect of this mapping between type II and heterotic theory is that in Borcherds-type one-loop integrals the automorphicity of the amplitudes under the full symmetry group of the lattice moduli space becomes explicit, due to the Borcherds-Harvey-Moore extension

[5] See [38] for further information on $K3$ surfaces in the context of string dualities

of the Howe or theta correspondence [44, 41]. In chapter 3, we will use heterotic-type II duality to compute worldsheet instanton numbers at arbitrary genus on chains of Calabi-Yau manifolds.

Another intriguing property of heterotic-type II duality has been pointed out in [40]. The number of vector- and hypermultiplets changes over the moduli space of heterotic $K3 \times \mathbb{T}^2$ compactifications when one explores different Higgs branches, passing through points of enhanced symmetry. On the type II side, this corresponds to jumping through successive Calabi-Yau spaces, and this process can be achieved via black hole condensation [22]. For more details on the geometric implications of this mapping, see chapter 3.

As far as the topological string amplitudes are concerned, the main drawback of heterotic-type II duality is that it applies only to Calabi-Yau spaces which are $K3$–fibrations, and much worse, the heterotic dilaton gets mapped to the Kähler modulus controlling the volume of the base space. This implies that the heterotic weak-coupling limit corresponds on the type II side to the region of the Kähler cone where the volume of the base space goes to infinity, and therefore, the only geometric information one can extract from heterotic-type II duality applies to the $K3$-fibers.

1.5 Topological strings and matrix models

According to a general principle put forward by 't Hooft [5], there should be a correspondence between matrix models at large N, where N is the rank of the gauge group, and string theories. In [32], Dijkgraaf and Vafa proposed that the topological B–model is indeed equivalent to a matrix model for some target space geometries. Recently, the authors of [34, 35] have completely reformulated the open and closed topological B-model in terms of matrix models, using the matrix model techniques of [33]. In this section, we sketch very briefly the main ideas, a more detailed review of matrix models and their intimate relation to topological strings will be given in chapter 4, while toric Calabi-Yau's and their mirrors are briefly reviewed in appendix C.3.

The crucial observation of [32] is that one can associate a matrix model to some topological string geometries by taking the spectral curve of the matrix model, a Riemann surface, to be the mirror curve Σ of the target geometry, the Riemann surface naturally defined by the topological string. Conversely, the target geometry is determined by the master field of the $1/N$ expansion.

The geometries considered in [32] are very restrictive and in particular don't include the geometrically interesting mirrors of toric geometries. However, there is a recursive reformulation of the $\frac{1}{N}$-expansion of matrix models in a geometric setup where the main ingredient is precisely the spectral curve [45, 33]. In [29, 35, 36], this was used to completely reformulate and substantially generalize the correspondence between matrix models and topological strings such that it can be applied to general toric Calabi-Yau's. These are CY threefolds described by an equation of the form

$$uv = \Sigma(X, Y), \tag{1.5.65}$$

where $\Sigma(X, Y) = 0$ describes a Riemann surface embedded in $\mathbb{C}^* \times \mathbb{C}^*$. The authors of [29, 35] then take this Riemann surface to be the spectral curve of a matrix model, and adapt the formalism of [33] such that it applies to the toric case, where X and Y are exponentiated variables taking values in $\mathbb{C}^*$. This allows one to compute open and closed amplitudes of the B-model using only the spectral curve without having to specify the potential of the matrix model.

This formalism has opened several new perspectives. For one thing, the matrix model recursion relations imply the holomorphic anomaly equations satisfied by the B-model amplitudes, however, they are considerably more general. In particular, they are completely determined and don't give rise to a holomorphic ambiguity. Furthermore, the matrix model equations yield holomorphic anomaly equations for both open and closed amplitudes, the standard holomorphic anomaly equations for closed amplitudes simply appear as a special case. Thus, the B-model

formalism implies that open string amplitudes should be seen as somewhat more fundamental quantities than closed amplitudes.

In chapter 5, we will show how the matrix description of the B-model can be used to obtain nonperturbative information about the topological string.

1.6 Nonperturbative Aspects

Some of the most fundamental aspects of quantum field theory such as quark confinement and spontaneous symmetry breaking are due to strong interactions or infinitely many degrees of freedom; in short, beyond the scope of perturbation theory. Furthermore, instanton transitions have been a source of astonishment and delight in both classical and quantum field theories; for a review, see [46, 47]. It is fair to say that without understanding these issues, we would not understand quantum field theory at all.

Contrary to quantum field theory, string theory has two expansion parameters, namely the string coupling g_s playing the role of $\hbar$, and the string tension α' that has no counterpart in the standard model. Nonperturbative effects related to the α'–expansion appear at the level of the worldsheet theory and are called worldsheet instantons. As we have seen in section 1.3.2, they correspond to different embeddings of the world-sheet in the Calabi-Yau and correct the topological string amplitudes, or, from a superstring point of view, the string scattering amplitudes. They are conceptually well understood, and in many cases even computable to high order, as we have explained above and will explicitly show in the following chapters.

However, the genus expansion in the string coupling g_s is more problematic. String theory is only defined perturbatively in g_s, and the perturbation series is an asymptotic, non-convergent series that does not define the theory nonperturbatively. Nonperturbative effects related to the g_s–expansion are due to space-time instantons associated to D-branes. Even though the understanding of such nonperturbative aspects has very much improved, in particular with the advent of string dualities, a full nonperturbative definition of string theory is still not available. In chapter 4 and 5, we will show how matrix models and large-order behaviour can shed some light on these issues.

Let us now briefly summarize nonperturbative effects in the context of topological strings. Consider the topological A-model free energy on a Calabi-Yau X,

$$F(Q, g_s) = \sum_{d,g} N_{d,g} Q^d g_s^{2g-2}. \tag{1.6.66}$$

Recall from section 1.3.2 that $N_{d,g}$ are the Gromov-Witten invariants counting embeddings of the world-sheet in X, the world-sheet instantons. This series is doubly perturbative, in the Kähler parameter $Q = \mathrm{e}^{-t}$ corresponding to the α'-expansion, as well as in the topological string coupling g_s[6]. Using mirror symmetry, we can go beyond perturbation theory in Q and obtain

$$F(Q, g_s) = \sum_{g} F_g(Q) g_s^{2g-2}, \tag{1.6.67}$$

where $F_g(Q)$ can be computed exactly as a modular function in Q. As in the type II theories, the g_s–expansion is more difficult. In the A-model, the genus expansion can be resummed using the topological vertex [31] to obtain an expression of the free energy as a sum over partitions,

$$F(Q, g_s) = \log \sum_{R_i} C(R_i, g_s) Q^{\ell(R_i)}, \tag{1.6.68}$$

where $\ell(R_i)$ is the length of the partition, and the coefficient $C(R_i, g_s)$ is exact in g_s. However, the price to pay is that this is again an expansion in Q only valid at the specific point in moduli

[6] A notational warning: by g_s we refer to both the topological string coupling and the type II coupling. Which one is meant should be clear from the context

space, called the large radius point, where Q is small. It is therefore desirable to incorporate nonperturbative corrections in g_s directly in the B-model, where one can go anywhere in moduli space.

It has been observed a long time ago by Shenker [48] that nonperturbative corrections of the order $\mathrm{e}^{-\frac{1}{g_s}}$ generically appear in string theory. When considering the embedding of the topological string in type IIB theory, these effects come from D-branes wrapping different cycles in the Calabi-Yau. However, they are known to depend on hypermultiplet moduli [28, 49], whereas the B-model a priori only sees vectormultiplet moduli. A nonperturbative completion of the B-model might therefore necessarily involve hypermultiplets.

Putting this complication aside for the moment, there are still nonperturbative effects related to space-time D-branes involving vector multiplet moduli only. These effects are precisely the generic $\mathrm{e}^{-\frac{1}{g_s}}$ effects appearing in B-model *topological* strings, where g_s is the topological string coupling. In the lift to type II theory, they are associated to *domain walls* interpolating between branes wrapped around different cycles. As will be reviewed in detail in chapter 4, these instantons are very closely related to perturbation theory, since they control the large-order asymptotics of the perturbative series! This is a standard connection that has made it into quantum field theory textbooks [50], but has until now been studied in string theory only in the context of minimal models [51].

In chapter 5, we test this connection between large-order behaviour of the perturbative amplitudes and instanton effects for matrix models and show that using the proposed matrix-model formalism for the B-model [29, 35] introduced in the last section, an instanton computation within the matrix model correctly predicts the large-order behaviour of B-model amplitudes and therefore allows one to go beyond perturbation theory in the topological string.

1.7 Disclaimer, Summary and Outline

In this chapter, we have sketched the main aspects of topological strings relevant to this thesis. Of course, it is not intended to be a comprehensive overview of the field, as many important areas of research have been left out for the sake of brevity, and due to the limited competence of the author. One important topic that has not been covered is the fascinating study of black hole microstates and the OSV-conjecture [52]. Fortunately, this is treated in many excellent reviews, for example [53]. Another area we have not mentioned at all is Landau-Ginzburg theory and the description of B-branes as matrix factorizations, see e.g. the short review [54]. On the pure mathematics side, we have only very briefly mentioned Gromov-Witten and Donaldson-Thomas theory. Furthermore, some beautiful applications of topological strings that we had to leave out are related to knot theory [55], for a general introduction to knot theory, see [56].

Let us now summarize the various approaches to solving the topological string, their range of application, and the role they will play in the remainder of this work. By solving the topological string on a given background, we generally mean computing the amplitudes F_g. This problem can be addressed at different levels. A complete solution would require a nonperturbative expression of the full partition sum, exact in both the string coupling g_s and the Kähler/complex structure parameter Q, and valid everywhere in moduli space. At the time of writing, this is far too ambitious. More modest solutions can however be found. Which part of the problem can be solved to what extent depends crucially on the type of background, in particular, whether it is compact or non-compact, as can be seen from Fig. 1.2. The case of non-compact, toric Calabi-Yau's is relatively well under control. For the A-model, we have mentioned the topological vertex, allowing to resum all-genus amplitudes as exact expressions in g_s. However, this approach is perturbative in Q and applies only at the large radius point in moduli space, where Q is small. On the more mathematical side, the available techniques are localization and relative Gromov-Witten theory, neither permitting a complete solution, but the amplitudes can at least in principle be computed to arbitrary genus. A related, quite recent mathematical development

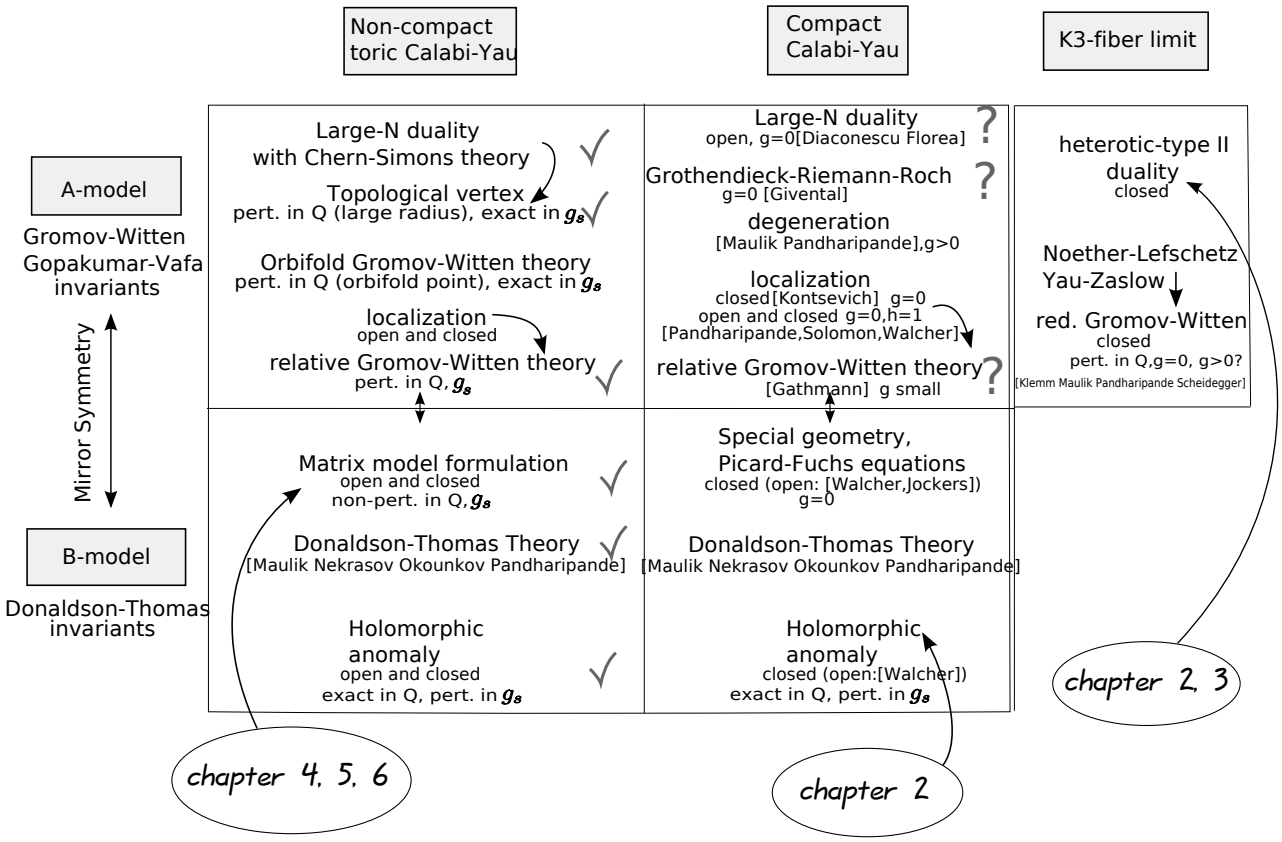

Figure 1.2: Solving the topological string on different types of backgrounds

is the study of orbifold Gromov-Witten invariants [57] and the crepant resolution conjectures [58, 59]. For the B-model on a non-compact Calabi-Yau, the most powerful techniques are integration of the holomorphic anomaly equations and the description in terms of matrix models. These have the advantage that they also apply to *open* amplitudes, while the corresponding open Gromov-Witten invariants are mathematically still poorly understood. A purely mathematical approach is Donaldson-Thomas theory. As we explained in section 1.3.2, Donaldson-Thomas invariants are conjectured to be the S-dual counterparts of Gromov-Witten invariants and accordingly we associate them to B-model rather than A-model computations. The exact correspondence between Donaldson-Thomas and Gromov-Witten theory has been proved for the case of local curves [25], and is conjectured for more general –including compact– backgrounds. Solutions of the B-model are generally automorphic functions, exact in Q and valid anywhere in moduli space, but perturbative in the genus expansion. The matrix model formulation allows to incorporate some nonperturbative effects, but these have to be computed instanton sector by instanton sector, as an expansion in $e^{\frac{-1}{g_s}}$.

If the target is compact, the problem turns out to be much more difficult. Few techniques are available. The A-model on compact Calabi-Yau manifolds has been addressed by Kontsevich via localization [60], and via relative Gromov-Witten theory by Gathmann, Maulik and Pandharipande [61, 62, 63]. In principle, the invariants can be computed at least for small genus, but few concrete results have been obtained, and most of these computations are limited to the comparatively simple cases of the Enriques Calabi-Yau studied in chapter 2 [63] and the quintic hypersurface in $\mathcal{P}^4$. Recently, Zinger has proved the mirror symmetry prediction made in [8] for the genus one Gromov-Witten invariants [64]. Open Gromov-Witten invariants have recently been addressed in [65, 66, 67] using localization and mirror symmetry, however, these approaches are limited to genus 0. Another approach to open Gromov-Witten invariants at genus 0 via geometric transitions is pursued in [68]. On the B-model side, the situation is

more encouraging, but the problem is still far from being solved. The holomorphic anomaly equations for closed strings have been integrated to genus 51 on the quintic hypersurface [69], and in chapter 2 of this work, we develop a technique to efficiently integrate them making use of modularity properties, which we apply on the Enriques Calabi-Yau to compute closed amplitudes up to genus six. However, this approach heavily relies on boundary conditions to fix the holomorphic ambiguities appearing at each genus, and even in these simple cases one invariably runs out of these conditions, so this is only a partial solution. Donaldson-Thomas theory is also defined on compact manifolds [25]. For some restricted compact cases, including low degrees on the quintic, the equivalence with Gromov-Witten theory has recently been proved in [70].

$\mathcal{N} = 2$ heterotic-type II duality applies to any targets which are $K3$-fibrations, but since one is limited to the heterotic weak coupling regime, it only determines the amplitudes in the $K3$-fiber limit, and the base directions cannot be addressed. From a purely mathematical point of view, one recent success is the proof of the Yau-Zaslow conjecture, determining the reduced Gromov-Witten invariants for $K3$ surfaces at genus 0.

The remainder of this thesis is organized as follows. The second part focuses on the problem of how to compute closed topological amplitudes. In chapter 2, we review $\mathcal{N} = 2$ special geometry and the holomorphic anomaly equations and develop an efficient method to integrate the latter. Chapter 3 presents a computation of geometric invariants of a large class of Calabi-Yau spaces using heterotic-type II duality. In the third part of this thesis, matrix models come into play. Chapter 4 presents an introduction to matrix models, instantons and the connection to topological strings. In chapter 5, we study the large-order behaviour and instanton effects in this context. In chapter 6, we consider multi-instanton effects and relate them to multicut matrix models. The last part contains a conclusion and remarks on open questions.

Part of the material presented in this thesis has been obtained in collaboration with M. Mariño, T. Grimm, A. Klemm and R. Schiappa and is published in [42, 43, 71], or will appear in [72].

Part II

COMPUTING TOPOLOGICAL AMPLITUDES

Chapter 2

Direct Integration of the Holomorphic Anomaly Equations

One of our main concerns throughout this thesis is solving the topological string on a given Calabi-Yau manifold. Recall from section 1.7 that while this problem is well under control – at least at the large-radius point– on non-compact, toric Calabi-Yau manifolds, it remains a challenge in the compact case. Currently, one of the best-suited approaches to obtain higher-genus amplitudes are the holomorphic anomaly equations due to Bershadsky, Cecotti, Ooguri and Vafa [19]. In this chapter, we develop a method to integrate them efficiently. The material presented is based on a publication with T. Grimm, A. Klemm and M. Marino [42].

We will make use of the fact that each Calabi-Yau manifold has a target space symmetry group which provides a symmetry of the topological partition function [73] and thereby drastically reduces the space of candidate solutions. The topological string amplitudes $F^{(g)}$ turn out to be polynomials in a finite set of generators which transform in a particularly simple way under the space-time symmetry group. Moreover, it can be shown that all non-holomorphic dependence in these amplitudes arises through a very special set of generators that are suitable generalizations of the non-holomorphic Eisenstein function $E_2(\tau, \bar{\tau})$. The remaining generators are holomorphic. Keeping track of these non-holomorphic contributions we will be able to directly integrate the holomorphic anomaly equations. This method turns out to be very efficient and gives us rich new information about the remaining holomorphic generators. A similar approach to the holomorphic anomaly equations was sketched in [19], in the analysis of toroidal orbifolds. For the quintic Calabi-Yau manifold a more complicated method was outlined in [74]. Other related approaches have been used before in [75, 76] to analyze rational elliptic surfaces, and in [77, 78] to study noncritical strings and $\mathcal{N} = 4$ super Yang–Mills theory.

The direct integration of the holomorphic anomaly equations can be performed for a generic Calabi-Yau manifold, as we show in the final section of [42]. However, in order to fully exploit the interplay of the holomorphic anomaly with the space-time symmetry, we will intensively discuss specific examples. To illustrate the general ideas we first study the local Calabi-Yau manifold associated to the Seiberg-Witten curve. Here the target-space symmetry group is a subgroup of $Sl(2, \mathbb{Z})$ and the generating modular functions are well-known.

Applying these methods to a compact Calabi-Yau manifold is far more involved. In most of this chapter we will focus on the specific example of the Enriques Calabi-Yau [39], arguably the simplest Calabi-Yau compactification with nontrivial topological string amplitudes [79, 62]. This manifold can be obtained as the free quotient $(\mathrm{K3} \times \mathbb{T}^2)/\mathbb{Z}_2$, where $\mathbb{Z}_2$ acts as the Enriques involution on the K3 fibers. The target space duality group of the Enriques Calabi-Yau is shown to be the discrete group $Sl(2, \mathbb{Z}) \times O(10, 2, \mathbb{Z})$, with the factors corresponding to the $\mathbb{T}^2$ base and Enriques fiber, respectively. The generating modular forms for $Sl(2, \mathbb{Z})$ are well-known, therefore we will be particularly concerned with the contributions from the Enriques fiber and

specially their mixing with the $\mathbb{T}^2$ base.

After integrating the holomorphic anomaly equations the only problem remaining is to fix the holomorphic ambiguities, i.e. the boundary conditions in the integration of the equations. These ambiguities are constrained by information coming from boundaries of the moduli space where the $F^{(g)}$ are known explicitly. In the Enriques case one can use the fiber limit, where all amplitudes can be determined by heterotic-type II duality [79], and a field theory limit where the manifold degenerates to give rise to $SU(2)$, $N_f = 4$ Seiberg-Witten theory. By making use of these boundary conditions we determine the full topological string amplitudes up to genus 6, improving in this way previous results in [79]. As a bonus of our analysis, we clarify the modularity properties of the conformal $N_f = 4$ theory and its gravitational corrections described in [80]. At present the available boundary conditions are not enough to completely solve topological string theory on the Enriques Calabi–Yau, but we provide efficient tools to analyze the amplitudes at all genus with the method of direct integration.

The rest of this chapter is organized as follows. In section 2.1 and 2.2 we review $\mathcal{N} = 2$ special geometry and the derivation of the holomorphic anomaly equations. Section 2.3 gives a simple example of the method of direct integration and the fixing of holomorphic ambiguities by application to Seiberg-Witten theory. Section 2.4 reviews what will be our main focus, the Enriques Calabi-Yau. We introduce modular and automorphic forms which will be relevant later and discuss the topological amplitudes on the Enriques fiber. Also an all-genus product formula for the fiber partition function will be introduced. In section 2.5, we show explicitly how one can solve for $F^{(g)}$ up to genus six and present the general recursive formalism. Furthermore, boundary conditions and a reduced Enriques model where part of the moduli space is blown down are investigated. In section 2.6 we analyze the field theory limit corresponding to $N_f = 4$ SYM and we relate it in detail to the Enriques Calabi–Yau.

2.1 $\mathcal{N} = 2$ special geometry

We now review some basic facts about $\mathcal{N} = 2$ special geometry [81, 82, 83, 84]. Let us start with some very basic definitions.

Definition 0**.**
A Kähler manifold is a hermitian complex manifold endowed with a metric $g_{i\bar{j}}$ such that the associated Kähler form

$$G = \mathrm{i} g_{i\bar{j}} dz^i \wedge d\bar{z}^{\bar{j}} \tag{2.1.1}$$

is closed, $dG = 0$. Locally, this implies that there is a Kähler potential $\mathcal{K}$ satisfying

$$g_{i\bar{j}} = \partial\bar{\partial}\mathcal{K}. \tag{2.1.2}$$

It turns out that we need a more restrictive object to allow for fermions, since they impose a quantisation condition on the Kähler form, and one finds that for consistency the Kähler form should be of integer cohomology [83], such that we can pick a line bundle $\mathcal{L}$ with

$$c_1(\mathcal{L}) = \frac{1}{2\pi}[G]. \tag{2.1.3}$$

By slight abuse of language, we call this type of Kähler manifold a *Hodge-Kähler* manifold.

Now let us focus on a type II compactification on a Calabi-Yau, and let's take IIB because of the absence of quantum corrections to the space of complex structure deformations $\mathcal{M}_V$. We can think of variations of complex structure as variations of Hodge structure:

$$H^3(Y, \mathbb{C}) = H^{3,0}(Y) + H^{2,1}(Y) + H^{1,2}(Y) + H^{0,3}(Y) = H^3(Y, \mathbb{Z}) \otimes_{\mathbb{Z}} \mathbb{C} \tag{2.1.4}$$

As we vary the complex structure, the embedding of the lattice $H^3(Y, \mathbb{Z})$ rotates with respect to this decomposition.

Comsider the holomorphic 3-from $\Omega \in H^{3,0}(Y)$, unique up to rescaling an nowhere vanishing by the Calabi-Yau condition. Choose a symplectic basis $\{A^a, B_a\}$ for $\mathcal{H}_3(Y)$, $a = 1, \cdots h^{2,1} + 1$, with intersections $A^a \cap B_b = \delta^a_b$.
Define the periods

$$X^a = \int_{A^a} \Omega; \qquad \mathcal{F}_a = \int_{B_a} \Omega \tag{2.1.5}$$

These periods span $\mathcal{M}_V$, however, since there are $2h^{2,1} + 2$ of them and the complex dimension of $\mathcal{M}_V$ is $h^{2,1}$, they cannot all be independent. Indeed, one can show that given all the X^a, the $\mathcal{F}_a$ are determined. Furthermore, the X^a can only be homogeneous coordinates since Ω is only determined up to a multiplicative constant, so we get the right dimension of $\mathcal{M}_V$ $h^{2,1} = \frac{2h^{2,1}+2}{2} - 1$. One can also show that we can define a *prepotential* $\mathcal{F}$ such that

$$\begin{aligned} \mathcal{F} =& \frac{1}{2} \sum X^a \mathcal{F}_a \\ \mathcal{F}(\lambda X^0, \lambda X^1, \cdots) =& \lambda^2 \mathcal{F}(X^0, X^1, \cdots) \\ \mathcal{F}_a =& \frac{\partial \mathcal{F}}{\partial X^a} \end{aligned} \tag{2.1.6}$$

This prepotential is the key quantity in special geometry, as will become clear below. It leads us to the first definition of a special Kähler manifold:
Definition 1.
A special Kähler manifold is a Hodge-Kähler manifold with a single holomorphic function $\mathcal{F}$ as above such that

(1) the Kähler potential is

$$\mathcal{K} = -\ln \mathrm{Im}(X^a \mathcal{F}_a), \tag{2.1.7}$$

(2) Transitions between local trivializations of $\mathcal{F}$ on overlaps of charts are given by holomorphic transition functions f_{ij} and $M_{ij} \in Sp(2n+2, \mathbb{R})$:

$$\begin{pmatrix} X \\ \partial \mathcal{F} \end{pmatrix}_i = \mathrm{e}^{f_{ij}(z)} M_{ij} \begin{pmatrix} X \\ \partial \mathcal{F} \end{pmatrix}_j . \tag{2.1.8}$$

Note that the geometry of $\mathcal{M}_V$ is completely determined by $\mathcal{F}$! In particular, the metric is given by the Kähler potential $\mathcal{K}$ according to (2.1.2). Notice also that $X^I \in \mathcal{L}$, $\overline{\mathcal{F}}_I \in \overline{\mathcal{L}}$, where $\mathcal{L}$ denotes the holomorphic line bundle over $\mathcal{M}_V$, the first Chern class of which equals the class of the Kähler form. Obviously the periods carry the information about the complex structure deformations. The X^I, $I = 0, \ldots h^{21}$ can serve locally as homogeneous coordinates on $\mathcal{M}$. Local special coordinates on $\mathcal{M}$ are defined by $t^i = X^i/X^0$, $i = 1, \ldots h^{(2,1)}$.

We can rephrase this in bundle language:
Definition 2.
A special Kähler manifold is a Hodge-Kähler manifold with

(1) a holomorphic $Sp(h^{2,1})$ vector bundle $\mathcal{H}$ over $\mathcal{M}_V$ with fibre $H^3(Y, \mathbb{C})$, and a holomorphic section Ω of $\mathcal{L} \otimes \mathcal{H}$ such that the Kähler 2-form G (equivalently, we can consider the Kähler potential $\mathcal{K}$) is

$$G = -\partial\bar{\partial} \ln\langle \bar{\Omega}, \Omega \rangle \qquad \text{or} \qquad \mathcal{K} = -\ln\langle \bar{\Omega}, \Omega \rangle. \tag{2.1.9}$$

(2) Ω satisfies $\langle \Omega, \partial\Omega \rangle = 0$.

These two definitions of special Kähler geometry, one inspired by $\mathcal{N} = 2$ supergravity, one from Calabi-Yau geometry, are completely equivalent [22, 83]! This is a highly nontrivial statement.

$\mathcal{K}$ thus induces the following Kähler metric structures on $\mathcal{M}_V$

$$\begin{aligned} G_{i\bar{\jmath}} &= \partial_i\partial_{\bar{\jmath}}\mathcal{K}, \quad \Gamma^k_{ij} = G^{k\bar{l}}\partial_i G_{j\bar{l}}, \quad \Gamma^{\bar{k}}_{\bar{\imath}\bar{\jmath}} = G^{l\bar{k}}\bar{\partial}_{\bar{\imath}}G_{l\bar{\jmath}} \\ R_{i\bar{\jmath}k\bar{l}} &= -\partial_i\bar{\partial}_{\bar{\jmath}}G_{k\bar{l}} + G^{m\bar{n}}(\partial_i G_{k\bar{n}})(\bar{\partial}_{\bar{\jmath}}G_{m\bar{l}}), \quad R_{i\bar{\jmath}k}{}^{l} = -\bar{\partial}_{\bar{\jmath}}\Gamma^l_{ik} \\ R_{i\bar{\jmath}} &\equiv G^{k\bar{l}}R_{i\bar{\jmath}k\bar{l}} = -\partial_i\bar{\partial}_{\bar{\jmath}}\log\det(G_{i\bar{\jmath}}) \ . \end{aligned} \tag{2.1.10}$$

Ω and $\bar{\Omega}$ are sections of holomorphic and anti-holomorphic lines bundles $\mathcal{L}$ and $\overline{\mathcal{L}}$ over $\mathcal{M}$ respectively and holomorphic gauge transformations $\Omega \to e^f\Omega$ in $\mathcal{L}$ correspond to Kähler transformations, i.e. $e^{-\mathcal{K}} \in \mathcal{L}\otimes\overline{\mathcal{L}}$. The derivatives ∂_i are with respect to coordinates t_i of $\mathcal{M}_V$, and sections like $V_{j\bar{\jmath}}$ in $T\mathcal{M}^*_{(1,0)}\otimes T\mathcal{M}^*_{(0,1)}\otimes\mathcal{L}^m\otimes\overline{\mathcal{L}}^n$ have a natural connection with respect to the Weil-Petersson metric $G_{i\bar{\jmath}}$ and the line bundle $K_i = \partial_i\mathcal{K}$, $K_{\bar{\imath}} = \partial_{\bar{\imath}}\mathcal{K}$

$$D_iV_{j\bar{\jmath}} = \partial_i - \Gamma^l_{ij}V_{l\bar{\jmath}} + mK_iV_{j\bar{\jmath}}, \quad D_{\bar{\imath}}V_{j\bar{\jmath}} = \partial_{\bar{\imath}} - \Gamma^{\bar{l}}_{\bar{\imath}\bar{\jmath}}V_{j\bar{l}} + nK_{\bar{\imath}}V_{j\bar{\jmath}} \ . \tag{2.1.11}$$

The forms Ω, $\chi_i \equiv D_i\Omega$, $\overline{\chi}_{\bar{\imath}} \equiv D_{\bar{\imath}}\bar{\Omega}$ and $\bar{\Omega}$ provide a basis which spans the above cohomology groups over $\mathbb{C}$. Since it depends on the complex structure we call it the moving basis. It can be expanded in terms of the fixed symplectic basis α_I, β^J given by the dual of $\{A^a, B_a\}$ as

$$\Omega = X^I\alpha_I - \mathcal{F}_I\beta^I \ , \qquad \chi_i = \chi^I_i\alpha_I - \chi_{Ii}\beta^I \ , \qquad \text{etc} \ . \tag{2.1.12}$$

By Kodaira theory, infinitesimal deformations of the complex structure are elements of $H^1(Y, TY)$. Ω induces an isomorphism $H^1(Y, TY) \sim H^{(2,1)}(Y)$. Hence the harmonic $(2,1)$-forms χ_i, $i = 1, \ldots, h^{21}$ can be identified as (co)tangent vectors to $\mathcal{M}_V$ and these deformations are unobstructed on a CY manifold [85, 86].

It turns out to be useful to introduce the second and third derivative of the prepotential as

$$\tau_{IJ} = \partial_I\partial_J\mathcal{F} \ , \qquad C_{IJK} = \partial_I\partial_J\partial_K\mathcal{F} \ , \tag{2.1.13}$$

which are homogeneous of degree zero and minus one respectively.

Special Kähler geometry describes the relation between the metric structure and the Yukawa coupling

$$C^{(0)}_{ijk} \equiv iC_{ijk} \equiv -\int_Y \Omega\wedge\partial_i\partial_j\partial_k\Omega = -\int_Y \Omega\wedge D_iD_jD_k\Omega \ , \tag{2.1.14}$$

a section of $C_{ijk} \in \mathrm{Sym}^3(T^*_{(1,0)})\otimes\mathcal{L}^2$. Using $\langle\chi_i, \bar{\chi}_{\bar{\imath}}\rangle = G_{i\bar{\jmath}}e^{-K}$ and transversality of $\langle,\rangle$ under the the decomposition (2.1.4), i.e. $\langle\gamma_{(k,l)}, \gamma_{(m,n)}\rangle = 0$ unless $k+m = l+n = 3$ one gets the special geometry identities [81]

$$D_iX^I \equiv \chi^I_i \ , \qquad D_i\chi^I_j = iC_{ijk}G^{k\bar{k}}\bar{\chi}^I_{\bar{k}}e^K \ , \qquad D_i\bar{\chi}^I_{\bar{\jmath}} = G_{i\bar{\jmath}}\bar{X}^I \ . \tag{2.1.15}$$

From (2.1.11) and (2.1.10) follows $[D_i, D_{\bar{\jmath}}]\chi_k = -G_{i\bar{\jmath}} + R_{i\bar{\jmath}k}{}^{l}\chi_l$ and using (2.1.15) one gets

$$[D_i, D_{\bar{k}}]_j{}^{l} = R_{i\bar{k}j}{}^{l} = G_{i\bar{k}}\delta^l_j + G_{j\bar{k}}\delta^l_i - C_{ijm}\bar{C}^{ml}_{\bar{k}} \ , \tag{2.1.16}$$

where we abbreviated

$$\bar{C}^{(0)ml}_{\bar{k}} = e^{2K}\bar{C}^{(0)}_{\bar{k}\bar{\imath}\bar{\jmath}}G^{m\bar{\imath}}G^{l\bar{\jmath}} \ , \qquad \bar{C}^{ml}_{\bar{k}} = i\bar{C}^{(0)ml}_{\bar{k}} \ . \tag{2.1.17}$$

Let us also summarize some relations obeyed by τ_{IJ} and C_{IJK}. One first notes that by homogeneity and (2.1.14) and (2.1.15) one has

$$C_{IJK}X^K = 0 \ , \qquad C_{ijk} = C_{IJK}\chi^I_i\chi^J_j\chi^K_k \ . \tag{2.1.18}$$

Using the above definitions and the degree two homogeneity of $\mathcal{F}$ one also shows that

$$2e^KX^I\mathrm{Im}\tau_{IJ}\bar{X}^J = 1 \ , \qquad \bar{X}^I\mathrm{Im}\tau_{IJ}\chi^J_i = 0 \ , \qquad 2e^K\chi^I_i\mathrm{Im}\tau_{IJ}\bar{\chi}^J_{\bar{\jmath}} = G_{i\bar{\jmath}} \ . \tag{2.1.19}$$

Denoting by $\mathrm{Im}\tau^{IJ}$ the inverse of $\mathrm{Im}\tau_{IJ}$ it follows from these conditions that

$$\chi_i^I G^{i\bar{j}} \bar{\chi}_{\bar{j}}^J e^K = \tfrac{1}{2}\mathrm{Im}\tau^{IJ} + X^I \bar{X}^J e^K \ . \tag{2.1.20}$$

We summarize once again the crucial points we learn from the above analysis:

- The holomorphic 3-form Ω is only defined up to rescaling, so the X^I are homogeneous coordinates and parametrize the so-called "big moduli space". In the following, we will mainly use the small moduli space, parametrized by the local special coordinates $t^i = \frac{X^i}{X^0}$.
- One can change the symplectic basis (and with it the periods) by any symplectic transformation. However, those symplectic transformations corresponding to automorphisms of the cohomology lattice will leave the complex structure invariant, so we get a subgroup $\Gamma \in Sp(2h^{2,1}+2)$ of monodromies under which $F^{(g)}(t^I)$, being functions of the complex structure itself, have to be *invariant*, as has been nicely made explicit in [73].
- There is a holomorphic line bundle $\mathcal{L}$, and a prepotential $F^{(0)}$ section of $\mathcal{L}^2$ such that $\mathcal{F}_I = \partial_I F^{(0)}$. This prepotential completely defines the geometry of the moduli space. In particular, it determines the Kähler potential K and the Kähler metric $G_{i\bar{j}}$.
- $\mathcal{L}$ has a natural connection $\partial_i \mathcal{K}$, such that we get the covariant derivatives $D_i = \partial_i + k\partial_i\mathcal{K}$ for sections of $\mathcal{L}^k$, which include the Christoffel symbols with respect to $G_{i\bar{j}}$ when acting on tensors.

For our paper, it is furthermore essential that the amplitudes $F^{(g)}$ transform as sections of $\mathcal{L}^{2-2g}$ with connection D_i [19], as we will see below.

2.2 The holomorphic anomaly equations

In this section, we review the derivation of the holomorphic anomaly equations of [19]. As we have seen in the previous section, the special geometry of the vector multiplet moduli space can be entirely encoded in a single holomorphic section of $\mathcal{L}^2$, the prepotential $F^{(0)} = \mathcal{F}(t)$, which is nothing else than the genus zero amplitude of the topological string. From a world-sheet point of view one does not obtain $F^{(0)}$ directly, but rather finds the three-point function

$$C^{(0)}_{ijk} = \langle \mathcal{O}^{(0)}_i \mathcal{O}^{(0)}_j \mathcal{O}^{(0)}_k \rangle_g = -\int_Y \Omega(t) \wedge \partial_i\partial_j\partial_k \Omega(t) \ , \tag{2.2.21}$$

where ∂_i are derivatives with respect to t^i. What about the higher genus amplitudes? From the point of view of the four-dimensional effective action, one is interested in the dependence of the $F^{(g)}$ on the complex moduli $t^i, \bar{t}^{\bar{i}}$ in the vector multiplets. These parametrize marginal deformations, which in the B-model correspond to complex structure deformation of the Calabi-Yau manifold. Infinitesimally the world-sheet action is perturbed by the $t^i, \bar{t}^{\bar{i}}$ as follows

$$S = S_0 + t^i \int_{\Sigma_g} \mathcal{O}^{(2)}_i + \bar{t}^{\bar{i}} \int_{\Sigma_g} \bar{\mathcal{O}}^{(2)}_{\bar{i}} \ , \tag{2.2.22}$$

where the sums run over $i = 1, \ldots, h^1(Y, TY) = h^{(2,1)}(Y)$. Here the marginal two-form operators are obtained using the descent equations as

$$\mathcal{O}^{(2)}_i = \{G_0^-, [\bar{G}_0^-, \mathcal{O}^{(0)}_i]\}\mathrm{d}z\mathrm{d}\bar{z} \ , \qquad \overline{\mathcal{O}}^{(2)}_{\bar{i}} = \{G_0^+, [\bar{G}_0^+, \bar{\mathcal{O}}^{(0)}_{\bar{i}}]\}\mathrm{d}z\mathrm{d}\bar{z} \ , \tag{2.2.23}$$

where G_0^+, G_0^- are the charges corresponding to the composite operators $G_{zz}, G_{\bar{z}\bar{z}}$ that were introduced as the BRST-operators of the topological string in section 1.3. In the above equations

we denoted by $\mathcal{O}_i^{(0)}$ the zero-form cohomological operators, which are in one-to-one correspondence with the $H^1(Y,TY)$ cohomology of the target space. The operators $\mathcal{O}_i^{(2)}$ are the only ones that can be inserted into the action without spoiling axial and vector symmetry.

From (2.2.23), one can show that $\overline{\mathcal{O}}_{\bar{\imath}}^{(2)}$ is $\mathcal{Q}_B$–exact, since the operators G_{ab} are the $\mathcal{Q}$–partners of the energy-momentum tensor while at the same time we have from the supersymmetry algebra (1.2.16)

$$\{\mathcal{Q}_\pm, \overline{\mathcal{Q}}_\pm\} = P \pm H, \tag{2.2.24}$$

therefore it is straightforward to show that

$$G_\pm = \pm\frac{1}{2}\mathcal{Q}_\pm, \tag{2.2.25}$$

and we find using $\mathcal{Q}_B = \overline{\mathcal{Q}}_+ + \overline{\mathcal{Q}}_-$

$$\left(\overline{\mathcal{O}_i}^{(2)}\right)_\pm = \frac{1}{4}\left\{\overline{\mathcal{Q}}_+, \left[\overline{\mathcal{Q}}_-, \overline{\mathcal{O}_i}^{(0)}\right]\right\} = \frac{1}{8}\left\{\mathcal{Q}_B, \left[\left(\overline{\mathcal{Q}}_- - \overline{\mathcal{Q}}_+\right), \mathcal{O}_i^{(2)}\right]\right\}. \tag{2.2.26}$$

According to our general arguments in section 1.2, these operators should have vanishing correlation functions and decouple from the theory, therefore all observables should be insensitive to any variation parametrized by $\bar{t}^{\bar{\imath}}$, and therefore simply $\bar{t}$–independent, that is, holomorphic. This would indeed be true if we were still considering the topological field theory constructed in section 1.2. But we are now dealing with topological string theory, and it turns out that the integration over the moduli space of worldsheet metric that couples the sigma model to gravity spoils the holomorphicity [8, 19]. However, it does so in a very subtle way: $\mathcal{Q}_B$–exact, non-holomorphic operators only fail to decouple at the *boundaries* of moduli space, where the genus g Riemann surface is degenerate with lower-genus surfaces, as shown in Fig. 2.1.

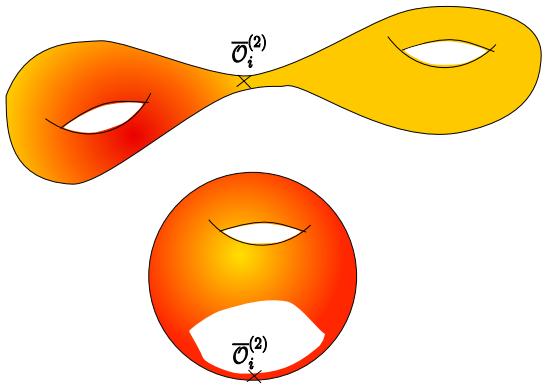

Figure 2.1: $\overline{\mathcal{O}}_i^{(2)}$, inserted in the throat of the Riemann surface at the point where it degenerates to one (or two) of lower genus do give a nonzero contribution to $\partial_{\bar{\imath}} F^{(g)}$

Note that as can be seen from Fig. 2.1, contributions to the antiholomorphic derivative of $F^{(g)}$ can only involve lower genus amplitudes. This startling phenomenon has been worked out by Bershadsky, Cecotti, Ooguri and Vafa [8, 19], whose results we briefly summarize as follows: *i.*) The $F^{(g)}$ transform as sections of $\mathcal{L}^{2-2g}$ with the connection (2.1.11).
ii.) The topological B-model correlation functions

$$C^{(g)}_{i_1\ldots i_n} = \begin{cases} \langle \int_{\Sigma_g} \mathcal{O}_{i_1}^{(2)} \cdots \int_{\Sigma_g} \mathcal{O}_{i_n}^{(2)} \rangle_g = D_{i_1} \ldots D_{i_n} F^{(g)} & \text{for } \; g \geq 1 \\ \langle \mathcal{O}_{i_1}^{(0)} \mathcal{O}_{i_2}^{(0)} \mathcal{O}_{i_3}^{(0)} \int_{\Sigma_g} \mathcal{O}_{i_4}^{(2)} \cdots \int_{\Sigma_g} \mathcal{O}_{i_n}^{(2)} \rangle_g = D_{i_4} \ldots D_{i_n} C^{(0)}_{i_1 i_2 i_3} & \text{for } \; g = 0 \end{cases} \tag{2.2.27}$$

can be obtained using the covariant derivatives (2.1.11) and obey

$$C^{(g)}_{i_1\dots i_n} = 0 \quad \text{for} \;\; 2g-2+n \leq 0 \; . \tag{2.2.28}$$

iii.) The anti-holomorphic derivative $\partial_{\bar\imath} = \frac{\partial}{\partial \bar t^{\bar\imath}}$ of the $F^{(g)}$,

$$\bar\partial_{\bar\imath} F^{(g)} = \int_{\overline{\mathcal{M}}_g} \bar\partial_{\bar\imath}\mu_g = \int_{\overline{\mathcal{M}}_g} \partial_m \bar\partial_{\bar m} \lambda_{\bar\imath,g} = \int_{\partial\overline{\mathcal{M}}_g} \lambda_{\bar\imath,g}, \tag{2.2.29}$$

receives only contributions from the complex codimension one locus in the moduli space of Riemann surfaces corresponding to world-sheets which are degenerate with lower genus components. These boundary contributions can be worked out and yield recursive equations for the $F^{(g)}$. For $g>1$ one gets

$$\bar\partial_{\bar\imath} F^{(g)} = \tfrac{1}{2}\bar C^{(0)jk}_{\bar\imath}\Big(D_j D_k F^{(g-1)} + \sum_{r=1}^{g-1} D_j F^{(r)} D_k F^{(g-r)}\Big) \tag{2.2.30}$$

and for $g=1$ a generalisation of the Quillen anomaly

$$\partial_i \bar\partial_{\bar\jmath} F^{(1)} = \tfrac{1}{2} C^{(0)}_{ikl}\bar C^{(0)kl}_{\bar\jmath} - \Big(\frac{\chi}{24}-1\Big) G_{i\bar\jmath} \; . \tag{2.2.31}$$

Here we defined

$$\bar C^{(0)kl}_{\bar\jmath} = e^{2K} G^{k\bar k} G^{l\bar l} \bar C^{(0)}_{\bar\jmath\bar k\bar l} \; , \tag{2.2.32}$$

where $G_{k\bar k} = \partial_k \bar\partial_{\bar k} K$ is the Weil-Petersson metric corresponding to the Kähler potential (2.1.9).

These are the recursive holomorphic anomaly equations, which we want to integrate directly in this paper. Note that there is no holomorphic anomaly at genus zero. $C^{(0)}_{ijk}$ has no world-sheet moduli dependence, hence no boundaries, and is therefore holomorphic. The genus zero data thus have to be provided from the outset. They can be determined from the period integrals of the manifold Y.

It is further shown in [19] that (2.2.30) can be integrated recursively. With an iterative procedure of complexity growing exponentially with the genus, one rewrites (2.2.30) as

$$\partial_{\bar k} F^{(g)}(t,\bar t) = \bar\partial_{\bar k}\Gamma^{(g)}(\hat\Delta^{ij}, \hat\Delta^i, \hat\Delta, C^{(r<g)}_{i_1\dots i_n}) \; , \tag{2.2.33}$$

and integrates it to

$$F^{(g)}(t,\bar t) = \Gamma^{(g)}(\hat\Delta^{ij}, \hat\Delta^i, \hat\Delta, C^{(r<g)}_{i_1\dots i_n}) + f^{(g)}(t) \; . \tag{2.2.34}$$

Here $\Gamma^{(g)}$ is a functional of some propagators $\hat\Delta^{ij}, \hat\Delta^i, \hat\Delta$ and the lower genus vertices $C^{(r)}_{i_1\dots i_n}$ with $r<g$. The holomorphic ambiguity $f^{(g)}(t)$ arises as an integration constant. To prove that the functional $\Gamma^{(g)}$ exists at every genus, [19] show that it is the disconnected Feynman graph expansion of an auxiliary action with the above vertices and propagators, whose partition function fulfills a master equation equivalent to (2.2.30) and (2.2.31). The propagators can be defined using the genus zero data as follows. Since

$$\bar D_{\bar\imath}\bar C^{(0)}_{\bar\jmath\bar k\bar l} = \bar D_{\bar\jmath}\bar C^{(0)}_{\bar\imath\bar k\bar l} \tag{2.2.35}$$

one can integrate

$$\bar C^{(0)}_{\bar\jmath\bar k\bar l} = -\tfrac{1}{2} e^{-2K}\bar D_{\bar\imath}\bar D_{\bar\jmath}\bar\partial_{\bar k}\hat\Delta \tag{2.2.36}$$

as

$$G_{\bar\imath j}\hat\Delta^j = \tfrac{1}{2}\bar\partial_{\bar\imath}\hat\Delta \; , \qquad G_{\bar\imath k}\hat\Delta^{kj} = \bar\partial_{\bar\imath}\hat\Delta^j \; , \qquad \bar C^{(0)jk}_{\bar\imath} = \bar\partial_{\bar\imath}\hat\Delta^{jk} \; . \tag{2.2.37}$$

Note that the propagators are defined by these equations only up to holomorphic ambiguities arising in the integration steps. Fixing these ambiguities directly affects the definition of the

holomorphic functions $f^{(g)}(t)$ in (2.2.34). It turns out that a preferred choice for this ambiguity is provided by relating the propagators in a canonical way to $F^{(1)}(t,\bar{t})$ [73].

The combinatorics of the Feynman graph expansion are useful to establish some general properties of the $F^{(g)}$, but its complexity grows exponentially with the genus. However, the $F^{(g)}$ are invariant under space-time modular transformations which are a symmetry of the full string compactification. As we will discuss later, they generically admit a split into a universal factor times a modular form. Here the weights of the modular forms grow linearly with the genus. Since the ring of modular forms is finitely generated, the complexity of modular invariant expressions grows only polynomially with the genus. The method of direct integration that we develop in this chapter uses this connection with modular forms such that its complexity also grows only polynomially with the genus. It has the advantage that the modular properties of the amplitudes are manifest in all steps of the derivation.

2.3 Solving Seiberg-Witten theory by direct integration

Local Calabi-Yau geometries provide simple and instructive examples for the interplay between holomorphicity and modular invariance in topological string theory. In this section we will explain the key features using the simplest example, namely the local Calabi-Yau corresponding to $SU(2)$ Seiberg-Witten theory with no matter [87]. In section 2.3.1 we first recall the geometry of Seiberg-Witten theory. We show that all genus zero data can be expressed in terms of a finite set of holomorphic modular forms. All higher amplitudes $F^{(g)}$ are invariant under the modular group. In section 2.3.2 we directly integrate the holomorphic anomaly equations, determining all $F^{(g)}$ up to a holomorphic modular ambiguity. Modularity restricts this ambiguity so much that simple boundary conditions set by the effective action near special points in the moduli space allow one to reconstruct all $F^{(g)}$. We review such a convenient set of boundary conditions in section 2.3.3. The general philosophy presented in this section will be later applied to the more complicated case of compact Calabi-Yau manifolds.

2.3.1 The Seiberg-Witten geometry

Seiberg-Witten theory with no matter [87] can be obtained in the A–model as a limit of the local Calabi-Yau geometry[1] $\mathcal{O}(-2,-2) \to \mathbb{P}^1 \times \mathbb{P}^1$ [88]. The mirror B–model geometry of this limit is the Seiberg-Witten elliptic curve $\mathcal{E}$

$$y^2 = (x-u)(x-\Lambda^2)(x+\Lambda^2) \ , \tag{2.3.38}$$

whose modular group is $\Gamma(2)$. This subgroup of $Sl(2,\mathbb{Z})$ acts on the period integrals

$$t = \int_a \lambda \ , \qquad\qquad t_D = \int_b \lambda \ , \tag{2.3.39}$$

where $\lambda = \frac{\sqrt{2}}{2\pi}\frac{y}{x^2-1}\mathrm{d}x$ is the Seiberg-Witten meromorphic differential. In the limit described above, λ is obtained as a reduction of the holomorphic $(3,0)$ form of the Calabi-Yau manifold. Rigid special geometry guarantees the existence of a prepotential $F^{(0)} = \mathcal{F}(t)$ with the properties

$$t_D = \frac{\partial \mathcal{F}}{\partial t} \ , \qquad\qquad \tau = -\frac{1}{4\pi}\frac{\partial^2 \mathcal{F}}{\partial^2 t} \ . \tag{2.3.40}$$

These conditions are obtained as the rigid limit of the special geometry relations presented in section 2.1. Note that τ is precisely the complex structure parameter of the torus and hence parametrizes the upper half-plane. In particular, $\mathrm{Im}\tau > 0$ is guaranteed by the Riemann

[1] for a short review of local Calabi-Yau geometry, see appendix C.3

inequality consistent with the fact that Imτ is the gauge kinetic coupling function of Seiberg-Witten theory. Moreover, a modular transformation acts on τ as

$$\tau \;\mapsto\; \frac{a\tau+b}{c\tau+d}\ . \tag{2.3.41}$$

The genus zero data are functions of τ and transform in a particularly simple way under (2.3.41). They can be expressed in terms of a finite set of modular generators, which we will specify in the following.

A modular function $f(\tau)$ of weight m is defined to transform as $f(\tau) \mapsto (c\tau+d)^m f(\tau)$ under (2.3.41). Focusing on the modular group of the Seiberg-Witten curve, we note that the ring of modular functions of $\Gamma(2)$ can be expressed as powers of the Jacobi θ-functions. Relevant properties of the Jacobian θ-functions are summarized in Appendix C.1. We introduce two generators

$$K_2 = \vartheta_3^4 + \vartheta_4^4, \qquad\qquad K_4 = \vartheta_2^8\ , \tag{2.3.42}$$

which are of modular weight two and four respectively. The modular transformation properties follow from (C.1.3). K_2, K_4 generate the graded ring of holomorphic modular forms $\mathcal{M}_*(\Gamma(2))$ of $\Gamma(2)$, which we will also denote by $\mathbb{C}[K_2, K_4]$. It turns out to be useful to also introduce

$$h = K_2\ , \qquad\qquad E_4 = \tfrac{1}{4}(K_2^2 + 3K_4)\ . \tag{2.3.43}$$

As we will see when we develop the method of direct integration, it is natural to take h, E_4 as the generators of the ring $\mathcal{M}_*(\Gamma(2))$.

Let us now express the genus zero data in terms of modular forms. The connection with the geometry of the Seiberg-Witten curve is given by the following relation

$$u(\tau) = \frac{K_2}{\sqrt{K_4}}\ . \tag{2.3.44}$$

The combination $z(\tau) = 1/u^2(\tau)$ is modular invariant and can be viewed as the analog of the mirror map for this non-compact Calabi-Yau manifold. The analog of the holomorphic triple coupling is

$$C \equiv C^{(0)}_{ttt} = \frac{\partial\tau}{\partial t} = \frac{32K_4^{1/4}}{K_2^2 - K_4} \tag{2.3.45}$$

Note that C^2 is a form of weight -6 under the modular transformations in $\Gamma(2)$. The modular group $\Gamma(2)$ also determines the periods t, t_D as weight 1 objects[2]

$$t(\tau) = \frac{E_2(\tau)+K_2(\tau)}{3K_4^{1/4}(\tau)}, \qquad t_D(\tau_D) = -i\frac{2E_2(\tau_D) - K_2(\tau_D) - 3K_4^{1/2}(\tau_D)}{3\big(2K_2(\tau_D) - 2K_4^{1/2}(\tau_D)\big)^{1/2}}\ , \tag{2.3.46}$$

where $\tau_D = -\frac{1}{\tau}$ and E_2 is the second Eisenstein series defined in (C.1.15). It is natural to give the periods in the above parameters. In the electric phase of Seiberg-Witten theory the $q = e^{2\pi i\tau}$ series converges and t is the physical expansion parameter, while in the magnetic phase the $q_D = e^{2\pi i\tau_D}$ series converges and t_D is the physical expansion parameter. Of course $t_D(\tau)$ and $t(\tau_D)$ can be obtained by performing an S-duality transformation on E_2 and the Jacobi theta functions.

2.3.2 Direct integration

Having discussed the genus zero geometry, let us now turn to the higher genus free energies $F^{(g)}$ and their holomorphic anomaly. Starting with $F^{(1)}$, we note that the holomorphic anomaly equation (2.2.31) specializes to

$$\partial_t\partial_{\bar t}F^{(1)} = \tfrac{1}{2}C^{(0)\,tt}_{\bar t}C^{(0)}_{ttt}\ . \tag{2.3.47}$$

[2]They can be calculated likewise using the Picard-Fuchs equation.

where the indices are raised with the Weil-Petersson metric $G_{t\bar{t}} = 2\mathrm{Im}\tau$. This equation integrates immediately to

$$F^{(1)} = -\tfrac{1}{2}\log\,\mathrm{Im}\tau - \log|\Phi(\tau)|\ , \tag{2.3.48}$$

where $\partial\tau/\partial t$ is evaluated using (2.3.45). The holomorphic object $\Phi(\tau)$ is the ambiguity at genus one. It is determined from modular constraints and the physical requirement that $F^{(1)}$ should only be singular at the discriminant of $\mathcal{E}$. Note that under a modular transformation (2.3.41) one finds that $\mathrm{Im}\tau \ \mapsto\ |c\tau+d|^{-2}\mathrm{Im}\tau$. Together with the invariance of $F^{(1)}$ this implies that $\Phi(\tau)$ must be a modular form of weight 1. The only modular form of weight 1 which has only poles at the discriminant of $\mathcal{E}$ is the square of the η function given in (C.1.4). This fixes the ambiguity at genus one as $\Phi(\tau) = \eta^2(\tau)$.

At genus one the non-holomorphic dependence was induced through the appearance of $\mathrm{Im}\tau$. As dictated by the holomorphic anomaly equations, all higher $F^{(g)}$ also depend on $\bar{t}$. We now show that this dependence arises through the propagator $\hat{\Delta}^{tt}$ only. $\hat{\Delta}^{tt}$ is obtained in the local limit of (2.2.37) and thus obeys

$$\partial_{\bar{t}}\hat{\Delta}^{tt} = C_{\bar{t}}^{(0)\,tt}\ . \tag{2.3.49}$$

All other propagators vanish in this limit. To integrate this condition, we first multiply both sides in (2.3.49) by $C^{(0)}_{ttt}$. The result is easily compared to the holomorphic anomaly equation (2.3.47) of $F^{(1)}$. Changing derivatives by inserting $\partial\tau/\partial t = C^{(0)}_{ttt}$ one evaluates with the help of (C.1.5)

$$\hat{\Delta}^{tt} = 2\partial_\tau F^{(1)}(\tau,\bar{\tau}) = -\tfrac{1}{12}\widehat{E}_2(\tau,\bar{\tau})\ , \qquad\qquad \partial_\tau = (2\pi i)^{-1}\tfrac{\partial}{\partial\tau} \tag{2.3.50}$$

The occurrence of the non-holomorphic extension of the second Eisenstein series $E_2(\tau)$

$$\widehat{E}_2(\tau,\bar{\tau}) = E_2(\tau) - \frac{3}{\pi\mathrm{Im}\tau}\ . \tag{2.3.51}$$

is forced by modular invariance. Since $F^{(1)}(\tau,\bar{\tau})$ is a modular function of weight zero, its derivative must be a modular form of weight 2 which is not holomorphic. The only form with these properties is the almost holomorphic form $\widehat{E}_2(\tau,\bar{\tau})$. This form is the canonical, almost holomorphic extension of the second Eisenstein series E_2, where E_2 is the unique holomorphic quasimodular form of weight 2 transforming as

$$E_2(\tau) \quad\mapsto\quad (c\tau+d)^2E_2(\tau) - \tfrac{6}{\pi}ic(c\tau+d) \tag{2.3.52}$$

under a modular transformation (2.3.41). The shift in the transformation of the anholomorphic piece in (2.3.51) cancels precisely the shift in (2.3.52). More generally the ring $\hat{\mathcal{M}}_*$ of almost holomorphic forms of $\Gamma(2)$ is generated as $\mathbb{C}[\widehat{E}_2, h, \Delta]$.

Using the propagator and general properties of the Feynman graph expansion one can extract the fact that the higher genus $F^{(g)}$ are weight 0 forms with the structure

$$F^{(g)}(\tau,\bar{\tau}) = C^{2g-2}\sum_{k=0}^{3g-3}\widehat{E}_2^k(\tau,\bar{\tau})c_k^{(g)}(\tau)\ , \qquad g>1\ , \tag{2.3.53}$$

where we defined $C = C^{(0)}_{ttt}$. Modular invariance implies then that the holomorphic forms $c_k^{(g)}(\tau)$ are modular of weight $6(g-1)-2k$ in $\mathbb{C}[h,\Delta]$. We will show next that all forms $c_k^{(g)}(\tau)$ with $k>0$ are very easily determined by direct integration of the holomorphic anomaly equation. The form $c_0^{(g)}(\tau)$ is not determined in this way and corresponds to a holomorphic modular ambiguity.

In order to analyze the holomorphic anomaly equations in the local case, it turns out to be very useful to discuss some general properties related to modular transformations. Let us first discuss how derivatives transform under the modular transformation (2.3.41). Denoting by f_k a

modular form of weight k it is elementary to check that its derivative transforms under (2.3.41) as

$$\partial_\tau f_k \quad \mapsto \quad (c\tau+d)^{k+2}\partial_\tau f_k + \frac{k}{2\pi i}c(c\tau+d)^{k+1}f_k \ . \tag{2.3.54}$$

Similarly, we can evaluate $\partial_t f_k = C^{-1}\partial_\tau f_k$, where as above $C = C^{(0)}_{ttt}$. In order to cancel the shift in (2.3.54) we will now introduce covariant derivatives. There are two possible ways to achieve this[3]. Firstly, one can cancel the shift against the shift of $(\mathrm{Im}\tau)^{-1}$ and set

$$D_t f_k = \Big(\partial_t - \frac{kC}{4\pi \mathrm{Im}\tau}\Big)f_k \ , \qquad D_\tau f_k = \Big(\partial_\tau - \frac{k}{4\pi \mathrm{Im}\tau}\Big)f_k \ . \tag{2.3.55}$$

Here D_t is the covariant derivative to the Weil-Petersson metric $G_{t\bar{t}}$ and D_τ is the so-called Mass derivative. D_t maps almost holomorphic forms of $\Gamma(2)$ of weight k into almost holomorphic forms of weight $k-1$, while D_τ increases the weight from k to $k+2$. Note that both derivatives in (2.3.55) are non-holomorphic due to the appearance of $\mathrm{Im}\tau$. There is however a second possibility to cancel the shift (2.3.54) which is manifestly holomorphic. More precisely, one can cancel the shift against the shift (2.3.52) of $E_2(\tau)$ and define

$$\hat{D}_t f_k = \big(\partial_t - \tfrac{1}{12}kCE_2\big)f_k \ , \qquad \hat{D}_\tau f_k = \big(\partial_\tau - \tfrac{1}{12}kE_2\big)f_k \ . \tag{2.3.56}$$

In this case $\hat{D}_\tau$ is known as the Serre derivative. Both $\hat{D}_t$ and $\hat{D}_\tau$ are holomorphic. They map holomorphic modular forms of weight k to holomorphic modular forms of weight $k-1$ and $k+2$ respectively. It is easy to check that the following identity holds

$$D_t f_k = \hat{D}_t f_k + \tfrac{1}{12}kC\widehat{E}_2\, f_k \ , \qquad D_\tau f_k = \hat{D}_\tau f_k + \tfrac{1}{12}k\widehat{E}_2\, f_k \ . \tag{2.3.57}$$

These equations also imply that whenever f_k is holomorphic all the non-holomorphic dependence of $D_t f_k$ and $D_\tau f_k$ lies in a term involving the propagator. In other words, once again all anti-holomorphic dependence arises through the propagator $\widehat{E}_2$ only. The generalizations of the modular derivatives (2.3.55) and (2.3.56) will reappear in later sections of this work. For the Enriques Calabi-Yau they are given in (2.1.11),(2.4.81) and (2.5.177).

Here we will us the covariant derivatives (2.3.55) and (2.3.56) to rewrite the holomorphic anomaly equations (2.2.30). Firstly, we will apply modularity and the fact that all non-holomorphic dependence arises through the propagator $\widehat{E}_2(\tau,\tau)$ to convert anti-holomorphic derivatives into derivatives with respect to $\widehat{E}_2$. Using (2.3.57) we will be able to carefully keep track of the $\widehat{E}_2$ dependence in the holomorphic anomaly equations. Eventually, a solution will be simply obtained by direct integration of a polynomial in $\widehat{E}_2$.

To begin with, note that the holomorphic anomaly equations specialize in the local limit to

$$\partial_{\bar{t}}F^{(g)} = \tfrac{1}{2}C^{(0)tt}_{\bar{t}}\Big(D_t\partial_t F^{(g-1)} + \sum_{r=1}^{g-1}\partial_t F^{(r)}\partial_t F^{(g-r)}\Big) \ . \tag{2.3.58}$$

Using the fact that all non-holomorphic dependence arises only through the propagator $\widehat{E}_2(\tau,\bar{\tau})$, this equation can be rewritten as

$$\frac{\partial F^{(g)}}{\partial \widehat{E}_2} = \tfrac{1}{48}\Big(D_t\partial_t F^{(g-1)} + \sum_{r=1}^{g-1}\partial_t F^{(r)}\partial_t F^{(g-r)}\Big) \ . \tag{2.3.59}$$

Here we used (2.3.49) to substitute $C^{(0)tt}_{\bar{t}}$ with the derivative $\partial_{\bar{t}}\widehat{E}_2$, which then cancels with the same factor arising on the left-hand side of this equation. Let us now manipulate the right-hand

[3]We thank Don Zagier for explaining us several manipulations involved in the following.

side of (2.3.62) and split off the derivative of $F^{(1)}$ in the second term

$$\frac{\partial F^{(g)}}{\partial \widehat{E}_2} = \begin{cases} \frac{1}{48}\Big(D_t\partial_t F^{(1)} + (\partial_t F^{(1)})^2\Big) & g=2\ , \\ \frac{1}{48}\Big((D_t + 2\partial_t F^{(1)})\partial_t F^{(g-1)} + \sum_{r=2}^{g-2}\partial_t F^{(r)}\partial_t F^{(g-r)}\Big) & g>2\ , \end{cases} \tag{2.3.60}$$

where the sum now runs from $r=2$ to $r=g-2$. One then notes that $\partial_t F^{(1)}$ can be replaced by $-\frac{1}{24}C\widehat{E}_2$ by using (2.3.50). Furthermore, we replace the non-holomorphic derivative D_t with its holomorphic counterpart $\hat{D}_t$ via (2.3.57). Altogether, one evaluates

$$\frac{\partial F^{(2)}}{\partial \widehat{E}_2} = -\tfrac{1}{48\cdot 24}\Big(\hat{D}_t(C\widehat{E}_2) - \tfrac{1}{8}(C\widehat{E}_2)^2\Big) \tag{2.3.61}$$

for genus two and for $g>2$

$$\frac{\partial F^{(g)}}{\partial \widehat{E}_2} = \tfrac{1}{48}\Big((\hat{D}_t - \tfrac{1}{6}C\widehat{E}_2)\partial_t F^{(g-1)} + \sum_{r=2}^{g-2}\partial_t F^{(r)}\partial_t F^{(g-r)}\Big)\ . \tag{2.3.62}$$

We are now in the position to make the dependence on $\widehat{E}_2$ explicit. This can be done by rewriting the right-hand side of (2.3.62) using (2.3.56). We also define $\hat{d}_t$ and $\hat{d}_\tau$ as covariant derivatives $D_t, \hat{D}_\tau$ not acting on the propagators $\widehat{E}_2$, such that e.g. $\hat{d}_\tau(\hat{E}_2^k\, c_k^{(r)}) = \hat{E}_2^k\,\hat{D}_\tau c_k^{(r)}$. Applying the chain rule we find

$$\partial_t F^{(r)} = \big[\hat{d}_t + (\hat{D}_t\widehat{E}_2)\partial_{\widehat{E}_2}\big]F^{(r)} = C\big[\hat{d}_\tau - \tfrac{1}{12}(E_4 + \widehat{E}_2^2)\partial_{\widehat{E}_2}\big]F^{(r)}\ , \tag{2.3.63}$$

where (2.3.51), (2.3.56) and (C.1.20) are applied to evaluate the derivative of E_2. The Eisenstein series E_4 arises naturally in rewriting the derivatives. We will therefore work with the ring $\mathbb{C}[\widehat{E}_2, h, E_4]$ introduced in (2.3.43).

Similarly, we rewrite the second derivative

$$\begin{aligned} \hat{D}_t\partial_t F^{(g-1)} \;=\; & \tfrac{1}{12^2}C^2\Big(12^2\hat{d}_\tau^2 + 6^2 h\hat{d}_\tau + 2E_4(\widehat{E}_2\partial_{\widehat{E}_2} + \widehat{E}_2^2\partial_{\widehat{E}_2}^2) \\ & -(3h+12\hat{d}_\tau)\widehat{E}_2^2\partial_{\widehat{E}_2} + 2\widehat{E}_2^3\partial_{\widehat{E}_2} + \widehat{E}_2^4\partial_{\widehat{E}_2}^2 \\ & +(-9E_4h + 2h^3 - 12E_4\hat{d}_\tau)\partial_{\widehat{E}_2} + E_4^2\partial_{\widehat{E}_2}^2\Big)F^{(g-1)}\ , \end{aligned} \tag{2.3.64}$$

where we have used that the derivative of C is given by $\hat{D}_\tau C = \frac{1}{4}h\,C$. This is how the holomorphic modular form h defined in (2.3.43) arises in the direct integration.

We can now actually perform the direct integration. This is done by inserting the expressions (2.3.63) and (2.3.64) for $\partial_t F^{(r)}$ and $\hat{D}_t\partial_t F^{(g-1)}$ into the holomorphic anomaly equation (2.3.62). Replacing all $F^{(r)}$ for $1<r<g$ with their propagator expansion (2.3.53), it is then straightforward to keep track of the number of propagators $\widehat{E}_2$ in each term of the right-hand side of (2.3.62). Finally, $F^{(g)}$ is determined up to a $\widehat{E}_2-$independent ambiguity by integrating the resulting polynomial in $\widehat{E}_2$. Without much effort this procedure can be repeated iteratively up to the desired genus.

Note that the equation (2.3.61) for $F^{(2)}$ is particularly simple to integrate. Using (2.3.56) and (C.1.20) one evaluates

$$\hat{D}_t(C\widehat{E}_2) - \tfrac{1}{8}(C\widehat{E}_2)^2 = \tfrac{1}{24}C^2\big(-5\widehat{E}_2^2 + 6\widehat{E}_2 h - 2E_4\big)\ . \tag{2.3.65}$$

Inserted into (2.3.62) it is straightforward to integrate this quadratic polynomial in $\widehat{E}_2$ to derive $F^{(2)}$ as

$$F^{(2)}(\tau,\bar{\tau}) = \tfrac{1}{2\cdot 24^3}C^2\Big(\tfrac{5}{3}\,\widehat{E}_2^3 - 3\,h\widehat{E}_2^2 + 2\,E_4\widehat{E}_2\Big) + C^2 c_0^{(2)}, \tag{2.3.66}$$

where $c_0^{(2)}(h, E_4)$ is the holomorphic ambiguity which can be fixed by additional boundary conditions as we discuss in the next section. For genus up to 7 the expressions for $F^{(g)}$ were calculated in [89] using the Feynman graph expansion. The direct integration using (2.3.62) provides a far more effective method to solve Seiberg-Witten theory and confirms the results of [89]. Furthermore, the modular properties of the expressions are manifest at each step. As we will discuss in the later sections, similar constructions will provide us with a powerful tool to determine the set of candidate modular generators for more complicated Calabi-Yau manifolds. In particular, holomorphic modular forms are needed to parametrize the holomorphic ambiguity. In case we know the ring of holomorphic modular forms, fixing the ambiguity reduces to a determination of a finite set of numerical factors at each genus. For Seiberg-Witten theory this can be done systematically, as we will discuss in the next section.

2.3.3 Boundary conditions

To systematically fix the $c_0^{(g)}$ we have to understand the boundary behavior of the $F^{(g)}$. As it is well known, there are three distinguished regions in the moduli space of pure $SU(2)$ $\mathcal{N} = 2$ SYM which correspond to the geometrical singularities of $\mathcal{E}$. We will parametrize the moduli space by the vacuum expectation value $u = \langle \mathrm{Tr}\Phi^2 \rangle$ of the scalar Φ in the $\mathcal{N} = 2$ vector multiplet. The first region occurs at $u \sim \frac{1}{2}t^2 \to \infty$, and it corresponds physically to the semiclassical regime. The monopole region occurs near $u \to \Lambda^2$, where a magnetic monopole of charge $(e, m) = (0, 1)$ becomes massless and the electric $SU(2)$ theory with gauge coupling $\mathrm{Im}\tau$ is strongly coupled. At the point $u \to -\Lambda^2$ a dyon of charge $(e, m) = (-1, 1)$ becomes massless. However, this point is identified with the monopole point by a $\mathbb{Z}_2$ exact quantum symmetry. For this reason there are no independent boundary conditions at $u \to -\Lambda^2$ and we focus on $u \to \Lambda^2$ and $u \sim \infty$. In both cases the elliptic curve acquires a node, i.e. a local singularity of the form $\xi^2 + \eta^2 = (u \pm \Lambda^2)$, where a cycle of $\mathbb{S}^1$ topology shrinks. In string theory, a point in the moduli space where a node in the target geometry develops is called a conifold point.

The natural physical parameter in the magnetic monopole region $u \to \Lambda^2$ is t_D. We get first a convergent expansion for the $F^{(g)}$ in the variable $q_D = \exp(2\pi i \tau_D)$ for $\tau_D = -\frac{1}{\tau} \to i\infty$, which corresponds to $t_D \to 0$. This is obtained by an S- transformation of the modular expressions for the $F^{(g)}(\tau, \bar{\tau})$ such as (2.3.66), which converge in the semiclassical region. The holomorphic magnetic expansions $\mathcal{F}_D^{(g)}(\tau_D)$ can be obtained by formally taking the limit $\bar{\tau}_D \to \infty$, while keeping τ_D fixed. Finally we obtain the expansion in t_D by inverting (2.3.46). In these magnetic expansions, a gap structure was observed near the monopole (or conifold) point [89]. One finds that the leading behavior of $\mathcal{F}_D^{(g)}(\tau_D)$ is of the form

$$\mathcal{F}_D^{(g)} = \frac{B_{2g}}{2g(2g-2)\tilde{t}_D^{2g-2}} + k_1^{(g)}\tilde{t}_D + \mathcal{O}(\tilde{t}_D^2) \ , \tag{2.3.67}$$

where the B_n are the Bernoulli numbers and we used a rescaled variable $\tilde{t}_D = i\frac{t_D}{2}$. The knowledge of the leading coefficients and the absence of the remaining $2g-3$ sub-leading negative powers in the $\tilde{t}_D$ expansion imposes $2g-2$ conditions. Since $\dim M_{6g-3}(\Gamma(2)) = \left[\frac{3g-1}{2}\right]$ this overdetermines the $c_0^{(g)}$, e.g. for $g = 2$ we find $c_0^{(2)} = -\frac{1}{2\cdot 24^3}\left(\frac{1}{2}E_4\, h + \frac{1}{30}h^3\right)$. It is very easy to integrate (2.3.62) using (2.3.63), (2.3.64) and the gap condition, which fixes the ambiguity to arbitrary genus. This solves the theory completely. One finds moreover a pattern in the first subleading term in the magnetic expansion

$$k_1^{(g)} = \frac{((2g-3)!!)^3}{g!2^{7g-2}} \ . \tag{2.3.68}$$

The gap can be explained by using the embedding of Seiberg-Witten theory into type IIA string theory compactified on a suitable Calabi–Yau manifold. The most generic singularity of

a d complex dimensional manifold is a node where an $\mathbb{S}^d$ shrinks. The codimension one locus in the moduli space where this happens is called the conifold. It was argued in [22, 90] that at the conifold a RR-hypermultiplet becomes massless. This hypermultiplet is charged and couples to the $U(1)$ vector multiplets. Its one loop effect on the kinetic terms of the vector multiplets in the effective action is captured by the local expansion of $F^{(0)}$ [22]. A gravitational one-loop effect yields the moduli dependence of the R_+^2 term in the effective action and is given by local expansion $F^{(1)}$ [90]. Using further one-loop arguments it was shown that the $F^{(g)}$, which capture the moduli dependence of the coupling of the self-dual part of the curvature to the self-dual part of the graviphoton $R_+^2\, F_+^{2g-2}$, have the following gap structure

$$F^{(g)}_{\text{conifold}} = \frac{(-1)^{g-1} B_{2g}}{2g(2g-2) t_D^{2g-2}} + \mathcal{O}(t_D^0), \tag{2.3.69}$$

where t_D is a suitable coordinate transverse to the conifold divisor [69]. The Seiberg-Witten gauge theory embedded in type IIA string theory inherits this structure, and the massless hypermultiplet at the conifold is identified as a monopole becoming massless at the monopole point. In this way, (2.3.69) explains the field theory result (2.3.67) and extends it to the full supergravity action.

Once the Seiberg-Witten amplitudes $F^{(g)}$ have been determined in terms of modular functions, these can be expanded around every point in the moduli space. For example, in the semiclassical regime $\tau \to i\infty$, $u \to \infty$ one finds the holomorphic amplitudes

$$\mathcal{F}^{(g)} = \frac{(-1)^g B_{2g}}{g(2g-2)(2t)^{2g-2}} + \frac{l^{(g)}_{2g+6}}{t^{2g+6}} + \mathcal{O}(t^{2g+10}) \ . \tag{2.3.70}$$

The higher order terms in this expansion correspond to gauge theory instantons and have been computed in [80].

2.4 A first look at the Enriques Calabi-Yau

In this section we review some basic properties of topological string theory on the Enriques Calabi-Yau. We begin by reviewing the $N = 2$ special geometry of the classical moduli space of Kähler and complex structure deformations. The first world-sheet instanton corrections arise from genus one Riemann surfaces as shown in refs. [39, 91, 79]. The holomorphic higher genus free energies, restricted to the K3 fiber, can also be derived by using heterotic-type II duality [79]. We briefly summarize these results. We then derive an all-genus product formula for the fiber amplitudes. In understanding and deriving the expression for the full $F^{(g)}$ an important hint is given by their transformation properties under the symmetry group of the full topological string theory on the Enriques Calabi-Yau. More precisely, generalizing the results of the previous section, one expects that all $F^{(g)}$ are built out of functions transforming in a particularly simple way under the group $Sl(2,\mathbb{Z}) \times O(10,2,\mathbb{Z})$. In paragraph 2.4.4, we will review some essentials about these modular and automorphic functions and forms.

2.4.1 Special geometry of the classical moduli space

The Enriques Calabi-Yau can be viewed as the first non-trivial generalization of the product space $\mathbb{T}^2 \times \text{K3}$. It is defined as the orbifold $(\mathbb{T}^2 \times \text{K3})/\mathbb{Z}_2$, where $\mathbb{Z}_2$ acts as a free involution [39]. This involution inverts the coordinates of the torus and acts as the Enriques involution on the K3 surface. The cohomology lattice of $\mathbb{T}^2 \times \text{K3}$ takes the form [38]

$$\Gamma^{6,22} = \Gamma^{2,2} \oplus [\Gamma^{1,1} \oplus E_8(-1)]_1 \oplus [\Gamma^{1,1} \oplus E_8(-1)]_2 \oplus \Gamma^{1,1}_g \oplus \Gamma^{1,1}_s \ , \tag{2.4.71}$$

where the inner products on the sublattices $E_8(-1)$ and $\Gamma^{1,1}$ are given by

$$(C^{\alpha\beta}) = -C_{E_8} \ , \qquad (C^{ij}) = \begin{pmatrix} 0 & 1 \\ 1 & 0 \end{pmatrix} \ . \tag{2.4.72}$$

with $\alpha, \beta = 1, \ldots, 8$ and $i, j = 1, 2$. Here C_{E_8} is the Cartan matrix of the exceptional group E_8. The lattice (2.4.71) splits into $H^1(\mathbb{T}^2) \oplus H_1(\mathbb{T}^2) = \Gamma^{2,2}$ and $H^*(K3) = \Gamma^{4,20}$. Under heterotic-type II duality it can be identified with the Narain lattice of the heterotic compactification on $\mathbb{T}^6$. The $\mathbb{Z}_2$ involution on the Enriques Calabi-Yau acts on the five terms of the lattice (2.4.71) as [39][4]

$$|p_1, p_2, p_3, p_4, p_5\rangle \to e^{\pi i \delta \cdot p_5} | - p_1, p_3, p_2, -p_4, p_5\rangle \ , \tag{2.4.73}$$

where p_i is an element of the i-th term in (2.4.71) and we denoted $\delta = (1, -1) \in \Gamma^{1,1}_s$.

The Enriques Calabi-Yau has holonomy group $SU(2) \times \mathbb{Z}_2$. This implies that type II string theory compactified on the Enriques Calabi-Yau will lead to a four-dimensional theory with $\mathcal{N} = 2$ supersymmetry. Nevertheless, due to the fact that it does not have the full $SU(3)$ holonomy of generic Calabi-Yau threefolds, various special properties related to $\mathcal{N} = 4$ compactification on $\mathbb{T}^2 \times K3$ are inherited.

As an example of the close relation of the Enriques Calabi-Yau to its $\mathcal{N} = 4$ counterpart $\mathbb{T}^2 \times K3$ one notes that the moduli space of Kähler and complex structure deformations are simply cosets. The complex dimensions of these moduli spaces are given by the dimensions $h^{(1,1)}$ and $h^{(2,1)}$ of the cohomologies $H^{(1,1)}$ and $H^{(2,1)}$. They can be determined constructing a basis of $H^{(p,q)}$ of forms of K3 and $\mathbb{T}^2$ invariant under the free involution. One obtains [39]

$$h^{(2,1)} = h^{(1,1)} = 11 \ , \tag{2.4.74}$$

while $H^{(0,0)}$, $H^{(3,3)}$ as well as $H^{(3,0)}$ are one-dimensional. Moreover, one can show that the Enriques Calabi-Yau is self-mirror and that both the Kähler and complex structure moduli spaces are given by the coset

$$\mathcal{M} = \frac{Sl(2, \mathbb{R})}{SO(2)} \times \mathcal{N}_8 \ , \tag{2.4.75}$$

where

$$\mathcal{N}_s = \frac{O(s+2, 2)}{O(s+2) \times O(2)}. \tag{2.4.76}$$

The actual moduli space is obtained after dividing $\mathcal{M}$ by the discrete groups $Sl(2, \mathbb{Z}) \times O(10, 2; \mathbb{Z})$. $\mathcal{M}$ is a simple example of a special Kähler manifold. We will discuss its properties in the following.

It is a well-known fact that the geometric moduli space of a Calabi-Yau manifold consists of two special Kähler manifolds corresponding to Kähler and complex structure deformations. A summary of some of the basic definitions and identities of special geometry can be found in section 2.1. Essentially all information is encoded in one holomorphic function, the prepotential $\mathcal{F}$. Let us for concreteness consider the moduli space of Kähler structure deformations of the Enriques Calabi-Yau which is of the form (2.4.75). Denoting by $\hat{\omega}$ the harmonic $(1,1)$-form in the $\mathbb{T}^2$-base and by ω_a the $(1,1)$ forms in the Enriques fiber, we obtain complex coordinates S, t^a by expanding the combination

$$J + iB_2 = \ S\, \hat{\omega} + t^a\, \omega_a \ , \qquad a = 1, \ldots, 10 \ , \tag{2.4.77}$$

where J is the Kähler form on the Enriques Calabi-Yau and B_2 is the NS-NS two-form. Note that in our conventions $\mathrm{Re}\, S > 0$ and $\mathrm{Re}\, t^a > 0$ such that the world-sheet instantons arise as series in $q_S = e^{-S}$ and $q_{t^a} = e^{-t^a}$ in the large radius expansion. We note that these complexified Kähler parameters t^a can be regarded as a parametrisation of the coset $\mathcal{N}_8$. The parametrisation

[4]The effect of the phase factor on the type II side was interpreted as turning on a Wilson line [39].

we are using here is the one suitable for the conventional large radius limit and corresponds to what was called in [79] the geometric reduction. In terms of (2.4.77), the prepotential takes the form

$$\mathcal{F} = -\tfrac{i}{2} C_{ab} t^a t^b S \ . \tag{2.4.78}$$

For the Enriques Calabi-Yau the cubic expression for the genus zero free energy $F^{(0)} = \mathcal{F}$ is exact and world-sheet instanton corrections will only arise at higher genus. This is precisely the reason for the simple form (2.4.75) of the moduli space. The symmetric matrix C_{ab} in (2.4.78) encodes the intersections in the Enriques fiber E such that

$$C_{ab} = \int_E \omega_a \wedge \omega_b \ . \tag{2.4.79}$$

The inverse matrix $C^{ab} \equiv C^{-1\,ab}$ can be calculated explicitly and coincide in an appropriate basis with the intersection matrix of the $\mathbb{Z}_2$ invariant lattice of the second and the third factor in (2.4.71), i.e.

$$\Gamma_E = \Gamma^{1,1} \oplus E_8(-1) \ , \qquad (C^{ab}) = \begin{pmatrix} 0 & 1 \\ 1 & 0 \end{pmatrix} \times (-C_{E_8}). \tag{2.4.80}$$

Here C_{E_8} is the Cartan matrix of the exceptional group E_8. The lattice Γ_E is identified with the second cohomology group of the Enriques surface.

The prepotential for the Enriques Calabi-Yau encodes the classical geometry of the moduli space (2.4.75). The Kähler potential is derived using equation (2.1.7) to be of the form

$$K = -\log\left[Y(S+\bar{S})\right] \ , \qquad Y = \tfrac{1}{2} C_{ab}(t^a + \bar{t}^a)(t^b + \bar{t}^b) \ . \tag{2.4.81}$$

Note that K as given in (2.1.7) contains a term $-\log|X^0|^2$, with X^0 being the fundamental period. Such a term can be removed by a Kähler transformation $K \to K - f - \bar{f}$, where f is a holomorphic function, such that our expression (2.4.81) corresponds to a certain Kähler gauge. In general, all objects we will consider below are sections of a line bundle $\mathcal{L}$ which parametrizes such holomorphic rescalings $V \to e^f V$. As an example e^{-K} is a section of $\mathcal{L} \otimes \bar{\mathcal{L}}$. Such Kähler transformations do not change the Kähler metric which is obtained by evaluating the holomorphic and anti-holomorphic derivative of K. The Kähler metric splits into two pieces

$$G_{S\bar{S}} = \frac{1}{(S+\bar{S})^2} \ , \qquad G_{a\bar{b}} = -\frac{C_{ab}}{Y} + \frac{C_{ac}(t+\bar{t})^c C_{bd}(t+\bar{t})^c}{Y^2} \ , \tag{2.4.82}$$

with all other components vanishing. The Christoffel symbols for this metric are easily evaluated to be

$$\Gamma^S_{SS} = 2K_S \ , \qquad \Gamma^c_{ab} = K_e C^{ed} \hat{\Gamma}^c_{ab|d} \ , \tag{2.4.83}$$

where K_S and K_a are the first derivatives of the Kähler potential (2.4.81) and we have defined

$$\hat{\Gamma}^b_{ac|d} = \left(\delta^b_c C_{ad} + \delta^b_a C_{cd} - \delta^b_d C_{ac}\right) \ . \tag{2.4.84}$$

It is also easy to derive the holomorphic Yukawa couplings $C^{(0)}_{ijk}$ defined in (2.1.14). In coordinates S, t^a one uses the prepotential (2.4.78) to show

$$C^{(0)}_{Sab} = C_{ab} \ . \tag{2.4.85}$$

In general $C^{(0)}_{Sab}$ is a section of $\mathcal{L}^2 \otimes \mathrm{Sym}^3(T^*\mathcal{M})$. In the case of the Enriques Calabi–Yau it is constant in the Kähler gauge and coordinates chosen above, and covariantly constant in a general gauge. The covariant derivative, acting on a section of $\mathcal{L}^m \otimes \bar{\mathcal{L}}^n$, is (2.1.11)

$$D_a = \partial_a + mK_a, \qquad D_{\bar{a}} = \partial_{\bar{a}} + nK_{\bar{a}}, \tag{2.4.86}$$

and includes the Christoffel symbols when acting on tensors. Applied to $C^{(0)}_{Sab}$ one shows

$$D_c C^{(0)}_{abS} = -\Gamma^d_{ca} C_{db} - \Gamma^d_{cb} C_{ad} + 2\partial_c K C_{ab} = 0 \ , \tag{2.4.87}$$

which vanishes by means of the equation (2.4.83) for the Christoffel symbols. A similar equation holds for the covariant derivative $D_S C^{(0)}_{abS}$, showing that $C^{(0)}_{abS}$ is indeed covariantly constant. Once again, this special property of the Yukawa couplings is immediately traced back to the fact that the prepotential $\mathcal{F}$ receives no instanton corrections.

The space $\mathcal{M}$ has two different types of singular loci in complex codimension one on the moduli space [39, 38] which lead to conformal field theories in four dimensions. The first degeneration comes from the shrinking of a smooth rational curve $e \in \Gamma_E$ with $e^2 = -2$. The shrinking $\mathbb{P}^1$ leads to an $SU(2)$ gauge symmetry enhancement together with a massless hypermultiplet, also in the adjoint representation of the gauge group. We then obtain for this point the massless spectrum of $\mathcal{N} = 4$ supersymmetric gauge theory. In terms of the complexified Kähler parameters introduced in (2.4.77) this singular locus occurs along

$$t^1 = t^2. \tag{2.4.88}$$

In order to understand the second singular locus, we first point out that the coset $\mathcal{N}_8$ can be parametrized in many different ways. In [79] it was noticed that there is a parametrisation of this coset in terms of some coordinates t^a_D, $a = 1, \cdots, 10$ which are related to what was called there the BHM reduction. By using the formulae in [79] it is easy to see that the coordinates t^a and t^a_D are related by the following simple projective transformation,

$$\begin{aligned} t^1 &= t^1_D - \frac{1}{4t^2_D} \sum_{i=3}^{10} (t^i_D)^2, \\ t^2 &= \frac{2\pi^2}{t^2_D}, \\ t^i &= -\pi \mathrm{i} \frac{t^i_D}{t^2_D}, \quad i = 3, \cdots, 10. \end{aligned} \tag{2.4.89}$$

The second singular locus occurs when

$$t^1_D = t^2_D. \tag{2.4.90}$$

On this locus one gets as well an $SU(2)$ gauge symmetry enhancement. In addition one gets four hypermultiplets in the fundamental representation of $SU(2)$, and the resulting gauge theory is $\mathcal{N} = 2$, $SU(2)$ Yang-Mills theory with four massless hypermultiplets. In Fig. 2.2 we represent schematically the two singular loci in moduli space, related by the projective transformation (2.4.89). In sections 2.5 and 2.6 of this paper we will explore in some detail the field theory limit of the topological string amplitudes and we will verify this picture of the moduli space.

2.4.2 Genus one and the free energies on the Enriques fiber

So far we have discussed the classical moduli space of the Enriques Calabi-Yau Y. We introduced the prepotential $\mathcal{F}$ which is cubic in the Kähler structure deformations and receives no worldsheet instanton corrections. One expects that such a simple structure will no longer persist at higher genus. This is already true at genus one as was shown in [91, 79]. Heterotic–type II duality can also be used to determine all higher genus free energies on the K3 fibers of the Enriques Calabi-Yau [79]. In this section we will summarize some results of [79] and present a closed expression for the fiber free energies also including the anti-holomorphic dependence.

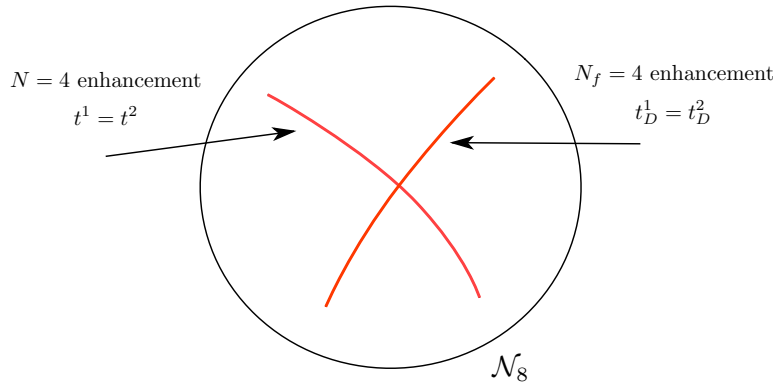

Figure 2.2: The singular loci in the moduli space $\mathcal{N}_8$, leading to two different gauge theories in the field theory limit.

Let us begin with a brief discussion of the free energies for the Enriques fiber. The fiber limit of the topological string amplitudes corresponds to blowing up the volume of the base space by taking

$$S \ \rightarrow \ \infty \ , \qquad\qquad q_S \equiv e^{-S} \ \rightarrow \ 0 \ . \tag{2.4.91}$$

In what follows we will need to distinguish the full topological string amplitudes $F^{(g)}$ from their fiber limits as well as from their holomorphic limits. We will denote,

$$F_E^{(g)}(t,\bar{t}) = \lim_{S\to\infty} F^{(g)}(t,\bar{t}) \tag{2.4.92}$$

and

$$\mathcal{F}_E^{(g)}(t) = \lim_{\bar{t}\to\infty} F_E^{(g)}(t,\bar{t}). \tag{2.4.93}$$

The fiber limit $F_E^{(g)}(t,\bar{t})$ can be calculated using heterotic-type II duality [18, 29, 79]. In the heterotic string they are given by a one–loop computation of the form

$$F_E^{(g)}(t,\bar{t}) = \int \mathrm{d}\tau\, \overline{\Theta}_\Gamma^g(\tau, v^+) f_g(\tau,\bar{\tau})/Y^{g-1} \tag{2.4.94}$$

where Y is defined in (2.4.81), and $\Theta_\Gamma^g(\tau, v^+)$ is a theta function with an insertion of $2g-2$ powers of the right–moving heterotic momentum. We will not need the precise definitions of Θ_Γ^g and f_g here. However, it is important to note that these amplitudes can be evaluated in closed form by using standard techniques for one–loop integrals. The holomorphic limit (2.4.93) was determined in [79] and it is given by

$$\mathcal{F}_E^{(g)}(t) = \sum_{r>0} c_g(r^2)\left[2^{3-2g}\mathrm{Li}_{3-2g}(e^{-r\cdot t}) - \mathrm{Li}_{3-2g}(e^{-2r\cdot t})\right] \ , \tag{2.4.95}$$

where Li_n is the polylogarithm of index n defined as

$$\mathrm{Li}_n(x) = \sum_{d=1}^{\infty} \frac{x^d}{d^n} \ . \tag{2.4.96}$$

In formula (2.4.95) we have also set $r^2 = C^{ab} r_a r_b$ and $r\cdot t = r_a t^a$. We will sometimes write

$$r = (n, m, \vec{q}). \tag{2.4.97}$$

The restriction $r > 0$ means $n > 0$, or $n = 0, m > 0$, or $n = m = 0$, $\vec{q} > 0$. Finally, we need to define the coefficients $c_g(n)$. They can be identified as the expansion coefficients of a particular quasi-modular form

$$\sum_n c_g(n) q^n = -2 \frac{\mathcal{P}_g(q)}{\eta^{12}(2\tau)}, \tag{2.4.98}$$

with $\mathcal{P}_g(q)$ given by

$$\left(\frac{2\pi \eta^3 \lambda}{\vartheta_1(\lambda|\tau)} \right)^2 = \sum_{g=0}^{\infty} (2\pi\lambda)^{2g} \mathcal{P}_g(q). \tag{2.4.99}$$

The definition of $\eta(\tau)$ and the theta-function $\vartheta_1(\lambda|\tau)$ can be found in Appendix C.1. From the definition (2.4.99) and the identities summarized in Appendix C.1 one also infers that the $\mathcal{P}_g$ are quasimodular forms of weight $2g$ and can be written as polynomials in the Eisenstein series E_2, E_4, E_6. We have for example

$$\mathcal{P}_1(q) = \tfrac{1}{12} E_2(q) \ , \qquad \mathcal{P}_2(q) = \tfrac{1}{1440}(5E_2^2 + E_4) \ . \tag{2.4.100}$$

In general, as we will see in section 2.5, it is very hard to include the $\mathbb{T}^2$-base in order to obtain the expressions $\mathcal{F}^{(g)}$ for the full Enriques Calabi-Yau. It turns out that only $\mathcal{F}^{(1)}$ factorizes nicely, namely we can write the A–model free energy $\mathcal{F}^{(1)}$ as [91, 79]

$$\mathcal{F}^{(1)}(S,t) = \mathcal{F}^{(1)}_{\text{base}} + \mathcal{F}^{(1)}_E \ , \tag{2.4.101}$$

where $\mathcal{F}^{(1)}_{\text{base}}$ and $\mathcal{F}^{(1)}_E$ are the contributions from the $\mathbb{T}^2$ base and the K3 fiber. $\mathcal{F}^{(1)}_{\text{base}}$ is the torus free energy given by [8]

$$\mathcal{F}^{(1)}_{\text{base}} = -12 \log \eta(S) \ , \tag{2.4.102}$$

where $\eta(S)$ is defined in (C.1.4), while

$$\mathcal{F}^{(1)}_E = -\tfrac{1}{2} \log \Phi(t), \tag{2.4.103}$$

where $\Phi(t)$ is the infinite product

$$\Phi(t) = \prod_{r>0} \left(\frac{1 - e^{-r\cdot t}}{1 + e^{-r\cdot t}} \right)^{2c_1(r^2)} \ . \tag{2.4.104}$$

This infinite product first appeared in the work of Borcherds [41]. As we will discuss in more detail later on, $\Phi(t)$ is the key example of a holomorphic automorphic form for the Enriques Calabi-Yau. It is also convenient to introduce,

$$\Phi(S,t) = \eta^{24}(S) \Phi(t), \tag{2.4.105}$$

so that we can write

$$\mathcal{F}^{(1)}(S,t) = -\tfrac{1}{2} \log \ \Phi(S,t). \tag{2.4.106}$$

We presented above formulae for the holomorphic limit of $F^{(g)}_E(t,\bar{t})$, but heterotic-type II duality can be used as well to obtain the antiholomorphic dependence on $\bar{t}$. At genus one, one finds [92, 29]

$$F^{(1)}_E(t,\bar{t}) = -2 \log Y - \log \big|\Phi(t)\big|. \tag{2.4.107}$$

The antiholomorphic dependence on $\bar{S}$ is the usual one for the torus [8] and one has

$$F^{(1)}(S,\bar{S},t,\bar{t}) = F^{(1)}_E(t,\bar{t}) - 6 \log\Big((S+\bar{S}) |\eta^2(S)|^2 \Big). \tag{2.4.108}$$

Equivalently, we can write

$$F^{(1)}(S,\bar{S},t,\bar{t}) = -2\log\left[(S+\bar{S})^3 Y\right] - \log\left|\Phi(S,t)\right|. \tag{2.4.109}$$

As a consistency check one shows that this anti-holomorphic dependence can also be inferred from the holomorphic anomaly equation (2.2.31) for $F^{(1)}$.

The antiholomorphic dependence in the heterotic calculation at higher genus is much more complicated, but was written down for the STU model in [29]. As we show in Appendix A.2, this computation can be considerably simplified and adapted to the Enriques case. We find that the non-holomorphic free energy $F_E^{(g)}(t,\bar{t})$ can be cast into the form

$$\begin{aligned} F_E^{(g)}(t,\bar{t}) &= \sum_{l=0}^{g-1} \sum_{C=0}^{\min(l,2g-3-l)} \begin{pmatrix} 2g-3-l \\ C \end{pmatrix} \frac{(t+\bar{t})^{a_1}\ldots(t+\bar{t})^{a_{l-C}}\partial_{a_1}\ldots\partial_{a_{l-C}}\mathcal{F}_E^{(g-l)}(t)}{(l-C)!2^l\ Y^l} \\ &\quad -\frac{1}{2^{g-2}(g-1)Y^{g-1}}\ , \end{aligned} \tag{2.4.110}$$

where $\mathcal{F}_E^{(r)}(t)$ is the holomorphic fiber expression given in (2.4.95). It is easy to check that the $F_E^{(g)}(t,\bar{t})$ fulfill the holomorphic anomaly equation on the fiber.

So far we have discussed the heterotic results for the fiber limit by using the Kähler parameters (2.4.77) appropriate for the large radius limit. As shown in [79], one can also compute them in the coordinates t_D^a introduced in (2.4.89). This was called the BHM reduction in [79], and leads to the holomorphic couplings,

$$\mathcal{F}_E^{(g)}(t_D) = \sum_{r>0} d_g(r^2/2)(-1)^{n+m}\mathrm{Li}_{3-2g}(\mathrm{e}^{-r\cdot t_D}) \tag{2.4.111}$$

where the coefficients $d_g(n)$ are defined by

$$\sum_n d_g(n)q^n = \frac{2^{2+g}\mathcal{P}_g(q^4) - 2^{2-g}\mathcal{P}_g(q)}{\eta^{12}(2\tau)}, \tag{2.4.112}$$

and in (2.4.111) we regard r as a vector in $\Gamma^{1,1}\oplus E_8(-2)$. Note that in comparison to (2.4.80) we now need to include the lattice $E_8(-2)$ with inner product given by -2 times the Cartan matrix of E_8, such that $r^2 = 2nm - 2\vec{q}^{\,2}$. One has, in particular,

$$\mathcal{F}_E^{(1)}(t_D) = -\tfrac{1}{2}\log\Phi_B(t_D)\ , \tag{2.4.113}$$

where

$$\Phi_B(t_D) = \prod_{r>0}\left(1-\mathrm{e}^{-r\cdot t_D}\right)^{(-1)^{n+m}c_B(r^2/2)} \tag{2.4.114}$$

with coefficients

$$\sum_n c_B(n)q^n = \frac{\eta(2\tau)^8}{\eta(\tau)^8\eta(4\tau)^8}. \tag{2.4.115}$$

This is the modular form introduced by Borcherds in [93], and the above expression for F_1 agrees with that found by Harvey and Moore in [91] (up to a factor of 1/2 due to different choice of normalizations).

2.4.3 An all–genus product formula on the fiber

As we have already mentioned, the infinite product (2.4.104) was first considered by Borcherds in [41]. Borcherds also noticed that (2.4.104) is the denominator formula for a generalized Kac–Moody (or Borcherds) superalgebra (see [94, 92] for a review of Borcherds algebras). The

root lattice of this superalgebra is $\Gamma^{1,1} \oplus E_8(-1)$ (i.e. the cohomology lattice of the Enriques surface), and the simple roots are the positive, norm 0 vectors. Each simple root appears also as a superroot, both with multiplicity 8, and this is why the product of (2.4.104) has a "supersymmetric" structure: the numerator is a trace over fermionic degrees of freedom, while the denominator traces over bosonic degrees of freedom. Both have the same multiplicity $2c_1(r^2)$. In addition, the fact that $c_1(-1) = 0$ is equivalent to the absence of tachyons in the spectrum.

We will now write down a formula for the total partition function of topological string theory, restricted to the fiber, and we will show that it preserves the structure found by Borcherds for (2.4.104). As a first step, we define a generating functional $\xi(q, g_s)$ closely related to (2.4.99),

$$\xi(q, g_s) = \prod_{n=1}^{\infty} \frac{(1-q^n)^2}{1 - 2q^n \cos\, g_s + q^{2n}}. \tag{2.4.116}$$

We have the identity

$$\sum_{g=0}^{\infty} \mathcal{P}_g(q) g_s^{2g-2} = \left(2 \sin\, \frac{g_s}{2}\right)^{-2} \xi^2(q, g_s), \tag{2.4.117}$$

Let us now define the Enriques degeneracies $\Omega_E(r, \ell)$ as

$$\sum_{r,\ell} 8\Omega_E(r,\ell) q^{r^2} q_s^{\ell} = \frac{2}{(q_s^{\frac{1}{4}} - q_s^{-\frac{1}{4}})^2} \frac{1}{\eta^{12}(2\tau)} (\xi^2(q, g_s/2) - \xi^2(-q, g_s/2)), \tag{2.4.118}$$

where

$$q_s = \mathrm{e}^{\mathrm{i} g_s}. \tag{2.4.119}$$

The right-hand side of (2.4.118) only involves *integer* powers of $q_s^{\pm 1}$. We can collect the Enriques degeneracies in the generating polynomials

$$\Omega_n(z) = \sum_{r^2 = 2n, \ell \geq 0} \Omega_E(r, \ell) z^{\ell}, \tag{2.4.120}$$

which are of degree n in z. We have for the first few:

$$\begin{aligned}
&\Omega_0(z) = 1, \\
&\Omega_1(z) = 12 + 2z, \\
&\Omega_2(z) = 90 + 24z + 3z^2, \\
&\Omega_3(z) = 520 + 180z + 36z^2 + 4z^3, \\
&\Omega_4(z) = 2538 + 1040z + 270z^2 + 48z^3 + 5z^4, \\
&\Omega_5(z) = 10944 + 5070z + 1560z^2 + 360z^3 + 60z^4 + 6z^5.
\end{aligned} \tag{2.4.121}$$

Notice that the constant terms of $\Omega_n(z)$ are closely related to the Euler characteristics of the Hilbert schemes of the Enriques surface, but there are "deviations" which become more and more important as the degree increases. Finally, notice that

$$\sum_{\ell} \Omega_E(r, \ell) q^{r^2} q_s^{\ell} = \Omega_n(q_s) + \Omega_n(q_s^{-1}) - \Omega_n(0). \tag{2.4.122}$$

We now define

$$F_E = \sum_{g=1}^{\infty} g_s^{2g-2} \mathcal{F}_E^{(g)}(t), \qquad Z_E = \mathrm{e}^{-2F_E}. \tag{2.4.123}$$

Notice that, as $g_s \to 0$, Z_E is precisely the Borcherds product $\Phi(t)$. It is now an easy exercise to evaluate it for finite g_s from (2.4.95), and we find

$$Z_E(g_s, t) = \prod_{r,\ell} \left(\frac{1 - q_s^{\ell} \mathrm{e}^{-r\cdot t}}{1 + q_s^{\ell} \mathrm{e}^{-r\cdot t}}\right)^{8\Omega_E(r,\ell)}. \tag{2.4.124}$$

As in the $g = 1$ case, (2.4.124) has a supersymmetric structure, with the same degeneracies for fermionic and bosonic states. This formula in fact suggests the existence of a superalgebra structure for the all–genus result as well. By including g_s we have extended the lattice to

$$\Gamma^{1,1} \oplus E_8(-1) \to \Gamma^{1,1} \oplus E_8(-1) \oplus \mathbb{Z} \tag{2.4.125}$$

which is reminiscent of the growth of an eleven–dimensional direction associated to the string coupling constant. The fact that the all–genus heterotic results seem to lead to an extra direction in the heterotic lattice has been pointed out in [95, 96]. It would be very interesting to see if there is indeed a superalgebra associated to the all–genus result (2.4.124). If this was the case, the quantities $8\Omega_E(r, \ell)$ would correspond to root multiplicities.

Finally, we mention that according to the conjecture in [25] and the results of [62], (2.4.124) is essentially the generating functional of an infinite family of Donaldson–Thomas invariants on the Enriques surface (written already in the right variables). Such product formulas for Z exist generically if the latter is expressed in terms of of Gopakumar-Vafa invariants [97]. Our comments above indicate that the Donaldson–Thomas theory on this manifold has a highly nontrivial algebraic structure (see section 3.2.6 in [62] for a related observation).

2.4.4 Automorphic forms

The free energies $F_E^{(g)}(t, \bar{t})$ on the fiber turn out to be automorphic forms on the coset space $\mathcal{N}_8$. Here we will study in some detail automorphic forms on the space $\mathcal{N}_s$. We will say that a function on the moduli space $\mathcal{N}_s$ is *automorphic* if it has well–defined transformation properties under the discrete subgroup $O(s + 2, 2; \mathbb{Z})$.

The transformation properties are easier to understand if we consider explicit generators of the symmetry group. We consider the explicit parametrisation of the coset space (2.4.75) induced by a reduction

$$\Gamma^{s+2,2} = \Gamma^{s+1,1} \oplus \Gamma^{1,1}, \tag{2.4.126}$$

and let $t \in \mathbb{C}^{s+1,1}$ be the vector of complex coordinates parametrizing the coset. Our conventions are such that t has *positive* real part. For an element $t^a \in \mathbb{C}^{s+1,1}$ we define the inner product

$$t^2 = \tfrac{1}{2} C_{ab} t^a t^b, \tag{2.4.127}$$

where C_{ab} is the intersection matrix.

The generators of the symmetry group are taken to be [92]:

- $t \mapsto t + 2\pi i\lambda$, $\lambda \in \Gamma^{s+1,1}$.
- $t \mapsto w(t)$, $w \in O(s + 1, 1; \mathbb{Z})$.
- The automorphic analog of an S–duality transformation

$$t^a \quad \mapsto \quad \tilde{t}^a = \frac{t^a}{t^2}. \tag{2.4.128}$$

We say that a function $\Psi(t)$ is an *automorphic function of weight* k if it is invariant under the first two transformations above, and if under (2.4.128), it behaves as follows:

$$\Psi_k(\tilde{t}) = t^{2k} \Psi_k(t). \tag{2.4.129}$$

We can also have automorphic forms of weight $(k, \bar{k})$ which transform as

$$\Psi_{k,\bar{k}}(\tilde{t}) = t^{2k}\ \bar{t}^{2\bar{k}} \Psi_{k,\bar{k}}(t). \tag{2.4.130}$$

Although we have not indicated it explicitly, these functions might have a non-holomorphic dependence on $\bar{t}$. Automorphic forms are in general non-holomorphic. Some automorphic forms

are meromorphic (they have poles at divisors). If they do not have poles, they are called *holomorphic*.

Notice that (2.4.128) transforms the metric $Y = (t+\bar{t})^2$ on the "upper half plane" as follows:

$$Y \;\mapsto\; t^{-2}\,\bar{t}^{-2} Y \;. \tag{2.4.131}$$

Following the definition (2.4.130) this identifies Y as an automorphic form of weight $(-1,-1)$. Recalling the form of the Kähler potential for the classical moduli space (2.4.81) this is nothing but a Kähler transformation [98]

$$K \;\mapsto\; K + \log t^2 + \log \bar{t}^2 \;. \tag{2.4.132}$$

in special coordinates where $X^0 = 1$. Note that, if we keep X^0, this shift can be absorbed by the transformation of X^0

$$X^0 \;\mapsto\; t^2 X^0 \;. \tag{2.4.133}$$

This can be traced back to the fact that K as given in (2.1.7) is a scalar under the full symplectic group.

In order to understand how the automorphic properties mix with taking derivatives, it is useful to derive the Jacobian J^b_a of the change of coordinates (2.4.128). We immediately find,

$$\frac{\partial \tilde{t}^a}{\partial t^b} \equiv (J^{-1})^a_b = \frac{1}{t^4}\Big(\delta^a{}_b t^2 - t^a C_{be} t^e\Big) \;, \qquad \frac{\partial t^a}{\partial \tilde{t}^b} = J^a_b = \delta^a{}_b t^2 - t^a C_{be} t^e \;. \tag{2.4.134}$$

Notice that J^b_a obeys the following useful identities

$$J^b_a = t^4 (J^{-1})^b_a \;, \qquad C_{ab} = t^{-4} C_{cd} J^c_a J^d_b \;, \qquad C^{ab} J^c_a J^d_b = t^4 C^{cd} \;. \tag{2.4.135}$$

Let us now assume that Ψ is an automorphic form of weight $(k,0)$. We want to determine the transformation behavior of $D_a\Psi$ and $D_aD_b\Psi$ under the dualities (2.4.128). D_a are here the derivatives covariant both with respect to Christoffel connection and the canonical connection on the vacuum bundle $\mathcal{L}$, as introduced in section 2.4.1. Therefore,

$$D_a\Psi = (\partial_a - kK_a)\Psi \;. \tag{2.4.136}$$

Notice that, since K transforms as given in (2.4.132), its first derivative K_a shifts as

$$K_a \;\mapsto\; J^b_a\big(K_b + t^{-2} C_{bc} t^c\big) \;. \tag{2.4.137}$$

Combining this with the transformation of the automorphic form Ψ itself we conclude

$$D_a\Psi \;\mapsto\; t^{2k} J^b_a D_b \Psi \;. \tag{2.4.138}$$

Similarly, we show that the second derivative of Ψ transforms as

$$D_bD_a\Psi \;\mapsto\; t^{2k} J^b_d J^c_a D_b D_c \Psi \;, \tag{2.4.139}$$

where we have used that the Christoffel symbols in the second connection transform as

$$J^d_b \partial_d J^c_a - \widetilde{\Gamma}^d_{ba} J^c_a = \Gamma^d_{ba} J^c_a \;. \tag{2.4.140}$$

Hence, we have shown that the covariant derivatives D_a of Ψ transform with a factor t^{2k} but are also rotated by the Jacobian J^a_b containing another factor of t^2. Note however, that we can easily obtain automorphic forms containing the derivatives $D_a\Psi$. More precisely, if Ψ and Ψ' are automorphic forms of weight $(k,0)$ and $(k',0)$ we find by using (2.4.135) that

$$C^{ab} D_a D_b \Psi \;, \qquad C^{ab} D_a\Psi D_b \Psi' \tag{2.4.141}$$

are automorphic forms of weight $k+2$ and $k+k'+2$ respectively. Such automorphic combinations arise in the derivation of all $F^{(g)}(S,\bar{S},t,\bar{t})$, $g>1$. More precisely, we will argue in the next sections that as function of $t,\bar{t}$, $F^{(g)}(S,\bar{S},t,\bar{t})$ itself is an automorphic form of weight $(2g-2,0)$ such that

$$F^{(g)} \;\mapsto\; t^{4g-4}F^{(g)} \qquad \text{for} \quad g>1\ . \tag{2.4.142}$$

An important example of an automorphic form is the heterotic integral (2.4.94). It is easy to show from the properties of the Narain–Siegel theta function that it has weight $(2g-2,0)$. Since this integral gives the fiber limit $F_E^{(g)}$, we obtain a check of the general property (2.4.142) from heterotic/type II duality. Note that it is straightforward to define amplitudes $F^{(g)}$ invariant under automorphic transformations by

$$(X^0)^{2-2g}\,F^{(g)}\ . \tag{2.4.143}$$

The invariance of this combination is readily checked by using (2.4.133) and (2.4.142). The expressions (2.4.143) are shown to be invariant under the full target space symmetry group $Sl(2,\mathbb{Z})\times O(10,2)$. They are the direct analogs of the invariant free energies encountered in the Seiberg-Witten example in section 2.3.

A particularly important and simple example occurs at $g=1$. Since $F_E^{(1)}$ is invariant, one deduces from (2.4.107) and (2.4.131) that $\Phi(t)$ is an automorphic form of weight $(4,0)$ i.e.

$$\Phi(\tilde{t}) = t^8\ \Phi(t)\ , \qquad\qquad \tilde{t}^a = \frac{t^a}{t^2}\ . \tag{2.4.144}$$

One can also show that $\Phi(t)$ is holomorphic. This is proved in [41], and it is in fact a consequence of the regularity of $\mathcal{F}_E^{(g)}(t)$ at the singular locus (2.4.88), which will be discussed in more detail in section 2.5.4. In addition, $\Phi(t)$ is what is called a singular automorphic form (see [99], section 3, for a definition). Singular automorphic forms are known to satisfy a wave equation

$$C^{ab}\frac{\partial^2}{\partial t^a\partial t^b}\Phi(t)=0. \tag{2.4.145}$$

Equivalently, they have Fourier expansions involving only vectors of zero norm. It follows that $\mathcal{F}_E^{(1)}(t)$ satisfies

$$C^{ab}\partial_a\partial_b\mathcal{F}_E^{(1)} = 2C^{ab}\partial_a\mathcal{F}_E^{(1)}\,\partial_b\mathcal{F}_E^{(1)}\ . \tag{2.4.146}$$

This is equivalent to the recursive relation found in [62] for genus one invariants on the fiber, and proves that the expression for $\mathcal{F}_E^{(1)}(t)$ obtained in [79] agrees with the Gromov–Witten calculation of [62].

2.5 Direct Integration on the Enriques Calabi-Yau

In this section we illustrate the power of the method of direct integration by studying the topological string amplitudes $F^{(g)}$ on the Enriques Calabi-Yau. Our approach will follow and generalize the strategy developed for the Seiberg-Witten example in section 2.3. To begin with, we perform a direct integration along the $\mathbb{T}^2-$base. Using the fiber results obtained in the previous section as additional input, the first six free energies $F^{(g)}$ can be determined in a closed form. We then present a more general formalism combining direct integration in base and fiber directions, and we introduce the relevant holomorphic and non-holomorphic $O(10,2,\mathbb{Z})$ forms. A closed recursive expression for $F^{(g)}$ will also be derived. It determines the $F^{(g)}$ up to a holomorphic ambiguity and we will briefly discuss possible boundary conditions. Finally, we consider a reduced Enriques model with three parameters only, which was already studied in [79]. This model has the advantage that the mirror map can be determined explicitly. We also study in more detail the boundary conditions (such as the gap condition), which lead to valuable conclusions also applying to the full model.

2.5.1 A simple direct integration and $F^{(g)}$ to genus six

Let us now perform the direct integration along the $\mathbb{T}^2$ base and derive the first few amplitudes $F^{(g)}$. In order to do that we carefully keep track of their dependence of on the base direction $S, \bar{S}$. As in the case of Seiberg–Witten theory studied in section 2.3, it is easy to see from the structure of the holomorphic anomaly equations that the only antiholomorphic dependence of $F^{(g)}$ on $\bar{S}$ appears through $\widehat{E}_2(S, \bar{S})$. By taking derivatives with respect to S we will also generate in the holomorphic anomaly equations the modular forms $E_4(S), E_6(S)$, and by keeping track of the modular weight one immediately finds that $F^{(g)}$ is an element of weight $2g-2$ in the ring generated by

$$\widehat{E}_2(S, \bar{S}), \quad E_4(S), \quad E_6(S) \ . \tag{2.5.147}$$

Our only assumption here is that the holomorphic ambiguity for $F^{(g)}$ is also a modular form of weight $2g-2$ in this ring. This assumption (as well as the details of the direct integration) can be checked in a highly nontrivial way by comparing the resulting expressions to the field theory limit in the $N_f = 4$ locus of Fig. 2.2. This check will be performed in section 2.6.

To perform the direct integration let us first rewrite the holomorphic anomaly equation for the base direction $\bar{S}$. The general expression (2.2.30) reduces to

$$\partial_{\bar{S}} F^{(g)} = -\frac{1}{2} \frac{C^{ab}}{(S+\bar{S})^2} \Big(D_a D_b F^{(g-1)} + \sum_{r=1}^{g-1} D_a F^{(r)} D_b F^{(g-r)} \Big) \ . \tag{2.5.148}$$

We now convert the derivative $\partial_{\bar{S}}$ into a derivative with respect to $\widehat{E}_2$. The definition of $\widehat{E}_2$ was already given in (2.3.51). Since we now consider an expansion in $q_S = e^{-S}$ it takes the form

$$\widehat{E}_2(S, \bar{S}) = -\frac{12}{S+\bar{S}} + E_2(S) \ . \tag{2.5.149}$$

Since the dependence of $F^{(g)}$ on $\bar{S}$ is only through this quantity, we can rewrite the anomaly equation as

$$\frac{\partial F^{(g)}}{\partial \widehat{E}_2} = -\tfrac{1}{24} C^{ab} \Big(D_a D_b F^{(g-1)} + \sum_{r=1}^{g-1} D_a F^{(r)} D_b F^{(g-r)} \Big) \ . \tag{2.5.150}$$

Here the covariant derivatives D_a are only taken with respect to the fiber directions and do not depend on the base due to the simple special geometry of the Enriques Calabi-Yau. This implies that all dependence on $\widehat{E}_2$ arises directly through the $F^{(r)}$. We thus expand $F^{(g)}$ in powers of $\widehat{E}_2$ by writing

$$F^{(g)} = \sum_{k=0}^{g-1} \widehat{E}_2^k(S, \bar{S}) \ c_k^{(g)} \ , \qquad g > 1 \ . \tag{2.5.151}$$

We see that (2.5.150) determines all the coefficients $c_k^{(g)}$ for $k = 1, \ldots, g-1$ in terms of quantities at lower genera. Explicitly, we have the solution

$$c_k^{(g)} = -\tfrac{1}{24k} C^{ab} \Big(D_a D_b c_{k-1}^{(g-1)} + \sum_{r=1}^{g-1} \sum_{l+m=k-1} D_a c_l^{(r)} D_b c_m^{(g-r)} \Big) \ , \tag{2.5.152}$$

where we have set

$$c_0^{(1)} = F^{(1)} \ , \qquad c_i^{(1)} = 0 \ , \qquad i \neq 0 \ . \tag{2.5.153}$$

The $\widehat{E}_2$-independent term $c_0^{(g)}$ arises as an integration constant and hence cannot be determined by the holomorphic anomaly equation. However, given our assumptions, we can fix it up to genus 6 as follows. Let us denote the coefficients in the fiber limit by

$$c_{E|\,k}^{(g)} = \lim_{S, \bar{S} \to \infty} c_k^{(g)} . \tag{2.5.154}$$

By also taking the fiber limit of (2.5.151) we find

$$\sum_{k=0}^{g-1} c^{(g)}_{E|\,k} = F^{(g)}_E(t,\bar{t}). \tag{2.5.155}$$

The free energies $F^{(g)}_E(t,\bar{t})$ are known from the heterotic computation and given in (2.4.110). Together with the fact that all $c^{(g)}_{E|\,k}$ for $k \geq 1$ are uniquely determined by the direct integration we can use (2.5.155) to derive $c^{(g)}_{E|\,0}$ i.e. the fiber limit of the integration constant. But the condition that $c^{(g)}_0$ is a modular form in the ring generated by (2.5.147) and does not involve $\widehat{E}_2$ fixes it uniquely in terms of $c^{(g)}_{E|\,0}$ as

$$\begin{aligned} &c^{(2)}_0 = 0\ , && c^{(3)}_0 = c^{(3)}_{E|\,0}\ E_4\ , && c^{(4)}_0 = c^{(4)}_{E|\,0}\ E_6\ , \\ &c^{(5)}_0 = c^{(5)}_{E|\,0}\ E_4^2\ , && c^{(6)}_0 = c^{(6)}_{E|\,0}\ E_4\,E_6\ , \end{aligned} \tag{2.5.156}$$

where $E_4(S)$ and $E_6(S)$ are the two holomorphic generators in (2.5.147). This can be checked by noting that the definition (C.1.15) of the Eisenstein series implies that

$$E_2\ ,\quad E_4\ ,\quad E_6 \quad\to\quad 1\ , \tag{2.5.157}$$

in the fiber limit $S, \bar{S} \to \infty$. For $g \geq 7$, the number of possible modular forms is greater than one and $c^{(g)}_{E|\,0}$ is no longer uniquely determined in terms of its fiber limit. For example, at genus seven $c^{(7)}_0$ can contain terms proportional to E_4^3 as well as E_6^2.

Let us now write down some explicit formula for lower genera. For $g = 2$ we find,

$$F^{(2)}(S,\bar{S},t,\bar{t}) = \widehat{E}_2(S,\bar{S})\ c^{(2)}_1\ , \tag{2.5.158}$$

where we use (2.5.156) and apply (2.5.152) to derive

$$c^{(2)}_1 = -\tfrac{1}{24} C^{ab}\left(D_a D_b F^{(1)}_E + D_a F^{(1)}_E D_b F^{(1)}_E\right). \tag{2.5.159}$$

Consistency of the fiber limit requires that $c^{(2)}_1 = F^{(2)}_E(t,\bar{t})$. This can be checked by using the heterotic expression (2.4.110) for $F^{(2)}_E(t,\bar{t})$, the property (2.4.146), and the identity [79]

$$\mathcal{F}^{(2)}_E = -\tfrac{1}{16} C^{ab}\partial_a\partial_b \mathcal{F}^{(1)}_E\ , \tag{2.5.160}$$

which follows directly from (2.4.94). In the holomorphic limit we find,

$$\mathcal{F}^{(2)}(S,t) = E_2(S)\mathcal{F}^{(2)}_E(t)\ , \tag{2.5.161}$$

in agreement with the results of [79, 62]. In the following sections we will also need a slightly different form of $F^{(2)}$. Namely, it is straightforward to apply (2.4.146) to write

$$F^{(2)} = -\tfrac{1}{8} C^{ab}\partial_a F^{(1)}\partial_b F^{(1)}\ . \tag{2.5.162}$$

Let us now consider the $g = 3$ case. The amplitude $F^{(3)}$ can be expanded by using (2.5.151) and (2.5.156) as

$$F^{(3)} = \widehat{E}_2^2(S,\bar{S})\, c^{(3)}_2 + E_4(S)\, c^{(3)}_{E|\,0}\ . \tag{2.5.163}$$

Using the result of the direct integration (2.5.152) we obtain

$$c^{(3)}_2 = -\tfrac{1}{48} C^{ab}\Big(D_a D_b F^{(2)}_E + 2 D_a F^{(2)}_E D_b F^{(1)}_E\Big)\ . \tag{2.5.164}$$

To determine $c^{(3)}_{E|0}$ we use (2.5.155), which gives

$$c^{(3)}_2 + c^{(3)}_{E|0} = F^{(3)}_E(t,\bar t)\ . \tag{2.5.165}$$

On the other hand, one finds that

$$F^{(3)}_E(t,\bar t) = -\tfrac{1}{24} C^{ab} D_a D_b F^{(2)}_E. \tag{2.5.166}$$

This can be derived in the holomorphic limit by using (2.4.94), and it is similar to (2.5.160). The antiholomorphic part can be checked with (2.4.110). Using all this, we finally obtain the following simple expression for $F^{(3)}(S,\bar S,t,\bar t)$,

$$F^{(3)} = -\tfrac{1}{24} E_4\, C^{ab} D_a D_b F^{(2)}_E - \tfrac{1}{48}(\widehat E_2^2 - E_4) C^{ab}\big(D_a D_b F^{(2)}_E + 2 D_a F^{(2)}_E D_b F^{(1)}_E\big)\ , \tag{2.5.167}$$

with the holomorphic limit

$$\mathcal{F}^{(3)}(S,t) = -\tfrac{1}{24} E_4\, C^{ab} \partial_a\partial_b \mathcal{F}^{(2)}_E - \tfrac{1}{48}(E_2^2 - E_4) C^{ab}\big(\partial_a\partial_b \mathcal{F}^{(2)}_E + 2\partial_a \mathcal{F}^{(2)}_E \partial_b \mathcal{F}^{(1)}_E\big)\ . \tag{2.5.168}$$

Note that the second term in these expressions vanishes identically in the fiber limit where $E_2, E_4 \to 1$. As we will discuss in more detail in section 2.5.4, this is the first $F^{(g)}$ where the inclusion of the base yields a behavior near the singular loci that differs significantly from the fiber limit.
Explicit calculations at genus 4 proceed in the same way. Modular invariance with respect to S gives

$$F^{(4)}(S,\bar S,t,\bar t) = \widehat E_2^3\ c^{(4)}_{E|3} + \widehat E_2 E_4\ c^{(4)}_{E|1} + E_6\ c^{(4)}_{E|0}. \tag{2.5.169}$$

Once again, the general equation (2.5.194) allows us to determine the coefficients as

$$\begin{aligned} c^{(4)}_{E|3} &= -\tfrac{1}{72} C^{ab}\big(D_a D_b c^{(3)}_{E|2} + 2 D_a F^{(1)}_E D_b c^{(3)}_{E|2} + D_a F^{(2)}_E D_b F^{(2)}_E\big)\ , \\ c^{(4)}_{E|1} &= -\tfrac{1}{24} C^{ab}\big(D_a D_b c^{(3)}_{E|0} + 2 D_a F^{(1)}_E D_b c^{(3)}_{E|0}\big)\ . \end{aligned} \tag{2.5.170}$$

The ambiguity $c^{(4)}_{E|0}$ is again determined by the heterotic computation in the fiber limit. More precisely, one specializes (2.5.155) to

$$c^{(4)}_{E|0} + c^{(4)}_{E|1} + c^{(4)}_{E|3} = F^{(4)}_E(t,\bar t)\ , \tag{2.5.171}$$

and solves for $c^{(4)}_{E|0}$ by inserting the fiber result (2.4.110). This determines the free energy $F^{(4)}$. A similar analysis also applies to $g = 5, 6$. As already discussed above, the main obstacle that has to be overcome in order to proceed to higher genus is the difficulty to fix the ambiguities $c^{(g)}_0$. We will discuss possible additional boundary conditions in sections 2.5.4, 2.5.5 and 2.6.

2.5.2 Propagators and holomorphic automorphic forms

In the previous section we calculated the first free energies $F^{(g)}$ by a direct integration along the base direction. The results were expressed in terms of the holomorphic fiber energies $\mathcal{F}^{(g)}_E$, which are known from heterotic-type II duality. Even though the results were rather compact and transparent, the information we have extracted is somewhat partial, since we have not used the holomorphic anomaly equations for the fiber moduli. In order to exploit the information they contain, we will construct building blocks for the automorphic forms in the fiber which enable us to perform the direct integration of the remaining holomorphic anomaly equations. Recall that we argued in the previous sections that the almost holomorphic modular form

$$\widehat E_2(S,\bar S) = -\frac{12}{S+\bar S} + E_2(S)\ , \qquad\qquad E_2(S) = \partial_S \log\Phi\ , \tag{2.5.172}$$

contains all non-holomorphic dependence of $F^{(g)}$ along the base direction S. It will be the task of this section to introduce the analog of $\widehat{E}_2$ for the fiber directions t^a. Furthermore we will define the fiber analogs of the holomorphic modular forms $E_4(S)$ and $E_6(S)$. This will lead us to the definition of a new class of holomorphic automorphic forms of $O(10,2,\mathbb{Z})$. Eventually, in section 2.5.3 we will argue that a direct integration along the fiber direction allows us to express all $F^{(g)}$ in terms of these almost holomorphic and holomorphic forms of $O(10,2,\mathbb{Z})$.

Let us now introduce the fiber analog of the almost holomorphic modular form $\widehat{E}_2(S,\bar{S})$. This can be done by recalling that the genus one free energy $F^{(1)}$ is an invariant of the full symmetry group $Sl(2,\mathbb{Z})\times O(10,2,\mathbb{Z})$ and hence its first derivatives transform in a particularly simple way. For the derivative with respect to S one finds $\partial_S F^{(1)} = \frac{1}{2}\widehat{E}_2$. The derivative with respect to t^a we denote by $\Delta^a = -\frac{1}{2}C^{ab}\partial_b F^{(1)}$ and evaluate

$$\Delta^a = \frac{t^a+\bar{t}^a}{Y} + \epsilon^a(t) = \epsilon^a(t) - K_b(t)C^{ba} \ , \qquad \epsilon^a(t) = \tfrac{1}{4}C^{ab}\partial_{t^b}\log\Phi \ , \tag{2.5.173}$$

where $Y = \frac{1}{2}C_{ab}(t+\bar{t})^b(t+\bar{t})^b$ and Φ is given in (2.4.104). The function $\epsilon^a(t)$ is holomorphic in the coordinates t^a and is the fiber analog of $E_2(S)$, while Δ^a plays the role of $\widehat{E}_2$. To see this note that ϵ^a transforms with a shift under the duality $t^a \mapsto t^a/t^2$:

$$\epsilon^a \quad \mapsto \quad t^4(J^{-1})^a_b(\epsilon^b + t^{-2}t^b) \ . \tag{2.5.174}$$

This shift is precisely canceled by the shift of the non-holomorphic term in (2.5.173) such that Δ^a simply transforms as

$$\Delta^a \quad \mapsto \quad t^4(J^{-1})^a_b\Delta^b(t) \ . \tag{2.5.175}$$

Note that $\widehat{E}_2$ and Δ^a are sufficient to parametrize all propagators $\hat{\Delta}^{ij},\hat{\Delta}^i,\hat{\Delta}$ introduced in (2.2.37). Indeed, one has

$$\begin{aligned} &\hat{\Delta}^{ab} = -\tfrac{1}{12}C^{ab}\widehat{E}_2 \ , && \hat{\Delta}^{aS} = \Delta^a \ , && \\ &\hat{\Delta}^S = -\tfrac{1}{2}C_{ab}\Delta^a\Delta^b \ , && \hat{\Delta}^a = \tfrac{1}{12}\widehat{E}_2\Delta^a \ , && \hat{\Delta} = -\tfrac{1}{12}\widehat{E}_2 C_{ab}\Delta^a\Delta^b \ . \end{aligned} \tag{2.5.176}$$

Using the explicit form of $\widehat{E}_2$ and Δ^a it is straightforward to check that these propagators fulfill the defining conditions (2.2.37). The fact that all $\hat{\Delta}-$propagators can be expressed as polynomials in $\widehat{E}_2$ and Δ^a implies that all non-holomorphic dependence of $F^{(g)}$ only arises through $\widehat{E}_2,\Delta^a$. However, we also have to extract the non-holomorphic dependence in the covariant derivatives D_a defined in (2.1.11). Following the logic of section 2.3 we will show that each derivative can be split into a holomorphic covariant derivative $\hat{D}_a$ plus holomorphic terms times the propagators Δ^a. As an important byproduct, the definition of $\hat{D}_a$ will also allow us to find an interesting construction of holomorphic automorphic forms.

Let us now construct a holomorphic covariant derivative $\hat{D}_a$, which has the same properties as D_a under automorphic transformations (2.4.128). More precisely, given an automorphic form Ψ of weight k we define its first derivative as

$$\hat{D}_a\Psi \equiv \big(\partial_a - kC_{ab}\epsilon^b\big)\Psi \ , \tag{2.5.177}$$

where ϵ^a is defined in (2.5.173), and note that $\hat{D}_a = D_a - kC_{ab}\Delta^b$. $\hat{D}_a$ can be viewed as the analog of the Serre derivative (2.3.56) for modular forms of subgroups of $Sl(2,\mathbb{Z})$. It is not hard to check that it transforms under (2.4.128) exactly as D_a. This transformation property was given in (2.4.138). Note however, that $\hat{D}_a$ maps holomorphic forms into holomorphic forms, while D_a contains an anti-holomorphic contribution. Moreover, by definition of ϵ^a one has

$$\hat{D}_a\Phi(t) = 0 \ , \tag{2.5.178}$$

for the automorphic form $\Phi(t)$ given in (2.4.104). In order to evaluate second derivatives we need to introduce the holomorphic analog of the Christoffel symbol in the definition (2.1.11) of

D_k. To do that, let us consider a section Ψ_a which transforms as $\Psi_a \mapsto t^{2k} J_a^b \Psi_b$ under the action (2.4.128). The covariant derivative is then defined to act as

$$\hat{D}_a \Psi_b = \big(\partial_a - kC_{ac}\epsilon^c\big)\Psi_b - \hat{\Gamma}^c_{ab}\Psi_c \ . \tag{2.5.179}$$

Here we have included the holomorphic Christoffel symbol

$$\hat{\Gamma}^c_{ab} = \hat{\Gamma}^c_{ab|d}\epsilon^d = \tfrac{1}{2}\hat{C}^{cd}\big(\partial_b \hat{C}_{da} + \partial_a \hat{C}_{db} - \partial_d \hat{C}_{ab}\big) \ , \tag{2.5.180}$$

where $\hat{\Gamma}^b_{cd|a}$ is defined in (2.4.84) and related to Γ^b_{cd} by $\Gamma^b_{cd} = \hat{\Gamma}^b_{cd|a} C^{ae} K_e$. We also have introduced the holomorphic 'metric' $\hat{C}_{ab}$. Explicitly, $\hat{C}_{ab}$ is defined as

$$\hat{C}_{ab} = \Phi^{1/2} C_{ab} \ , \qquad \hat{C}_{ab} \ \mapsto \ J_a^c J_b^d \hat{C}_{cd} \ , \tag{2.5.181}$$

where Φ is given in (2.4.104) and we have also displayed the transformation behavior of $\hat{C}_{ab}$ under (2.4.128) as inferred from (2.4.144) and (2.4.135). Once again we evaluate the transformation behavior of $\hat{D}_a\Psi_b$ under (2.4.128) and finds the holomorphic analog of (2.4.139). It is now easy to show that every non-holomorphic derivative D_a can be split as

$$D_a \Psi_b = \hat{D}_a \Psi_b + kC_{ac}\Delta^c \, \Psi_b + \hat{\Gamma}^c_{ab|d}\Delta^d \, \Psi_c \ . \tag{2.5.182}$$

In other words, whenever Ψ_b is holomorphic the non-holomorphic dependence in $D_a\Psi_b$ arises through the propagators Δ^a only.

Let us now discuss a second interesting application of the holomorphic covariant derivative $\hat{D}_a$. Namely, we will now show how it can be used to construct new holomorphic automorphic forms. To start with let us note that $\epsilon_a = C_{ab}\epsilon^b$ transforms in (2.5.174) similarly to a vector field. We can use this analogy and define a field strength

$$\epsilon^4_{ab} = \partial_a \epsilon_b - \tfrac{1}{2}\hat{\Gamma}^c_{ab}\epsilon_c = \partial_a \epsilon_b - \epsilon_a \epsilon_b + C_{ab}\epsilon^2 \ , \qquad\qquad \epsilon_a = C_{ab}\epsilon^b \ , \tag{2.5.183}$$

which transforms covariantly, $\epsilon^4_{ab} \ \mapsto \ J_a^c J_b^d \epsilon^4_{cd}$, under automorphic transformations (2.4.128). Note that by using the wave-equation (2.4.146) one shows that $\partial_a \epsilon^a = -4C_{ab}\epsilon^a\epsilon^b$ such that

$$C^{ab}\epsilon^4_{ab} = 0 \ . \tag{2.5.184}$$

Nevertheless, we can use ϵ^4_{ab} to construct holomorphic automorphic forms. To do that, we define

$$\epsilon^{2k}_{a_1 \ldots a_k} = \hat{D}_{a_k} \ldots \hat{D}_{a_3} \epsilon^4_{a_2 a_1} \ , \tag{2.5.185}$$

which is shown to be totally symmetric in the indices. Holomorphic automorphic forms are now constructed by contraction with C^{ab}. For example, forms of weight 4 and 6 are given by

$$\begin{aligned} &\text{weight } 4: && C^{ab}C^{cd}\epsilon^4_{ac}\epsilon^4_{bd} \ , && \\ &\text{weight } 6: && C^{ac}C^{be}C^{df}\epsilon^4_{ab}\epsilon^4_{cd}\epsilon^4_{ef} \ , && C^{ac}C^{be}C^{df}\epsilon^6_{abd}\epsilon^6_{cef} \ . \end{aligned} \tag{2.5.186}$$

It is tempting to conjecture that holomorphic automorphic forms of this type are sufficient to parametrize the holomorphic ambiguity of $F^{(g)}$. The fact that there is no holomorphic weight 2 automorphic form of this type due to (2.5.184) matches nicely the fact that there is no holomorphic ambiguity for $F^{(2)}$. Also the forms in (2.5.186) can be shown to be sufficient to parametrize the ambiguities of $F^{(3)}$ and $F^{(4)}$. This will be analyzed in further work.

2.5.3 Direct integration of the holomorphic anomaly

We will now use the material developed in the previous section to perform the direct integration in both fiber and base directions. This will allow us to give closed expressions which determine the $F^{(g)}$ up to a holomorphic ambiguity. To begin with, we show that each $F^{(g)}$ can be written as

$$F^{(g)} = \sum_{k=0}^{g-1} \sum_{n=0}^{2g-2} \widehat{E}_2^k \Delta^{a_1} \dots \Delta^{a_n} c^{(g)}_{k\,|\,a_1 \dots a_n} \ , \qquad g > 1 \tag{2.5.187}$$

where $c^{(g)}_{k\,|\,a_1 \dots a_n}$ are holomorphic functions of S, t^a and all anti-holomorphic dependence arises through the propagators Δ^a and $\widehat{E}_2$ introduced in (2.5.172) and (2.5.173). Note that by using the transformation properties of $F^{(g)}$ and Δ^a given in (2.4.142) and (2.5.175) one infers that

$$c^{(g)}_{k\,|\,a_1 \dots a_n} \ \mapsto \ t^{4g-4-4n} J^{b_1}_{a_1} \dots J^{b_n}_{a_n} \, c^{(g)}_{k\,|\,b_1 \dots b_n} \tag{2.5.188}$$

under automorphic transformations (2.4.128).

Let us now show that each $F^{(g)}$ for $g > 1$ can indeed be written as (2.5.187) by using induction. We first note that $F^{(2)}$ is of the form (2.5.187),

$$F^{(2)} = -\tfrac{1}{2} \widehat{E}_2 C_{ab} \Delta^a \Delta^b \ , \tag{2.5.189}$$

as is immediately inferred from (2.5.162) and (2.5.173). So let us assume that (2.5.187) is true for all $r < g$ and show that this implies that (2.5.187) is true for g. In order to do that we use the Feynman graph expansion (2.2.34) of $F^{(g)}$ [19], which states that each $F^{(g)}$ can be written as an expansion with propagators $\hat{\Delta}^{ij}, \hat{\Delta}^i, \hat{\Delta}$ and vertices $C^{(r)}_{i_1 \dots i_n}$ with $r < g$. We have already shown that the $\hat{\Delta}$-propagators are polynomials in $\widehat{E}_2$ and Δ^a in (2.5.176). Hence, it remains to show that also the vertices $C^{(r)}_{i_1 \dots i_n}$ are polynomials in $\widehat{E}_2$ and Δ^a. By definition (2.2.27) and our assertion, the vertices are defined as the covariant derivatives of amplitudes $F^{(r)}$ of the form (2.5.187). Using (2.5.182) each of these covariant derivatives D_a can be split into a holomorphic covariant derivative $\hat{D}_a$ and an expansion in Δ^a. So we only have to show that $\hat{D}_a \Delta^b$ admits again an expansion into Δ's. A straightforward computation shows that

$$\hat{D}_a \Delta^b = C^{bd} \epsilon^4_{da} - \tfrac{1}{2} \hat{\Gamma}^b_{cd|a} \Delta^c \Delta^d \ , \tag{2.5.190}$$

where ϵ^4_{ab} and $\hat{\Gamma}^b_{cd|a}$ are defined in (2.5.183) and (2.4.84). Altogether one infers that all vertices and $\hat{\Delta}$-propagators are polynomial in Δ^a and hence that $F^{(g)}$ is of the form (2.5.187).

Having shown that every $F^{(g)}$ is of the form (2.5.187) we will now derive a closed expression for $F^{(g)}$ by direct integration of the holomorphic anomaly equation (2.2.30). Applying the definition (2.2.37) of the propagators we can write the holomorphic anomaly equation as

$$\partial_{\bar{\imath}} F^{(g)} = \tfrac{1}{2} \partial_{\bar{\imath}} \hat{\Delta}^{ik} \Big(D_j D_k F^{(g-1)} + \sum_{r=1}^{g-1} D_j F^{(r)} D_k F^{(g-r)} \Big) \ . \tag{2.5.191}$$

This equation captures the anti-holomorphic derivatives $\partial_{\bar{S}} F^{(g)}$ along the base as well as the derivative $\partial_{\bar{a}} F^{(g)}$ along the fiber of the Enriques Calabi-Yau. Recall that the only non-vanishing propagators are $\hat{\Delta}^{ab} = -\frac{1}{12} C^{ab} \widehat{E}_2$ and $\Delta^a = \hat{\Delta}^{aS}$. As we have shown, they contain all anti-holomorphic dependence such that we can rewrite (2.5.191) as

$$\frac{\partial F^{(g)}}{\partial \widehat{E}_2} \ = \ -\tfrac{1}{24} C^{ab} \Big(D_a D_b F^{(g-1)} + \sum_{r=1}^{g-1} D_a F^{(r)} D_b F^{(g-r)} \Big) \ , \tag{2.5.192}$$

$$\frac{\partial F^{(g)}}{\partial \Delta^a} \ = \ D_a D_S F^{(g-1)} + \sum_{r=1}^{g-1} D_a F^{(r)} D_S F^{(g-r)} \ . \tag{2.5.193}$$

As we have seen above, the first equation is already very powerful and can be integrated easily. We can write the solution (2.5.152) as

$$F^{(g)} = -\tfrac{1}{24}\sum_{k=1}^{\infty}\tfrac{1}{k}\widehat{E}_2^k C^{ab}\Big(D_aD_bc_{k-1}^{(g-1)} + \sum_{r=1}^{g-1}\sum_{l+m=k-1} D_ac_l^{(r)}D_bc_m^{(g-r)}\Big) + c_0^{(g)}\ , \tag{2.5.194}$$

where $c_m^{(1)}$ is defined in (2.5.153). Note that $c_0^{(g)}(\Delta,S,t)$ arises an integration constant of the $\widehat{E}_2$ integration and hence can be a function of the propagators Δ^a but not $\widehat{E}_2$.

Let us now determine a second closed expression for $F^{(g)}$ by integrating the second anomaly equation (2.5.193). Since $F^{(1)}$ is not of the form (2.5.187) we first split off terms involving $F^{(1)}$. Inserting the definitions of the propagators Δ^a and $\widehat{E}_2$ we find for $g>2$ that

$$\frac{\partial F^{(g)}}{\partial\Delta^a} = (D_S+\tfrac{1}{2}\widehat{E}_2)D_aF^{(g-1)} - 2C_{ac}\Delta^cD_SF^{(g-1)} + \sum_{r=2}^{g-2}D_aF^{(r)}D_SF^{(g-r)}. \tag{2.5.195}$$

To make the dependence on the propagators Δ^a explicit we expand the covariant derivative $D_aF^{(g)}$. The covariant derivative D_a can be split into a holomorphic derivative $\hat{D}_a$ defined in (2.5.179) plus a propagator expansion using (2.5.182). Moreover, using the chain rule one rewrites

$$\hat{D}_a = \hat{d}_a + (\hat{D}_a\Delta^b)\partial_{\Delta^b}\ , \tag{2.5.196}$$

where $\hat{d}_a$ is the covariant holomorphic derivative not acting on the propagators, i.e. we set

$$\hat{d}_a\big(\Delta^{a_1}\dots\Delta^{a_n}c_{a_1\dots a_n}\big) = \Delta^{a_1}\dots\Delta^{a_n}\hat{D}_ac_{a_1\dots a_n}\ . \tag{2.5.197}$$

Combining (2.5.182), (2.5.196) and (2.5.190) we immediately derive

$$D_aF^{(g)} \;=\; \Big[\hat{d}_a + \epsilon_{ac}^4C^{cb}\partial_{\Delta^b} + (2g-2)C_{ad}\Delta^d - \tfrac{1}{2}\hat{\Gamma}^b_{cd|a}\Delta^c\Delta^d\partial_{\Delta^b}\Big]F^{(g)}\ . \tag{2.5.198}$$

This expansion makes the dependence of D_a on the propagators Δ^a explicit. We note that the $\hat{d}_a$ term on the right-hand side of this expansion does not change the number of propagators. The second term lowers the number of propagators by one, while the two last terms raise the number of propagators by one. Inspecting the holomorphic anomaly equation we note that only the first derivative along the fiber direction appears on the right-hand side of (2.5.195). Hence, at least for the integration of (2.5.195) it will not be necessary to evaluate the second derivative $D_aD_bF^{(g)}$ as a propagator expansion.

To integrate expressions such as (2.5.198) for $D_aF^{(g)}$ we also need to keep track of the number of propagators in the expansion of $F^{(g)}$. Therefore, we introduce the following shorthand notation

$$F^{(g)} = \sum_n c^{(g)}_{(n)}\ , \qquad\qquad c^{(g)}_{(n)} = \sum_{k=0}^{g-1}\widehat{E}_2^k\Delta^{a_1}\dots\Delta^{a_n}c^{(g)}_{k\,|\,a_1\dots a_n}\ , \tag{2.5.199}$$

where each $c^{(g)}_{(n)}$ contains n propagators Δ^a. By counting the number of propagators one finds

$$\int D_aF^{(g)}d\Delta^a = \sum_n\Big\{\tfrac{1}{n+1}\Delta^a\hat{d}_a + \tfrac{1}{n}\Delta^a\epsilon_{ac}^4C^{cb}\partial_{\Delta^b} + \tfrac{4g-4-n}{n+2}\Delta^2\Big\}c^{(g)}_{(n)}\ , \tag{2.5.200}$$

where as defined above $\Delta^2 = \frac{1}{2}C_{ab}\Delta^a\Delta^b$. This integral together with similar ones for the remaining terms in (2.5.195) yields a closed expression for $F^{(g)}$ of the form

$$\begin{aligned} F^{(g)} \;=\;& (D_S+\tfrac{1}{2}\widehat{E}_2)\sum_n\Big\{\tfrac{1}{n+1}\Delta^a\hat{d}_a + \tfrac{1}{n}\Delta^a\epsilon_{ac}^4C^{cb}\partial_{\Delta^b} + \tfrac{4g-8-n}{n+2}\Delta^2\Big\}c^{(g-1)}_{(n)} \\ &- \sum_n\tfrac{4}{n+2}\Delta^2D_Sc^{(g-1)}_{(n)} + \sum_{r=2}^{g-2}\sum_n\sum_{k+l=n}D_Sc^{(g-r)}_{(l)}\Big\{\tfrac{1}{n+1}\Delta^a\hat{d}_a \\ &+\tfrac{1}{n}\Delta^a\epsilon_{ac}^4C^{cb}\partial_{\Delta^b} + \tfrac{4r-4-n}{n+2}\Delta^2\Big\}c^{(r)}_{(k)} + c^{(g)}_{(0)}\ . \end{aligned} \tag{2.5.201}$$

Here $c^{(g)}_{(0)}(\widehat{E}_2, S, t)$ is the integration constant of the Δ^a integration and hence can depend on $\widehat{E}_2$ but not on Δ^a.

Before turning to the discussion of an explicit example, let us consider the fiber limit of (2.5.201). We therefore apply (C.1.20) and (2.5.157) to show that

$$\lim_{S,\bar{S}\to\infty} D_S F^{(g)} = 0 \ . \tag{2.5.202}$$

We also denote by $c^{(g)}_{E\,(k)}$ the fiber limit of the coefficients $c^{(g)}_{(k)}$ in (2.5.199). Inserting (2.5.202) into the formula (2.5.201) for direct integration along the fiber direction one finds

$$F^{(g)}_E = \tfrac{1}{2}\sum_n \Big(\tfrac{1}{n+1}\Delta^a \hat{d}_a + \tfrac{1}{n}\Delta^a \epsilon^4_{ac} C^{cb}\partial_{\Delta^b} + \tfrac{4g-8-n}{n+2}\Delta^2\Big) c^{(g-1)}_{E\,(n)} + c^{(g)}_{E\,(0)} \ , \tag{2.5.203}$$

where $c^{(g)}_{E\,(0)}(t)$ is a holomorphic ambiguity in the fiber. Recall that the full expression (2.4.110) for $F^{(g)}_E(t,\bar{t})$ is known from heterotic-type II duality. Therefore, verifying that this closed expression fulfills the differential equation (2.5.203) provides a non-trivial check of our derivations.

Let us end this section by presenting the first non-trivial solution to the closed expressions (2.5.194) and (2.5.201) for $F^{(g)}$. More precisely, one derives that the free energy $F^{(3)}$ admits the following propagator expansion

$$\begin{aligned} F^{(3)} \ &= \ -\tfrac{1}{48}\hat{E}_2^2\big(14\Delta^4 + 10\epsilon^4_{ab}\Delta^a\Delta^b - \epsilon^4_{ac}\epsilon^4_{bd}C^{ab}C^{cd}\big) \\ &\quad -\tfrac{1}{48}E_4\big(-2\Delta^4 + 2\epsilon^4_{ab}\Delta^a\Delta^b - \epsilon^4_{ac}\epsilon^4_{bd}C^{ab}C^{cd}\big) \ , \end{aligned} \tag{2.5.204}$$

where ϵ^4_{ab} is defined in (2.5.183). Note that the last term in the first line has to be determined by the direct integration with respect to $\widehat{E}_2$ by using (2.5.194). Moreover, the purely holomorphic term

$$f^{(3)}(S,t) = \tfrac{1}{48}E_4\epsilon^4_{ac}\epsilon^4_{bd}C^{ab}C^{cd} \tag{2.5.205}$$

is the holomorphic ambiguity at genus 3, determined by the fiber limit. In other words, applying (2.5.157) one easily derives

$$F^{(3)}_E = -\tfrac{1}{4}\epsilon^4_{ab}\Delta^a\Delta^b - \tfrac{1}{4}\Delta^4 + \tfrac{1}{24}\epsilon^4_{ac}\epsilon^4_{bd}C^{ab}C^{cd} \ , \tag{2.5.206}$$

which is readily compared with the general expression (2.4.110) for the fiber free energies. It is straightforward to derive all $F^{(g)}$ for $g < 7$ by evaluating (2.5.194) and (2.5.201) and fixing the ambiguity by comparison with the fiber result (2.4.110). Clearly, at genus greater than 6 we will encounter the same difficulties as in section 2.5.1. Only additional boundary conditions can help to fix the ambiguities in these cases. In the next section we will summarize possible additional conditions.

2.5.4 Boundary conditions

One important feature of the formalism of direct integration is that modular and holomorphic properties of the $F^{(g)}$ are manifest. In particular the ambiguity is holomorphic, modular invariant and for given genus expressible in terms of a modular form of finite weight. This implies that a finite number of data will fix it. The latter must be provided from additional information at the boundaries of the moduli space of the Calabi-Yau manifold. Let us give a short overview over the the nature of these boundary conditions.

In the large radius limit the holomorphic limit of the $F^{(g)}$ has an expansion in terms of Gromov-Witten invariants $N^{(g)}_\beta$. Since the an-holomorphic part is fixed, the $F^{(g)}$ can be completely determined by calculating a finite number of Gromov-Witten invariants. The reorganisation of the expansion in terms of Gopakumar-Vafa invariants $n^{(g)}_\beta$ is useful here, because the

latter vanish if the degree is higher then the maximal degree for which a smooth curve exists in a given class.

For K3-fibered Calabi-Yau threefolds, the limit of large base volume corresponds generically to a perturbative heterotic string theory on K3$\times\mathbb{T}^2$. If the heterotic theory is known one can calculate the dependence of the $F^{(g)}$ on the fiber moduli by calculating a BPS saturated one loop amplitude in the heterotic string [29, 79]. In the Enriques CY case this yields most of the information and is the reason that one can tackle an 11 parameter model at all. Even if the heterotic dual is not known, one may get all the holomorphic $F^{(g)}$ in the fiber from the modular properties of the B-model on the K3 and the formula for the cohomology of the Hilbert scheme of points on the fiber [97].

If the Calabi-Yau admits controllable local limits, e.g. to toric Fano varieties with anti-canonical bundle, then the $F^{(g)}$ can be unambiguously calculated using the topological vertex [31]. One can also find boundary conditions by looking at the behavior of the topological string amplitudes near the conifold point, as we discussed in section 2.3.3. When there is only one hypermultiplet becoming massless at the conifold point, the amplitudes behave like (2.3.69), where t_D is a suitable coordinate transverse to the conifold divisor. This yields $2g-2$ independent conditions on the holomorphic ambiguity.

In contrast to generic $\mathcal{N}=2$ compactifications, the four dimensional massless spectrum at singularities of the Enriques Calabi-Yau is conformal, which requires hyper- and vector multiplets to become simultaneously massless. The leading behavior of the corresponding effective action is less characteristic. We will find a partial gap in the reduced model considered in section 2.5.5, which is similar to the partial gap structures that were found in [69] at a point where likewise several RR states become massless. The determination of the subleading behavior is possible in the field theory limit and yields conditions on the anomaly. We will consider here only the complex codimension singularities that we discussed in section 2.4. The nontrivial information about the $F^{(g)}$ comes from the $N_f=4$ locus: as we will show in section 2.6, the residue of the leading singularity near (2.4.88) can be computed using instanton counting in field theory.

Let us now analyze the leading singularity of $\mathcal{F}^{(g)}$ near the singular loci in the fiber limit. This can be done with the heterotic computations of [79] reviewed in section 2.4. These computations give us expansions around two special regions in moduli space, the large radius limit (where t^a are large) and the region appropriate to the BHM reduction (where t^a_D are large). As in [18, 29], we can use the computation at large radius to obtain the leading behavior of the fiber amplitudes near (2.4.88), and the computation in the BHM reduction to obtain the behavior near (2.4.90).

Let us first look at the behavior near (2.4.88). A possible singular behavior there must come from the vector $r=(1,-1)$ in (2.4.95), since this leads to a polylogarithm which, when expanded at the singular locus (2.4.88),

$$\mathrm{Li}_{3-2g}(\mathrm{e}^{-z}) = \frac{(2g-3)!}{z^{2g-2}} + \mathcal{O}(z^0), \quad g\geq 2, \tag{2.5.207}$$

exhibits a pole. Here, $z=t^1-t^2$. However, since $c_g(-2)=0$, the coefficient of this polylogarithm vanishes and we conclude that the amplitudes are regular at (2.4.88). This is indeed consistent with the fact that the field theory limit of this model at (2.4.88) is massless $SU(2)$, $\mathcal{N}=4$ super Yang–Mills theory, which has $\mathcal{F}^{(g)}=0$ for all $g\geq 2$ [80, 100, 101].

Let us now look at the behavior near (2.4.90). To understand this, we look at the heterotic result for the holomorphic couplings in the BHM reduction (2.4.111). Again, the singular behavior comes from the vector $r=(1,-1)$. Since the coefficients are defined now by (2.4.112), we find

$$d_g(-1) = \frac{4^g-1}{2^{g-2}}\frac{|B_{2g}|}{2g(2g-2)!}. \tag{2.5.208}$$

If we set

$$\mu = t^1_D - t^2_D, \tag{2.5.209}$$

and we take into account the behavior of the polylogarithm (2.5.207), we find that the singular behavior of $\mathcal{F}_E^{(g)}(t_D)$ near (2.4.90) is given by

$$\mathcal{F}_E^{(g)}(t_D) \to \frac{4^g-1}{2^{g-2}} \frac{|B_{2g}|}{2g(2g-2)} \frac{1}{\mu^{2g-2}} + \mathcal{O}(\mu^0) \tag{2.5.210}$$

for $g \geq 2$, while for $g = 1$ we have a logarithm singularity

$$-\frac{1}{2} \log \mu. \tag{2.5.211}$$

Since the full $\mathcal{F}^{(g)}(S, t_D)$ can be written for $g \leq 6$ in terms of (2.4.111), as we showed in section 2.5.1, we can compute its leading singular behavior at the locus (2.4.90). This will be useful in section 2.6 to compare to the field theory limit. The above computation shows that along the fiber direction the topological string amplitudes $\mathcal{F}_E^{(g)}$ show the gap behavior discovered in [89, 69]. In order to see if the gap also holds in the mixed directions, it is clear from the formulae above that we need a precise knowledge of the regular terms in μ in the expansion of $\mathcal{F}_E^{(g)}$. Unfortunately, this is something we cannot extract from the heterotic expressions. We will however be able to do this in the reduced model introduced in [79] and studied in more detail below. We will see that indeed the strong gap condition obtained for the fiber direction in (2.5.210) does not hold for the mixed directions.

2.5.5 The reduced Enriques model

We now discuss a reduced model for the Enriques Calabi-Yau introduced in [79]. The main advantage of this model is that the target symmetry group becomes much simpler, and one can easily parametrize the holomorphic functions which appear in the expansion of $F^{(g)}$ in the propagators $\Delta^a(t, \bar{t})$ and $\widehat{E}_2(S, \bar{S})$. In particular, the holomorphic ambiguity can be parametrized in terms of a finite number of coefficients at each genus. Also the mirror map is known explicitly and can be used to translate the $F^{(g)}$ into a simple polynomial form. In these aspects, the reduced model is very closely related to the Seiberg–Witten theory studied in section 2.3.

Special geometry and the mirror map

We begin with a brief discussion of the reduced special geometry and recall the mirror map derived in [79]. Out of the eleven special coordinates S, t^a the reduced model is only parametrized by three parameters. More precisely, it is obtained by shrinking 8 out of the 10 cycles in the Enriques fiber as

$$(S, t^a) = (S, t^i, t^\alpha) \quad \to \quad (S, t^i, 0) \ , \qquad i = 1, 2 \ , \quad \alpha = 3, \ldots, 10 \ . \tag{2.5.212}$$

We denote the reduced moduli space spanned by the remaining coordinates S, t^1, t^2 by $\mathcal{M}_{\rm r}$. Explicitly, the full coset (2.4.75) reduces in this limit to

$$\mathcal{M}_{\rm r} = \frac{Sl(2,\mathbb{R})}{SO(2)} \times \left(\frac{Sl(2,\mathbb{R})}{SO(2)} \right)^2 \ , \tag{2.5.213}$$

inducing a split of the full target space symmetry group as

$$Sl(2,\mathbb{Z}) \times O(10,2,\mathbb{Z}) \quad \to \quad Sl(2,\mathbb{Z}) \times \Gamma(2) \times \Gamma(2) \ . \tag{2.5.214}$$

The generators of $Sl(2,\mathbb{Z})$ are precisely the Eisenstein series $\widehat{E}_2(S, \bar{S})$, $E_4(S)$, $E_6(S)$ as already introduced for the full model in (2.5.147). The generators for $\Gamma(2)$ have been introduced in the Seiberg-Witten section 2.3. More precisely, we will generate the ring of almost holomorphic

modular forms of $\Gamma(2)$ by $\widehat{E}_2(t,\bar{t})$, $K_2(t)$ and $K_4(t)$ explicitly defined in (2.5.149) and (2.3.42). In the following we will simplify expressions by abbreviating

$$\begin{aligned} E_2 &= E_2(t^1)\ , & K_2 &= K_2(t^1)\ , & K_4 &= K_4(t^1)\ , \\ \tilde{E}_2 &= E_2(t^2)\ , & \tilde{K}_2 &= K_2(t^2)\ , & \tilde{K}_4 &= K_4(t^2)\ . \end{aligned} \tag{2.5.215}$$

Whenever not stated otherwise, we will keep the S-dependence explicit. Let us also note that the matrix C_{ab} splits as

$$C_{ab} = \begin{pmatrix} C_{ij} & 0 \\ 0 & C_{\alpha\beta} \end{pmatrix}\ , \qquad C_{ij} = \begin{pmatrix} 0 & 1 \\ 1 & 0 \end{pmatrix}\ , \tag{2.5.216}$$

as already given in (2.4.80). Hence, the holomorphic prepotential (2.4.78) and the fiber Kähler potential $Y = (t+\bar{t})^2$ reduce to

$$\mathcal{F}_{\rm r} = iSt^1t^2\ , \qquad Y_{\rm r} = (t^1+\bar{t}^1)(t^2+\bar{t}^2)\ . \tag{2.5.217}$$

As we have already noted in section 2.4.1 this prepotential and fiber potential are exact and receive no instanton corrections.

Let us now turn to a discussion of the mirror map for the reduced Enriques model. In order to determine this duality map we first note that the reduced Enriques has an algebraic realization. Applying standard techniques, one can thus derive the three Picard-Fuchs equations for the holomorphic three-form $\Omega(z)$ as

$$\mathcal{L}_1\Omega(z) = 0\ , \qquad \mathcal{L}_2\Omega(z) = 0\ , \qquad \mathcal{L}_3\Omega(z) = 0\ , \tag{2.5.218}$$

where $z^i(t), z^3(S)$ with $i = 1,2$ are the mirror coordinates of t^i, S respectively. The Picard-Fuchs operators are found to be

$$\mathcal{L}_i = \theta_i^2 - 4(4\theta_i + 4\theta_j - 3)(4\theta_i + 4\theta_j - 1)z_i\ , \qquad i,j = 1,2\ ,\quad i \neq j\ , \tag{2.5.219}$$

$$\mathcal{L}_3 = 36(z^3-1)^2(z^3-2)\theta_3^2 + 36z^3(z^3-1)\theta_3 + z^3\big(8z^3 - 4(z^3)^2 - 31\big)\ , \tag{2.5.220}$$

where $\theta_i = z^i\frac{\partial}{\partial z^i}$. The Picard-Fuchs equations (2.5.218) can be solved to determine the mirror maps $z^i(t), z^3(S)$. This was done in [79] and we will only quote the result here. We first abbreviate

$$z(q_i) = \frac{K_4(t^i)}{K_2^2(t^i)}\ . \tag{2.5.221}$$

Using this shorthand notation the fiber mirror map reads

$$z^1(t) = z(q_1)\big(1 - z(q_2)\big)\ , \qquad z^2(t) = z(q_2)\big(1 - z(q_1)\big)\ . \tag{2.5.222}$$

These coordinates are related by a factor of 64 to z_1, z_2 used in ref. [79]. In the base one evaluates

$$z^3(S) = 1 - E_4^{-3/2}E_6\ . \tag{2.5.223}$$

Compared to [79] we have rescaled z^3 by a factor 864. Using these explicit expressions for z^1, z^2 and z^3, one immediately verifies their invariance under the target space symmetry group $Sl(2,\mathbb{Z}) \times \Gamma(2) \times \Gamma(2)$. Also the fundamental period X^0 can be obtained from the Picard-Fuchs system (2.5.218) and reads

$$X^0 = x^0\hat{X}^0\ , \qquad (\hat{X}^0)^2 = \tfrac{1}{4}K_2\tilde{K}_2\ , \qquad (x^0)^4 = E_4\ . \tag{2.5.224}$$

We immediately verify that X^0 is not invariant under the symmetry group $Sl(2,\mathbb{Z}) \times \Gamma(2) \times \Gamma(2)$. The S-duality transformation (2.4.128) reads for the reduced model $t^1 \mapsto 1/t^2$ and $t^2 \mapsto 1/t^1$. Applied to X^0 this yields precisely the transformation behavior given in (2.4.133). Before turning

to the higher genus amplitudes in the next section let us also note that the discriminant of the reduced model is given by

$$\Delta(z^1, z^2)\ D(z^3)\ , \tag{2.5.225}$$

where $\Delta(z^1, z^2)$ is the discriminant along the fiber and $D(z^3)$ is the discriminant along the base. Explicitly, we find in the coordinates (2.5.221) and (2.5.222) that

$$\begin{aligned} \Delta(z^1, z^2) &= \big(1 - z(q_1) - z(q_2)\big)^2 && (2.5.226)\\ &= 1 - 2(z^1 + z^2 + z^1 z^2) + (z^1)^2 + (z^2)^2\ . && (2.5.227) \end{aligned}$$

The second discriminant $D(z^3)$ is given by

$$D(z^3) = \tfrac{1}{2^6 3^3}\big((z^3)^2 - z^3\big)\ . \tag{2.5.228}$$

In the next section we will use the mirror coordinates z^1, z^2 to express the reduced free energies $F_r^{(g)}$. Since along the base direction all equations are expressed in terms of simple Eisenstein series $E_{2n}(S)$ we choose to keep this S-parametrisation also in the following discussions.

Reduced free energies and direct integration

Let us now discuss the free energies $F_r^{(g)}$ and their holomorphic limits $\mathcal{F}_r^{(g)}$ for the reduced model. In the limit (2.5.212) they are simply defined as

$$F_r^{(g)}(S, t^1, t^2) = F^{(g)}(S, t^1, t^2, t^\alpha = 0)\ . \tag{2.5.229}$$

The reduced form of $F^{(1)}$ can be derived by direct computation as was already discussed in [79]. Explicitly one finds

$$F_{\rm r}^{(1)} = -2\log\big[(S+\bar S)^3(t^1+\bar t^1)(t^2+\bar t^2)\big] - \log|\Phi_{\rm r}(S,t)|\ , \tag{2.5.230}$$

where

$$\Phi_{\rm r}(S, t^1, t^2) = \eta^{24}(S)\prod_{m,n}\Big(\frac{1-q^n q^m}{1+q^n q^m}\Big)^{c_1^{\rm r}(2mn)}\ . \tag{2.5.231}$$

The coefficients $c_1^r(n)$ are given through the modular form

$$\sum_n c_1^{\rm r}(n) q^n = -\frac{64}{3\eta^6(q)\vartheta_2^6(q)} E_2(q) E_4(q^2)\ . \tag{2.5.232}$$

Note that in comparison with the expression (2.4.98) for the full Enriques model the Eisenstein series $E_4(q^2)$ appears in (2.5.232). This extra factor arises due to the summation over the E_8 vectors in (2.4.104) and precisely counts their degeneracy. It was further shown in [79] that the following denominator formula holds

$$\Phi_{\rm r}(S, t^1, t^2) = \tfrac{1}{16}\eta^{24}(S)\ \delta = \eta^{24}(S)(\hat X^0)^4\Delta^{1/2} \tag{2.5.233}$$

where

$$\delta(t^1, t^2) = K_2^2\tilde K_2^2 - K_4\tilde K_2^2 - K_2^2\tilde K_4\ . \tag{2.5.234}$$

Here the $\Gamma(2)$ generators $K_2, \tilde K_2$ as well as $K_4, \tilde K_4$ are defined in (2.5.215), while the fundamental period $\hat X^0$ and the discriminant Δ were given in (2.5.224) and (2.5.226).

The holomorphic reduced amplitudes restricted to the Enriques fiber can also be computed directly by reducing the heterotic expressions (2.4.95) and (2.4.111). The result reads [79]

$$\begin{aligned} \mathcal{F}_{{\rm r},E}^{(g)}(t) &= \sum_{r>0} c_g^{\rm r}(r^2)\Big[2^{3-2g}{\rm Li}_{3-2g}(e^{-r\cdot t}) - {\rm Li}_{3-2g}(e^{-2r\cdot t})\Big]\ ,\\ \mathcal{F}_{{\rm r},E}^{(g)}(t_D) &= \sum_{r>0} d_g^{\rm r}(r^2/2)(-1)^{n+m}{\rm Li}_{3-2g}({\rm e}^{-r\cdot t_D})\ , \end{aligned} \tag{2.5.235}$$

where the coefficients $c^{\mathrm{r}}(n)$, $d_g^{\mathrm{r}}(n)$ are defined by

$$\begin{aligned}\sum_n c_g^{\mathrm{r}}(n)q^n &= -2E_4(q^2)\frac{\mathcal{P}_g(q)}{\eta^{12}(2\tau)}\ ,\\ \sum_n d_g^{\mathrm{r}}(n)q^n &= E_4(q^2)\frac{2^{2+g}\mathcal{P}_g(q^4)-2^{2-g}\mathcal{P}_g(q)}{\eta^{12}(2\tau)}\ .\end{aligned} \tag{2.5.236}$$

Once again we recognize the additional factor $E_4(q^2)$ counting the degeneracies of the E_8 lattice. Clearly, also the expressions $\mathcal{F}^{(g)}_{\mathrm{r},E}(t)$ and $\mathcal{F}^{(g)}_{\mathrm{r},E}(t_D)$ can be expressed in terms of the holomorphic generators (2.5.215) depending on t^i and t^i_D respectively.

Let us now turn to the discussion of the complete reduced amplitudes including the base and the non-holomorphic dependence. In order to do that we describe the direct integration for the reduced model focusing on the essential differences to the considerations presented in section 2.5.3. To begin with, note that the propagators of the full model reduce as

$$\Delta^i \quad\to\quad \Box^i\ , \qquad\qquad \Delta^\alpha \quad\to\quad 0\ , \tag{2.5.237}$$

where $\Box^i$ is obtained from (2.5.173) by setting $t^\alpha = 0$ and using (2.5.231). That Δ^α reduces to zero arises from the fact that in summation over the E_8 lattice the vectors cancel pairwise. In order to perform the direct integration we first have to find recursive relations which are valid for the reduced free energies $F^{(g)}_{\mathrm{r}}$. Recall that in the full Enriques model we found two sorts of recursive relations (2.5.192) and (2.5.193) capturing the properties $F^{(g)}$ in the base and in the fiber of the Enriques. It turns out that only the second anomaly equation (2.5.193) admits a simple reduction. More precisely, it can be rewritten for the reduced model as

$$\frac{\partial F^{(g)}_{\mathrm{r}}}{\partial \Box^i} = D_S D_i F^{(g-1)}_{\mathrm{r}} + \sum_{r=1}^{g-1} D_i F^{(r)}_{\mathrm{r}} D_S F^{(g-r)}_{\mathrm{r}}\ , \tag{2.5.238}$$

since performing the reduction $t^\alpha = 0$ interchanges with the differentiation with respect to t^1, t^2. Note that this is no longer true for derivatives with respect to t^α. In particular, the first equation (2.5.192) involves a summation over the α indices and one shows that the resulting terms do not vanish under the reduction $t^\alpha = 0$. Nevertheless, one can directly integrate (2.5.238) for the reduced free energies

$$F^{(g)}_{\mathrm{r}} = \sum_{n=1}^{2g-2} \Box^{i_1}\ldots\Box^{i_n}\,\hat{c}^{(g)}_{i_1\ldots i_n} + \hat{c}^{(g)}\ , \qquad g>1\ . \tag{2.5.239}$$

The function $\hat{c}^{(g)}$ is holomorphic in t^i and generally depends on $\widehat{E}_2(S,\bar{S}), E_4(S), E_6(S)$. Note that due to (2.5.237) the coefficients of the full and reduced model are related by $\hat{c}^{(g)}_{i_1\ldots i_n} = c^{(g)}_{i_1\ldots i_n}(t^\alpha = 0)$. The direct integration is performed in analogy to the integration in the full model and results in a closed expression similar to (2.5.201). The important difference is that the $\epsilon^4_{\mathrm{r}\,ij}$ as well as the covariant derivatives $\hat{D}^{\mathrm{r}}_a$ are not obtained from the full ϵ^4_{ab} and $\hat{D}_a$ by simply restricting to the i,j indices and setting $t^\alpha = 0$. Both $\epsilon^4_{\mathrm{r}\,ij}$ as well as $\hat{D}^{\mathrm{r}}_a$ have to be defined with respect to a new holomorphic metric $\hat{C}^{\mathrm{r}}_{ij} = \Phi_{\mathrm{r}}^{1/2} C_{ij}$ but otherwise analog to (2.5.183) and (2.5.179). If one had been using the old connection, an additional summation over the α indices would arise and yield extra contributions. Applied to the specific free energy $F^{(3)}$ one finds the reduction of the holomorphic ambiguity (2.5.205)

$$f^{(3)}_{\mathrm{r}}(S,t) = \tfrac{1}{48}E_4\big(\epsilon^4_{\mathrm{r}\,ik}\epsilon^4_{\mathrm{r}\,jl}C^{ij}C^{kl} + \tfrac{1}{8}(\epsilon^4_{\mathrm{r}\,ij}C^{ij})^2\big) \tag{2.5.240}$$

After these considerations it is not surprising that the contraction of the new $\epsilon^4_{\mathrm{r}\,ij}$ with C^{ij} does not vanish as it is the case in the full model (2.5.184).

The free energies $F^{(g)}$ on the mirror

So far the reduced free energies $F_{\rm r}^{(g)}$ were expressed as functions of the variables t^i, S or t^i_D, S. In the reduced model we know the mirror map explicitly and thus will be able to translate the expansion (2.5.239) of $F_{\rm r}^{(g)}$ into a function of the complex coordinates z^i. We will show that the holomorphic coefficients become polynomials in z^i divided by an appropriate power of the discriminant. Since the dependence of $F_{\rm r}^{(g)}$ is rather transparent we chose to keep this variable and do not replace it by its mirror counterpart z^3.

The $F^{(g)}$ transform non-trivially under the reduced automorphic transformations. We already discussed the actually invariant combination in (2.4.143). In the coordinates z^i, S we thus set

$$F^{(g)}(z,\bar z,S,\bar S) = (\hat X^0)^{2-2g}\, F^{(g)}(t,\bar t,S,\bar S)\ . \tag{2.5.241}$$

This definition is consistent with the fact that the $z^i(t)$ are invariant under the target space group (2.5.214), while $(\hat X^0)^{2g-2}$ transforms exactly as $F^{(g)}(t,S)$. To rewrite the expansion (2.5.239) we first note that the propagator $\Box^i$ can be written in the z^i coordinates as

$$\Box^i = (\hat X^0)^2 \frac{\partial t^i}{\partial z^j}\Box^{z^j}\ , \qquad\qquad \Box^{z^i} = -C^{z^i z^j}\big(\hat K_{z^j} - \tfrac{1}{8}\partial_{z^j}\log\Delta\big)\ , \tag{2.5.242}$$

where $\Box^{z^i}$ is a function of $z^i, \bar z^i$ and we have used

$$C_{ij} = (\hat X^0)^{-2} C_{z^k z^l}\frac{\partial z^k}{\partial t^i}\frac{\partial z^l}{\partial t^j}\ , \qquad\qquad \hat K(z,\bar z) \equiv -\log\big[|\hat X^0|^2 Y_{\rm r}(z,\bar z)\big]. \tag{2.5.243}$$

It is not hard to use the expressions (2.5.222) for z^1 and z^2 to evaluate $C_{z^i z^j}$ explicitly as

$$C_{z^1 z^2} = \frac{1}{z^1 z^2\Delta}(1-z^1-z^2)\ , \qquad C_{z^1 z^1} = \frac{1}{z^1 z^2\Delta}2z^2\ , \qquad C_{z^2 z^2} = \frac{1}{z^1 z^2\Delta}2z^1\ . \tag{2.5.244}$$

Once again (2.5.242) and (2.5.243) are in accordance with the transformation behavior of the $\Box^i$ and C_{ij} given in (2.5.175) and (2.4.135). Similarly, we transform the coefficients $\hat c^{(g)}_{i_1\ldots i_n}$ in (2.5.239) and set

$$\hat c^{(g)}_{i_1\ldots i_n} = (\hat X^0)^{2g-2-2n}\ \frac{\partial z^{j_1}}{\partial t^{i_1}}\cdots\frac{\partial z^{j_n}}{\partial t^{i_n}}\ \hat c^{(g)}_{z^{j_1}\ldots z^{j_n}}(z)\ , \tag{2.5.245}$$

which is consistent with (2.5.189). It is also straightforward to rewrite the direct integration expression for $F_{\rm r}^{(g)}$ by using the z^i coordinates. Let us once again only discuss the appearing building blocks. We begin by noting that the holomorphic covariant derivative transforms as

$$\hat D_i V_j = (\hat X^0)^{2k}\frac{\partial z^l}{\partial t^i}\frac{\partial z^m}{\partial t^j}\hat D_{z^l} V_{z^m}\ , \tag{2.5.246}$$

where the covariant derivative $\hat D_{z^i}$ is given by

$$\hat D_{z^i} V_{z^j} = \partial_{z^i} V_{z^j} - \tfrac{k}{8}(\partial_{z^i}\log\Delta)V_{z^j} + \hat\Gamma^{z^l}_{z^i z^j}V_{z^l}\ . \tag{2.5.247}$$

The holomorphic Christoffel symbol in this expression is defined by

$$\hat\Gamma^{z^l}_{z^i z^j} = \tfrac{1}{2}\hat C^{z^l z^m}\big(\partial_{z^i}\hat C_{z^m z^j} + \partial_{z^j}\hat C_{z^i z^m} - \partial_{z^m}\hat C_{z^i z^j}\big)\ , \qquad \hat C_{z^i z^j} = \Delta^{1/4} C_{z^i z^j}\ . \tag{2.5.248}$$

The second important object in the general equation for the direct integration is the automorphic form $\epsilon^4_{{\rm r}\,ij}$. One shows that it can be decomposed as

$$\epsilon^4_{{\rm r}\,ij} = \frac{1}{z^1 z^2\Delta^2}\frac{\partial z^l}{\partial t^i}\frac{\partial z^m}{\partial t^j}\ \epsilon^4_{z^l z^m}\ . \tag{2.5.249}$$

where for $i=1,2$, $i\neq j$ one finds that

$$\begin{aligned}\epsilon^4_{z^i z^i} &= -\tfrac{1}{16} z^j \left((z^i)^2\,\left(1+3\,z^j\right)+\left(-1+z^j\right)^2\,\left(1+3\,z^j\right)-2\,z^i\,\left(1-5\,z^j+3\,(z^j)^2\right)\right)\,,\\ \epsilon^4_{z^i z^j} &= \tfrac{3}{16}\,z^i\,z^j\,\left(-2+z^i+(z^i)^2+z^j+(z^j)^2-2\,z^i\,z^j\right)\,.\end{aligned} \tag{2.5.250}$$

Note that $\epsilon^4_{z^i z^i}$ is polynomial due to the fact that we extracted the denominator $z^1 z^2 \Delta^2$ in (2.5.249). This turns out to be possible for all the coefficients $\hat{c}^{(g)}_{z^{i_1}\ldots z^{i_n}}$ appearing in (2.5.245). We thus define

$$P^{(g)}_{i_1\ldots i_n}(z,\widehat{E}_2,E_4,E_6) = (z^1 z^2\Delta)^{g-1}\;\hat{c}^{(g)}_{z^{i_1}\ldots z^{i_n}}\;, \tag{2.5.251}$$

where $P^{(g)}$ are polynomials in z^i as well as $\widehat{E}_2, E_4, E_6$. The reduced free energies are thus of the form

$$F^{(g)}_{\rm r}(z,\bar{z},S,\bar{S}) = \frac{1}{(z^1 z^2\Delta)^{g-1}}\sum_n \Box^{z^{i_1}}\ldots\Box^{z^{i_n}}\;P^{(g)}_{i_1\ldots i_n}\;,\qquad g>1\;. \tag{2.5.252}$$

In particular, this implies that at each genus the holomorphic ambiguity is parametrized by a polynomial $P^{(g)}(z,E_4,E_6)$ holomorphic in z^i and S. As it was the case before the coefficients in $P^{(g)}$ have to be determined by boundary conditions. For the lower genera this can be done explicitly by using the fiber limes. At higher genus additional information are needed and we will discuss in the next section the possible input from a small gap condition. We believe that essentially all results on the mirror rewriting can be generalized to the full model in case one is able to determine the full mirror map. For the ten parameters along the fiber this is however a technically challenging task.

Boundary conditions and the small gap

As we have seen in (2.5.214), the automorphism group acting on the fiber variables is simply

$$\Gamma(2)\times\Gamma(2)\;, \tag{2.5.253}$$

where these groups act on $t^{1,2}$, respectively, plus the exchange $t^1\leftrightarrow t^2$. Moreover, we see from (2.4.89) that the $\{t^i=0: i=3,\cdots,10\}$ locus maps to the $\{t^i_D=0: i=3,\cdots,10\}$ locus. If we now define

$$2\pi{\rm i}\tau^{1,2} = -t^{1,2},\quad 2\pi{\rm i}\tau^{1,2}_D = -t^{1,2}_D. \tag{2.5.254}$$

we see that the transformation (2.4.89) relating the geometric and the BHM expressions reduces to

$$\tau^1_D = \tau^1,\quad \tau^2_D = -\frac{1}{2}\frac{1}{\tau^2}. \tag{2.5.255}$$

By using the explicit expressions for $\mathcal{F}^{(g)}_{{\rm r},E}(t)$ in terms of modular forms (which can be obtained for example by direct integration), one finds that under (2.5.255)

$$\mathcal{F}^{(g)}_{{\rm r},E}(t)\to 2^{1-g}\mathcal{F}^{(g)}_{{\rm r},E}(t_D), \tag{2.5.256}$$

where the factor of 2 is inherited from the factor of 2 in (2.5.255) and $\mathcal{F}^{(g)}_{{\rm r},E}(t_D)$ are also given in (2.5.235). Therefore, one can obtain expressions for the amplitudes in the BHM reduction in terms of modular forms by simply applying the transformation (2.5.255) to the results of the direct integration in the reduced model (which are valid for the geometric reduction).

These expressions for the BHM amplitudes can also be used to study in detail the behavior near the singularity (2.4.90), and in particular to calculate the subleading terms. One can verify that the discriminant (2.5.226) transforms under (2.5.255) as

$$\Delta(t^1,t^2)\quad\mapsto\quad \Delta(t^1_D,t^2_D) = (z(q^1_D)-z(q^2_D))^2, \tag{2.5.257}$$

which vanishes at the locus (2.4.90). This leads to the singular behavior of $\mathcal{F}_{\rm r}^{(g)}(t_D)$, and one can now verify the behavior (2.5.210) by expanding the expressions in terms of modular forms. One finds,

$$\begin{aligned}
\mathcal{F}^{(1)}_{{\rm r},E}(t_D) &= -\frac{1}{2}\log(\mu) - \frac{1}{2}\log\Big[\frac{1}{128}K_2K_4(K_2^2-K_4)(q_D^2)\Big] + \mathcal{O}(\mu),\\
\mathcal{F}^{(2)}_{{\rm r},E}(t_D) &= \frac{1}{16\mu^2} - \frac{80E_2^2K_2^2 - 16K_2^4 + 3K_2^2K_4 + 9K_4^2 + 16E_2(K_2^2+3K_2K_4)}{9216K_2^2}(q_D^2) + \mathcal{O}(\mu),\\
\mathcal{F}^{(3)}_{{\rm r},E}(t_D) &= \frac{1}{32\mu^4} + \frac{1}{53084160K_2^4}\big(-800E_2^4K_2^4 + 214K_2^8 - 726K_2^6K_4 + 1431K_2^4K_4^2\\
&\quad + 405K_4^4 - 320E_2^3(K_2^5+3K_2^3K_4) + 120E_2^2(10K_2^6 - 15K_2^4K_4 + 9K_2^2K_4^2)\\
&\quad -540K_2^2K_4 - 40E_2(14K_2^7 - 54K_2^5K_4 + 27K_2^3K_4^2 - 27K - 2K_4^3)\big)(q_D^2) + O(\mu).
\end{aligned} \tag{2.5.258}$$

However, if one includes the base directions, the gap is "partially filled" starting at genus three (for $\mathcal{F}^{(2)}(S,t_D)$, the gap property away from the fiber limit is trivially satisfied). Indeed, one finds that the term $C^{ab}\partial_a\mathcal{F}_E^{(1)}(t_D)\partial_b\mathcal{F}_E^{(2)}(t_D)$, leads, in the reduced model, to the expansion

$$\begin{aligned}
&\partial_1\mathcal{F}^{(1)}_{{\rm r},E}(t_D)\partial_2\mathcal{F}^{(2)}_{{\rm r},E}(t_D) + \partial_2\mathcal{F}^{(1)}_{{\rm r},E}(t_D)\partial_1\mathcal{F}^{(2)}_{{\rm r},E}(t_D) =\\
&-\frac{1}{8\mu^4} - \frac{20E_2^2K_2 + 17K_2^3 + 3K_2K_4 + 4E_2(K_2^2+3K_4)}{9216K_2}(q_D^2)\frac{1}{\mu^2} + \cdots
\end{aligned} \tag{2.5.259}$$

Although there are some nontrivial cancellations (for example, there is no term in μ^{-3}), generically one finds, for finite S, singular terms in μ beyond the leading one.

2.6 The field theory limit

As we reviewed in section 2.4, there is a line of enhanced symmetry in the moduli space of the Enriques Calabi–Yau which leads in the field theory limit to $SU(2)$, $\mathcal{N}=2$ QCD with four massless hypermultiplets. This occurs at the locus (2.4.90). Similarly to what happens for other K3 fibrations [102], we expect that near this locus the leading singularities of the topological string partition functions become field theory amplitudes of the $N_f=4$ theory. At genus zero one should recover the prepotential, and at higher genus the gravitational amplitudes introduced by Nekrasov in [80] by using instanton counting techniques. In this section we will explain this in some detail, and as spin-off we will obtain some new results on the modularity properties of the $N_f=4$ theory and its gravitational corrections.

We first note that the behavior of the amplitudes near (2.4.88), in the fiber limit, has been already determined with heterotic techniques in (2.5.210). The results of section 2.5 including the base were obtained in principle in the large radius limit, in terms of the "electric" coordinates t. However, the calculations of $F^{(g)}$ performed there are also valid in the t_D coordinates, due to general covariance. In particular, the holomorphic limit $\mathcal{F}^{(g)}(S,t_D)$ can be expanded in polynomials in $E_2(S), E_4(S), E_6(S)$ as explained before (2.5.147), and we can write

$$\mathcal{F}^{(g)}(S,t_D) = \sum_k p_k^g(S) f_k^g(t_D). \tag{2.6.260}$$

Near the locus (2.4.90) the f_k^g should show display a singular behavior of the form

$$f_k^g(t_D) = \frac{b_k^g}{\mu^{2g-2}} + \cdots, \tag{2.6.261}$$

as we checked in the fiber limit in (2.5.210). How does this compare to the field theory?

The prepotential and gravitational corrections of the massless $N_f = 4$, $SU(2)$ $\mathcal{N} = 2$ Yang–Mills theory depend on the vector multiplet variable a and on the microscopic coupling τ_0. They can be put together into a generating functional

$$\mathcal{F}^{\rm YM}(a, \tau_0, \hbar) = \sum_{g=0}^{\infty} \hbar^{2g} \mathcal{F}_g^{\rm YM}(a, \tau_0), \tag{2.6.262}$$

where $\mathcal{F}_0^{\rm YM}(a, \tau_0)$ is the $\mathcal{N} = 2$ prepotential and the higher g amplitudes are the gravitational corrections. The statement that the type II theory on the Enriques Calabi–Yau has this gauge theory as its field theory limit near the locus (2.4.90) implies that the leading singularity of the topological string amplitudes is given by

$$\mathcal{F}^{(g)}(S, t_D) \to \frac{1}{\mu^{2g-2}} \sum_k b_k^g p_k^g(S) = \mathcal{F}_g^{\rm YM}(a, \tau), \tag{2.6.263}$$

where S is related to the coupling constant of the theory τ_0, and μ is related to the a variable of Seiberg and Witten in a way that we will make precise in a moment. Let us first look at the prepotential. While it has been originally assumed [87] that the prepotential of the self-dual theories with $\mathcal{N} = 2$, gauge group $SU(N)$ and $2N$ flavors is classically exact, it was found in [103] that it does get instanton corrections. Those can however be absorbed in the following redefinition of the coupling [104],

$$\tau_0 \to \tau = \frac{1}{2} \frac{\partial^2}{\partial a^2} \mathcal{F}_0^{\rm YM}(a, \tau_0) = \tau_0 + \sum_k c_k q_0^k, \tag{2.6.264}$$

where

$$q_0 = \exp(2\pi i \tau_0). \tag{2.6.265}$$

We then have for the instanton-corrected prepotential

$$\mathcal{F}_0^{\rm YM}(a, \tau_0) = \frac{1}{2} \tau a^2, \tag{2.6.266}$$

in terms of the renormalized coupling τ. This is needed in order to match the type II prepotential (2.4.78), which does not exhibit instanton corrections. We will then express the $\mathcal{F}_g^{\rm YM}$ obtained by instanton computations not as functions of q_0, but of $q = \mathrm{e}^{2\pi i \tau}$.

The computation of the field theory amplitudes proceeds as follows. The functional (2.6.262) has the structure

$$\mathcal{F}^{\rm YM}(a, \tau_0, \hbar) = \mathcal{F}^{\rm YM}_{\rm pert}(a, \hbar) - \hbar^2 \log Z(a, \tau_0, \hbar), \tag{2.6.267}$$

where

$$\mathcal{F}^{\rm YM}_{{\rm pert},g}(a, \hbar) = -\frac{2B_{2g}}{4^{(g-1)} 2g(2g-2)} (1 - 4^g) \frac{1}{a^{2g-2}} \tag{2.6.268}$$

is the perturbative piece computed in [100], and

$$Z(a, \tau_0, \hbar) = \sum_k Z_k(a, \hbar) q_0^k \tag{2.6.269}$$

is an instanton sum. Nekrasov's formula for the k-instanton contribution to the partition sum $Z_k(a, \hbar)$ can be written as [101]

$$Z_k(a, \hbar) = \sum_{\{Y_\lambda\}} \prod_\lambda^N \prod_{s \in Y_\lambda} \frac{\varphi_\lambda(s)^4}{\prod_{\tilde{\lambda}} E(s)^2}. \tag{2.6.270}$$

The sum runs over sets $\{Y_\lambda\}$ of Young diagrams labeled in the $SU(2)$ case by $\lambda = 1, 2$. For massless flavors,

$$\varphi_\lambda(s) = a_\lambda - (s_j - s_i)\hbar, \tag{2.6.271}$$

where s_i, s_j are the coordinates of the cell s inside the Young diagram Y_λ. We also have

$$E(s) = a_{\lambda\tilde{\lambda}} - \hbar(h(s) - v(s) - 1), \qquad h(s) = \nu_{s_i} - s_j, \qquad v(s) = \tilde{\nu}'_{s_j} - s_i, \tag{2.6.272}$$

where ν_{s_i} is the length of row s_i in Y_λ, $\tilde{\nu}'_{s_j}$ the length of column s_j in $Y_{\tilde{\lambda}}$ and $h(s), v(s)$ are the number of boxes to the right of s inside Y_λ respectively above s inside $Y_{\tilde{\lambda}}$, see Fig. 2.3. The constants $a_\lambda = (a_1, a_2)$ are set to $(-a, a)$.

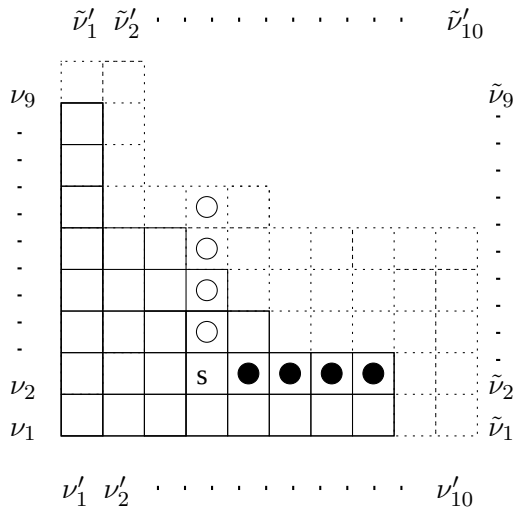

Figure 2.3: A sample pair of Young diagrams $Y_\lambda, Y_{\tilde{\lambda}}$ contributing to (2.6.270).

The relative normalizations between the results in [80] and the Calabi–Yau case can be obtained from the limit $q \to 0$, which is the limit $S \to \infty$. The only remaining singularity on the Enriques is then (2.5.210), while in the Yang–Mills case we are left with the perturbative piece (2.6.268). Comparing this to (2.5.210) and taking into account the relative sign in (2.6.263) we find

$$(-2)^{g-1}\frac{a^{2g-2}}{\mu^{2g-2}} = 1, \tag{2.6.273}$$

and one can immediately read off the normalization of a with respect to $\mu = t^1_D - t^2_D$:

$$a = \frac{\mu}{i\sqrt{2}}. \tag{2.6.274}$$

We notice the following factorization,

$$\mathcal{F}^{\mathrm{YM}}_g(q_0, a) = \frac{1}{a^{2g-2}}\Xi_g(q_0), \tag{2.6.275}$$

where $\Xi_g(q_0)$ is a power series in q_0. The relation between q_0 and q is defined by

$$q = q_0 \exp[\Xi_0(q_0)], \tag{2.6.276}$$

which can be inverted to obtain the relation between q_0 and q. The explicit power series one finds is

$$q_0 = q - \frac{q^2}{2} + \frac{11q^3}{64} - \frac{3q^4}{64} + \frac{359q^5}{32768} - \frac{75q^6}{32768} + \frac{919q^7}{2097152} - \frac{41q^8}{524288} + \mathcal{O}(q^9). \tag{2.6.277}$$

If we now plug this series into $\mathcal{F}_g^{\rm YM}(a,q_0)$ we find that all gravitational couplings are functions of q^2, that is to say, there are no odd instanton contributions, as it should be since those are forbidden by a $\mathbb{Z}_2$–symmetry of the theory [87]. The power series (2.6.277) should be given by a mirror map, corresponding to some algebraic realization of an elliptic curve. Indeed, when expressed in terms of

$$q = 2^4 q_S^{\frac{1}{2}}, \quad q_S = \mathrm{e}^{-S}, \tag{2.6.278}$$

we find

$$q_0 = 16\, q_S^{\frac{1}{2}} - 128\, q_S + 704\, q_S^{\frac{3}{2}} - 3072\, q_S^2 + \cdots = \frac{\vartheta_2^4(q_S)}{\vartheta_3^4(q_S)}, \tag{2.6.279}$$

which is (up to an overall factor 16) the Hauptmodul of $\Gamma_0(4)$. This equality between q_0 and the Hauptmodul has only be checked for the first few terms of the instanton expansion, and we don't have a general proof.

We can now express the couplings $\mathcal{F}_g^{\rm YM}(a,q_0)$, computed from (2.6.270), in terms of q_S, μ. Due to the connection to the Enriques results and the field theory limit (2.6.263), we expect them to be (up to an overall factor μ^{2-2g}) quasi–modular forms in q_S of weight $2g-2$, and belonging to the ring generated by $E_2(S)$, $E_4(S)$ and $E_6(S)$. The results obtained with the instanton expansion are in perfect agreement with this. We find at $g=2$

$$\begin{aligned} \mu^2 \mathcal{F}_2^{\rm YM} &= \frac{1}{16} - \frac{3q_S}{2} - \frac{9q_S^2}{2} - 6q_S^3 - \frac{21q_S^4}{2} - 9q_S^5 + 18q_S^6 + \mathcal{O}\left(q_S^7\right) \\ &= \frac{1}{2^4} E_2(q_S)\ . \end{aligned} \tag{2.6.280}$$

Proceeding in the same way we find,

$$\begin{aligned} \mu^4 \mathcal{F}_3^{\rm YM} &= \frac{1}{2^5}\Big(\frac{2}{3}E_2^2 + \frac{1}{3}E_4\Big)\ , \\ \mu^6 \mathcal{F}_4^{\rm YM} &= \frac{1}{2^6}\Big(\frac{11}{12}E_2^3 + \frac{4}{3}E_2E_4 + \frac{7}{12}E_6\Big)\ , \\ \mu^8 \mathcal{F}_5^{\rm YM} &= \frac{1}{2^7}\Big(\frac{17}{9}E_2^4 + \frac{97}{18}E_2^2E_4 + \frac{32}{9}E_4^2 + \frac{14}{3}E_2E_6\Big)\ , \\ \mu^{10} \mathcal{F}_6^{\rm YM} &= \frac{1}{2^8}\Big(\frac{619}{120}E_2^5 + \frac{218}{9}E_2^3E_4 + \frac{427}{9}E_2E_4^2 + \frac{4501}{144}E_2^2E_6 + \frac{4337}{144}E_4E_6\Big)\ , \\ \mu^{12} \mathcal{F}_7^{\rm YM} &= \frac{1}{2^9}\Big(\frac{1418}{81}E_2^6 + \frac{52837}{432}E_2^4E_4 + \frac{12848}{27}E_2^2E_4^2 + \frac{22631}{108}E_2^3E_6 + \frac{5423}{9}E_2E_4E_6 \\ &\qquad + \frac{6529}{54}E_6^2 + \frac{352069}{1296}E_4^3\Big)\ , \end{aligned} \tag{2.6.281}$$

We point out that we have not proved these equalities, but rather verified them by using the instanton expansion up to high order. It is however highly non–trivial that this expansion can be matched to a quasimodular form of the required weight. In addition, one can verify that the coefficients of the above combinations agree with the Enriques results. For example, if we look at the singular behavior of (2.5.168) by using (2.5.210), one finds,

$$\mathcal{F}^{(3)}(S,t_D) \to \frac{1}{32\mu^4}E_4(S) + \frac{1}{48\mu^4}(E_2^2(S) - E_4(S)) = \frac{1}{96}(2E_2^2(S) + E_4(S)), \tag{2.6.282}$$

in agreement with the result above. We have checked that the above polynomials are in accordance with the field theory limit of the Enriques model also for $g = 4, 5, 6$. For higher genus the instanton results for the $N_f = 4$ theory provide a boundary condition for the holomorphic anomaly equation, since they determine the coefficient of the leading singularity near (2.4.90) as a function of S, and generalize the heterotic result (2.5.210) away from the fiber.

In summary, we have verified with the instanton computations of [80] our general results about the structure of the topological string amplitudes in the Enriques Calabi–Yau (in particular our assumption after (2.5.147) about the modular properties of the holomorphic ambiguity). Conversely, the results on the Enriques side have been instrumental in clarifying the modularity structure of the massless $N_f = 4$ theory.

Conclusion

In this chapter we have developed a new approach to solving the holomorphic anomaly equations of [19], based on the interplay between modularity and non-holomorphicity, which makes possible to perform a direct integration of the equations at each genus. This approach is more efficient than the diagram expansion of [19] and leads to closed expressions for the topological string amplitudes, once the ambiguities are fixed by appropriate boundary conditions. The amplitudes obtained with this procedure can be written as polynomials in a finite set of generators that transform in a particularly simple way under the space-time symmetry group, making the modularity properties manifest.

Chapter 3

Topological Amplitudes and Heterotic-Type II Duality

In this chapter, we report on a computation of topological amplitudes on a chain of Calabi-Yau manifolds, using $\mathcal{N} = 2$ heterotic-type II duality. This duality connects the heterotic string compactified on $K3 \times \mathbb{T}^2$ with compactifications of type IIA theory on $K3$-fibrations, as we briefly reviewed in section 1.4. The material presented here is based on the publication [43].

Recall that the 4d effective action of these $\mathcal{N} = 2$ compactifications contains a series of BPS protected higher-loop terms of the form

$$S \sim \int F^{(g)}(t, \bar{t}) T^{2g-2} R^2 + \cdots , \tag{3.0.1}$$

where R is the Riemann tensor, T the graviphoton field strength, and the couplings $F^{(g)}$ are amplitudes of the topological string on the internal Calabi-Yau [18, 19]. On the heterotic side, these amplitudes appear at 1–loop [20] and are therefore in general accessible to computation [44, 29, 97, 79]. The result can be mapped to the type II side, yielding striking predictions in enumerative geometry.

The Higgs transitions on the heterotic side correspond to geometric transitions between the corresponding Calabi-Yaus on the type II side. A more precise picture of how the heterotic moduli spaces are connected might therefore provide some insight into the web of type II vacua. Until now, most explicit comparisons between heterotic and type II models have been restricted to cases with a small number n_v of massless Abelian vector multiplets, namely $n_v = 3, 4, 5$. These vector multiplets are the graviphoton, the heterotic dilaton S, one or two ($n_v = 4$) moduli T, U from the compactification torus, and if $n_v = 5$, one Wilson line modulus V. However, by now there is a myriad of conjectured heterotic-type II pairs with higher numbers of vector multiplets waiting to be analyzed.

In [105], the authors obtained chains of heterotic-type II duals by compactifying the heterotic string on $K3 \times \mathbb{T}^2$ in various orbifold realizations. In each chain, subsequent models are connected by a sequential Higgs mechanism reducing the number of generic Wilson line moduli by one. $K3$ is realized as an orbifold $\mathbb{T}^4/\mathbb{Z}_N$, $N = 2, 3, 4, 6$ and the $\mathbb{Z}_N$ is simultaneously embedded in the gauge connection in a modular invariant way. For the last models in the chains, the candidate type II duals can be explicitly constructed.

The classical vector multiplet moduli space of compactifications with $k = n_v - 4$ Wilson lines is given by the special Kähler space

$$\frac{SU(1,1)}{U(1)} \times \frac{SO(2+k,2)}{SO(2+k) \times SO(2)}, \tag{3.0.2}$$

where the first factor corresponds to the dilaton and the second to the torus and Wilson line moduli. The T-duality group, under which the vector multiplet couplings have to transform as

automorphic functions, is $SO(2+k,2;\mathbb{Z})$ [106, 107, 108].
For the $SO(2,2;\mathbb{Z})$ case with four vector multiplets, i.e. the well-known STU model, the higher derivative couplings have been computed in [29]. They can be expressed in terms of expansion coefficients of ordinary modular forms. The case with five vector multiplets (one Wilson line) has been studied at the level of prepotential and $F^{(1)}$ in [109]. This case is somewhat special, as the T-duality group is here $SO(3,2;\mathbb{Z}) \cong Sp(4,\mathbb{Z})$ [108], and the corresponding automorphic functions are given by Siegel modular forms [108]. The effective couplings can be expressed in terms of Jacobi forms of index one, yielding a prescription how to split off the part depending on the Wilson line modulus from the gauge lattice.
In this chapter, we present the results of [43] about the generic case, involving more general automorphic forms. We define a splitting procedure analogous to the one in [109], and show how the split lattice sum can be explicitly expressed in terms of ordinary Jacobi Theta functions. Once this split is determined, we use the technique of lattice reduction [41] to explicitly compute higher-derivative F-terms for heterotic $\mathcal{N}=2$ compactifications with an arbitrary number of Wilson lines. The final result involves the q-expansion coefficients of the moduli independent Higgsed part of the lattice sum. Even though the computation is done at the orbifold point, the results are fully valid at generic points of $K3$ moduli space, since the couplings $F^{(g)}$ only depend on vector multiplets and therefore cannot mix with the $K3$ moduli, belonging to hypermultiplets. While the formalism can be applied to almost any symmetric $\mathbb{Z}_N$ orbifold limit of $K3$, we mainly focus on the dual pairs found in [105]. We compute the corresponding topological amplitudes $F^{(g)}$ in closed form. For genus zero, our results agree with the numbers of rational curves found on the type II side wherever those are known [110]. The present computation extends previous work on threshold corrections for models with a single Wilson line [96, 109, 111], and also provides a more explicit realization, extended to higher genus, of the general results of [92].

The rest of this chapter is organized as follows. In section 3.1, we review heterotic compactifications with $\mathcal{N}=2$ supersymmetry and the Higgs chains of [105]. In section 3.2, we explain how to compute partition sums and higher derivative F-terms in general heterotic orbifold setups. Section 3.3 introduces the lattice splits in the presence of Wilson lines. A general expression for the amplitudes $F^{(g)}$ in the presence of Wilson lines is derived. In section 3.4, we use our results to extract geometric information on the dual Calabi-Yau manifold. This provides a highly nontrivial check of our computation in those cases where instanton numbers are known on the type II side.

3.1 Heterotic $\mathcal{N}=2$ compactifications

In this section, we briefly discuss the construction of heterotic $\mathcal{N}=2$ compactifications and their matter spectrum. There are two main approaches to analyzing these models. Section 3.1.1 reviews the purely geometrical approach of [40], while section 3.1.2 reviews the exact CFT construction via orbifolds of [105]. Even though the two approaches are completely equivalent, it proves very useful to keep the two in mind simultaneously, as sometimes one is more convenient, sometimes the other. Section 3.1.3 reviews how these compactifications fall into chains of models connected by a sequential Higgs mechanism [105].

3.1.1 The Calabi-Yau approach

Consider compactification of the heterotic string on $K3\times\mathbb{T}^2$. In order to break the gauge group $\mathcal{G}=E_8\times E_8$ of the ten-dimensional heterotic string down to a subgroup G, one gives gauge fields on K3 an expectation value in H, where $G\times H$ is a maximal subgroup of $\mathcal{G}$. Geometrically, this corresponds to embedding a H-bundle V on K3. This bundle can be chosen to be the tangent bundle of K3, an $SU(2)$-bundle with instanton number $\int_{K3} c_2(V)=24$. This is the standard embedding, where the spin connection on K3 is equal to the gauge connection. More generally,

one can embed several stable holomorphic SU(N)-bundles V_a, as long as the constraints from modular invariance

$$\sum_a c_2(V_a) = 24 \qquad c_1(V_a) = 0 \tag{3.1.3}$$

are satisfied. We will here only consider embeddings of one or two $SU(2)$-bundles on one respectively both E_8 and write their instanton numbers according to (3.1.3) as $(d_1, d_2) = (12+n, 12-n)$. The number of gauge neutral hypermultiplets is determined as follows [40]. There is a universal gravitational contribution of 20, and each of the $SU(N_a)$-bundles $V_a \to K3$ with $\int_{K3} c_2(V_a) = A$ has an extra $AN_a + 1 - N_a^2$ moduli, therefore we get additional 45 moduli for one and 51 for two embedded $SU(2)$ bundles. The rank of the gauge group is reduced by the rank of the embedded bundle, N-1. For the standard embedding, we thus find 65 hypermultiplets and an enhanced gauge group $E_7 \times E_8$, the first model in the $\mathbb{Z}_2$ chain in [105]. The Cartan subalgebra of $E_7 \times E_8$ contains 15 generators, and there is an extra $U(1)^4$ from the SUGRA multiplet and torus compactification, therefore this model has $n_v = 19$ vector multiplets.

3.1.2 Exact CFT construction via orbifolds

Rather than following the approach presented above, we will here realize the heterotic models following [105] in the so-called exact CFT construction via orbifolds. In this approach, the K3 is realized as a $\mathbb{Z}_N$ orbifold, while simultaneously the spin connection is embedded into the gauge degrees of freedom. We will mainly concentrate on the $\mathbb{Z}_N$–embeddings given in table 3.1. The orbifold $\mathbb{Z}_N$ twist θ acts on two of the four complex bosonic transverse coordinates as $\mathrm{e}^{\pm\frac{2\pi\mathrm{i}}{N}}$. Since we impose $\mathcal{N} = 2$ SUSY, N can only take on the values $2, 3, 4, 6$ [92]. The action of θ on the gauge degrees of freedom is strongly restricted by worldsheet modular invariance. We implement it as a shift of the gauge lattice, writing for the torus and gauge lattice sum

$$\mathbf{Z}^{18,2}\begin{bmatrix}a\\b\end{bmatrix} = \sum_{p\in\Gamma^{18,2}+a\gamma} \mathrm{e}^{2\pi\mathrm{i}b\gamma\cdot p} q^{\frac{|p_L|^2}{2}} \bar{q}^{\frac{|p_R|^2}{2}}, \tag{3.1.4}$$

where $a, b \in \{1/N, \cdots (N-1)/N\}$. The shift $\gamma \in \Gamma^{18,2}$ has to fulfill the modular invariance and level-matching constraints [13]

$$\sum_{i=1}^{8} \gamma_i = \sum_{i=9}^{16} \gamma_i = 0 \bmod 2 \tag{3.1.5}$$

and

$$\gamma^2 = 2 \bmod 2N. \tag{3.1.6}$$

One then finds the possible inequivalent $\mathbb{Z}_N$ orbifolds: There are 2 for $\mathbb{Z}_2$, 5 for $\mathbb{Z}_3$, 12 for $\mathbb{Z}_4$ and 61 for $\mathbb{Z}_6$ [111]. Note that in those cases where the same type of shift is modular invariant for different N, those models are equivalent as far as the topological amplitudes $F^{(g)}$ are concerned. The reason for this is that they are only distinguished by the specific orbifold realization of the K3-surface. Since the moduli of the K3 live in hypermultiplets which do not mix with the vector multiplets, the higher-derivative couplings should be identical for the different $\mathbb{Z}_N$ embeddings. They can however differ if we turn on Wilson line moduli corresponding to the gauge groups only present in the orbifold limit [92], as will be explained in section 3.3.2.
Some non-standard embeddings, along with their perturbative gauge group, are given in table 3.3. These groups are easily read off from the simple root system for E_8 given below, table 3.2. The unbroken group is generated by the roots α_i invariant under the shift γ, i.e. fulfilling

$$\mathrm{e}^{\frac{2\pi\mathrm{i}\gamma\cdot\alpha_i}{N}} = 1. \tag{3.1.7}$$

$\mathbb{Z}_2$	γ^1=(1,-1,0,0,0,0,0,0);		
	γ^2=(0,0,0,0,0,0,0,0)	$SU(2) \times E_7 \times E_8'$	n=12
$\mathbb{Z}_3$	γ^1=(1,1,2,0,0,0,0,0);		
	γ^2=(1,-1,0,0,0,0,0,0)	$SU(3) \times E_6 \times U(1)' \times E_7'$	n=6
$\mathbb{Z}_4$	γ^1=(1,1,1,-3,0,0,0,0);		
	γ^2=(1,1,-2,0,0,0,0,0)	$SO(10) \times SU(4) \times E_6' \times SU(2)' \times U(1)'$	n=4
$\mathbb{Z}_6$	γ^1=(1,1,1,1,-4,0,0,0);		
	γ^2=(1,1,1,1,1,-5,0,0)	$SU(5) \times SU(4) \times U(1) \times SU(6)' \times SU(3)' \times SU(2)'$	n=2

Table 3.1: Embeddings of the spin connection in the gauge degrees of freedom

0	1	1	0	0	0	0	0	α_1
0	0	-1	1	0	0	0	0	α_2
0	0	0	-1	1	0	0	0	α_3
0	0	0	0	-1	1	0	0	α_4
0	0	0	0	0	-1	-1	0	α_5
0	0	0	0	0	0	1	1	α_6
$-\frac{1}{2}$	$-\frac{1}{2}$	$\frac{1}{2}$	$\frac{1}{2}$	$\frac{1}{2}$	$\frac{1}{2}$	$-\frac{1}{2}$	$-\frac{1}{2}$	α_7
0	0	0	0	0	0	1	-1	α_8

Table 3.2: A simple root system for E_8

In the first embedding in table 3.3, the invariant roots on the first E_8 are the 126 roots of E_7, generated by the roots $\alpha_2, \cdots, \alpha_8$. One realization is given in table 3.2. For a general $\mathbb{Z}_N$ embedding, the gauge group from the first E_8 would then be $U(1) \times E_7$. For $N = 2$, γ itself is also a root, orthogonal to the others, fulfilling (3.1.7), and the $U(1)$ is enhanced to an $SU(2)$. On the second E_8, the invariant roots are the roots of $SO(14)$ $\alpha_1, \cdots, \alpha_6, \alpha_8$, and an extra root $(1, -1, 0^6)$ such that the unbroken gauge group is $SO(16)$. The second embedding is obviously analogous, only in this case $N = 3$, therefore $(1, -1, 0^6)$ is not an invariant root anymore. For the left-hand side of the third embedding, the unbroken roots are $\alpha_1, (1, -1, 0^6)$, and the second system, orthogonal to the first $\alpha_3, \cdots \alpha_8$, yielding a perturbative gauge group $SU(3) \times E_6$. On the second E_8, the unbroken roots are $\alpha_1, \cdots, \alpha_7, (\frac{1}{2}, -\frac{1}{2}, -\frac{1}{2}, -\frac{1}{2}, -\frac{1}{2}, -\frac{1}{2}, \frac{1}{2}, -\frac{1}{2})$, forming the Dynkin diagram of $SU(9)$. The other examples work out similarly. Note that each of these realizations breaks the original gauge group $E_8 \times E_8$ to a different rank 16 subgroup, containing a nonabelian rank r group G and a $U(1)^{16-r}$ that may be enhanced as in the example above. However, this latter factor is only present in the orbifold limit; for a smooth K3, the gauge group

$$\begin{pmatrix} 2 & -1 & 0 & & \cdots & & & 0 \\ -1 & 2 & -1 & 0 & & & & 0 \\ 0 & -1 & 2 & -1 & 0 & & & 0 \\ \vdots & 0 & -1 & 2 & -1 & 0 & & 0 \\ & & 0 & -1 & 2 & -1 & 0 & -1 \\ & & & 0 & -1 & 2 & -1 & 0 \\ & & & & 0 & -1 & 2 & 0 \\ 0 & & \cdots & & -1 & 0 & \cdots & 2 \end{pmatrix} \tag{3.1.8}$$

Figure 3.1: Cartan matrix of E_8

consists merely of G.

The perturbative gauge group $G \times G'$ can subsequently be spontaneously broken to a subgroup $G_1 \subset G$ via maximal Higgsing, as explained in section 3.1.1 within the Calabi-Yau approach of [40]. This subgroup depends on the embedding γ only via its instanton numbers: For the standard embedding with $n = 12$, there are no instantons on the second E_8 and the gauge group E_8' can not be broken at all. For the cases $n = 0, 1, 2$, complete Higgsing is possible. For $n = 3, 4, 6, 8$, there are too few hypermultiplets on E_8' that could be used for Higgsing, and G' can only be broken to a terminal subgroup $G_1 = SU(3), SO(8), E_6, E_7$ [111]. Once again, we consider the standard $\mathbb{Z}_2$ orbifold as an example. The hypermultiplets in the untwisted (θ^0) and twisted (θ^1) sectors transform under $E_7 \times SU(2)$ in the following representations:

$$\begin{aligned} (56, 2) + 4(1, 1) \qquad & (\text{untwisted},\ \theta^0) \\ 8\left((56, 1) + 4(1, 2)\right) \qquad & (\text{twisted},\ \theta^1). \end{aligned} \tag{3.1.9}$$

We can now Higgs the $SU(2)$ giving vevs to three scalars, and we are left with 10 hypermultiplets transforming in the **56** of E_7 and 65 singlet hypermultiplets, as advertised in section 3.1.1. We can then break E_7 further by sequential Higgs mechanism. Since the instanton numbers corresponding to this embedding are $(24, 0)$, we can not break the E_8' from the second E_8 lattice at all. A complete classification of orbifold limits of $K3$ along with their instanton numbers can be found in [111].

$\mathbb{Z}_2$	$(1, -1, 0, 0, 0, 0, 0, 0)$; $(2, 0, 0, 0, 0, 0, 0, 0)$	$SU(2) \times E_7 \times SO(16)'$	$n = 4$
$\mathbb{Z}_3$	$(2, 0, 0, 0, 0, 0, 0, 0)$; $(2, 0, 0, 0, 0, 0, 0, 0)$	$U(1) \times SO(14) \times U(1)' \times SO(14)'$	$n = 0$
$\mathbb{Z}_3$	$(1, 1, -2, 0, 0, 0, 0, 0)$; $(-2, 1, 1, 1, 1, 1, 2, 1)$	$SU(3) \times E_6 \times SU(9)'$	$n = 3$
$\mathbb{Z}_4$	$(3, -1, 0, 0, 0, 0, 0, 0)$; $(0, 0, 0, 0, 0, 0, 0, 0)$	$SU(2) \times U(1) \times SO(12) \times E_8'$	$n = 12$
$\mathbb{Z}_6$	$(3, -1, -1, -1, -1, -1, 1, 1)$; $(3, -3, 2, 0, 0, 0, 0, 0)$	$U(1)^2 \times SU(7) \times U(1)' \times SU(2)'^2 \times SO(10)'$	$n = 2$

Table 3.3: Other $\mathbb{Z}_N$ embeddings of the spin connection

3.1.3 Chains of dual models and the sequential Higgs mechanism

Once one has chosen a modular invariant embedding of $SU(N)$ bundles, and maximally Higgsed the gauge group on the E_8 lattice where the embedding has the lower instanton number, one can perform a cascade breaking on the remaining gauge group along the chain $E_8 \to E_7 \to E_6 \to SO(10) \to SU(5) \to SU(4) \to SU(3) \to SU(2) \to$ (nothing). For the example of the standard $\mathbb{Z}_2$ orbifold, this goes as follows.

Starting with the (65,19) model with $E_7 \times E_8$ symmetry remaining after the gauge embedding, one can move to a point in moduli space where the E_7 gauge symmetry is restored. Under the maximal subgroup $E_6 \times U(1) \in E_7$, the **56** of E_7 decomposes as $\mathbf{56} = \mathbf{27} + \overline{\mathbf{27}} + \mathbf{1} + \mathbf{1}$. At this point, there are 10 **56**, therefore 20 E_6 singlets charged under the U(1). We now give a generic vev to the adjoint scalars in the unbroken vector multiplets, thereby giving masses to all hypermultiplets charged with respect to E_6, and at the same time breaking E_6 to its maximal Abelian subgroup $U(1)^6$. Using one scalar to Higgs the $U(1)$, we get 19 extra gauge singlet fields: the new spectrum is $(84, 18)$, the second model in the corresponding chain in [105]. We can then move to a point in moduli space where the $U(1)^6$ is enhanced to E_6 and continue this procedure until no gauge symmetry remains on this lattice. In this way, one easily finds a chain

of models with characteristics (n_h, n_v) [105]

$$(65,19),(84,18),(101,17),(116,16),(167,15),(230,14),(319,13),(492,12) \tag{3.1.10}$$

The same mechanism can be applied to the other embeddings in table 3.1. For the $\mathbb{Z}_3$ orbifold, $n = 6$, therefore we can maximally Higgs on the second lattice down to E_6. On the first E_8 lattice, we first Higgs down to the rank-reduced subgroup and then start cascade breaking as explained above. The result is a chain $E_6 \to SO(10) \to \cdots \to SU(2) \to 0$ passing through models with characteristics

$$(76,16),(87,15),(96,14),(129,13),(168,12),(221,11),(322,10). \tag{3.1.11}$$

For the $\mathbb{Z}_4$ orbifold, $n = 4$, maximal Higgsing leaves an $SO(8)$ on the second lattice and the embedding of the spin connection leaves a rank-reduced subgroup $SU(4)$ on the first. The resulting chain reads

$$(123,11),(154,10),(195,9),(272,8). \tag{3.1.12}$$

The $\mathbb{Z}_6$ orbifold in table 3.1, finally, has $n = 2$ and therefore allows for complete Higgsing. The rank-reduced subgroup is $SU(5)$, Higgsed via the chain

$$(118,8),(139,7),(162,6),(191,5),(244,4). \tag{3.1.13}$$

The last four models in each chain have candidate type II duals, i.e. known K3 fibrations with the right Betti numbers. It is interesting to note that on the type-II side, the cascade breaking procedure corresponds precisely to moving between moduli spaces of different Calabi-Yau manifolds. Indeed, as pointed out in [40], this is strikingly similar to the specific type-II process described in [112].

3.2 Higher derivative couplings for $\mathbb{Z}_n$ orbifolds

We will consider here the $E_8 \times E_8$ formulation of the 10 dimensional heterotic string, where the gauge degrees of freedom are encoded by 16 left-moving bosons, and compactify it on $K3 \times \mathbb{T}^2$, yielding another two left- and two right-moving bosons. These fields take their values on an even self–dual lattice of signature $(18,2)$ that will be denoted by $\Gamma^{18,2}$. One can identify $\Gamma^{18,2}$ as obtained from a Euclidean standard lattice by an $SO(18,2)$ rotation. The moduli space of inequivalent lattices is therefore given by

$$\frac{SO(18,2)}{SO(18)\times SO(2)}. \tag{3.2.14}$$

This homogeneous space can be parametrized following [44],[92] by

$$u(y) = (\vec{y}, y^+, y^-; 1, -\frac{1}{2}(y,y)),\ y \in \mathbb{C}^{17,1} \tag{3.2.15}$$

with $y_2 > 0, (y_2, y_2) < 0$ and inner product

$$(x,y) = (\vec{x},\vec{y}) - x^+y^- - x^-y^+. \tag{3.2.16}$$

The right-moving components of a vector in $\Gamma^{18,2}$ with respect to a vector $(\vec{b}, m_-, n_+, m_0, n_0)$ in the fixed Euclidean standard lattice are then denoted by $p_R = p \cdot u(y)$, and we have

$$\frac{p_L^2 - p_R^2}{2} = \frac{1}{2(y_2,y_2)}\big(\vec{b}\cdot\vec{b} + m_-n_+ + m_0n_0\big), \tag{3.2.17}$$

$$\frac{p_R^2}{2} = \frac{-1}{2(y_2,y_2)}\big|\vec{b}\cdot\vec{y} + m_+y^- - n_-y^+ + n_0 + \frac{1}{2}m_0(y,y)\big|^2, \tag{3.2.18}$$

The general expression for $F^{(g)}$ is given by [20, 113, 79]

$$F^{(g)} = \frac{1}{Y^{g-1}} \int_{\mathcal{F}} \frac{d^2\tau}{\tau_2} \frac{1}{|\eta|^4} \sum_{\text{even}} \frac{i}{\pi} \partial_\tau \left(\frac{\vartheta[{}^{\alpha}_{\beta}](\tau)}{\eta(\tau)} \right) Z_g^{\text{int}}[{}^{\alpha}_{\beta}], \tag{3.2.19}$$

where

$$Z_g^{\text{int}}[{}^{\alpha}_{\beta}] = \langle : \left(\partial X\right)^{2g} : \rangle = \mathcal{P}_g C_g^{\text{int}}[{}^{\alpha}_{\beta}]. \tag{3.2.20}$$

$\mathcal{P}_g(q)$ is a one-loop correlation function of the bosonic fields and is given by [114],[20]

$$\mathrm{e}^{-\pi\lambda^2\tau_2} \left(\frac{2\pi\eta^3\lambda}{\vartheta_1(\lambda|\tau)} \right)^2 = \sum_{g=0}^{\infty} (2\pi\lambda)^{2g} \mathcal{P}_g(q), \tag{3.2.21}$$

and $C_g^{\text{int}}[{}^{a}_{b}]$ denotes the trace over the (a,b) sector of the internal CFT with an insertion of p_R^{2g-2}, namely

$$\sum_{a,b} c(a,b) (-1)^{2\alpha+2\beta+4\alpha\beta} \frac{\vartheta[{}^{\alpha}_{\beta}] \vartheta[{}^{\alpha+a}_{\beta+b}] \vartheta[{}^{\alpha-a}_{\beta-b}]}{\eta^3} \cdot Z_{4,4}[{}^{a}_{b}] \cdot Z^g_{\mathbb{T}^2}[{}^{a}_{b}], \tag{3.2.22}$$

where $c(a,b)$ are constants ensuring modular invariance.
Note that for g=1, (3.2.19) is just the unregularized one-loop gravitational threshold correction

$$F^{(1)} = \int_{\mathcal{F}} \frac{d^2\tau}{\tau_2^2} \left(\frac{\tau_2}{|\eta|^4} \sum_{\text{even}} \frac{i}{\pi} (-1)^{2\alpha+2\beta+4\alpha\beta} \partial_\tau \left(\frac{\vartheta[{}^{\alpha}_{\beta}](\tau)}{\eta(\tau)} \right) \frac{\widehat{E}_2}{12} C_g^{\text{int}}[{}^{\alpha}_{\beta}] \right). \tag{3.2.23}$$

The contribution from the bosonic (4,4) blocks reads

$$Z_{4,4}[{}^{a}_{b}] = 16 \frac{\eta^2 \bar{\eta}^2}{\vartheta^2[{}^{1-a}_{1-b}] \bar{\vartheta}^2[{}^{1-a}_{1-b}]} \qquad (a,b) \neq (0,0) \tag{3.2.24}$$

while the bosons on the $\mathbb{T}^2$ together with the 16 bosons corresponding to the gauge degrees of freedom contribute [92]

$$Z^g_{\mathbb{T}^2}[{}^{a}_{b}] = \frac{1}{\eta^{18}} e^{-2\pi i a b \gamma^2} \sum_{p \in \Gamma^{18,2} + a\gamma} p_R^{2g-2} e^{2\pi i b\gamma \cdot p} q^{\frac{|p_L|^2}{2}} \bar{q}^{\frac{|p_R|^2}{2}}. \tag{3.2.25}$$

Using

$$\frac{\mathrm{i}}{4\pi} \sum_{(\alpha,\beta)\text{even}} (-1)^{2\alpha+2\alpha+4\alpha\beta} \partial_\tau \left(\frac{\vartheta[{}^{\alpha}_{\beta}]}{\eta} \right) \frac{\vartheta[{}^{\alpha}_{\beta}] \vartheta[{}^{\alpha+a}_{\beta+b}] \vartheta[{}^{\alpha-a}_{\beta-b}]}{\eta^3} \frac{Z_{4,4}[{}^{a}_{b}]}{|\eta|^4} = 4 \frac{\eta^2}{\bar{\vartheta}[{}^{1+a}_{1+b}] \bar{\vartheta}[{}^{1-a}_{1-b}]}, \tag{3.2.26}$$

one can write for (3.2.19)

$$F^{(g)} = \frac{1}{Y^{g-1}} \int_{\mathcal{F}} \frac{d^2\tau}{\tau_2^2} \tau_2^{2g-1} \mathcal{P}_{2g}(q) \sum_{a,b} \frac{c(a,b) \mathrm{e}^{2\pi i a b (2-\gamma^2)}}{\eta^{18} \vartheta[{}^{1+a}_{1+b}] \vartheta[{}^{1-a}_{1-b}]} \sum_{p \in \Gamma^{18,2} + a\gamma} p_R^{2g-2} e^{2\pi i b\gamma \cdot p} q^{\frac{|p_L|^2}{2}} \bar{q}^{\frac{|p_R|^2}{2}}. \tag{3.2.27}$$

The constants $c(a,b)$ can be determined by the modular invariance constraints [92]

$$\begin{aligned} c(0,b) &= 4 \sin^4(\pi b) \\ c(a,b) &= \mathrm{e}^{\pi i a^2 (2-\gamma^2)} c(a, a+b) \\ c(a,b) &= \mathrm{e}^{-2\pi i a b (2-\gamma^2)} c(b, -a). \end{aligned} \tag{3.2.28}$$

Introducing the Siegel-Narain theta function with insertion and shifts (see Appendix C.1)

$$\Theta^g_\Gamma(\tau, \gamma, a, b) = \sum_{p \in \Gamma + a\gamma} p_R^{2g-2} q^{\frac{|p_L|^2}{2}} \bar{q}^{\frac{|p_R|^2}{2}} \mathrm{e}^{\pi i b\gamma \cdot p}, \tag{3.2.29}$$

we can rewrite (3.2.27) as

$$F^{(g)} = \frac{1}{Y^{g-1}} \int_{\mathcal{F}} \frac{d^2\tau}{\tau_2^2} \tau_2^{2g-1} \mathcal{P}_{2g}(q) \sum_{a,b} \frac{c(a,b) \mathrm{e}^{2\pi \mathrm{i} ab(2-\gamma^2)}}{\eta^{18} \vartheta[^{1+a}_{1+b}] \vartheta[^{1-a}_{1-b}]} \Theta^g_{\Gamma^{18,2}}(\tau, \gamma, a, b). \tag{3.2.30}$$

For the special cases of $\mathcal{N}$=2 compactifications with a factorized $\mathbb{T}^2$, the prepotential and $F^{(1)}$ have been shown to be universal, i.e. independent of the specific model [114]. In other words, they are identical for all compactifications on $K3 \times \mathbb{T}^2$ with all Wilson lines set to zero. Everything then only depends on the torus moduli. It is easy to see that this also applies to the amplitudes $F^{(g)}$: When we set all Wilson line moduli to zero, the lattice sum obviously factorizes as

$$\sum_{p \in \Gamma^{16,0} + a\gamma} q^{\frac{|p_L|^2}{2}} \mathrm{e}^{2\pi \mathrm{i} bp\cdot\gamma} \sum_{\widehat{p} \in \Gamma^{2,2}} q^{\frac{|\widehat{p}_L|^2}{2}} \bar{q}^{\frac{|\widehat{p}_R|^2}{2}}, \tag{3.2.31}$$

and we obtain

$$\begin{aligned} F^{(g)}_{0\mathrm{WL}} =& \frac{1}{Y^{g-1}} \int_{\mathcal{F}} \frac{d^2\tau}{\tau_2^2} \tau_2^{2g-1} \mathcal{P}_{2g}(q) \sum_{a,b} \frac{c(a,b)}{\eta^{18} \vartheta[^{1+a}_{1+b}] \vartheta[^{1-a}_{1-b}]} \sum_{p \in \Gamma^{16,0} + a\gamma} q^{\frac{p^2}{2}} \mathrm{e}^{\pi \mathrm{i} g\gamma\cdot p} \Theta^g_{\Gamma^{2,2}}(\tau) \\ =& \int \frac{d^2\tau_2}{\tau_2^2} \tau_2^{2g-1} \mathcal{P}_{2g} \Theta^g_{\Gamma^{2,2}} \frac{1}{\eta^{24}} \Omega, \end{aligned} \tag{3.2.32}$$

where

$$\Omega = \sum_{a,b} \frac{c(a,b)\eta^6}{\vartheta[^{1+a}_{1+b}] \vartheta[^{1-a}_{1-b}]} \sum_{p \in \Gamma^{16,0} + a\gamma} q^{\frac{p^2}{2}} \mathrm{e}^{\pi \mathrm{i} b\gamma\cdot p}. \tag{3.2.33}$$

For modular invariance, Ω then has to be a modular form of weight (10,0). Since the spaces of modular forms of even weight $2 < w < 12$ are one-dimensional, Ω has to be proportional to the single generator of weight 10 holomorphic modular forms $E_4 E_6$. Indeed, one finds easily

$$\Omega = \sum_{a,b} \frac{\eta^6}{\vartheta[^{1+a}_{1+b}] \vartheta[^{1-a}_{1-b}]} \sum_{A,B \in \{0,1\}} \prod_{i=1}^{8} \vartheta[^{A+a\gamma_i}_{B+b\gamma_i}] \tag{3.2.34}$$

which can be checked to be $-E_4 E_6$. An abstract proof of this identity based on 6d anomaly cancellation can be found in [15]. We thus find that (3.2.32) yields precisely the expression for the STU-model without Wilson line moduli given in [29]. This universality property is related to the structure of the elliptic genus [114, 115].
We will now consider the nontrivial case with non-vanishing Wilson lines. The lattice sum does not factorize completely anymore. However, it should factorize partly, into a preserved and a Higgsed part. Indeed, it turns out that one can now write $F^{(g)}$ as

$$F^{(g)} = \frac{1}{Y^{g-1}} \int_{\mathcal{F}} \frac{d^2\tau}{\tau_2^2} \tau_2^{2g-2} \bar{\mathcal{P}}_{2g}(q) \sum_{a,b} \frac{c(a,b) \mathrm{e}^{2\pi \mathrm{i} ab(2-\gamma^2)}}{\eta^{18} \vartheta[^{1+a}_{1+b}] \vartheta[^{1-a}_{1-b}]} \sum_{J} \bar{\Theta}^g_{J,k}(\tau) \Phi^k_J[^a_b](q) \tag{3.2.35}$$

with

$$\bar{\Theta}^g_{J,k} = \sum_{p \in \Gamma^{k+2,2}_J} \bar{p}_R^{2g-2} q^{\frac{|p_L|^2}{2}} \bar{q}^{\frac{|p_R|^2}{2}}, \tag{3.2.36}$$

where $\Gamma^{k+2,2}_J$ denotes the conjugacy class J inside the lattice $\Gamma^{k+2,2}$, and $\Phi^k_J[^a_b](q)$ is a sum over theta functions that will be determined in the following section. Note that (3.2.35) is manifestly automorphic under the T-duality group $SO(2+k,2;\mathbb{Z})$, since it has the structure of a Borcherds' type one-loop integral [41].

3.3 Wilson lines: Splitting the lattice

3.3.1 Decompositions of the E_8 lattice

Recall from section 3.1.3 that the sequential Higgs mechanism is realized by moving along specific branches of moduli space, away from the generic point. This corresponds to imposing constraints on the Wilson line moduli, such that at each step in the chain, the number of free Wilson line moduli is reduced by one. The lattice then splits non-trivially into a Higgsed part with $p \cdot y = 0$ and a part depending on the remaining unconstrained moduli from Wilson lines and the torus.

First of all, we will determine how the lattice sum of E_8 behaves under decomposition into the maximal subgroups involved in the cascade breaking. Consider the Dynkin diagram of E_8 (Fig. 3.2) and the simple root system given in table 3.2. In all the figures, crosses correspond to Higgsed generators of the group, while the generators remaining in the Coulomb phase due to Wilson lines are shown as circles. Note that as can be seen from the labeling of the Dynkin

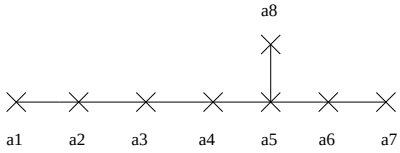

Figure 3.2: E_8 Higgsed completely (no Wilson lines)

diagram, the subgroup E_7 of E_8 is spanned by $\alpha_2, \cdots, \alpha_8$, E_6 by $\alpha_3, \cdots, \alpha_8$, $E_5 = SO(10)$ by $\alpha_4, \cdots, \alpha_8$, and so on for $SU(5), SU(4), SU(3), SU(2)$. We denote the simple roots of the second E_8 by α'_i.

We can now turn on one Wilson line, $y \sim \alpha_1$. On the other hand, turning on seven Wilson line moduli can be encoded in the constraint $\alpha_1 \cdot y = 0$. Both cases result in a split of the lattice sum of E_8 into

$$\begin{aligned}
\sum_{p\in\Gamma_{E_8}} q^{\frac{p^2}{2}} &= \sum_{n_i\in\mathbb{Z}} q^{n_1^2+\cdots+n_8^2-n_1n_2-n_2n_3-n_3n_4-n_4n_5-n_5n_6-n_5n_8-n_6n_7} \\
&= \sum_{n_i\in\mathbb{Z}} q^{(n_1-\frac{n_2}{2})^2+\frac{3}{4}n_2^2+n_3^2+\cdots+n_8^2-n_2n_3-\cdots-n_6n_7} \\
&= \sum_{j=0,1}\sum_{n_1} q^{(n_1-\frac{j}{2})^2} \sum_{n_2,\cdots n_8\in\mathbb{Z}} q^{\frac{3}{4}(2n_2-j)^2+n_3^2+\cdots+n_8^2-(2n_2-j)n_3-\cdots-n_6n_7} \\
&= \sum_{j=0,1} \vartheta\left[{}^{j/2}_{0}\right](2\cdot) \sum_{n_2,\cdots,n_8} q^{\frac{3}{4}(2n_2-j)^2+n_3^2\cdots+n_8^2-(2n_2-j)n_3-\cdots-n_6n_7}.
\end{aligned} \tag{3.3.37}$$

Here and in the following, arguments $(m\cdot)$ stand for $m \cdot \tau$, see appendix C.1. The second sum in the last line is nothing else than the sum over the conjugacy class of E_7 corresponding to $(\alpha_1, p) = j$:

$$\begin{aligned}
(\alpha_1, p) = 2n_1 - n_2 &\stackrel{!}{=} j \qquad \Rightarrow n_2 = 2n_1 - j \\
&\Rightarrow p = n_1\alpha_1 + (2n_1 - j)\alpha_2 + n_3\alpha_3 + \cdots + n_8\alpha_8, \\
p^2 &= \frac{3}{2}(2n_1 - j)^2 + \frac{j^2}{2} + 2n_3^2 - 2n_3(2n_1 - j) - \cdots
\end{aligned} \tag{3.3.38}$$

and therefore

$$q^{\frac{j^2}{4}} \sum_{n_2,\cdots,n_8} q^{\frac{3}{4}(2n_2-j)^2+n_3^2\cdots+n_8^2-(2n_2-j)n_3-\cdots-n_7n_8} = \sum_{(p,\alpha_1)=j}^{E_8} q^{\frac{p^2}{2}} = q^{\frac{j^2}{4}} \sum_{E_7^{(1)}} q^{\frac{p^2}{2}}. \tag{3.3.39}$$

We can also express the above in terms of theta functions. Rewriting the exponent in the second sum in the last line of (3.3.37) as a sum over p with $(p,\alpha_1)=0$ i.e. as

$$\begin{aligned} p &= (n_1-\frac{j}{2})\alpha_1+(2n_1-j)\alpha_2+n_3\alpha_3+\cdots n_8\alpha_8 \\ &= (-\frac{n_7}{2}, n_1-\frac{j}{2}-\frac{n_7}{2}, -n_1+\frac{j}{2}+\frac{n_7}{2}, 2n_1-j-n_3+\frac{n_7}{2}, n_3-n_4+\frac{n_7}{2}, \\ &\qquad n_4-n_5+\frac{n_7}{2}, -n_5+n_6-\frac{n_7}{2}+n_8, n_6-\frac{n_7}{2}-n_8), \end{aligned} \tag{3.3.40}$$

we can write this sum as

$$\begin{aligned} &\sum_{n_2,\cdots,n_8} q^{\frac{3}{4}(2n_2-j)^2+n_3^2\cdots+n_8^2-(2n_2-j)n_3-\cdots-n_7n_8} = \sum_{p\in E_7^{(1)}} q^{\frac{p^2}{2}} = \sum_{\substack{p\in\Gamma_{E_8}-j\frac{\alpha_1}{2}\\(p,\alpha_1)=0}} q^{\frac{p^2}{2}} \\ &= \sum_{\substack{N_1,N_3,\cdots N_8\\ N_3+\cdots+N_8=j \bmod 2\\ a=0,1}} q^{(N_1-\frac{j}{2}-\frac{a}{2})^2} q^{\frac{1}{2}\left((N_3-\frac{a}{2})^2+\cdots+(N_8-\frac{a}{2})^2\right)} \\ &= \sum_{\substack{N_1,\cdots N_8\in\mathbb{Z}\\ a=0,1\\ b=0,1}} q^{(N_1-\frac{j}{2}-\frac{a}{2})^2} q^{\frac{1}{2}\left((N_3-\frac{a}{2})^2+\cdots+(N_8-\frac{a}{2})^2\right)} (-1)^{b(N_3+\cdots+N_8-j)} \\ &= \sum_{a,b\in\{0,1\}} \vartheta[{}^{a/2+j/2}_{0}](2\cdot)\vartheta[{}^{a/2}_{b/2}]^6(-1)^{jb}. \end{aligned} \tag{3.3.41}$$

We thus have decomposed the E_8-lattice according to $P_{E_8} \to P_{E_7^{(0)}}P_{A_1^{(0)}} + P_{E_7^{(1)}}P_{A_1^{(1)}}$, as shown in Fig. 3.3. This split has already been constructed in [109]. Indeed (3.3.37) is completely equivalent to the hatting procedure for Jacobi theta functions developed in [109] for this particular split.

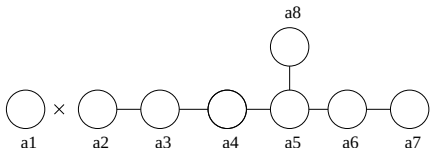

Figure 3.3: $E_8 \to E_7 \times SU(2)$

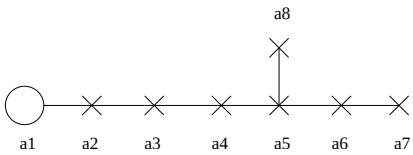

Figure 3.4: E_8 with 1 Wilson line

The same procedure applies when we split the lattice in other maximal subgroups. Namely, we can decompose with respect to $E_8 \supset E_6 \times SU(3)$:

$$\begin{aligned} \sum_{p\in\Gamma_{E_8}} q^{\frac{p^2}{2}} &= \sum_{j_2=0,1,2} \sum_{\substack{n_1,n_2\in\mathbb{Z}\\ j_1\in\{0,1\}}} q^{(n_1-\frac{j_1}{2})^2+3(n_2+\frac{j_1}{2}-\frac{j_2}{3})^2} \sum_{n_3,\cdots,n_8\in\mathbb{Z}} q^{\frac{2}{3}(3n_3-j_2)^2+n_4^2+\cdots+n_8^2-(3n_3-j_2)n_4-\cdots-n_6n_7} \\ &= \sum_{\substack{j_1=0,1\\ j_2=0,1,2}} \vartheta[{}^{j_1/2}_{0}](2\cdot)\vartheta[{}^{j_1/2+j_2/3}_{0}](6\cdot) \sum_{a,b\in\{0,1\}} \vartheta[{}^{a/2+j_2/3}_{b/2}](3\cdot)\vartheta[{}^{a/2}_{b/2}]^5(-1)^{b\cdot j_2} \\ &= P_{E_6^{(0)}}\cdot P_{A_2^{(0)}} + 2P_{E_6^{(1)}}\cdot P_{A_2^{(1)}}, \end{aligned} \tag{3.3.42}$$

The last relation in (3.3.42) follows from

$$\sum_{n_3,\cdots,n_8\in\mathbb{Z}} q^{6(n_3-\frac{j}{3})^2+n_4^2+\cdots+n_8^2-n_3n_4-\cdots-n_6n_7} = q^{-\frac{j^2}{3}} \sum_{\substack{p\in\Gamma_{E_8}\\(p,\alpha_1)=0\\(p,\alpha_2)=j}} q^{\frac{p^2}{2}} = \sum_{E_6^{(j)}} q^{\frac{p^2}{2}}, \tag{3.3.43}$$

and from the fact that $E_6^{(j=1)}$ and $E_6^{j=2}$ are equivalent. This case corresponds to 2 respectively 6 Wilson lines.
Analogously, we have lattice decompositions with respect to $E_8 \supset SO(10)\times SU(4)$ (3 or 5 Wilson lines)

$$\begin{aligned}
&\sum_{p\in\Gamma_{E_8}} q^{\frac{p^2}{2}}\\
&= \sum_{j_3=0,1,2,3} \sum_{\substack{n_1,n_2,n_3\in\mathbb{Z}\\ j_1\in\{0,1\}\\ j_2\in\{0,1,2\}}} q^{(n_1-\frac{j_1}{2})^2+3(n_2+\frac{j_1}{2}-\frac{j_2}{3})^2+6(n_3+\frac{j_2}{3}-\frac{j_3}{4})^2} \sum_{n_4,\cdots,n_8\in\mathbb{Z}} q^{\frac{3}{8}(4n_4-j_3)^2+\cdots+n_8^2-(4n_4-j_3)n_5-\cdots-n_6n_7}\\
&= \sum_{j_3=0,1,2,3} \sum_{\substack{j_1=0,1\\ j_2=0,1,2}} \vartheta[{}^{j_1/2}_{0}](2\cdot)\vartheta[{}^{j_2/3-j_1/2}_{0}](6\cdot)\vartheta[{}^{j_3/4-j_2/3}_{0}](12\cdot) \sum_{a,b\in\{0,1\}} \vartheta[{}^{a/2+j_3/4}_{0}](4\cdot)\vartheta[{}^{a/2}_{b/2}]^4(-1)^{b\cdot j_3}\\
&= P_{D_5^{(0)}}\cdot P_{A_3^{(0)}} + 2P_{D_5^{(1)}}\cdot P_{A_3^{(1)}} + P_{D_5^{(2)}}\cdot P_{A_3^{(2)}},
\end{aligned} \tag{3.3.44}$$

and for $E_8 \supset SU(5)\times SU(5)$ (4 Wilson lines)

$$\begin{aligned}
\sum_{p\in\Gamma_{E_8}} q^{\frac{p^2}{2}} &= \sum_{j_4=0,\cdots,4} \sum_{\substack{j_1=0,1\\ j_2=0,1,2\\ j_3=0,\cdots,3}} \vartheta[{}^{j_1/2}_{0}](2\cdot)\vartheta[{}^{j_2/3-j_1/2}_{0}](6\cdot)\vartheta[{}^{j_3/4-j_2/3}_{0}](12\cdot)\vartheta[{}^{j_4/5-j_3/4}_{0}](20\cdot)\cdot\\
&\qquad \cdot \sum_{a,B\in\{0,1\}} \vartheta[{}^{a/2+j_4/5}_{B/2}](5\cdot)\vartheta[{}^{a/2}_{B/2}]^3(-1)^{B\cdot j_4}\\
&= P_{A_4^{(0)}}\cdot P_{A_4^{(0)}} + 2P_{A_4^{(1)}}\cdot P_{A_4^{(1)}} + 2P_{A_4^{(2)}}\cdot P_{A_4^{(2)}}.
\end{aligned} \tag{3.3.45}$$

Note, however, that there are many other ways to decompose the lattice under other maximal subgroups. As an example, we can decompose $E_8 \to SO(14)\times SU(2)$ as shown in Fig. 3.5:

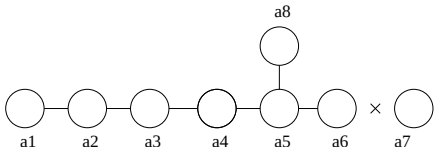

Figure 3.5: The split $E_8 \to SO(14)\times SU(2)$

$$\sum_{p\in\Gamma_{E_8}} q^{\frac{p^2}{2}} = \sum_{j=0,1}\sum_{n_7} q^{(n_7-\frac{j}{2})^2} \sum_{n_1,\cdots,n_6,n_8} q^{\frac{3}{4}(2n_6-j)^2+n_8^2+n_5^2\cdots+n_1^2-(2n_6-j)n_5-n_5n_8\cdots-n_7n_8}. \tag{3.3.46}$$

Denoting the lattice sum $\sum_{p\in\Gamma_{E_8}} q^{\frac{p^2}{2}}$ by $f(\tau)$, the splittings (3.3.37)-(3.3.45) labeled by the lower number of Wilson lines $k=1,\cdots,4$ can be cast into the general form

$$f(\tau) = f_0^k\theta_0^{(8-k)} + \cdots f_k^k\theta_k^{(8-k)}, \tag{3.3.47}$$

where

$$\theta_J^{(k)} := \sum_{\substack{j_1=0,1 \\ \vdots \\ j_{k-1}=0,\cdots k-1}} \vartheta[{}^{\frac{j_1}{2}}_{0}](2\cdot)\vartheta[{}^{\frac{j_2}{3}-\frac{j_1}{2}}_{0}](6\cdot)\cdots\vartheta[{}^{\frac{j_{k-1}}{k}-\frac{j_{k-2}}{k-1}}_{0}]((k-1)\cdot k)\vartheta[{}^{\frac{J}{(k+1)}-\frac{j_{k-1}}{k}}_{0}](k\cdot(k+1)), \tag{3.3.48}$$

and

$$f_J^k = q^{-\frac{kJ^2}{2(k+1)}} \sum_{\substack{p\in\Gamma_{E_8} \\ (p,\alpha_1)=\cdots=(p,\alpha_{k-1})=0 \\ (p,\alpha_k)=J}} q^{\frac{p^2}{2}}. \tag{3.3.49}$$

For the chains of models in [105], we find the explicit expressions

$$f_J^k = \sum_{a,b=0,1} \vartheta[{}^{a/2+J/(k+1)}_{b/2}]((k+1)\cdot)\vartheta[{}^{a/2}_{b/2}]^{(7-k)}(-1)^{b\cdot J} \tag{3.3.50}$$

for k even and

$$f_J^k = \sum_{a,b=0,1} \vartheta[{}^{a/2+J/(k+1)}_{0}]((k+1)\cdot)\vartheta[{}^{a/2}_{b/2}]^{(7-k)}(-1)^{b\cdot J} \tag{3.3.51}$$

for k odd.
We can write down the same decompositions including the shifts due to the orbifold embedding. In the chains of models in [105], the shifts are of the form $\gamma = (\alpha_1 + 2\alpha_2 + \cdots + m\alpha_m)$ and thus deform p to $p + a\gamma = (n_1 + a)\alpha_1 + (n_2 + 2a)\alpha_2 + \cdots + (n_m + m\cdot a)\alpha_j$. Therefore, $\theta_J^{(k)}$ gets deformed to

$$\theta^{(k)}_{J,\gamma}[{}^{a}_{b}](q) = \sum_{\substack{j_1=0,1 \\ \vdots \\ j_{k-1}=0,\cdots k-1}} \vartheta[{}^{\frac{j_1}{2}}_{0}](2\cdot)\vartheta[{}^{\frac{j_2}{3}-\frac{j_1}{2}}_{0}](6\cdot)\cdots\vartheta[{}^{\frac{jm}{(m+1)}-\frac{j_{m-1}}{m}-m\cdot a}_{-m(m+1)b}](m\cdot(m+1))\cdots\vartheta[{}^{\frac{J}{(k+1)}-\frac{j_{k-1}}{k}}_{0}](k\cdot(k+1)). \tag{3.3.52}$$

Similar realizations exist for other types of shifts. On the part of the lattice denoted by f_J^k, it is more convenient to write in an orthogonal basis $\gamma = (\gamma_1, \cdots, \gamma_{7-k}, 0, \cdots, 0)$ and we get for f_J^k with k even

$$f^k_{J,\gamma}[{}^{a}_{b}] = \sum_{A,B=0,1} \mathrm{e}^{-\pi\mathrm{i}\sum_i \gamma_i Ba}\vartheta[{}^{A/2+J/(k+1)}_{B/2}]((k+1)\cdot)\prod_{i=1}^{7-k}\vartheta[{}^{A/2+a\gamma_i}_{B/2+b\gamma_i}](-1)^{B\cdot J}, \tag{3.3.53}$$

respectively for k odd,

$$f^k_{J,\gamma}[{}^{a}_{b}] = \sum_{A,B=0,1} \mathrm{e}^{-\pi\mathrm{i}\sum_i \gamma_i Ba}\vartheta[{}^{A/2+J/(k+1)}_{0}]((k+1)\cdot)\prod_{i=1}^{7-k}\vartheta[{}^{A/2+a\gamma_i}_{B/2+b\gamma_i}](-1)^{B\cdot J}. \tag{3.3.54}$$

Cases with more than $7-k$ non-vanishing entries in γ have to be considered separately, see section 3.3.2.
The lattice splits derived above are the main ingredients for computing the $F^{(g)}$ in models with Wilson lines. Indeed, turning on one Wilson line in the chains of [105] corresponds to preserving a $U(1)$ that can be enhanced to an $SU(2)$ while Higgsing an E_7, and will therefore be reflected by a split as in (3.3.37). On the other hand, turning on seven Wilson lines Higgses an $SU(2)$ while preserving a $U(1)^7$ that can be enhanced to E_7 and therefore corresponds to the same split with sides exchanged, or equivalently: the same modified Dynkin diagram (Fig. 3.3) with circles replaced by crosses. Similarly, (3.3.42) corresponds to 2, respectively 6 and (3.3.44) to 3, respectively 5 Wilson lines. For 4 Wilson lines, one can choose to Higgs either side of the lattice.

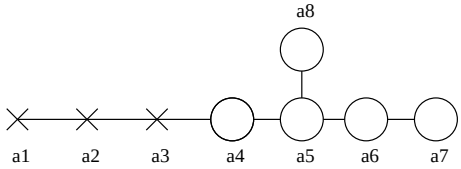

Figure 3.6: E_8 with 5 Wilson lines

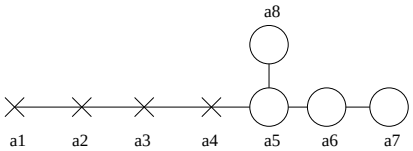

Figure 3.7: E_8 with 4 Wilson lines

3.3.2 Moduli dependence

We can now use the above to decompose the full lattice sum with torus moduli, Wilson moduli, shifts and insertions. Note that when the vector of Wilson line moduli y is *not* orthogonal to the shifts, i.e. $\gamma \cdot y \neq 0$, we turn on Wilson line moduli corresponding to the part of the gauge group only present in the orbifold limit. This results in freezing the vector moduli at that special point of moduli space, and the degeneracy of vacua gets lifted: The couplings corresponding to equivalent embeddings with different N can be different [92].
We therefore impose here $\gamma \cdot y = 0$, restricting the Wilson lines to the part of the lattice orthogonal to the shift. We have to distinguish the cases of less than four Wilson lines from those with four and more. In the latter, $\gamma \cdot y = 0$ is automatically fulfilled for the shifts given in table 3.1, as the Wilson lines are active on the right-hand side of the Dynkin diagram while the shifts act on the left. If we turn on less than four Wilson lines, those are active on the left-hand side of the diagram, as explained in section 3.3.1. This means that we have to choose the shift such that it does not interfere with the Wilson lines, and in such a way that it preserves the part of the diagram where the Wilson lines are active. For the $\mathbb{Z}_2, \mathbb{Z}_3$ and $\mathbb{Z}_4$ embeddings on the first E_8 lattice (see table 3.1), it is sufficient to move the shift to the other end of the diagram, redefining $\gamma^1_{\mathbb{Z}_2} \to \gamma'^1_{\mathbb{Z}_2} = (0^6, -1, 1), \gamma^1_{\mathbb{Z}_3} \to \gamma'^1_{\mathbb{Z}_3} = (0^5, -2, 1, 1), \gamma_{\mathbb{Z}_4} \to \gamma'^1_{\mathbb{Z}_4} = (0^4, -3, 1, 1, 1)$. In the case of the $\mathbb{Z}_6$ orbifold, this does the trick for one and two Wilson lines, but if we turn on a third one, it is not orthogonal to $\gamma'^1_{\mathbb{Z}_6}$ anymore. However, we can choose the equivalent embedding $\gamma'^1 = (2, 2, 2, 2, 2, 0^3)$, orthogonal to $y \in \text{span}(\alpha_1, \alpha_2, \alpha_3)$. In this case, this is also a valid choice for zero, one and two Wilson lines. The Wilson lines on the second E_8, unchanged throughout the sequential Higgs mechanisms, work out similarly. Only the $\mathbb{Z}_4$ orbifold is slightly more delicate, as the Wilson lines corresponding to maximal Higgsing on the second E_8 preserve an $SO(8)$, and therefore act in the center of the diagram. The combination of theta functions corresponding to the Higgsed lattice can however be determined using (3.3.49).

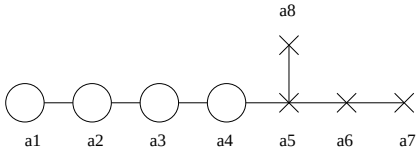

Figure 3.8: E_8 with 4 Wilson lines, alternative split

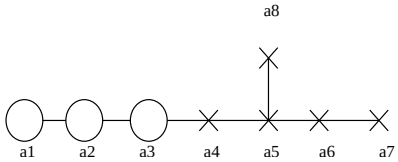

Figure 3.9: E_8 with 3 Wilson lines

For one Wilson line, we thus write

$$\begin{aligned}
&\sum_{p\in\Gamma^{18,2}+a\gamma} p_R^{(2g-2)} q^{\frac{|p_L|^2}{2}} \bar{q}^{\frac{|p_R|^2}{2}} \mathrm{e}^{2\pi \mathrm{i} b\gamma\cdot p} = \sum_{p\in\Gamma^{18,2}+a\gamma} (p\cdot u(y))^{(2g-2)} q^{\frac{p^2}{2}} |q|^{(p\cdot u(y))^2} \mathrm{e}^{2\pi \mathrm{i} b\gamma\cdot p} \\
&\quad = \sum_{J=0,1} \sum_{\substack{A,B\in\{0,1\}\\ \alpha,\beta\in\{0,1\}}} \mathrm{e}^{-\pi \mathrm{i} \sum_i \gamma_i' Ba} \left(\prod_{i=3}^{8} \vartheta[{}^{A/2+a\gamma_i'}_{B/2+b\gamma_i'}]\right) \vartheta[{}^{A/2+J/2}_{0}](2\cdot)(-1)^{BJ} \\
&\cdot \mathrm{e}^{-\pi \mathrm{i} a \sum_{i=9}^{16} \gamma_i \beta} \left(\prod_{j=9}^{16} \vartheta[{}^{\alpha/2+a\gamma_j}_{\beta/2+b\gamma_j}]\right) \cdot \sum_{n_1,n_\pm,m_\pm} (p\cdot u(y))^{2g-2} q^{(n_1-\frac{J}{2})^2 - m_+ n_- + n_0 m_0} |q|^{(p\cdot u(y))^2} \\
&\quad = \sum_J f_J^1[{}^a_b](q) \bar{\Theta}^g_{J,1}(q,y),
\end{aligned} \tag{3.3.55}$$

where $\Theta^g_{J,k}(q,y)$ is defined in (3.2.36), and

$$\begin{aligned}
f_J^1[{}^a_b](q) = &\sum_{\substack{A,B\in\{0,1\}\\ \alpha,\beta\in\{0,1\}}} \mathrm{e}^{-\pi \mathrm{i} a \sum_{i=3}^{8} \gamma_i' B} \left(\prod_{i=3}^{8} \vartheta[{}^{A/2+a\gamma_i'}_{B/2+b\gamma_i'}]\right) \vartheta[{}^{A/2+J/2}_{0}](2\cdot)(-1)^{BJ} \\
&\cdot \mathrm{e}^{-\pi \mathrm{i} a \sum_{i=9}^{16} \gamma_i \beta} \left(\prod_{j=9}^{16} \vartheta[{}^{\alpha/2+a\gamma_j}_{\beta/2+b\gamma_j}]\right).
\end{aligned} \tag{3.3.56}$$

This is nothing else than (3.3.54) applied to the whole lattice of two E_8 and the torus, and including the shifts. Analogously, we get for $k \le 4$ Wilson lines

$$\sum_{p\in\Gamma^{18,2}+a\gamma} p_R^{(2g-2)} q^{\frac{|p_L|^2}{2}} \bar{q}^{\frac{|p_R|^2}{2}} \mathrm{e}^{2\pi \mathrm{i} b\gamma\cdot p} = \sum_J f_J^k[{}^a_b](q) \bar{\Theta}^g_{J,k}(q,y), \tag{3.3.57}$$

where for k=3

$$\begin{aligned}
f_J^3[{}^a_b](q) = &\sum_{\substack{A,B\in\{0,1\}\\ \alpha,\beta\in\{0,1\}}} \mathrm{e}^{-\pi \mathrm{i} a \sum_{i=5}^{8} \gamma_i' B} \left(\prod_{i=5}^{8} \vartheta[{}^{A/2+a\gamma_i'}_{B/2+b\gamma_i'}]\right) \vartheta[{}^{A/2+J/4}_{0}](4\cdot)(-1)^{BJ} \\
&\mathrm{e}^{-\pi \mathrm{i} a \sum_{i=9}^{16} \gamma_i \beta} \left(\prod_{j=9}^{16} \vartheta[{}^{\alpha/2+a\gamma_j}_{\beta/2+b\gamma_j}]\right),
\end{aligned} \tag{3.3.58}$$

and for $k = 2$ or $k = 4$ Wilson lines, using (3.3.53),

$$\begin{aligned}
f_J^k[{}^a_b](q) = &\sum_{\substack{A,B\in\{0,1\}\\ \alpha,\beta\in\{0,1\}}} \mathrm{e}^{-\pi \mathrm{i} a \sum_{i=k+2}^{8} \gamma_i B} \left(\prod_{i=k+2}^{8} \vartheta[{}^{A/2+a\gamma_i'}_{B/2+b\gamma_i'}]\right) \vartheta[{}^{A/2+J/(k+1)}_{B/2}]((k+1)\cdot)(-1)^{BJ} \\
&\mathrm{e}^{-\pi \mathrm{i} a \sum_{i=9}^{16} \gamma_i \beta} \left(\prod_{j=9}^{16} \vartheta[{}^{\alpha/2+a\gamma_j}_{\beta/2+b\gamma_j}]\right).
\end{aligned} \tag{3.3.59}$$

When more than four Wilson lines are turned on ($k \geq 4$), we decompose analogously as

$$\sum_{p\in\Gamma^{18,2}+a\gamma} p_R^{(2g-2)} q^{\frac{|p_L|^2}{2}} \bar{q}^{\frac{|p_R|^2}{2}} \mathrm{e}^{2\pi \mathrm{i} b\gamma\cdot p} = \sum_J \theta_J^k[{}^a_b](q)\bar{\Theta}^g_{J,k}(q,y), \tag{3.3.60}$$

where $\theta_J^k[{}^a_b](q)$ is (3.3.52), supplemented by the contribution from the second E_8 lattice. Any other split for any number of Wilson lines fulfilling the constraint $\gamma \cdot y = 0$ can be realized similarly. In the above, we have assumed that the second E_8 lattice is Higgsed completely, without any Wilson lines. If this is not the case, as for example for the $\mathbb{Z}_2, \mathbb{Z}_3$ and $\mathbb{Z}_4$ models in [105], the second lattice also has to be split according to the above prescription.

Note that these splits describe a "generalized hatting procedure" analogous to the 1-Wilson line case analyzed in [109] for generalized Jacobi forms. In the 1 Wilson line $STUV$ model, the relevant forms are standard Jacobi forms

$$f(\tau, V) = \sum_{\substack{n\geq 0\\ l\in\mathbb{Z}}} c(4n-l^2) q^n r^l \tag{3.3.61}$$

with $q = \mathrm{e}^{2\pi \mathrm{i}\tau}, r = \mathrm{e}^{2\pi V}$, admitting a decomposition

$$f(\tau, V) = f_{ev}(\tau)\theta_{ev}(\tau, V) + f_{odd}(\tau)\theta_{odd}(\tau, V), \tag{3.3.62}$$

where $\theta_{ev} = \theta_3(2\tau, 2V)$, $\theta_{odd} = \theta_2(2\tau, 2V)$. The effect of turning on a Wilson line can be described by replacing $f(\tau, V)$ by its hatted counterpart [109]

$$\hat{f}(\tau, V) = f_{ev}(\tau) + f_{odd}(\tau) \tag{3.3.63}$$

In the generic, k Wilson line case considered here, we decompose the lattice sum as in (3.3.47).

When $k \leq 4$, the "generalized hatting" due to the Wilson lines is

$$\hat{f}[{}^a_b](\tau, V_1, \cdots V_k) = f_0^k[{}^a_b](\tau) + \cdots f_k^k[{}^a_b](\tau), \tag{3.3.64}$$

where f_J^k and f_{k+1-J}^k are equivalent. When $k \geq 4$, we have to keep the other part of the split lattice. This yields the "complementary hatting"

$$\breve{f}(\tau, V_1, \cdots V_n) = \theta_0^{8-k}[{}^a_b](\tau) + \cdots \theta_k^{8-k}[{}^a_b](\tau), \tag{3.3.65}$$

with $\theta_J^{8-k} = \theta_{k+1-J}^{8-k}$.

3.3.3 Computation of $F^{(g)}$

In the following, we will denote the number of Wilson lines by k and write the split lattice sum as

$$\sum_J \Phi_J^k[{}^a_b](q)\bar{\Theta}^g_{k,J}(q), \tag{3.3.66}$$

where $\Phi_J^k[{}^a_b](q)$ is the function appearing in (3.2.35) and stands for $f_J^k[{}^a_b]$ or $\theta_J^k[{}^a_b](q)$, whichever is applicable. We expand the modular function in the integrand of (3.2.35) as

$$\mathcal{P}_{2g}(q)\mathcal{F}_J^k(q) := \mathcal{P}_{2g}(q)\sum_{a,b} \frac{c(a,b)\mathrm{e}^{2\pi \mathrm{i} ab(2-\gamma^2)}}{\eta^{18}\vartheta[{}^{1+a}_{1+b}]\vartheta[{}^{1-a}_{1-b}]}\Phi_J^k[{}^a_b](q) = \sum_{n\in\mathbb{Q}_J} c^k_{g,J}(n)q^n, \tag{3.3.67}$$

where $\mathbb{Q}_J$ denotes the subset of $\mathbb{Q}$ containing the powers of q appearing in the conjugacy class J. Since different conjugacy classes correspond to different rational powers of q, we can sum over J without loss of information and write

$$\sum_{n\in\mathbb{Q}} c^k_g(n)q^n = \sum_J \sum_{n\in\mathbb{Q}_J} c^k_{g,J}(n)q^n. \tag{3.3.68}$$

We can now evaluate the integral (3.2.27) using Borcherds' technique of lattice reduction [41] reviewed in appendix A.1. We choose the reduction vector to lie in the torus part of the lattice, the result is therefore only valid in the chamber of the T, U torus moduli space where the projected reduction vector z_+ is small. The result looks very similar to what was obtained in [29] for the STU-model and can be simplified to read[1] $F^{(g)} = F^{(g)}_{\text{deg}} + F^{(g)}_{\text{nondeg}}$ where

$$F^{(g)}_{\text{deg}} = \frac{(y_2,y_2)8\pi^3}{T_2}\delta_{g,1} + \frac{1}{2(2T_2)^{2g-3}} \sum_{\lambda\in\Gamma^{k,0}} \sum_{l=0}^{g} \text{Li}_{2l-2g+4}(q^{\text{Re}(\bar{\lambda}\cdot\bar{y})}) c^k_{g-l}(\frac{\lambda^2}{2}) \frac{1}{\pi^{2l+3}} (-\frac{T_2^2}{2y_2^2})^l \quad (3.3.69)$$

$$\begin{aligned} F^{(g)}_{\text{nondeg}} = & \\ & \sum_{l=0}^{g-1} \sum_{C=0}^{\min(l,2g-3-l)} \sum_{r\in\Gamma^{k+1,1}} \binom{2g-l-3}{C} \frac{1}{(l-C)!2^C} \frac{(-\text{Re}(r\cdot y))^{l-C}}{(y_2,y_2)^l} c^k_{g-l}(\frac{r^2}{2}) \text{Li}_{3-2g+l+C}(\mathrm{e}^{-r\cdot y}) \\ & + \frac{c^k_1(0)}{2^g(g-1)(y_2,y_2)^{g-1}} + \sum_{l=0}^{g-2} \frac{c^k_{g-l}(0)}{l!(2(y_2,y_2))^l} \zeta(3+2(l-g)) \frac{(2g-3-l)!}{(2g-3-2l)!} \end{aligned} \quad (3.3.70)$$

This can also be compared to the expressions obtained in [92] for genus one. The lattice sum in (3.3.70) is over the so-called reduced lattice $\Gamma^{k+1,1}$. This is a sublattice of the original lattice $\Gamma^{k+2,2}$, parametrized by (n_0, m_0, b_i).

A highly nontrivial check of the computation is provided by the Euler characteristics of the corresponding Calabi-Yau manifolds, respectively the difference $n_h - n_v$ on the heterotic side. Heterotic-type II duality implies [29] that it should be given by the normalized q^0 coefficient of $\mathcal{F}^k_J$, namely

$$2(n_h - n_v) = \chi(X) = 2\frac{c^k_0(0)}{c^k_0(-1)}. \quad (3.3.71)$$

One indeed finds precisely the chains of Euler characteristics given in [105], see table 3.4. The corresponding K3-fibrations are listed in table B.1.

$\mathbb{Z}_2$	92	132	168	200	304	412	612	960
$\mathbb{Z}_3$		120	144	164	232	312	420	624
$\mathbb{Z}_4$					224	288	372	528
$\mathbb{Z}_6$				220	264	312	372	480

Table 3.4: Euler characteristics χ for the models in [105]

3.4 Heterotic-type II duality and instanton counting

3.4.1 Moduli map

In this section, we will determine geometric quantities on the dual Calabi-Yau manifolds on the type II side using the heterotic expressions obtained above.

The heterotic dilaton S gets mapped to the Kähler modulus t_2, therefore heterotic weak coupling regime corresponds to $t_2 \to \infty$. This restricts the instanton numbers accessible to our computation to those classes where the corresponding coefficient l_2 vanishes. The mapping of the remaining heterotic moduli from the Torus and the Wilson lines $(T, U, V_1, \cdots V_k)$ to the Kähler moduli $(t_1, \cdots t_{k+3})$ on the type II side can be determined for models with small number

[1] see the appendix of [42] for details of the simplification

of Kähler moduli comparing the classical pieces of the prepotential [109]. In order to compare with the instanton numbers in [110], we extend the map of [109] to two Wilson lines as follows:

$$\begin{aligned} T &\to t_1 + 2t_4 + 3t_5 \\ U &\to t_1 + t_3 + 2t_4 + 3t_5 \\ V_1 &\to t_4 \\ V_2 &\to t_5 \end{aligned} \tag{3.4.72}$$

implying that the numbers (n_0, m_0, b_i) in (3.2.18) map to the numbers l_i on the type II side as

$$\begin{aligned} l_1 &= n_0 + m_0 \qquad & l_4 &= 2(n_0 + m_0) + b_1 \\ l_2 &= 0 & l_5 &= 3(n_0 + m_0) + b_2 \\ l_3 &= n_0. \end{aligned} \tag{3.4.73}$$

For higher numbers of Wilson lines, we cannot conclusively determine the map due to lack of information on the type II side, but it is clear that such a map exists and that it is linear. In order to extract genus g instanton numbers from the expansion (3.3.67), we have to specify the norm (p, p). Redefining the indices in (3.3.37)-(3.3.45) as

$$\begin{aligned} (n_1 - \frac{a}{2})^2 &\to \frac{b_1^2}{4} \\ (n_1 - \frac{a}{2})^2 + 3(n_2 + \frac{a}{2} - \frac{b}{3})^2 &\to \frac{b_1^2}{4} + 3(\frac{b_1}{2} - \frac{b_2}{3})^2 = b_1^2 - b_1 b_2 + \frac{b_2^2}{3} \\ (n_1 - \frac{a}{2})^2 + 3(n_2 + \frac{a}{2} - \frac{b}{3})^2 + 6(n_2 + \frac{b}{3} - \frac{c}{4})^2 &\to \frac{b_1^2}{4} + 3(\frac{b_1}{2} - \frac{b_2}{3})^2 + 6(\frac{b_2}{3} - \frac{b_3}{4})^2 \\ &= b_1^2 + b_2^2 - b_1 b_2 - b_2 b_3 + \frac{3b_3^2}{8}, \\ &\vdots \end{aligned} \tag{3.4.74}$$

we find the norms given in table 3.5. We thus have for the instanton numbers

$$\begin{aligned} c_k^g(n_0, m_0, b_1, \cdots b_k) &= c_k^g(n_0 m_0 - b_1^2 - \cdots - b_{k-1}^2 + b_1 b_2 \cdots b_{k-1} b_k - \frac{k b_k^2}{2(k+1)}), \qquad k \le 4 \\ c_k^g(n_0, m_0, b_{9-k}, \cdots b_8) &= c_k^g(n_0 m_0 - \frac{(10-k) b_{9-k}^2}{2(9-k)} - b_{10-k}^2 - \cdots - b_8^2 + b_{9-k} b_{10-k} + \cdots b_5 b_8, \\ & \qquad\qquad\qquad\qquad\qquad\qquad\qquad\qquad\qquad\qquad\qquad\qquad k \ge 4, \end{aligned} \tag{3.4.75}$$

confirming the conjecture made in [109]. Note that the last b_p determines the conjugacy class.

3.4.2 Extracting geometric information

The topological couplings $F^{(g)}$ are the free energies of the A-model topological string. They have a geometric interpretation as a sum over instanton sectors,

$$F^{(g)}(t) = \sum_\beta N_{g,\beta} Q^\beta, \tag{3.4.76}$$

where $Q_i = \mathrm{e}^{-t_i}$, $\beta = \{n_i\}$ in a basis of $H_2(X)$ denotes a homology class, $Q^\beta := \mathrm{e}^{-t_i n_i}$, and $N_{g,\beta}$ are the Gromov-Witten invariants, in general *rational* numbers. With the work of Gopakumar and Vafa [23, 24], a hidden integrality structure of the $N_{g,\beta}$ has been uncovered. The generating functional of the $F^{(g)}$,

$$F(t, g_s) = \sum_{g=0}^{\infty} F^{(g)}(t) g_s^{2g-2}, \tag{3.4.77}$$

k	$p^2_{\rm het}$
0	$n_0 m_0$
1	$n_0 m_0 - \frac{b_1^2}{4}$
2	$n_0 m_0 - b_1^2 + b_1 b_2 - \frac{b_2^2}{3}$
3	$n_0 m_0 - b_1^2 - b_2^2 + b_1 b_2 + b_2 b_3 - \frac{3b_3^2}{8}$
4	$n_0 m_0 - b_1^2 - b_2^2 - b_3^2 + b_1 b_2 + b_2 b_3 + b_3 b_4 - \frac{2b_4^2}{5}$
5	$n_0 m_0 - \frac{5b_4^2}{8} - b_5^2 - b_6^2 - b_7^2 - b_8^2 + b_4 b_5 + b_5 b_6 + b_5 b_8 + b_6 b_7 + b_7 b_8$
6	$n_0 m_0 - \frac{2b_3^2}{3} - b_4^2 - b_5^2 - b_6^2 - b_7^2 - b_8^2 + b_3 b_4 + b_4 b_5 + b_5 b_6 + b_5 b_8 + b_6 b_7 + b_7 b_8$
7	$n_0 m_0 - \frac{3b_2^2}{4} - b_3^2 - b_4^2 - b_5^2 - b_6^2 - b_7^2 - b_8^2 + b_2 b_3 + b_3 b_4 + b_4 b_5 + b_5 b_6 + b_5 b_8 + b_6 b_7 + b_7 b_8$

Table 3.5: The norm $(p_{\rm het}, p_{\rm het})_k$ for $k = (0, 1, \cdots 7)$ Wilson lines

can be written as a generalized index counting BPS states in the corresponding type IIA theory:

$$F(t, g_s) = \sum_{g=0} \sum_{\beta} \sum_{d=1}^{\infty} n_\beta^g \frac{1}{d} \left(2 \sin \frac{d g_s}{2} \right)^{2g-2} Q^{d\beta}, \tag{3.4.78}$$

where the numbers n_β^g are now *integers* called Gopakumar-Vafa invariants. Since the homology classes β are labeled by lattice vectors p, we write the Gopakumar-Vafa invariants for models with k Wilson lines as $n_g^k(p) \equiv n_g^k(\frac{p^2}{2})$. We also write, in terms of the instanton degrees on the type II side, $n_g^k(l_1, \cdots, l_{k+3})$.
From the structure of the $F^{(g)}$, one can deduce that the coefficients $c_g^k(\frac{p^2}{2})$ appearing in (3.3.69),(3.3.70) are related to the Gopakumar-Vafa invariants through

$$\sum_{g \geq 0} n_g^k(p) \left(2 \sin \frac{\lambda}{2} \right)^{2g-2} = \sum_{g \geq 0} c_g^k(\frac{p^2}{2}) \lambda^{2g-2}. \tag{3.4.79}$$

The Gopakumar-Vafa invariants can be obtained efficiently using the formula [79]

$$\sum_{p \in {\rm Pic}(K3)} \sum_{g=0}^{\infty} n_g^k(p) z^g q^{\frac{p^2}{2}} = \sum_J \mathcal{F}_J^k(q) \xi^2(z, q), \tag{3.4.80}$$

where $\mathcal{F}_J^k(q)$ is defined in (3.3.67), and

$$\xi(z, q) = \prod_{n=1}^{\infty} \frac{(1-q^n)^2}{(1-q^n)^2 + z q^n}. \tag{3.4.81}$$

3.4.3 Gopakumar-Vafa invariants

Table 3.6- table 3.8 show conjectural GV invariants n_g^k for the K3 fibrations dual to the STU-, the $STUV$-, and the $STUV_1V_2$-model. Similar tables for the other models considered in this work can be found in appendix B.1, along with a list of the dual pairs of [105].

For comparison with [110], we give the genus 0 instanton numbers in notation $[l_1 \cdots l_{k+3}] = n_0^k(l_1, \cdots l_{k+3})$ for models with one and two Wilson lines in table 3.9, 3.10. We find indeed perfect agreement with [110].

Another nontrivial check is provided by the requirement of consistent truncation: in [110], the authors deduce that the following relations have to hold between instanton numbers with 3,4,and 5 moduli

$$n_0^0(l_1, l_2, l_3) = \sum_x n_0^1(l_1, l_2, l_3, x) \qquad n_0^1(l_1, l_2, l_3, l_4) = \sum_x n_0^2(l_1, l_2, l_3, l_4, x). \tag{3.4.82}$$

g	$\frac{p^2}{2}=-1$	0	1	2	3	4	5
0	-2	480	282888	17058560	477516780	8606976768	115311621680
1	0	4	-948	-568640	-35818260	-1059654720	-20219488840
2	0	0	-6	1408	856254	55723296	1718262980
3	0	0	0	8	-1860	-1145712	-76777780
4	0	0	0	0	-10	2304	1436990

Table 3.6: $n_g^k(\frac{p^2}{2})$ for $\mathbb{Z}_6$, 0 Wilson lines (STU), dual to $X^{1,1,2,8,12}$

g	$\frac{p^2}{2}=-1$	$-\frac{1}{4}$	0	$\frac{3}{4}$	1	$\frac{7}{4}$	2	$\frac{11}{4}$	3
0	-2	56	372	53952	174240	3737736	9234496	110601280	237737328
1	0	0	4	-112	-732	-108240	-350696	-7799632	-19517380
2	0	0	0	0	-6	168	1084	162752	528582
3	0	0	0	0	0	0	8	-224	-1428

Table 3.7: $\mathbb{Z}_6$,1 Wilson line (STUV), dual to $X^{1,1,2,6,10}$

g	$\frac{p^2}{2}=-1$	$-\frac{1}{3}$	0	$\frac{2}{3}$	1	$\frac{5}{3}$	2	$\frac{8}{3}$	3
0	-2	30	312	26664	120852	1747986	5685200	49588776	135063180
1	0	0	4	-60	-612	-53508	-243560	-3656196	-12097980
2	0	0	0	0	-6	90	904	80472	367458
3	0	0	0	0	0	0	8	-120	-1188
4	0	0	0	0	0	0	0	0	-10

Table 3.8: $\mathbb{Z}_6$, 2 Wilson lines (STUV_1V_2), dual to $X^{1,1,2,6,8}$

[0001]	56	[1001]	56	[1003]	56	[3014]	174240
[0002]	-2	[1002]	372	[1000]	-2	[1011]	56
[1004]	-2	[2012]	372	[0003]	0	[2013]	53952

Table 3.9: Numbers of rational curves of degree $[l_1,0,l_2,l_3,l_4]$ on $X^{1,1,2,6,10}$ (dual to $\mathbb{Z}_6$,1 WL)

[00001]	30	[10011]	30	[00002]	0	[10023]	312
[00010]	-2	[10022]	30	[00012]	30	[10010]	-2
[00023]	-2	[20101]	26664	[00011]	30	[20169]	312
[00101]	0	[30141]	0	[00013]	-2	[30144]	30
[30145]	26664	[30146]	120852	[30147]	26664	[30148]	30

Table 3.10: Numbers of rational curves of degree $[l_1,0,l_3,l_4,l_5]$ on $X^{1,1,2,6,8}$ (dual to $\mathbb{Z}_6$, 2 WL)

Our numbers indeed fulfill this constraint, as for example

$$n_0^2(0,0,0,1,0)+\cdots+n_0^2(0,0,0,1,3)=-2+30+30-2=56=n_0^1(0,0,0,1), \tag{3.4.83}$$

$$n_0^1(0,0,0,0)+\cdots+n_0^1(0,0,0,4)=-2+56+372+56-2=480=n_0^0(0,0,0), \tag{3.4.84}$$

and

$$n_0^2(3,0,1,4,0)+\cdots+n_0^2(3,0,1,4,8)=174240=n_0^1(3,0,1,4). \tag{3.4.85}$$

This relation should also hold at higher genus and for higher numbers of Kähler moduli [97], namely we expect

$$n_g^k(l_1, l_2, \cdots l_{k+3}) = \sum_x n_g^{k+1}(l_1, l_2, \cdots l_{k+3}, x). \tag{3.4.86}$$

Indeed, we have for example for truncation from 2 to 1 Wilson line (tables 3.7, 3.8) $4-60-60+4 = -112$, $-6+90+90-6 = 168$, and $90+904+90 = 1084$. All instanton numbers produced, including those in tables B.2-B.15, fulfill the truncation identities

$$\begin{aligned}
n_g^0(1) &= 2\left(n_g^1(0) + n_g^1(\frac{3}{4})\right) + n_g^1(1) & n_g^0(2) &= 2\left(n_g^1(-\frac{1}{4}) + n_g^1(1) + n_g^1(\frac{7}{4})\right) + n_g^1(2) \\
n_g^1(1) &= 2\left(n_g^2(-\frac{1}{3}) + n_g^2(\frac{2}{3})\right) + n_g^2(1) & n_g^1(2) &= 2\left(n_g^2(-1) + n_g^2(\frac{2}{3}) + n_g^2(\frac{5}{3})\right) + n_g^2(2) \\
n_g^2(1) &= 2\left(n_g^3(-\frac{1}{2}) + n_g^3(\frac{5}{8})\right) + n_g^3(1) & n_g^2(2) &= 2\left(n_g^3(\frac{1}{2}) + n_g^3(\frac{13}{8})\right) + n_g^3(2) \\
n_g^2(\frac{2}{3}) &= n_g^3(-\frac{3}{8}) + n_g^3(0) + n_g^3(\frac{1}{2}) + n_g^3(\frac{5}{8}) & n_g^3(0) &= n_g^4(-\frac{2}{5}) + n_g^4(0).
\end{aligned} \tag{3.4.87}$$

Note that these identities hold –as far as we can verify– at general genus and independently of the specific chain, as expected. Again, this provides a non-trivial check of our results.

Conclusion

In this chapter, we have shown how to compute higher derivative couplings for general symmetric $\mathbb{Z}_N$, $\mathcal{N}=2$ orbifold compactifications of the heterotic string with any number of Wilson lines. In particular, this provides conjectural instanton numbers for each of the models in the chains of heterotic-type II duals of [105]. Unfortunately, our results can so far only be checked for up to two Wilson lines, since for higher numbers of vector multiplets the type II computation becomes very involved. They do however fulfill nontrivial constraints coming from the geometric transitions on the type II side [110].

Part III

INSTANTONS IN MATRIX MODELS AND TOPOLOGICAL STRINGS

It is a well-known fact that the $1/N$ expansion of gauge theories has nonperturbative corrections which behave as e^{-N} [116, 48]. Physically, these corrections are due to instantons in the collective field theory describing the large N limit. In cases where the gauge theory has a string dual, they typically correspond to D–brane instanton effects. Based on general arguments, one should expect that these e^{-N} effects are in turn related to the large–order behavior of the $1/N$ expansion, as in standard field theory [117].

Perhaps the simplest class of large N gauge theories with dual string theories are matrix models. These dual pairs fall in two classes. One is noncritical string theory, i.e. whose conformal algebra has central charge $c < 1$, corresponding to matrix models in a certain double-scaling limit near the critical point (see [118] for a review). The second class is the B-model topological string, corresponding to matrix models off criticality. This duality, mentioned in chapter 1 and to be reviewed in more detail in section 4.2, was first proposed for some geometries in [32] and has recently been extended to the mirrors of toric manifolds [29, 36]. In these examples, the matrix model is evaluated at *generic* values of the couplings, corresponding to generic complex structure moduli. If one further tunes the couplings to the critical point taking a double-scaling limit, one finds that the free energies near this point of moduli space satisfy the Painlevé I equation describing two-dimensional gravity, see, e.g., [119].

The instanton configurations in the $1/N$ expansion have been identified long ago in terms of eigenvalue tunneling [48, 120, 121], and they have been studied in great detail in the double–scaling limit. In [120, 121], David derived the action of the instanton configuration corresponding to the tunneling of a single matrix eigenvalue across the well of the unstable effective potential. This is a one–instanton effect; we refer to tunneling of several eigenvalues as multi–instanton effects. David explicitly showed that, near the critical point, this one–instanton action correctly predicts the large–genus behaviour of the free energy of the matrix model in the double–scaling limit, where the latter is obtained independently of the instanton computation via a solution to the so–called string equation. In the dual non-critical string theory, the instanton effects considered by David were later identified as D–instanton effects [122, 123] due to the so–called ZZ branes [124], and it was shown in [122, 51] that a direct D–brane calculation reproduces the instanton action obtained from the double–scaled matrix model. This line of research thus made explicit the connection between D–instantons in string theory and eigenvalue tunneling in the matrix model dual. Quantum fluctuations around this one–instanton configuration, again restricted to the double–scaling limit, were further analyzed in [125], and more recently in [126, 127], but the connection to the large–order behavior of perturbation theory was never explicitly addressed in any of those papers. In fact, it is surprising that to this date there has been no detailed study of instanton configurations in the matrix model off–criticality, nor of their connection to the large–order behaviour of the $1/N$ expansion. In [126, 127] a general setting for this study was presented but the results of these papers are incorrect once we move away from the critical point.

The main goal of this part is to fill this gap. In chapter 4, we review the relevant material about matrix models, the duality with topological string theory and the connection between instantons and large-order behaviour. We then present a computation of the instanton amplitude in generic one-cut hermitian matrix models up to two loops, published in [71], in chapter 5. We test our results with the large-order asymptotics of both matrix models and their proposed dual topological string theories, obtaining excellent agreement [71]. This is not only a check of the duality beyond perturbation theory, but also shows that the matrix model description contains nonperturbative information about the topological string that is difficult to define let alone compute directly. Chapter 6 extends the computation to multi-cut respectively multi-instanton models [72].

Chapter 4

Topological Strings at Large Order from Matrix Model Instantons

This chapter contains an introduction to the main concepts relevant for the rest of this part. The organization is as follows. Section 4.1 contains a review of hermitian matrix models and their instanton configurations. In section 4.2, we review the relation between matrix models and topological strings, focusing on the Dijkgraaf-Vafa conjecture and its recent generalization. Section 4.3 reviews how instantons determine large-order behaviour in field theory and quantum mechanics.

4.1 Matrix Models

4.1.1 The $1/N$ expansion and the Eynard-Orantin recursion

Matrix models are quantum gauge theories in zero dimensions, and thus in a sense the simplest examples of quantum field theories. Nevertheless, they are surprisingly complex and share many features with ordinary QFTs, such as nonperturbative effects and a nontrivial phase structure. Much of the magic of matrix models lies in their large-N expansion, where N is the rank of the gauge group respectively the size of the matrices. This expansion, also known as topological, is known to have enumerative content [128, 129], and is therefore the one we are interested in. We will summarize in the following some of the main properties of matrix models at large N. For a more detailed introduction to the subject, see e.g. [118, 9].

A matrix model is defined by the partition function

$$Z = \frac{1}{\mathrm{vol}(U(N))} \int dM \mathrm{e}^{-\frac{1}{g_s}\mathrm{Tr}V(M)}, \tag{4.1.1}$$

where the integration is over some ensemble of random matrices, in the cases considered here, hermitian matrices. $V(M)$ is a polynomial potential of the form

$$M^2 + \sum_p g_p M^p, \tag{4.1.2}$$

therefore the action has the obvious gauge symmetry

$$M \to UMU^\dagger. \tag{4.1.3}$$

Integrating over eigenvalues instead of matrix elements, we obtain

$$Z_N = \frac{1}{N!(2\pi)^N} \int \prod_{i=1}^{N} \mathrm{d}\lambda_i \, \Delta^2(\lambda) \, \mathrm{e}^{-\frac{1}{g_s}\sum_{i=1}^{N} V(\lambda_i)}, \tag{4.1.4}$$

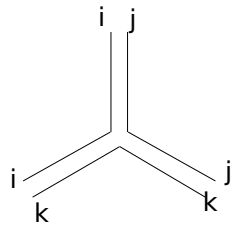

Figure 4.1: cubic vertex in double-line notation

where $\Delta(\lambda) = \prod_{i<j}(\lambda_i - \lambda_j)$ is the familiar Vandermonde determinant. Note that this can also be written as

$$Z_N = \frac{1}{N!}\int \prod_{i=1}^{N} \frac{dz_i}{2\pi} \mathrm{e}^{-\frac{1}{g_s}V_{eff}(z_i)} \tag{4.1.5}$$

with the effective potential

$$V_{\text{eff}}(z_i) = V(z_i) - 2g_s \sum_{i\neq j} \log|z_i - z_j|. \tag{4.1.6}$$

In the above expression, V_{eff} contains an effective Coulomb repulsion, resulting in eigenvalues spreading out over an interval $\mathcal{C}$. This correlation of eigenvalues is due to the constraint from the matrix ensemble; even though the matrices are random, their eigenvalues are not. This property of matrix models has led to various applications in statistics, ranging from the distribution of mexican buses to financial data [130, 131].

In the ordinary perturbative expansion, each Feynman diagram will generically give rise to several terms with different powers of N. In order to resum the perturbative expansion collecting powers of N, we introduce the double-line notation due to 't Hooft [5]. Since the fundamental field M_{ij} is in the adjoint representation which is the tensor product of fundamental and antifundamental representation, we can consider the indices i, j separately as indices of the (anti-)fundamental representations $N, \bar{N}$, and replace the ordinary, single-line propagator by a double-line propagator keeping track of these indices. In this notation, the cubic vertex

$$\mathrm{Tr}M^3 = \sum_{ijk} M_{ij}M_{jk}M_{ki} \tag{4.1.7}$$

is represented as shown in Fig. 4.1. The propagator of the theory reads

$$\langle M_{ij}M_{kl}\rangle = g_s\delta_{il}\delta_{jk} \tag{4.1.8}$$

In the fatgraph notation, there are now two ways of joining two cubic vertices together by three propagators, shown in Fig. 4.2. Both correspond to the *same* Feynman diagram in the ordinary, perturbative expansion, but give rise to *different* factors of N, depending on how the lines are glued together. The first one contributes

$$\sum_{ijkmno} \langle M_{ij}M_{nm}\rangle\langle M_{jk}M_{on}\rangle\langle M_{ki}M_{mo}\rangle = g_s^3N^3. \tag{4.1.9}$$

The second one contributes

$$\sum_{ijkmno} \langle M_{ij}M_{nm}\rangle\langle M_{jk}M_{mo}\rangle\langle M_{ki}M_{on}\rangle = g_s^3N. \tag{4.1.10}$$

Obviously, the power of N corresponding to a given fatgraph is equal to the number of closed loops that it contains.

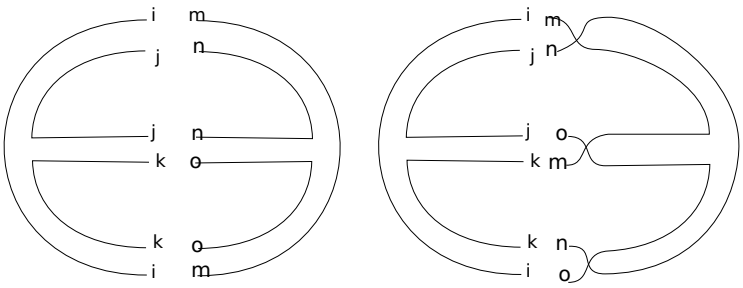

Figure 4.2: two cubic vertices

What if we try to draw the fatgraphs in Fig. 4.2 on a Riemann surface without letting any lines cross, such that the lines can be seen as edges of holes in the surface? It is easy to see that this is possible on a sphere for the graph on the left, while it takes at least a torus for the one on the right. We thus define the genus of a fatgraph as the minimal genus of such a surface, given by the standard topological relation

$$2g - 2 = P - V - h, \tag{4.1.11}$$

where P is the number of double-line propagators, V the number of vertices and h the number of closed loops, or holes in the surface. Each fatgraph then comes with a factor

$$g_s^{P-V} N^h \prod_p g_p^{V_p} = g_s^{2g-2} t^h \prod_p g_p^{V_p} = t^{2g-2+h} N^{2-2g} \prod_p g_p^{V_p}, \tag{4.1.12}$$

where we have introduced the 't Hooft parameter

$$t = N g_s. \tag{4.1.13}$$

This is a crucial step. In the seminal paper [128], it has been shown that the infinite number of fatgraphs of genus 0, called "planar", can be summed up to obtain the genus 0 partition function in closed form. In [132] the analysis has been extended to higher-genus quantities. Note also that at fixed 't Hooft parameter, the genus expansion in g_s is completely equivalent to an expansion in $\frac{1}{N}$. In the large–N limit, the distribution of eigenvalues becomes continuous and one can write

$$V_{\text{eff}}(\lambda) = V(\lambda) - 2t \int \rho(\lambda') \log|\lambda - \lambda'| d\lambda', \tag{4.1.14}$$

Here, $\rho(z)$ is the density of eigenvalues. Due to their mutual Coulomb repulsion, they are equally distributed over an interval $\mathcal{C}$, the "cut". This density is completely determined by the requirement that the effective potential be constant along the cut,

$$V_{\text{eff}}(\lambda) = t\xi(t), \quad \lambda \in \mathcal{C}. \tag{4.1.15}$$

A fundamental quantity at large N is the so-called resolvent, defined by the correlator

$$\omega(\lambda) = \frac{1}{N} \langle \text{Tr} \frac{1}{\lambda - M} \rangle = \sum_g g_s^{2g} \omega_g(\lambda). \tag{4.1.16}$$

The discontinuity of its genus zero piece across the cut encodes the density of eigenvalues,

$$\rho(\lambda) = -\frac{1}{2\pi \mathrm{i}} \left(\omega_0(\lambda + \mathrm{i}\epsilon) - \omega_0(\lambda - \mathrm{i}\epsilon) \right). \tag{4.1.17}$$

A convenient way to encode the genus-0 solution is to define the so-called *spectral curve*

$$y(\lambda) = W'(\lambda) - 2t\omega_0(\lambda), \tag{4.1.18}$$

where we have introduced

$$W'(\lambda) = -t\left(\omega_0(\lambda + \mathrm{i}\epsilon) + \omega_0(\lambda - \mathrm{i}\epsilon)\right). \tag{4.1.19}$$

The spectral curve $y(z)$ is a hyperelliptic curve that will play a fundamental role in the next section when we discuss the connection with topological string theory. It has a branch cut along $\mathcal{C}$ and can also be written as

$$y(p) = M(p)\sqrt{(p-a)(p-b)}, \tag{4.1.20}$$

where $M(p)$, known as the *moment function*, is given by

$$M(p) = \oint_\infty \frac{\mathrm{d}z}{2\pi\mathrm{i}} \frac{V'(z)}{z-p} \frac{1}{\sqrt{(z-a)(z-b)}}, \tag{4.1.21}$$

with the contour of integration being around the point at ∞. The endpoints of the cut follow from the equations

$$\begin{aligned} \oint_{\mathcal{C}} \frac{\mathrm{d}z}{2\pi\mathrm{i}} \frac{V'(z)}{\sqrt{(z-a)(z-b)}} &= 0, \\ \oint_{\mathcal{C}} \frac{\mathrm{d}z}{2\pi\mathrm{i}} \frac{zV'(z)}{\sqrt{(z-a)(z-b)}} &= 2t. \end{aligned} \tag{4.1.22}$$

There is also a useful formula for the moments of the function $M(p)$, which are defined as

$$M_{a,b}^{(k)} = \frac{1}{(k-1)!} \frac{\mathrm{d}^{k-1}}{\mathrm{d}p^{k-1}} M(p)\Big|_{p=a,b}, \qquad k \geq 1, \tag{4.1.23}$$

given in terms of contour integrals [45]:

$$M_a^{(k)} = \oint_{\mathcal{C}} \frac{\mathrm{d}z}{2\pi\mathrm{i}} \frac{V'(z)}{(z-a)^{k+\frac{1}{2}}(z-b)^{\frac{1}{2}}}, \qquad M_b^{(k)} = \oint_{\mathcal{C}} \frac{\mathrm{d}z}{2\pi\mathrm{i}} \frac{V'(z)}{(z-a)^{\frac{1}{2}}(z-b)^{k+\frac{1}{2}}}. \tag{4.1.24}$$

The object we will mainly be interested in in the following is the normalized free energy, defined by

$$F = \log \frac{Z_N}{Z_N^G}, \tag{4.1.25}$$

where Z_N^G is the partition function of the Gaussian matrix model, defined by the potential $V(M) = \frac{1}{2}M^2$. The free energy has a perturbative genus expansion

$$F(t) = \log Z = \sum_{g\geq 0} F_g(t) g_s^{2g-2}. \tag{4.1.26}$$

Another important set of quantities in a matrix model are the connected correlation functions

$$W_h(p_1, \ldots, p_h) = \left\langle \operatorname{Tr} \frac{1}{p_1 - M} \cdots \operatorname{Tr} \frac{1}{p_h - M} \right\rangle_{(\mathrm{c})}, \tag{4.1.27}$$

where the subscript (c) means connected. These correlation functions are generating functions for multi–trace correlators of the form

$$W_h(p_1, \ldots, p_h) = \sum_{n_i \geq 1} \frac{1}{p_1^{n_1+1} \cdots p_h^{n_h+1}} \left\langle \operatorname{Tr} M^{n_1} \cdots \operatorname{Tr} M^{n_h} \right\rangle_{(\mathrm{c})}, \tag{4.1.28}$$

and they further have a g_s expansion of the form

$$W_h(p_1, \ldots, p_h) = \sum_{g=0}^{+\infty} g_s^{2g+h-2} W_{g,h}(p_1, \ldots, p_h; t). \tag{4.1.29}$$

Eynard-Orantin recursion

It turns out that the quantities $F_g(t)$ and $W_{g,h}(p_1,\dots,p_h;t)$ can be computed in terms of the spectral curve alone. More precisely, knowledge of the endpoints of the cut, a and b, and of the moments (4.1.23), is all one needs in order to compute them. This was first made clear in [45] and later culminated in the geometric formalism of [133, 134, 33]. The central quantities in this formalism are meromorphic differentials $W_{g,k}(p_1,\cdots,p_k)$ on the curve. If the spectral curve happens to correspond to a matrix model, these are just the correlation functions of the matrix model as defined in (4.1.29). However, the crucial insight of Eynard and Orantin was that these objects could be constructed on *any* affine curve, even if it is not connected to a matrix model at all. Given such an affine curve, which we will denote by $\mathcal{C}=\{(x,y)\in\mathbb{C}^2|\Sigma(x,y)=0\}\subset\mathbb{C}^2$, the matrix model recursion relations of [33] then proceed as follows, as is very clearly summarized in [35]. The necessary ingredients are

- the meromorphic differential $\Phi(p)=y(p)\mathrm{d}x(p)$ on $\mathcal{C}$
- the *ramification points* q_i, defined by $\partial_y\Sigma(q_i)=0$
- the Bergmann kernel $B(p,q)$, uniquely defined as the meromorphic differential on $\mathcal{C}$ with a double pole at $p=q$ with no residue, and no other pole, normalized to have vanishing integral on the A_I–cycles of a chosen canonical symplectic basis A_I,B^I on $\mathcal{C}$. Note that modular transformations correspond to changes in this basis (recall section 2.1) and thus transform the Bergmann kernel. This is crucial since it turns out that the Bergmann kernel alone is enough to promote the F_g from holomorphic to modular invariant, non-holomorphic topological string amplitudes.
- the prime form differential $dE_q(p)=\int_q^{\bar q}B(p,\xi)\mathrm{d}\xi$.

The recursion relation of [33] then reads

$$W_{g,h+1}(p,p_1,\cdots p_h)=\sum_{q_i}\mathrm{Res}_{q=q_i}\frac{\mathrm{d}E_q(p)}{\Phi(q)-\Phi(\bar q)}\cdot \\ \cdot\left(W_{g-1,h+2}(q,\bar q,p_1,\cdots,p_h)+\sum_{\ell=0}^{g}\sum_{J\subset H}W_{g-\ell,|J|+1}(q,p_J)W_{\ell,h-|J|+1}(\bar q,p_{H\setminus J})\right), \tag{4.1.30}$$

where $H=1,\cdots,h$ and $p_J\equiv p_{i_1},\cdots p_{i_j}$ for any subset $J=\{i_1,\cdots i_j\}\subset H$. The recursion starts with

$$W_{0,1}(p_1)=0,\quad W_{0,2}(p_1,p_2)=B(p_1,p_2). \tag{4.1.31}$$

Note that these are *not* the resolvent and annulus amplitudes as the notation suggests, and as it is true for any genera and numbers of holes $(g,h)\neq(0,1),(0,2)$, but artificial, auxiliary quantities just defined to generate the higher correlators [33]. Indeed, the resolvent and the genus zero free energy are the only quantities *not* completely determined by the spectral curve alone. The genus zero free energy is given by

$$F_0(t)=-\frac{t}{2}\int_{\mathcal{C}}\mathrm{d}\lambda\,\rho(\lambda)V(\lambda)-\frac{1}{2}t^2\xi(t). \tag{4.1.32}$$

The free energies for $g>1$ are then generated by

$$F_g=\frac{1}{2-2g}\sum_{q_i}\mathrm{Res}_{q=q_i}\phi(q)W_{g,1}(q), \tag{4.1.33}$$

for any $\phi(p)$ fulfilling $\mathrm{d}\phi(p)=\Phi(p)$.

In terms of the moment function (4.1.21), one finds in this way for the genus–one free energy [45]

$$F_1 = -\frac{1}{24}\log\left[M(a)M(b)(a-b)^4\right]. \tag{4.1.34}$$

The two and three–point correlators at genus zero are given by [135]

$$\begin{aligned} W_{0,2}(p,q) &= \frac{1}{2(p-q)^2}\left(\frac{pq-\frac{1}{2}(p+q)(a+b)+ab}{\sqrt{(p-a)(p-b)(q-a)(q-b)}}-1\right), \\ W_{0,3}(p,q,r) &= \frac{1}{8\sqrt{(p-a)(p-b)(q-a)(q-b)(r-a)(r-b)}}\cdot \\ &\cdot\left(\frac{a-b}{M(a)}\,\frac{1}{(p-a)(q-a)(r-a)}+\frac{b-a}{M(b)}\,\frac{1}{(p-b)(q-b)(r-b)}\right), \end{aligned} \tag{4.1.35}$$

while the one–point function at genus one is given by [45]

$$\begin{aligned} W_{1,1}(p) = &\frac{1}{16M(a)(p-a)\sqrt{(p-a)(p-b)}}\left(\frac{2p+b-3a}{(p-a)(b-a)}-\frac{M'(a)}{M(a)}\right)+ \\ &+\frac{1}{16M(b)(p-b)\sqrt{(p-a)(p-b)}}\left(\frac{2p+a-3b}{(p-b)(a-b)}-\frac{M'(b)}{M(b)}\right). \end{aligned}$$

4.1.2 Critical behaviour

If one takes the limit $N\to\infty$ in a standard matrix model, only planar surfaces are retained, since all others are suppressed by powers of $\frac{1}{N}$. However, at the same time there is generally a specific, critical value of the coupling λ_c where the free energy diverges as

$$F_g \sim (\lambda-\lambda_c)^{(2-\gamma)(1-g)}, \tag{4.1.36}$$

where γ is some critical exponent. If we see the matrix model as describing random triangulations of surfaces, this is the limit where the total area of the surface diverges. We can then rescale the area of the individual triangles to zero to produce a continuum surface of finite area, and therefore this limit is called the continuum limit. Note that higher-genus contributions have poles of higher order at this point in moduli space, so they are enhanced with respect to the lower genus amplitudes. If one now takes a combined, so called double-scaling limit, where N is taken to ∞ while simultaneously tuning the coupling to its critical value, the large-genus suppression and enhancement can compensate each other and one gets coherent contributions from continuum surfaces at any genus. Explicitly, this double-scaling limit is

$$z = -\frac{1}{\lambda_c}(\lambda-\lambda_c)\left(\frac{t}{N}\right)^{\frac{1}{\gamma/2-1}}, \qquad N\to\infty,\ g\to g_c,\ z \text{ fixed}, \tag{4.1.37}$$

with $t=g_sN$ the usual 't Hooft parameter. The critical exponent γ here can be determined by standard methods. In particular, it doesn't depend on the details of the matrix model under consideration, but only on the universality class of the critical point. The critical behaviour we will be interested in corresponds to a critical exponent $\gamma=-\frac{1}{2}$ or equivalently, a critical point of order 2. It seems natural from the discussion above that in the double-scaling limit, the theory is described by two-dimensional pure gravity. Indeed, it turns out that as a function of the new, double-scaled variable z the second derivative of the free energy $u=-F''(z)$ satisfies the Painlevé I equation

$$z = u^2 - \frac{u''}{6}, \tag{4.1.38}$$

controlling nonperturbative 2d gravity.

4.1.3 Instantons

One of the nice, nontrivial features of matrix models is that they admit instanton transitions.

We consider here cases where the potential has at least two extrema. For concreteness, let us first focus on the one-cut case. The effective potential (4.1.14) is constant along the cut and has a saddle point at some value λ_0, as shown in Fig. 4.3.

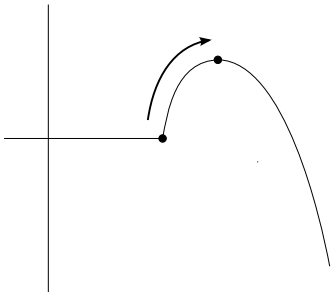

Figure 4.3: Instanton configuration: an eigenvalue from the endpoint of the cut moves to the saddle of the effective potential barrier

The instanton transition consists in one eigenvalue moving from the endpoint of the cut to this saddle. The corresponding instanton action is given by the integral over the spectral curve [120, 48]:

$$\mathcal{A}_{\rm inst} = \int_a^{x_0} y(z)dz. \tag{4.1.39}$$

Geometrically, the spectral curve is a curve of genus zero pinched at x_0 (Fig. 4.4). This was observed in [136] in the context of spectral curves for double–scaled matrix models, and their relation with minimal strings.

$\mathcal{A}_{\rm inst}$ can be seen as a contour integral from the endpoint of the cut to the singularity of the spectral curve, as shown in Fig. 4.4.

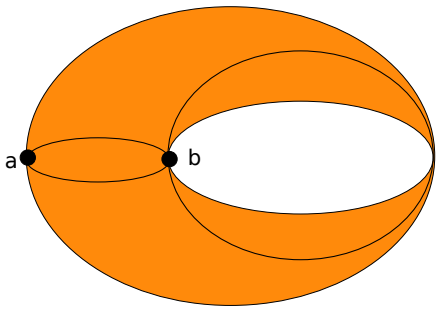

Figure 4.4: The instanton configuration as a contour integral on the spectral curve

The standard $1/N$ expansion is computed by considering the saddle–point configuration in which all of the N eigenvalues have support in the cut $\mathcal{C}$. As was first pointed out in [120, 121, 48], a k–instanton configuration corresponds to a distinct saddle–point, in which $N-k$ of the eigenvalues remain in the interval $\mathcal{C}$, while k eigenvalues are placed at the local maximum x_0.

The matrix integral for the one–instanton sector is given by [126]

$$Z_N^{(1)} = \frac{N}{N!(2\pi)^N} \int_{x\in\mathcal{I}} {\rm d}x\, {\rm e}^{-\frac{1}{g_s}V(x)} \int_{\lambda\in\mathcal{I}_0} \prod_{i=1}^{N-1} {\rm d}\lambda_i\, \Delta^2(x,\lambda_1,\ldots,\lambda_{N-1})\, {\rm e}^{-\frac{1}{g_s}\sum_{i=1}^{N-1}V(\lambda_i)}, \tag{4.1.40}$$

where the first integral in x is over the nontrivial saddle–point contour, which we have denoted by $x\in\mathcal{I}$, while the rest of the $N-1$ eigenvalues are integrated around the standard saddle–point

contour $\mathcal{I}_0$. The overall factor of N in front of the integral is a symmetry factor, counting the N possible distinct ways of choosing one eigenvalue out of a set of N. One can easily write similar integrals for the k–instanton contribution (see [126]).

In the one–instanton computation that we will perform in the next chapter, we will need some derivatives with respect to t of various quantities that characterize the large N solution. A result we need is (see [118])

$$\frac{\partial(t\omega_0(p))}{\partial t} = \frac{1}{\sqrt{(p-a)(p-b)}} \tag{4.1.41}$$

together with the following derivatives, which follow from the defining relations (4.1.22) and (4.1.24),

$$\frac{\partial a}{\partial t} = \frac{4}{a-b}\,\frac{1}{M(a)}, \qquad \frac{\partial b}{\partial t} = \frac{4}{b-a}\,\frac{1}{M(b)}. \tag{4.1.42}$$

Using these formulae one finds,

$$\begin{aligned} \partial_t y(z) &= -\frac{2}{\sqrt{(z-a)(z-b)}}, \\ \partial_t M(z) &= \frac{2}{(z-a)(z-b)}\left(\frac{(z-b)M(z)}{(a-b)M(a)} + \frac{(z-a)M(z)}{(b-a)M(b)} - 1\right), \end{aligned} \tag{4.1.43}$$

as well as

$$\begin{aligned} \partial_t M(a) &= \frac{6}{a-b}\,\frac{M'(a)}{M(a)} + \frac{2}{(a-b)^2}\left(1 - \frac{M(a)}{M(b)}\right), \\ \partial_t M(b) &= \frac{6}{b-a}\,\frac{M'(b)}{M(b)} + \frac{2}{(b-a)^2}\left(1 - \frac{M(b)}{M(a)}\right). \end{aligned} \tag{4.1.44}$$

Finally, we will also need derivatives of the free energies. One finds[1] [127]

$$\begin{aligned} \partial_t F_0(t) &= -t\xi(t) = -V_{\text{eff}}(b), \\ \partial_t^2 F_0(t) &= -\partial_t V_{\text{eff}}(b) = 2\log(b-a) - 2\log 4, \end{aligned} \tag{4.1.45}$$

while higher derivatives with respect to t follow from (4.1.42).

4.2 The B-model as a Matrix Model

As early as 1973, 't Hooft suggested that the large N limit of a $U(N)$ gauge theory could be interpreted as a closed string theory [5]. This deep idea had been around for over 20 years before it could celebrate a huge success with the AdS/CFT-conjecture due to Maldacena [4], and the discovery by Gopakumar and Vafa that Chern-Simons theory at large N is dual to the topological A-model [27]. Since then, large N limits of gauge theories and their (string) duals have been studied more extensively than ever before.

4.2.1 Geometric transitions and Dijkgraaf-Vafa conjecture

In 2002, Dijkgraaf and Vafa put forward a duality between the B-model topological string on certain local Calabi-Yau geometries and the large-N expansion of a matrix model. Their work builds on the somewhat analogous duality of the A-model with Chern-Simons theory[2], and on the previously developed geometric transitions between open and closed backgrounds [137].

[1] Notice that $\partial_t V_{\text{eff}}(b)$ can be obtained by integrating $\partial_t y(z)$ from $-\infty$ to b, an integral which diverges logarithmically. Sensible results are obtained [127] by always considering its regulated version, where one simply drops the divergent $\log z$ term.

[2] Note that this is *not* a mirror of the B-model setup

The concept of geometric transitions was originally developed in the context of type IIB superstrings [137, 138, 139, 140]. Let us briefly review this construction. Consider the so-called deformed conifold, with defining equation

$$x^2 + y^2 + u^2 + v^2 = \mu. \tag{4.2.46}$$

Replacing the coordinates x, y, u, v by $x_j + \mathrm{i}v_j$, $j = 1, \cdots, 4$, one can see that this is nothing else than the tangent bundle of the three-sphere T^*S^3: the above defining equation takes the form

$$\sum_i x_i^2 - v_i^2 = \mu, \quad x_i v_i = 0. \tag{4.2.47}$$

Hence, x_i parametrize the three-sphere as can be seen from the first equation at $v_i = 0$, and v_i its tangent space, according to the second. The so-called conifold singularity arises as $\mu \to 0$. There is another way to smooth out this singularity, apart from keeping $\mu \neq 0$. This option, referred to as *resolution* of a singularity, consists of replacing the singular point by a $\mathbb{P}^1$. For the conifold, this is done as follows. Introduce new coordinates X, Y, U, V defined as $x+\mathrm{i}y, x-\mathrm{i}y, u+\mathrm{i}v, u-\mathrm{i}v$. The conifold singularity is then at $XY = UV$ or equivalently

$$\det \begin{pmatrix} Y & U \\ V & X \end{pmatrix} = 0. \tag{4.2.48}$$

Now introduce two new parameters $\lambda_1, \lambda_2 \in \mathbb{C}$ and consider the subspace of $\mathbb{C}^4 \times \mathbb{P}^1$ defined by $Y\lambda_1 = -U\lambda_2$ and $V\lambda_1 = -X\lambda_2$. This can also be written as

$$\begin{pmatrix} Y & U \\ V & X \end{pmatrix} \begin{pmatrix} \lambda_1 \\ \lambda_2 \end{pmatrix} = 0, \tag{4.2.49}$$

therefore it implies the previous equation. Note that the eigenvector equation determines λ_1, λ_2 only up to scaling, that's why they are coordinates on $\mathbb{P}^1$. At $(Y, U, X, V) \neq (0, 0, 0, 0)$, the point $(\lambda_1, \lambda_2) \in \mathbb{P}^1$ is fixed, while at the origin of $\mathbb{C}^4$, it can move freely all over $\mathbb{P}^1$. Thus, the singularity has been resolved by blowing up the origin to a sphere. It turns out that the new space can be described in a different way. It can be parametrized by two overlapping charts, for the two regions where $\lambda_i \neq 0$. Then for the first region, we have $Y = -\frac{\lambda_2}{\lambda_1}U$, $V = -\frac{\lambda_2}{\lambda_1}X$ and coordinates are $(\lambda = \frac{\lambda_2}{\lambda_1}, U, X)$. Similarly, the second chart leads to coordinates $(\frac{1}{\lambda} = \frac{\lambda_1}{\lambda_2}, Y, V)$, and on the overlap, we get $U = -\frac{1}{\lambda}Y$, $X = -\frac{1}{\lambda}V$. These are precisely the transition functions for two $\mathcal{O}(-1)$-bundles over $\mathbb{P}^1$, and the above resolution of the conifold is nothing else than the total space of the bundle[3]

$$\mathcal{O}(-1) \oplus \mathcal{O}(-1) \to \mathbb{P}^1. \tag{4.2.50}$$

Geometrically, we have started with the deformed conifold, passed through the singularity at the origin by letting the radius of the S^3 shrink to zero, then blown up the singularity by letting grow an S^2. This procedure is the principle behind what is called geometric transitions. This construction actually applies to a larger class of geometries, of the form

$$uv + W'(x)^2 + y^2 = 0. \tag{4.2.51}$$

The special case $W'(x) = x$ is the conifold geometry. Indeed, we get conifold-like singularities at any point $W''(x) = 0$. Now resolve the singularity as we have done above by letting grow two-spheres at all the singular points, and consider stacks of space-filling D5-branes wrapped over these S^2's. In the limit where the number of branes N gets large, gaugino condensation takes place, and the S^2's are "blown down" and get replaced by "blown up" S^3's without any branes, resulting in a closed string theory on a deformed geometry similar to (4.2.46) [137, 139]. This

[3] see also appendix C.3

transition can be naturally lifted to a transition between open and closed topological strings, as one should expect, and one finds that at large N, the open topological B-model on geometries with resolved conifold singularities is equivalent to the closed B-model on deformed conifolds.

At the same time, deforming the geometry corresponds to turning on a superpotential in the string field theory description of the open string, and the resulting action can be shown to be a matrix model with potential $W(\Phi)$.

Summarizing, we thus have a two-fold result: there is a string field description of the open topological B-model on the resolved conifold in terms of a matrix model, and in the limit of large N, the latter is dual to closed B-model topological strings on the deformed conifold.

4.2.2 Remodeling the B-model

The main drawback of the beautiful duality found by Dijkgraaf and Vafa is that the geometries they consider in the original and subsequent papers [32, 141, 142] are highly restrictive, and in particular exclude the myriad of Calabi-Yau manifolds with toric mirrors. However, a new development on the matrix model side has enabled a new point of view of the connection between matrix models and topological strings, leading to a reformulation and generalization of the Dijkgraaf-Vafa setup. The starting point was the work of Eynard and Orantin [33], where the authors develop a recursive formalism to solve matrix models based on an algebraic-geometric point of view. Starting from the spectral curve introduced above, this formalism allows one to compute all higher matrix amplitudes recursively. The crucial point is that one completely circumvents the potential of the matrix model: all that is needed to define the amplitudes is some geometric input in the form of the spectral curve. This implies that its scope goes far beyond ordinary matrix models. In [34], Mariño made use of this fact to define a general, matrix-model inspired formalism to compute *open* string amplitudes. The key point is that the spectral curve, a Riemann surface, has an analogous counterpart in the topological string, namely the curve determining the mirror geometry. The formalism has been extended and generalized in [35], leading to a complete reformulation of the open B-model in terms of matrix models.

For the reader not familiar with mirror symmetry for toric Calabi-Yau manifolds, the main ideas are reviewed in appendix C.3. Here, we just state that the mirror of a toric Calabi-Yau can be constructed and generically takes the form of a bundle over $\mathbb{C}^* \times \mathbb{C}^*$

$$xz = \Sigma_t(u, v), \tag{4.2.52}$$

where $\Sigma_t(u, v) = 0$ determines a family of Riemann surfaces, parametrized by the Kähler parameter t. It is of crucial importance that $\Sigma_t(u, v)$ is embedded in $\mathbb{C}^* \times \mathbb{C}^*$ rather than in $\mathbb{C} \times \mathbb{C}$, since the variables u, v are exponentials. The matrix model recursion relations of [33] that we have summarized at the end of section 4.1.1 thus have to be adapted to apply to the $\mathbb{C}^* \times \mathbb{C}^*$–case, as it has been done in [35]. The main modification concerns the meromorphic differential $d\Phi(p) = y(p)dx(p)$, where $y(p)$ is the spectral curve. In the original setup, this is related to the standard symplectic form $dx \wedge dy$ on $\mathbb{C}^2$. On $(\mathbb{C}^*)^2$, it is replaced by the symplectic form $\frac{dx}{x} \wedge \frac{dy}{y}$, which can in turn be integrated to the new meromorphic differential, appropriate for $(\mathbb{C}^*)^2$, $\theta(P) = \log(y(p))\frac{dx(p)}{x(p)}$. The recursion then proceeds essentially as in [33], and produces a set of amplitudes and correlation functions F_g, $W_{g,h}$.

The interpretation of these quantities is most conveniently stated in A-model terms. Namely, the free energies F_g correspond, after plugging in the closed mirror map, to the A-model closed string amplitudes, as we have advertised above. However, this is not yet the end. In [143], it has been observed that D-branes show the so-called framing phenomenon, that is, they depend on the parametrisation of the mirror curve. This information has to be somehow contained in the open string amplitudes. In fact, it turns out that once one has chosen a parametrisation of the mirror curve, the correlation functions $W_{g,h}(p_1, \cdots, p_k)$ can be integrated and mapped to the A-model by open and closed mirror maps to yield A-model open string amplitudes on the mirror threefold [35].

In chapter 5, we perform a nonperturbative check of this identification for the closed amplitudes, by showing that a nonperturbative matrix computation correctly predicts the large-order asymptotics of the topological string. This is not only a highly nontrivial check of the matrix model approach to the B-model, but also indicates that the matrix model can be useful in finding a nonperturbative completion of the topological string.

As we have mentioned briefly in section 1.5, the matrix formulation of the B-model puts several issues in a new light. In a sense, the matrix model recursion relations can be seen as a generalization of the holomorphic anomaly equations of [19]. Indeed, the latter can be derived from the former [144], but the matrix model version differs from its traditional counterpart in two important aspects. One is that the non-holomorphicity of the matrix amplitudes only comes in almost trivially through the Bergmann Kernel [144, 35], in order to promote the originally holomorphic amplitudes to modular invariant topological string amplitudes. Thus, the equations are completely determined and there is no holomorphic ambiguity. This setting fits well in the picture advertised in [73], where the mutually exclusive properties of holomorphicity and modularity appeared as essentially a matter of choice of polarization. The other difference between the original holomorphic anomaly equations and the matrix model equations is that the matrix model equations naturally involve both open and closed amplitudes, purely closed amplitudes are never more than a special case. This implies that open amplitudes should be seen as more fundamental than closed amplitudes, in that they contain considerably more information.

4.3 Instantons and Large Order in Field Theory

In this section we review the connection between instantons and the large–order behavior of perturbation theory. Good references on this subject include [117, 145, 50, 146].

Standard, stable potentials in field theory and quantum mechanics show an obvious vacuum instability at negative coupling, where particles can tunnel away from the original vacuum to states of lower energy. According to an old argument due to Dyson, we should therefore not a priori expect the perturbation series to have a nonzero radius of convergence, as this will be in many cases impossible[4].

This is a sign of a fundamental connection between vacuum instability due to instanton effects and large-order behaviour of the perturbative expansion. The method of Borel resummation provides a way to make sense of the (divergent) perturbation series via analytic continuation: To a perturbative series

$$S = \sum_n a_n z^n, \tag{4.3.53}$$

we associate a Borel sum

$$B_S^\beta = \sum_n \frac{a_n}{(\beta n!)} w^n, \tag{4.3.54}$$

where β is related to the large-order behaviour of a_n as $a_n \propto (n\beta)!$. Using

$$(\beta n)! = \int_0^\infty dt \mathrm{e}^{-t} t^{\beta n}, \tag{4.3.55}$$

it is now easy to see that

$$f(z) = \int_0^\infty dt \mathrm{e}^{-t} B_S^\beta(t^\beta z) \tag{4.3.56}$$

defines an analytic continuation of $S(z)$. This may however be ambiguous, in many cases, there will be a nonperturbative ambiguity. We distinguish the following three special cases:

- S has finite radius of convergence r: B_S will be analytic everywhere and $f(z) = S|_{z<r}$.

[4]This argument should be applied carefully, as there exist loopholes

- S has zero r.o.c., but B_S has a finite radius of convergence, an analytic continuation to an ϵ-tube around the positive real axis, and $f(z)$ is absolutely convergent: S is called *Borel summable*.

- B_S does have singularities on the positive real axis: In this case, S is *not* Borel summable, and there is a nonperturbative ambiguity related to the choice of integration contour around the singularities.

The Borel transform provides a link between instantons and large order behaviour. Namely, if a QFT admits an instanton configuration ϕ with finite action $S(\phi)$, B_S will be singular at $S(\phi)$. In turn, the singularities of B control the large-order behaviour of the perturbation series. $f(z)$ can acquire an imaginary part when integrating around a pole of B_S, this reflects an *instability* of the theory which is not seen in its perturbative expansion.

As an example, let us start by considering a quantum mechanical or field theoretical model which depends on a coupling constant, g, in such a way that for $g > 0$ the theory has an unstable vacuum and that this vacuum gets stabilized for $g < 0$. A simple example of such a situation is the familiar quartic anharmonic oscillator with potential

$$V = \frac{1}{2}x^2 - gx^4. \tag{4.3.57}$$

Due to the instability, there will be instanton solutions (sometimes called *bounces* in this context)

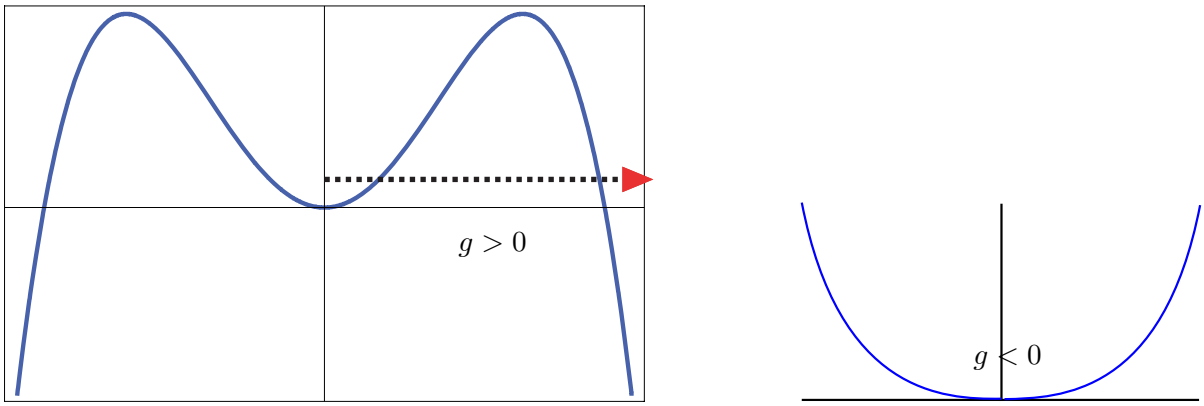

Figure 4.5: The potential for the quartic anharmonic oscillator. When $g > 0$ the theory has an unstable vacuum at the origin, which decays via instanton tunneling. This vacuum gets stabilized when $g < 0$.

which mediate the decay of the false vacuum. This is illustrated in Fig. 4.5. As one analytically continues the coupling constant to the full complex plane, one finds that the partition function will have a branch cut along the real, positive g axis, with a discontinuity which is purely imaginary. In particular, one may write for the full partition function [147]

$$Z(g \pm \mathrm{i}\epsilon) = Z^{(0)}(g) \pm \frac{1}{2}\,\mathrm{disc}\, Z(g), \tag{4.3.58}$$

defining both $Z^{(0)}$ and the discontinuity across the branch cut $\mathrm{disc}\, Z(g) = Z(g + \mathrm{i}\epsilon) - Z(g - \mathrm{i}\epsilon)$. A careful analysis of the physics of this problem, in the particular example of the anharmonic oscillator [147, 148, 145], shows that $Z^{(0)}$ is given by the path integral around the perturbative vacuum (or zero–instanton configuration), while the leading contribution to $\mathrm{disc}\, Z(g)$ turns out to be given by the path integral calculated around the one–instanton configuration, i.e. the instanton configuration with the lowest action in absolute value. We denote this path integral by $Z^{(1)}(g)$.

Let us be slightly more precise on this point. If we want the partition function to remain meaningful, as one performs the analytical continuation in the coupling constant from the stable to the unstable case, it is required that the contour of integration is also rotated, in a compensating way [147] (*e.g.*, in the quartic oscillator as one continues $-g$ to $-g\exp(\pm\mathrm{i}\pi)$ one must rotate x to $x\exp(\mp\mathrm{i}\pi/4)$). The rotated integration contours are illustrated in Fig. 4.6. What the analysis in [147, 148, 145] shows is that $Z^{(0)}$ is computed as the integral over the *sum* of both contours, $\mathcal{C}^+ + \mathcal{C}^-$. In particular, if one is to compute the path integral in a saddle–point approximation, the contribution to $Z^{(0)}$ arises from the saddle–point at the origin. On the other hand, the discontinuity $\mathrm{disc}\, Z(g)$ is computed on the *difference* of the two rotated contours, $\mathcal{C}^+ - \mathcal{C}^-$. This immediately implies that the saddle–point at the origin cancels, between the two contours. One thus needs to consider the sub–leading saddle–points, which correspond to the one–instanton configuration. These sub–leading saddle–point contributions are also illustrated in Fig. 4.6. In particular, notice that

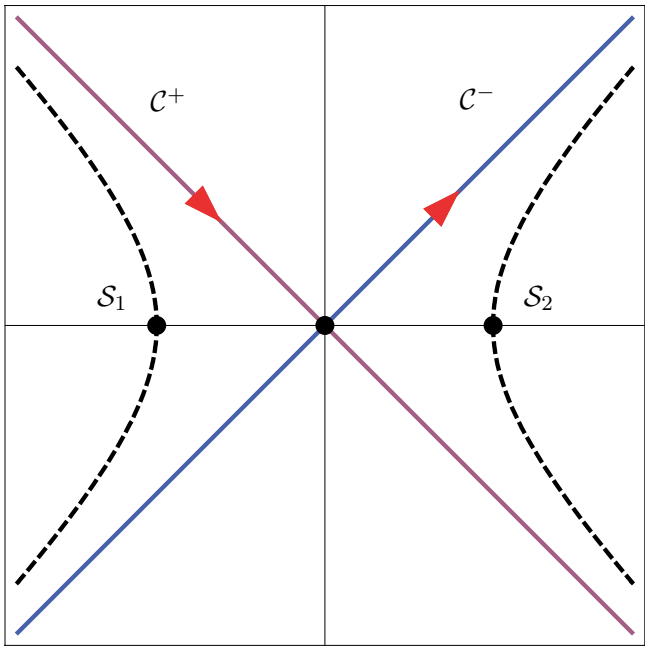

Figure 4.6: The complex plane for the functional integration. Here, $\mathcal{C}^+$ and $\mathcal{C}^-$ are the rotated contours one needs to consider for $g > 0$. Their sum may be evaluated by the contribution of the saddle–point at the origin. Their difference is evaluated by the contribution of the sub–leading saddle–points, here denoted as $\mathcal{S}_1$ and $\mathcal{S}_2$.

$$Z^{(1)}(g) \sim \mathrm{e}^{-1/g} \tag{4.3.59}$$

and it is exponentially suppressed for small g as compared to $Z^{(0)}$. This is exactly as one should expect from the discussion above. If we now consider the free energy, defined by $F = \log Z$, we similarly have

$$F(g \pm \mathrm{i}\epsilon) = F^{(0)}(g) \pm \frac{1}{2}\mathrm{disc}\, F(g), \tag{4.3.60}$$

where $F^{(0)}(g) = \log Z^{(0)}(g)$ and

$$\mathrm{disc}\, F(g) = \log \frac{Z(g+\mathrm{i}\epsilon)}{Z(g-\mathrm{i}\epsilon)} = \frac{Z^{(1)}(g)}{Z^{(0)}(g)} + \cdots, \tag{4.3.61}$$

at leading order in e^{-1/g_s}. We will denote by

$$F^{(1)}(g) = \frac{Z^{(1)}(g)}{Z^{(0)}(g)} \tag{4.3.62}$$

the one–instanton contribution to the discontinuity. The zero–instanton sector has a perturbative expansion around $g = 0$ given by

$$F^{(0)}(g) = \sum_{k=0}^{+\infty} a_k g^k, \tag{4.3.63}$$

while the contribution from the one–instanton sector to the discontinuity $\operatorname{disc} F(g)$ turns out to have an expansion of the form

$$F^{(1)}(g) = \mathrm{i} g^{-b} \mathrm{e}^{-A/g} \sum_{n=0}^{+\infty} c_n g^n. \tag{4.3.64}$$

In this equation, A is the action of the single instanton, b is a characteristic exponent, and c_n is the $(n+1)$–loop contribution around the instanton configuration.

If one now assumes analyticity of $F(g)$ in the g–plane, except for the branch cut along the positive real axis which we alluded to before, as well as some suitable conditions on the $g \to \infty$ behavior, one can deduce the following relation between the coefficients of the perturbative expansion around the zero–instanton sector and the discontinuity across the cut

$$a_k = \frac{1}{2\pi \mathrm{i}} \int_0^\infty \mathrm{d}z \, \frac{F^{(1)}(z)}{z^{k+1}}. \tag{4.3.65}$$

Plugging the expansion for $F^{(1)}$ (4.3.64) in the above formula (4.3.65) we find an asymptotic expansion for large k,

$$a_k \sim \frac{1}{2\pi} \sum_{n=0}^{+\infty} c_n A^{-k-b+n} \Gamma(k+b-n). \tag{4.3.66}$$

This can be equivalently written as

$$a_k \sim \frac{A^{-b-k}}{2\pi} \, \Gamma(k+b) \left[c_0 + \frac{c_1 A}{k+b-1} + \frac{c_2 A^2}{(k+b-2)(k+b-1)} + \cdots \right]. \tag{4.3.67}$$

What one learns from this analysis is that the computation of the one–instanton partition function, at one–loop, determines the leading order of the asymptotic expansion for the perturbative coefficients of the zero–instanton partition function, while higher–loop corrections yield the $1/k$ corrections. Notice that instanton configurations with an action $A' > A$ (in particular, multi–instanton configurations with action nA, $n \geq 2$) give corrections to the asymptotics of a_k which are exponentially suppressed in k, and will not be considered in here. The relation between a nonperturbative instanton computation and the large–order behavior of perturbation theory was first implemented by Bender and Wu in the case of the quartic anharmonic oscillator in quantum mechanics [149]. They used the WKB method in order to perform a two–loop computation around the bounce, and thus obtain precise numerical values for c_0 and c_1. Furthermore, they performed accurate numerical tests of their prediction (4.3.65) for the large–order behavior of the a_k coefficients. Their results were later reproduced in path integral language [147].

In this quantum mechanical example the analyticity conditions for the free energy can be justified rigorously (see [150] for a review). In more general situations (such as in quantum field theory) one cannot justify these same assumptions; however the relation (4.3.65) can be tested in a number of examples with surprising numerical precision (see, *e.g.*, [145, 50] for a review of these tests).

Chapter 5

Instantons in One-Cut Models and Large Order

In this chapter, we study in detail the perturbative expansion around a one–instanton configuration in a generic, one–cut matrix model, and apply it to predict the large-order behaviour of both matrix models and the topological string, along the lines of what has been explained in the previous chapter. The material presented is based on the publication [71] with M. Mariño and R. Schiappa.

We will give explicit formulae for both the one– and two–loop contributions to the instanton amplitude in terms of geometric data of the spectral curve associated to the matrix model. This is a crucial aspect of our analysis, since it allows one to apply the results not only to full-fledged matrix models but also to topological strings via the formalism of [29, 35]. Using this description, we deduce that the nonperturbative completion of the topological string theories considered in this chapter includes an infinite number of nontrivial topological sectors, corresponding to the different instanton sectors of the matrix model. Geometrically, we interpret these nonperturbative effects as due to domain walls interpolating between D–brane configurations, as it had already been anticipated in [32].

We test our results against the large-order behaviour of the perturbative amplitudes in the quartic matrix model, topological strings on local curves, Hurwitz theory, and 2d gravity. We confirm and improve the predictions of [29] about the large–order behavior of these models, and we will also consider a special limit of topological strings on local curves which describes simple Hurwitz numbers (studied in [151]). All of these models have a critical point, describing pure 2d gravity, which is controlled by the Painlevé I equation. The double–scaling limit of our instanton calculations provides results for the large–order behavior of 2d gravity which refine those obtained [119, 152] and agree with the analysis of the asymptotics in [153]. In fact, with the help of the Painlevé I equation one can derive the full perturbative expansion around the one–instanton sector, and in this way we provide a further check of our explicit two–loop calculation.

Mathematically, our results are highly nontrivial predictions for the asymptotics of the $1/N$ expansion of a one–cut matrix model, and they provide some clues concerning the analytic structure of the total free energy of topological string theory, as a function of the string coupling constant. In the case of topological strings, our tests of large–order behavior provide a further check of the conjecture in [29], as well as new conjectures about asymptotic properties of enumerative invariants that have not been explored so far.

This chapter is organized as follows. In section 5.1, we explain why instantons are expected to control the large-order asymptotics of the string perturbation series just as in the field theory case discussed in the last chapter. In section 5.2, we apply the technology developed in chapter 4 explicitly to the analysis of one–instanton effects in matrix models. We present com-

plete formulae for both the one–loop and the two–loop corrections around the one–instanton configuration, in generic one–cut matrix models, following the general strategy put forward in [126, 127]. Section 5.3 reviews the numerical techniques used to extrapolate low-genus results to high genus. The following sections contain applications of these results. In section 5.4, we consider the quartic matrix model both off–criticality and in the double–scaling limit where it becomes pure 2d gravity. We further present numerical tests of the predictions given by the instanton calculation, by analyzing the large–order behavior of both the quartic matrix model and the Painlevé I equation. In section 5.5 we consider topological string theory on local curves, verifying and extending the predictions of [29], and we discuss the spacetime interpretation of the instanton effects in terms of domain walls. Then, in section 5.6, we analyze in detail the large–order behavior of the generating functionals for simple Hurwitz numbers as a further example of our formalism. In all cases, we find impressive agreement between theoretical and numerical results.

5.1 The $1/N$ Expansion and String Theory

The existence of a connection between instantons and large–order behavior has also been addressed in the context of the $1/N$ expansion; for example in [154] where one considers vector models in low dimension. In the case of matrix models and their double–scaling limit, such a connection was used in [120, 121, 119] in order to infer on the large–order behavior of pure 2d gravity, by computing the instanton action directly in the matrix model (see [118] for a review). However, precise tests at one–loop or higher (the c_n coefficients in the expressions above) have not been performed to date, and we fill such a gap in the present work. In order to proceed to loop–level, one first needs a generalization of both the dispersion relation (4.3.65) and the expression for the perturbation theory asymptotics (4.3.66), to the present setting.

We will proceed in a heuristic way. Let us first consider the perturbative series in the zero–instanton sector of a closed string theory or its matrix model dual,

$$F^{(0)}(g_s) = \sum_{g=0}^{+\infty} F_g(t)\, g_s^{2g-2}. \tag{5.1.1}$$

In this equation the sum is over all genera, g_s is the string coupling constant and t is the 't Hooft coupling $t = g_s N$ in the context of matrix models, or a geometric modulus in string theory. Observe that while in the previous case of the anharmonic oscillator one wanted to study the asymptotics of a standard numerical series, one now wants to address the asymptotics of a series of functions, naturally enlarging the complexity of the problem [154]. In order to have a perturbative series with standard structure, we consider instead

$$\mathcal{F}(g_s) = g_s^2\, F(g_s). \tag{5.1.2}$$

In this case, the one–instanton path integral yields a series of the form

$$\mathcal{F}^{(1)}(z) = \mathrm{i} z^{-b/2} \mathrm{e}^{-\frac{A}{\sqrt{z}}} \sum_{n=0}^{+\infty} c_n z^{n/2}, \tag{5.1.3}$$

where $z = g_s^2$. This is an important feature distinguishing matrix models and string theory from field theory: the action of an instanton goes like $1/\sqrt{z}$, and not as $1/z$. Similarly, the perturbation series around the instanton sector is a series in powers of $\sqrt{z}$, and not a series in powers of z. As such, we may now write

$$\mathcal{F}^{(0)}(z) = \sum_{g=0}^{+\infty} F_g(t)\, z^g. \tag{5.1.4}$$

Our basic assumption is that a dispersion relation of the form (4.3.65) holds in here, as it did in field theory. In this case, one finds

$$F_g = \frac{1}{2\pi}\int_0^\infty \frac{\mathrm{d}z}{z^{g+1}} z^{-b/2} \mathrm{e}^{-\frac{A}{\sqrt{z}}} \sum_{n=0}^{+\infty} c_n z^{n/2} \sim \frac{1}{\pi}\sum_{n=0}^{+\infty} c_n A^{-2g-b+n}\Gamma(2g+b-n), \tag{5.1.5}$$

which may be explicitly written as

$$F_g \sim \frac{A^{-2g-b}}{\pi}\,\Gamma(2g+b)\,\mu_1\left[1+\frac{\mu_2 A}{2g+b-1}+\frac{\mu_3 A^2}{(2g+b-2)(2g+b-1)}+\cdots\right], \tag{5.1.6}$$

where we have introduced for later convenience

$$\mu_1 = c_0, \qquad \mu_{i+1} = \frac{c_i}{c_0}, \quad i \geq 1. \tag{5.1.7}$$

The series inside the brackets in (5.1.6) must be understood as an asymptotic expansion in powers of $1/g$, therefore up to two loops we can write it as

$$F_g \sim \frac{A^{-2g-b}}{\pi}\,\Gamma(2g+b)\,\mu_1\left[1+\frac{\mu_2 A}{2g}+\cdots\right]. \tag{5.1.8}$$

Justifying that the dispersion relation (4.3.65) holds in the present context is more delicate. The underlying reason is that g_s^2 or $1/N^2$ appear naturally as coupling constants only in a collective field treatment of the problem (or, equivalently, in a formulation in terms of a closed string field theory). In spite of this, one could still present a heuristic derivation of (5.1.5) by making use of the Lipatov approach to the large–order behavior, and applying it within the context of collective/string field theory. In this approach one does not use the analyticity properties of the free energy, but instead performs a saddle–point evaluation in both field space and coupling space [155]. Another heuristic derivation of (5.1.5) can be done by using Borel transforms [118]. Instead of trying to provide a more rigorous foundation for (5.1.5), we proceed to test it in various examples, also in the spirit of the many tests performed in field theory.

In writing (5.1.6) we have implicitly assumed that there is a single instanton solution that contributes to the asymptotic behavior. In general there might be various instanton configurations in the system, with the same action in absolute value, and in this case $F^{(1)}$ will denote the sum of all these contributions. For example, in the quartic matrix model, which we will analyze in section 5.4, due to the symmetry of the potential there are two instantons which contribute equally. It is also common to have complex instanton solutions which give complex conjugate contributions to $F^{(1)}$, and in this case the asymptotic behavior of F_g is again obtained by adding their contributions [156]. If we write

$$A = |A|\mathrm{e}^{\mathrm{i}\theta_A}, \qquad \mu_1 = |\mu_1|\mathrm{e}^{\mathrm{i}\theta_{\mu_1}}, \tag{5.1.9}$$

the leading asymptotics will read in this case

$$F_g \sim \frac{|A|^{-2g-b}}{\pi}\,\Gamma(2g+b)\,|\mu_1|\,\cos\big((2g+b)\theta_A+\theta_{\mu_1}\big). \tag{5.1.10}$$

We also find examples of this situation in the models studied in the next chapter.

5.2 One–Instanton Computation for Matrix Models

We now compute the "path" integral around the one–instanton configuration of the matrix model. In this process, we will adopt the framework put forward in [126], but we use saddle–point technology rather than the approach based on orthogonal polynomials. Such a strategy

has been considered before, as the approach of [126] was first rephrased in terms of the saddle–point perspective in [127] (for a third point of view, based on collective field theory, see [157]). At this stage, it is important to point out that our calculation will improve on the calculations in [126, 127] in three different ways. First of all, we fully exploit the saddle–point technology in order to present a much more succinct derivation of the final results. Secondly, we compute explicit formulae for the quantum expansion around the one–instanton solution up to two loops. Thirdly, and more importantly, we correct both the approach and the one–loop result in [126, 127] which, as they stand, are incorrect once one moves away from criticality. Taking all normalization factors into careful account, one finds for (4.1.40) [126]

$$\begin{aligned} Z_N^{(1)} &= \frac{N}{N!(2\pi)^N}\,(2\pi)^{N-1}(N-1)!\,Z_{N-1}^{(0)}\int_{x\in\mathcal{I}}\mathrm{d}x\,\left\langle\det(x\mathbf{1}-M')^2\right\rangle_{N-1}^{(0)}\,\mathrm{e}^{-\frac{1}{g_s}V(x)} \\ &\equiv \frac{1}{2\pi}\,Z_{N-1}^{(0)}\int_{x\in\mathcal{I}}\mathrm{d}x\,f(x). \end{aligned} \tag{5.2.11}$$

The notation in this equation is as follows. $Z_N^{(0)}$ is the partition function evaluated around the standard saddle–point, and within the standard $1/N$ expansion. M' is an $(N-1)\times(N-1)$ hermitian matrix, and all of its eigenvalues are still integrated around the standard saddle–point. $\langle\mathcal{O}\rangle_N^{(0)}$ is the normalized vacuum expectation value of the gauge–invariant operator $\mathcal{O}$, again computed around the standard saddle–point,

$$\langle\mathcal{O}\rangle_N^{(0)} = \frac{\int_{\lambda\in\mathcal{I}_0}\prod_{i=1}^N\mathrm{d}\lambda_i\,\Delta^2(\lambda)\,\mathcal{O}(\lambda)\,\mathrm{e}^{-\frac{1}{g_s}\sum_{i=1}^N V(\lambda_i)}}{\int_{\lambda\in\mathcal{I}_0}\prod_{i=1}^N\mathrm{d}\lambda_i\,\Delta^2(\lambda)\,\mathrm{e}^{-\frac{1}{g_s}\sum_{i=1}^N V(\lambda_i)}}. \tag{5.2.12}$$

Finally, we have also defined

$$f(x) = \left\langle\det(x\mathbf{1}-M')^2\right\rangle_{N-1}^{(0)}\,\mathrm{e}^{-\frac{1}{g_s}V(x)}. \tag{5.2.13}$$

As we have seen in (4.3.61), the one–instanton contribution to the free energy may be expressed in terms of the partition function, at leading order in $\mathrm{e}^{-1/g}$, by

$$F^{(1)} = \frac{Z_N^{(1)}}{Z_N^{(0)}} = \frac{1}{2\pi}\,\frac{Z_{N-1}^{(0)}}{Z_N^{(0)}}\int_{x\in\mathcal{I}}\mathrm{d}x\,f(x). \tag{5.2.14}$$

In the rest of this section we present a careful computation of this quantity.

In order to calculate the instanton contribution (5.2.14), we first compute $f(x)$, as defined above in (5.2.13). Making use of the familiar relation $\det(x\mathbf{1}-M) = \exp\left(\mathrm{tr}\ln(x\mathbf{1}-M)\right)$ we obtain,

$$\left\langle\det(x\mathbf{1}-M)^2\right\rangle = \exp\left[\sum_{s=1}^{+\infty}\frac{2^s}{s!}\left\langle(\mathrm{tr}\ln(x\mathbf{1}-M))^s\right\rangle_{(\mathrm{c})}\right], \tag{5.2.15}$$

which is written in terms of connected correlation functions (recall that the cumulant expansion precisely relates the generating functional of *standard* correlation functions to the generating functional of *connected* correlation functions as in this equality). The correlation functions appearing in (5.2.15) are nothing but integrated versions of the W_h correlators in (4.1.27), evaluated at coincident points. Let us define

$$\begin{aligned} A_{g,h}(x;t) &= \int^{x_1}\mathrm{d}p_1\cdots\int^{x_h}\mathrm{d}p_h\,W_{g,h}(p_1,\cdots,p_h)\Big|_{x_1=\cdots=x_h=x}, \\ \mathcal{A}_n(x;t) &= \sum_{k=0}^{\left[\frac{n}{2}\right]}\frac{2^{n-2k+1}}{(n-2k+1)!}\,A_{k,n-2k+1}(x;t), \quad n\geq 1. \end{aligned} \tag{5.2.16}$$

In this notation, the general perturbative formula for the determinant follows as

$$\left\langle \det(x\mathbf{1} - M)^2 \right\rangle = \exp\left(\sum_{n=0}^{+\infty} g_s^{n-1} \mathcal{A}_n(x;t) \right), \tag{5.2.17}$$

where $\mathcal{A}_n(x;t)$ is the n–loop contribution. We have, for example,

$$\begin{aligned} \mathcal{A}_0(x;t) &= 2A_{0,1}(x;t), \\ \mathcal{A}_1(x;t) &= 2A_{0,2}(x;t), \\ \mathcal{A}_2(x;t) &= \frac{4}{3} A_{0,3}(x;t) + 2A_{1,1}(x;t), \\ \mathcal{A}_3(x;t) &= \frac{2}{3} A_{0,4}(x;t) + 2A_{1,2}(x;t). \end{aligned} \tag{5.2.18}$$

One observes that in order to compute the determinant at n–loops, one would require analytic expressions for the $W_{g,h}$ with $(g,h) = (0,n+1), (1,n-1), (2,n-3), \ldots, (\frac{n}{2}, 1)$. Let us also point out that the integration constants involved in the integrations in (5.2.16) may be simply fixed by the large x expansion of the correlators. Indeed, we have the expansion

$$\left\langle (\mathrm{tr}\ln(x\mathbf{1} - M))^s \right\rangle_{(\mathrm{c})} = \sum_{n_i \geq 1} \frac{(-1)^s}{\prod_{i=1}^s n_i} \left\langle \mathrm{Tr}\, M^{n_1} \cdots \mathrm{Tr}\, M^{n_s} \right\rangle_{(\mathrm{c})} x^{-\sum_{i=1}^s n_i}. \tag{5.2.19}$$

Next, we define the *holomorphic* effective potential, which combines the matrix model potential together with $\mathcal{A}_0(x;t)$, as

$$V_{\mathrm{h,eff}}(x;t) = V(x) - 2t \int^x \mathrm{d}p\, \omega_0(p) = V(x) - 2t \int \mathrm{d}p\, \rho(p) \log(x-p), \tag{5.2.20}$$

which satisfies

$$V'_{\mathrm{h,eff}}(x;t) = y(x) \tag{5.2.21}$$

as well as

$$\mathrm{Re}\, V_{\mathrm{h,eff}}(x;t) = V_{\mathrm{eff}}(x), \tag{5.2.22}$$

where $V_{\mathrm{eff}}(x)$ was earlier defined in (4.1.14). Altogether, one finally has for the integrand

$$f(x) = \exp\left(-\frac{1}{g_s} V_{\mathrm{h,eff}}(x;t') + \sum_{n=1}^{+\infty} g_s^{n-1} \mathcal{A}_n(x;t') \right), \tag{5.2.23}$$

where

$$t' = g_s(N-1) = t - g_s. \tag{5.2.24}$$

This shift in the 't Hooft parameter is due to the fact that the correlation function involved in (5.2.13) is computed in a matrix model with $N-1$ eigenvalues (recall we removed one eigenvalue from the single–cut). Since we are computing the one–instanton contribution in the theory with N eigenvalues, we thus have to expand (5.2.23) around t. This gives further corrections in g_s, which we make explicit as

$$f(x) = \exp\left(-\sum_{k=0}^{+\infty} g_s^{k-1} \frac{(-1)^k}{k!} \partial_t^k V_{\mathrm{h,eff}}(x;t) + \sum_{n=1}^{+\infty} \sum_{k=0}^{+\infty} g_s^{n+k-1} \frac{(-1)^k}{k!} \partial_t^k \mathcal{A}_n(x;t) \right). \tag{5.2.25}$$

We write this expression as

$$f(x) = \exp\left(-\frac{1}{g_s} V_{\mathrm{h,eff}}(x) + \Phi(x) \right), \tag{5.2.26}$$

where we define

$$\Phi(x) \equiv \sum_{n=1}^{+\infty} g_s^{n-1}\, \Phi_n(x) \equiv \sum_{n=1}^{+\infty} g_s^{n-1} \left[\frac{(-1)^{n-1}}{n!}\, \partial_t^n V_{\rm h,eff}(x) + \sum_{k=0}^{n-1} \frac{(-1)^k}{k!}\, \partial_t^k \mathcal{A}_{n-k}(x) \right]. \quad (5.2.27)$$

One finds, for example,

$$\begin{aligned} \Phi_1(x) &= \mathcal{A}_1(x) + \partial_t V_{\rm h,eff}(x), \\ \Phi_2(x) &= \mathcal{A}_2(x) - \partial_t \mathcal{A}_1(x) - \frac{1}{2!}\, \partial_t^2 V_{\rm h,eff}(x), \\ \Phi_3(x) &= \mathcal{A}_3(x) - \partial_t \mathcal{A}_2(x) + \frac{1}{2!}\, \partial_t^2 \mathcal{A}_1(x) + \frac{1}{3!}\, \partial_t^3 V_{\rm h,eff}(x). \end{aligned} \quad (5.2.28)$$

In expression (5.2.26) all quantities now depend on the standard 't Hooft parameter t for the model with N eigenvalues, and we have thus dropped the explicit dependence on t. The derivatives with respect to t can be performed by using the formulae we presented at the end of the last subsection.

One may now proceed with the integration of $f(x)$,

$$\int_{x\in\mathcal{I}} {\rm d}x\, \exp\left(-\frac{1}{g_s} V_{\rm h,eff}(x) + \Phi(x) \right). \quad (5.2.29)$$

If we wish to evaluate this integral as a perturbative expansion around small string coupling, g_s, we can do it using a saddle–point evaluation [126, 127]. The integration contour is over the nontrivial saddle characterizing the one–instanton sector, which is defined by the usual saddle–point requirement

$$V'_{\rm h,eff}(x_0) = 0 \quad \Rightarrow \quad y(x_0) = 0, \quad (5.2.30)$$

with x_0 located *outside* of the cut. If we use the explicit form of the spectral curve (4.1.20) we find the equivalent condition

$$M(x_0) = 0. \quad (5.2.31)$$

The saddle–point x_0 is typically a local maximum of the effective potential, as depicted in Fig. 4.3. Of course, it can happen that there is more than one solution to (5.2.31). In this case, there will be various instantons and we will have to add up their contributions (the leading contribution arising from the instanton with the highest action, in absolute value). The calculation of (5.2.29) is now completely standard, and it reduces to Gaussian integrations. The result is

$$\int_{x\in\mathcal{I}} {\rm d}x\, f(x) = \sqrt{\frac{2\pi g_s}{V''_{\rm h,eff}(x_0)}}\, \exp\left(-\frac{1}{g_s} V_{\rm h,eff}(x_0) + \Phi_1(x_0) \right) \left(1 + \sum_{n=2}^{+\infty} g_s^n\, f_n \right), \quad (5.2.32)$$

where the f_n can be systematically computed in terms of the functions $\Phi_n(x)$ and their derivatives, evaluated at the saddle–point x_0, by making use of the Gaussian integral and the Gaussian moments. This is a long and tedious process, where one should be very careful with factors of g_s. In particular, one splits the integrand into the standard Gaussian integrand plus the rest, where the rest should be power–series expanded in order to produce Gaussian moments. This process is source to some extra factors of g_s that must be properly considered. In any case, there are no conceptual difficulties in taking this calculation to arbitrary order. In order to find an explicit expression for the two–loop contribution to the one–instanton path integral, we will need

$$\begin{aligned} f_2 = \Phi_2(x_0) &+ \frac{1}{2V''_{\rm eff}(x_0)} \left\{ \partial_x^2 \Phi_1(x_0) + (\partial_x \Phi_1(x_0))^2 \right\} - \\ &- \frac{1}{2\left(V''_{\rm h,eff}(x_0) \right)^2} \left\{ \frac{1}{4}\, \partial_x^4 V_{\rm h,eff}(x_0) + \partial_x^3 V_{\rm h,eff}(x_0) \partial_x \Phi_1(x_0) \right\} + \frac{5\left(\partial_x^3 V_{\rm h,eff}(x_0) \right)^2}{24\left(V''_{\rm h,eff}(x_0) \right)^3}. \end{aligned} \quad (5.2.33)$$

Observe that the required evaluation of derivatives at x_0, in the expression above, is a rather straightforward exercise as we are dealing in this case with rational functions.

The last ingredient needed to compute the one–instanton contribution is the quotient of partition functions in the expression for $\operatorname{disc} F$, (5.2.14). This quotient can be written in terms of the standard, perturbative free energies, since

$$\frac{Z^{(0)}_{N-1}}{Z^{(0)}_N} = \exp\big(F(t') - F(t)\big)\,. \tag{5.2.34}$$

In the rest of this section both $F(t)$ and $F_g(t)$ denote the *unnormalized* free energies, *i.e.*, $F = \log Z_N$. If one explicitly expands in g_s, by both writing the above expression in terms of the standard 't Hooft parameter t alone, and further expanding the free energy in its perturbative genus expansion (4.1.26), it follows

$$\frac{Z^{(0)}_{N-1}}{Z^{(0)}_N} = \exp\left(\sum_{n=0}^{+\infty} g_s^{n-1}\mathcal{G}_n\right), \qquad \mathcal{G}_n \equiv \sum_{k=0}^{\left[\frac{n}{2}\right]} \frac{(-1)^{n-2k+1}}{(n-2k+1)!}\,\partial_t^{n-2k+1} F_k(t). \tag{5.2.35}$$

One has, for example,

$$\begin{aligned} \mathcal{G}_0 &= -\partial_t F_0(t), \\ \mathcal{G}_1 &= \frac{1}{2}\,\partial_t^2 F_0(t), \\ \mathcal{G}_2 &= -\frac{1}{3!}\,\partial_t^3 F_0(t) - \partial_t F_1(t). \end{aligned} \tag{5.2.36}$$

Putting together (5.2.32) and (5.2.35) above, we finally find that $F^{(1)}$ has the structure

$$F^{(1)} = \mathrm{i}\, g_s^{\frac{1}{2}}\,\mu_1\,\exp\left(-\frac{A}{g_s}\right)\left\{1 + \sum_{n=1}^{+\infty}\mu_{n+1} g_s^n\right\}. \tag{5.2.37}$$

Collecting results above we obtain the following contributions to $F^{(1)}$, up to two loops:

$$\begin{aligned} A &= V_{\mathrm{h,eff}}(x_0) - \mathcal{G}_0(t), \\ \mu_1 &= -\mathrm{i}\sqrt{\frac{1}{2\pi V''_{\mathrm{h,eff}}(x_0)}}\,\exp\Big(\Phi_1(x_0) + \mathcal{G}_1(t)\Big), \\ \mu_2 &= f_2 + \mathcal{G}_2(t). \end{aligned} \tag{5.2.38}$$

Let us now give explicit expressions for these quantities in terms of data associated to the spectral curve (4.1.20). First of all, by using (5.2.36), (4.1.45) and (5.2.21) we find

$$A = V_{\mathrm{h,eff}}(x_0) - V_{\mathrm{h,eff}}(b) = \int_b^{x_0} \mathrm{d}z\, y(z), \tag{5.2.39}$$

which is the instanton action (here, we use the fact that $V_{\mathrm{h,eff}}(b) = V_{\mathrm{eff}}(b)$). Notice that, as pointed out in [136], this expression also has a geometric interpretation as the contour integral of the one–form $y(z)\,\mathrm{d}z$, from the endpoint of the cut $\mathcal{C}$ to the singular point x_0 (recall Fig. 4.4).

We next move to the one–loop contribution, and begin with the computation of $\Phi_1(x)$. One can find the result for $A_{0,2}(x;t)$ (which enters in the expression of $\mathcal{A}_1$) simply by integrating the first formula in (4.1.35) [127]

$$A_{0,2}(x;t) = \log\left(1 + \frac{x - (a+b)/2}{\sqrt{(x-a)(x-b)}}\right) - \log 2. \tag{5.2.40}$$

Using (4.1.41) one further finds,

$$\partial_t V_{\mathrm{h,eff}}(x) = -4\log\Big[\sqrt{x-a}+\sqrt{x-b}\Big] + 4\log 2, \tag{5.2.41}$$

and both these results together is all one requires to obtain

$$\Phi_1(x) = -\log\Big[(x-a)(x-b)\Big]. \tag{5.2.42}$$

Adding to $\Phi_1(x)$ the result for $\mathcal{G}_1(t)$, which follows from (4.1.45), it is simple to put all expressions together and obtain the contribution, μ_1, of the one–loop fluctuations around the one–instanton configuration,

$$\mu_1 = -\mathrm{i}\,\frac{b-a}{4}\,\sqrt{\frac{1}{2\pi M'(x_0)\Big[(x_0-a)(x_0-b)\Big]^{\frac{5}{2}}}}. \tag{5.2.43}$$

This formula is valid for any one–cut matrix model with an unstable potential. Notice that if x_0 is a local maximum of $V_{\mathrm{eff}}(x)$, one will have that $M'(x_0) < 0$, and hence μ_1 will be real. It is also important to point out that our result (5.2.43) is *different* from the result obtained in [126, 127]. The reason is that, in these references, no distinction is made between correlation functions computed at t' and those computed at t. Correspondingly, the contribution of (5.2.41) is never taken into account. While this contribution vanishes at the critical point, it is non–zero for generic values of the parameters, making it crucial in order to obtain a generic result. In this chapter we present substantial evidence that (5.2.43) is the correct result, by using the connection to the large–order behavior of perturbation theory explained in the last section.

The computation at two loops does not present any conceptual difficulty, but it is much more involved. One needs the explicit expressions

$$\begin{aligned}
A_{0,3}(x;t) &= \frac{\left(\sqrt{x-a}-\sqrt{x-b}\right)^3}{(a-b)^2}\left(\frac{1}{M(a)(x-a)^{\frac{3}{2}}}-\frac{1}{M(b)(x-b)^{\frac{3}{2}}}\right),\\
A_{1,1}(x;t) &= -\frac{1}{12(a-b)^2}\left(\frac{1}{M(a)}+\frac{1}{M(b)}\right)+\\
&\quad+\frac{1}{24(a-b)^2}\left(\frac{(2(x-a)+(b-a))\sqrt{x-b}}{M(a)\,(x-a)^{\frac{3}{2}}}+\frac{(2(x-b)+(a-b))\sqrt{x-a}}{M(b)\,(x-b)^{\frac{3}{2}}}\right)-\\
&\quad-\frac{\sqrt{x-a}-\sqrt{x-b}}{8(a-b)^2}\left(\frac{2M(a)+(a-b)M'(a)}{M^2(a)\sqrt{x-a}}-\frac{2M(b)+(b-a)M'(b)}{M^2(b)\sqrt{x-b}}\right).
\end{aligned} \tag{5.2.44}$$

After very long but straightforward computations, one finally obtains the two–loop coefficient as

$$\begin{aligned}
\mu_2 &= \frac{1}{4(a-b)\sqrt{(x_0-a)(x_0-b)}}\left(\frac{(x_0-b)M'(a)}{M^2(a)}-\frac{(x_0-a)M'(b)}{M^2(b)}\right)-\\
&\quad-\frac{\sqrt{(x_0-a)(x_0-b)}}{12(a-b)^2}\left(\frac{8(x_0-a)+17(a-b)}{(x_0-a)^2M(a)}+\frac{8(x_0-b)+17(b-a)}{(x_0-b)^2M(b)}\right)+\\
&\quad+\frac{5\left(M''(x_0)\right)^2-3M'(x_0)M^{(3)}(x_0)}{24\left(M'(x_0)\right)^3\sqrt{(x_0-a)(x_0-b)}}+\frac{35\left(2x_0-(a+b)\right)M''(x_0)}{48\left(M'(x_0)\right)^2\left((x_0-a)(x_0-b)\right)^{\frac{3}{2}}}+\\
&\quad+\frac{140\left(2x_0-(a+b)\right)^2+33(a-b)^2}{96M'(x_0)\left((x_0-a)(x_0-b)\right)^{\frac{5}{2}}}.
\end{aligned} \tag{5.2.45}$$

As one immediately realizes from the explicit expressions above, both μ_1 and μ_2 depend uniquely on data specified by the spectral curve. More precisely, they depend on the endpoints of the

cut, a and b, the position of the saddle–point, x_0, and on the moments of the function $M(p)$, evaluated at a, b or x_0. It is not hard to convince oneself that the rest of the coefficients μ_n in (5.2.37) must also share this property. This has two important consequences. First of all, it displays the universality of the results, in the sense that two matrix models which lead to the same spectral curve will also share the same discontinuity, $\operatorname{disc} F$. In particular, since taking the double–scaling limit commutes with the geometric computation of the amplitudes, different models that lead to the same critical theory will also lead to the same one–instanton contribution at criticality [126, 127]. Secondly, since the description of the B–model on mirrors of toric manifolds in [29, 36] only depends on the geometry of the spectral curve, we may also compute nonperturbative effects in these models by simple application of the formulae above for $F^{(1)}$: one just has to apply them to the spectral curves described in [29, 36]. Notice that in this chapter we restrict ourselves to the one–cut case, therefore our formalism will only apply to the mirrors of local curves, worked out in [29]. The multi-cut case is discussed in chapter 6.

5.3 Numerical Methods and Richardson Transforms

The instanton computations we perform in this work yield predictions for the quantities A, b, μ_1 and μ_2 appearing in (5.1.6) above. In order to test these predictions, one has to extract these quantities from the asymptotics of the sequence $\{F_g\}_{g\geq 0}$. However, computation of the amplitudes F_g is, in most cases, rather involved and therefore they will typically only be available at low genus, of order $g < 20$. This will also be the case for our examples, apart from 2d gravity where the Painlevé I equation allows for a computation to arbitrarily high genus. We therefore use a standard numerical technique known as Richardson extrapolation (see, *e.g.*, [158]), in order to be able to extract the asymptotic behavior more accurately from the very first terms of the series. This method removes the first terms of the subleading tail and thus accelerates convergence towards the leading asymptotics.

The basic idea of Richardson extrapolation is as follows. Given a sequence

$$S(g) = s_0 + \frac{s_1}{g} + \frac{s_2}{g^2} + \cdots , \tag{5.3.46}$$

its Richardson transform is defined as

$$A_S(g, N) = \sum_{k\geq 0} \frac{S(g+k)(g+k)^N(-1)^{k+N}}{k!(N-k)!}. \tag{5.3.47}$$

This cancels the sub–leading terms in $S(g)$ up to order g^{-N}. Indeed, one can show that if $S(g)$ truncates at order g^{-N}, the Richardson transform gives exactly the leading term s_0.

The first quantity that one may extract from the sequence $\{F_g\}_{g\geq 0}$, assuming it is of the form (5.1.6), is the instanton action. In order to apply the Richardson method, we need a sequence with large g asymptotics of the form (5.3.46). This is achieved by considering the sequence

$$Q_g = \frac{F_{g+1}}{4g^2 F_g} = \frac{1}{A^2}\left(1 + \frac{1+2b}{2g} + \mathcal{O}\left(\frac{1}{g^2}\right)\right). \tag{5.3.48}$$

Once A has been found, one can then simply extract the parameter b from the new sequence

$$2g\left(A^2 \frac{F_{g+1}}{4g^2 F_g} - 1\right) = 1 + 2b + \mathcal{O}\left(\frac{1}{g}\right). \tag{5.3.49}$$

Finally, one obtains the coefficients μ_1 and μ_2 from the sequences

$$\frac{\pi A^{2g+b} F_g}{\Gamma(2g+b)} = \mu_1\left(1 + \frac{\mu_2 A}{2g} + \mathcal{O}\left(\frac{1}{g^2}\right)\right) \tag{5.3.50}$$

and

$$\frac{2g}{A}\left(\frac{\pi A^{2g+b}F_g}{\mu_1\Gamma(2g+b)}-1\right)=\mu_2+\mathcal{O}\left(\frac{1}{g}\right), \tag{5.3.51}$$

whose asymptotics are already of the form (5.3.46), with leading terms μ_1 and μ_2, respectively. This is the basic picture behind most of our numerical work.

The situation is slightly more complicated when we have to deal with two complex conjugate instantons. In this case, the ansatz for F_g is given by (5.1.10). If the absolute value of the instanton action is known, its phase θ_A can be checked using the sequence

$$\frac{|A|^{2g+2}F_{g+1}}{(2g+b+1)(2g+b)F_g}-\frac{|A|^{2g-2}F_{g-1}(2g+b-2)(2g+b-1)}{F_g}=2\cos(2\theta_A)\left(1+\mathcal{O}\left(\frac{1}{g^2}\right)\right). \tag{5.3.52}$$

5.4 Application I: Quartic Matrix Model and 2d Gravity

Before proceeding towards the realm of topological string theory, we test our results in the case of a rather familiar matrix model, the quartic matrix model both off and at criticality.

5.4.1 The Quartic Matrix Model

The quartic matrix model is defined by the potential

$$V(z)=\frac{1}{2}z^2+\lambda z^4, \tag{5.4.53}$$

with λ the quartic coupling constant. The properties of this model at large N were addressed long ago in [128, 132]. The density of eigenvalues has support on the single cut $\mathcal{C}=[a,b]\equiv[-2\alpha,2\alpha]$, where α is a function of λ and the 't Hooft parameter t, as

$$\alpha^2=\frac{1}{24\lambda}\left(-1+\sqrt{1+48\lambda t}\right). \tag{5.4.54}$$

The spectral curve follows as

$$y(z)=M(z)\sqrt{z^2-4\alpha^2}, \tag{5.4.55}$$

with

$$M(z)=1+8\lambda\alpha^2+4\lambda z^2. \tag{5.4.56}$$

This function has two zeros which give two non–trivial saddle–points, namely $\pm x_0$ with

$$x_0^2=-\frac{1}{4\lambda}\left(1+8\lambda\alpha^2\right). \tag{5.4.57}$$

These two saddle–points are evident in Fig. 5.1, where we have displayed the effective potential for the quartic matrix model. If we wish to compare the large–order prediction of our formulae with the real behavior of the perturbation theory in this model, one is required to actually compute the free energies at high genera. The set–up for such a calculation was first described in [132], but the calculation was only carried out in that paper up to genus $g=2$. We have extended this computation to genus $g=10$ and we review in the following how to compute F_g in the quartic matrix model at large g.

The calculation of the $1/N$ expansion of the free energy in the quartic matrix model was set up in [132] using the method of orthogonal polynomials. A review of such method and subsequent calculation would lead us too far apart from the main line of this work, so that in the following we restrict ourselves to presenting an algorithmic prescription to compute F_g which summarizes the results of [132]. The interested reader should consult the original reference [132] for full details. Also, for simplicity, we set $t=1$ in the following and will follow the exact same

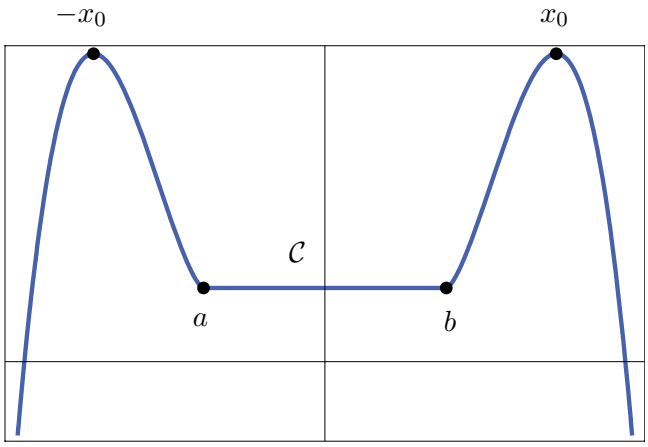

Figure 5.1: The effective potential $V_{\text{eff}}(x)$ for the quartic matrix model. There are two saddle–points located at x_0 and $-x_0$.

conventions as in [132]. In particular, in this section our convention for the free energy, following [132], is that $F = -\log Z$. There are several components that make up the calculation of F_g. It starts with the so–called pre–string equation

$$R_n\big\{1 + 4\lambda\,(R_n + R_{n-1} + R_{n+1})\big\} = n g_s, \tag{5.4.58}$$

for the coefficients R_n which determine the partition function in the orthogonal polynomial formalism. One then considers a continuous version of these coefficients, corresponding to a family of polynomials, $r_{2s}(x;\lambda)$, which, in light of the pre–string equation (5.4.58), satisfy a simple algebraic, recursive relation. For $s = 0$

$$r_0(x;\lambda) = \frac{1}{24\lambda}\left(-1 + \sqrt{1 + 48\lambda x}\right), \tag{5.4.59}$$

while for $s > 0$ the pre–string equation yields the recursive expression

$$r_{2s}(x;\lambda) + 4\lambda \sum_{m+n=s} r_{2m}(x;\lambda)\left(r_{2n}(x;\lambda) + 2\sum_{k+p=n}\frac{r^{(2p)}_{2k}(x;\lambda)}{(2p)!}\right) = 0. \tag{5.4.60}$$

In this way it is rather simple to compute the polynomials $r_{2s}(x;\lambda)$ to very high s. These polynomials are crucial in other to find F_g. Indeed, the general formula for the total free energy is [132]

$$\begin{aligned} g_s^2 F(\lambda) = &-\int_0^1 \mathrm{d}x\ (1-x)\log\Xi(x;\lambda) + \mathcal{H}(\lambda) - \\ &-\sum_{p=1}^{+\infty} g_s^{2p}\,\frac{B_{2p}}{(2p)!}\,\frac{\mathrm{d}^{2p-1}}{\mathrm{d}x^{2p-1}}\Big((1-x)\log\Xi(x;\lambda)\Big)\Big|_{x=0}^{x=1}, \end{aligned} \tag{5.4.61}$$

where the function $\Xi(x;\lambda)$ is precisely built using the $r_{2s}(x;\lambda)$ polynomials as

$$\Xi(x;\lambda) = \sum_{s=0}^{+\infty} g_s^{2s}\,\frac{r_{2s}(x;\lambda)}{x}. \tag{5.4.62}$$

In the expression above, B_{2p} are Bernoulli numbers and $\mathcal{H}(\lambda)$ is the function

$$\mathcal{H}(\lambda) = -\frac{1}{2}\,g_s\left[\log\int_{-\infty}^{+\infty}\mathrm{d}\mu\,\mathrm{e}^{-\frac{1}{2}\mu^2 - g_s\lambda\mu^4} - \log\int_{-\infty}^{+\infty}\mathrm{d}\mu\,\mathrm{e}^{-\frac{1}{2}\mu^2 + g_s\lambda\mu^4}\right]. \tag{5.4.63}$$

An expansion of (5.4.61) in powers of g_s then yields explicit expressions for F_g. Moreover, this is an algorithmic prescription of calculation, which may be simply implemented with a symbolic computation program. This calculation was carried out analytically up to $g = 2$ in [132] and we have implemented it in a computer program, obtaining in this way explicit results up to $g = 10$. A partial list of our F_g can be found in appendix B.2.1. Here, let us just recall that [132] conjectured that, for genus $g \geq 2$, the general structure should be of the form

$$F_g(\alpha^2) = \frac{\left(1-\alpha^2\right)^{2g-1}}{\left(2-\alpha^2\right)^{5(g-1)}} \mathcal{P}_g(\alpha^2), \tag{5.4.64}$$

with $\mathcal{P}_g(\alpha^2)$ a polynomial in α^2 such that

$$\mathcal{P}_g(\alpha^2 = 1) = \frac{1}{2 \cdot 6^{2g-1}} \frac{(4g-3)!}{g!(g-1)!}. \tag{5.4.65}$$

We have checked this conjecture up to genus $g = 10$ and further found that the polynomial $\mathcal{P}_g(\alpha^2)$ is of order $3g-4$ in α^2.

5.4.2 Instanton Effects and Large–Order Behavior

Let us now present explicit formulae for the terms contributing to the one–instanton sector, in the quartic matrix model. As we did before, in the following we will set $t = 1$ for simplicity. The first thing to notice is that, since the potential is symmetric, there are *two* instanton solutions, corresponding to eigenvalue tunneling from $\mathcal{C}$ to the two saddles $\pm x_0$ (see Fig. 5.1). Both instantons have the same action, which is computed via direct integration of the spectral curve

$$A = -\frac{\sqrt{3}\,\alpha^2}{4\left(1-\alpha^2\right)} \sqrt{4-\alpha^4} - 2\log\left[\sqrt{3}\sqrt{-2+\alpha^2} + \sqrt{-2-\alpha^2}\right] + \log 4\left(1-\alpha^2\right), \tag{5.4.66}$$

and therefore contribute equally to the large–order behavior. The one–loop contribution μ_1 can be easily obtained from the general formula we derived before, but it has an extra factor of 2 in order to account for the two instantons. It reads,

$$\mu_1 = -\frac{1}{3^{\frac{3}{4}}\sqrt{\pi}} \frac{1-\alpha^2}{\left(2-\alpha^2\right)^{\frac{5}{4}} \left(2+\alpha^2\right)^{\frac{1}{4}}}. \tag{5.4.67}$$

After some tedious but straightforward analysis, one likewise obtains for the two–loop contribution μ_2

$$\mu_2 = \frac{1}{4\sqrt{3}} \frac{1}{\left(2-\alpha^2\right)^{\frac{5}{2}} \left(2+\alpha^2\right)^{\frac{3}{2}}} \left(40 - 12\alpha^2 - 21\alpha^4 - 10\alpha^6\right). \tag{5.4.68}$$

Using these formulae, we see that $b = -5/2$ in (5.1.3), and the asymptotics of $F_g(\lambda)$ is then given by

$$F_g(\lambda) \sim \frac{\mu_1}{\pi}\, A^{-2g+5/2}\, \Gamma\left(2g - \frac{5}{2}\right) \left[1 + \frac{\mu_2 A}{2g} + \mathcal{O}\left(\frac{1}{g^2}\right)\right]. \tag{5.4.69}$$

The goal is now to compare this "theoretical" large–order prediction with the actual, "experimental" behavior of the $1/N$ expansion, using the results we have obtained for the free energies F_g up to $g = 10$, in the quartic matrix model. We first focus on the range of values of λ where the instanton action, as well as the F_g, are real. This is precisely the interval between $\lambda = 0$ and the critical point $\lambda = -\frac{1}{48}$ (we will come back to this critical point in the next subsection). In Fig. 5.2–Fig. 5.4 we have displayed the asymptotic values of the instanton action as well as the one and two–loop results for the quartic potential. This is done at specific values of the coupling. The graphs include results extracted from the original sequence F_g (the uppermost sequence of data), and its Richardson transforms, alongside with the prediction from instanton calculus. In

Fig. 5.5 we have plotted the asymptotic values of μ_1 and μ_2, obtained as a function of λ from the third Richardson transform, divided by the corresponding prediction from instanton calculus. It is rather clear that this quotient is very close to 1, with a small error of roughly 0.1% over most of moduli space. The larger error found at $\lambda \approx 0$ is due to numerical difficulties related to the divergence of the instanton action in this region. Indeed, at very small λ, the Richardson transformations converge too slowly to fall on a horizontal line at low genus—in this case, we would need higher–genus data to obtain better agreement with the predictions. In any case, the complete set of displayed numerical results strongly supports our analytical predictions.

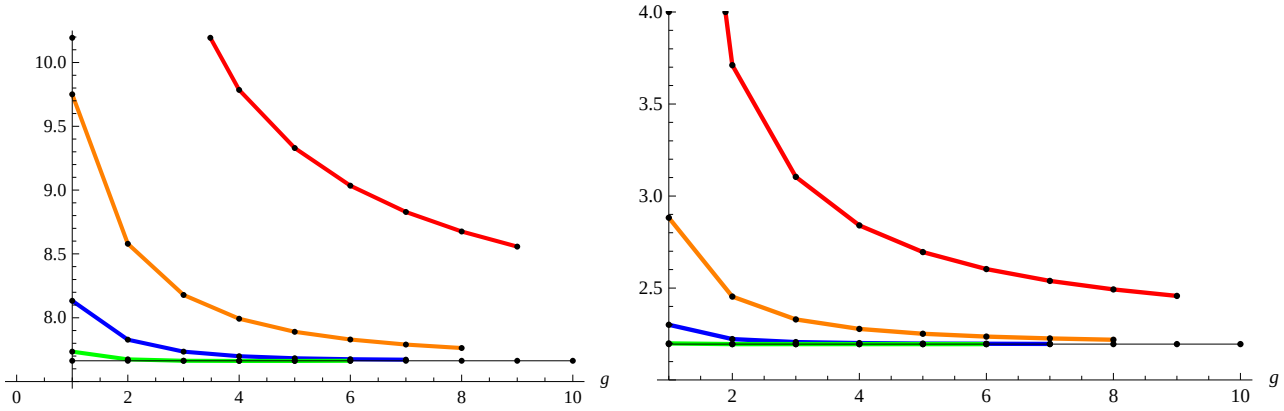

Figure 5.2: The sequence $\sqrt{1/Q_g}$ with Q_g as defined in (5.3.48) and the corresponding Richardson transforms for the quartic matrix model, at fixed values $\lambda = -0.005$ (left) and $\lambda = -0.01$ (right). The prediction for the leading asymptotics is given by the instanton action $A(\lambda)$, shown as a straight line. The error for $g = 10$ is 0.01% at $\lambda = -0.005$, respectively 0.0047% at $\lambda = -0.01$.

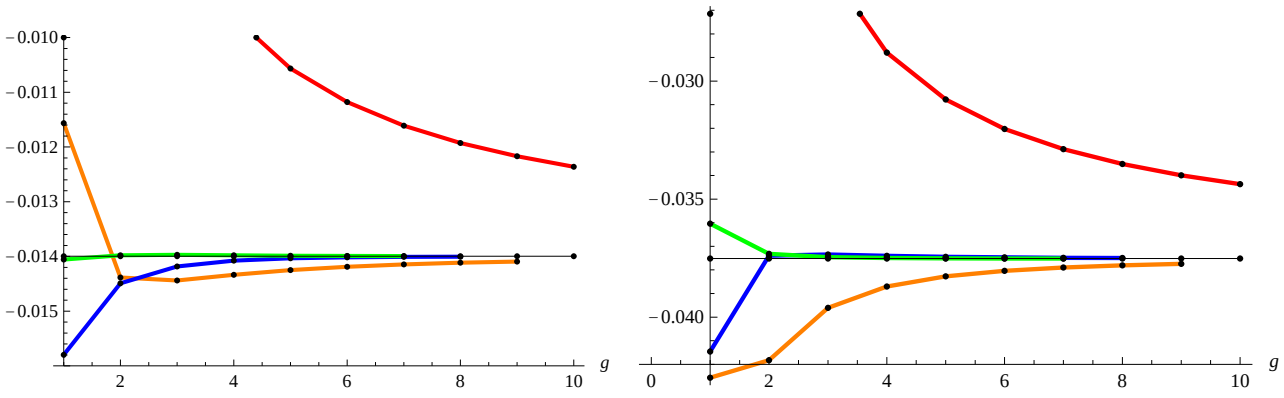

Figure 5.3: The sequence $\pi F_g A^{2g-\frac{5}{2}}/\Gamma(2g-\frac{5}{2})$ and its Richardson transforms for the quartic matrix model, at fixed values $\lambda = -0.005$ (left) and $\lambda = -0.01$ (right). The prediction for the asymptotic value is the one–loop result μ_1 (straight line). The error is 0.003% at $\lambda = -0.005$, respectively 0.002% at $\lambda = -0.01$.

Let us now consider the range of moduli space where $\lambda > 0$. In this region the amplitudes F_g are still real, as are the endpoints of the cut $\pm 2\alpha$. However, the saddle–points x_0 given in (5.4.57) now become purely imaginary and conjugate to each other. This implies that there are now *four* instanton solutions, corresponding to eigenvalues tunneling from both endpoints of the cut to both of the saddle–points, as depicted in Fig. 5.6. The corresponding instanton actions are complex conjugate by a constant shift of $\pm i\pi$. We therefore expect the leading asymptotics

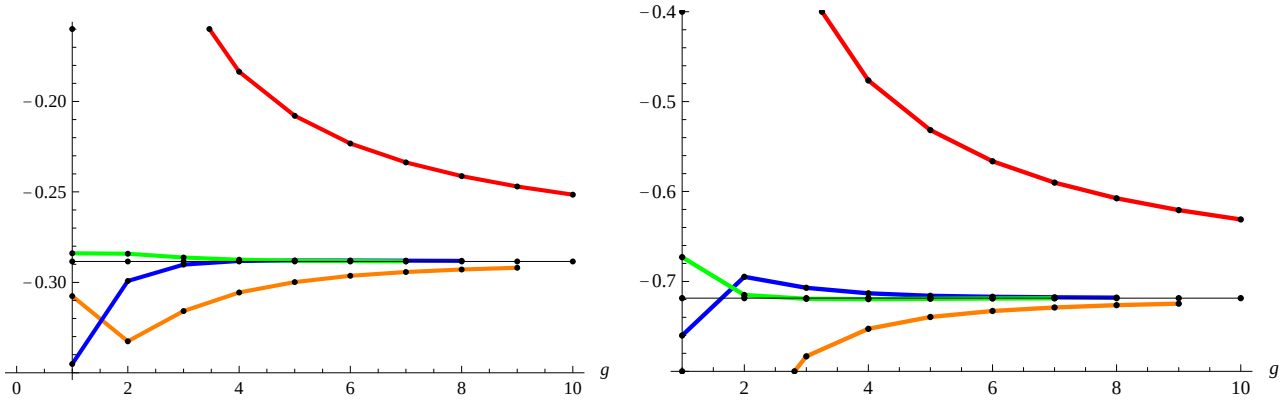

Figure 5.4: The sequence (5.3.51) and its Richardson transforms for the quartic matrix model, at $\lambda = -0.005$ (left) and $\lambda = -0.01$ (right). The prediction for the leading asymptotics is given by the two–loop result μ_2. The error is 0.05% at $\lambda = -0.005$, respectively 0.016% at $\lambda = -0.01$.

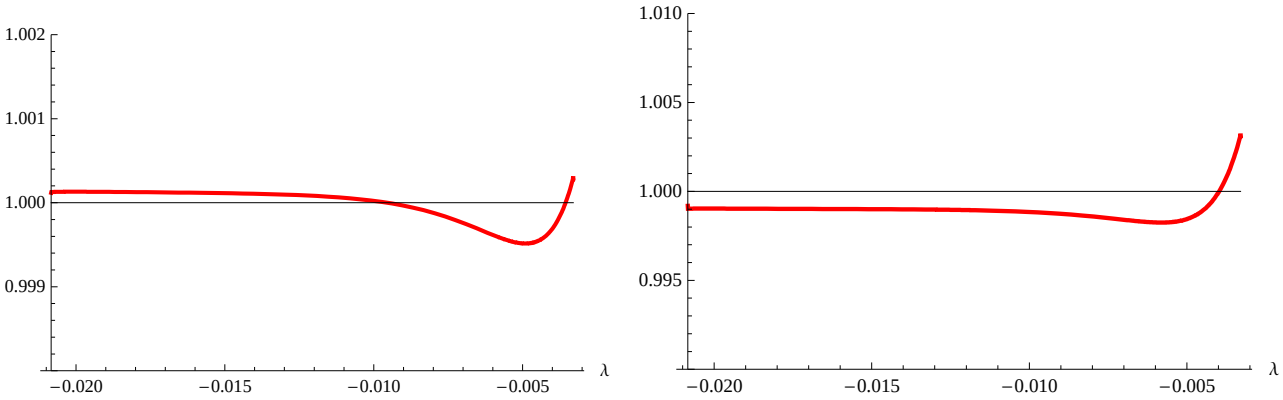

Figure 5.5: The left figure shows the asymptotic value of $\pi F_g A^{2g-\frac{5}{2}}/\Gamma(2g-\frac{5}{2})$ for the quartic matrix model, as extracted as a function of λ by the third Richardson transform, divided by the analytic prediction μ_1. The figure on the right shows the analogous quotient for μ_2. For $\lambda < -0.004$ the error is always less than 0.06%.

to be of the form (5.1.10), implying that

$$\frac{\pi F_g |A|^{2g-\frac{5}{2}}}{|\mu_1|\Gamma(2g-\frac{5}{2})} = 2\cos\left((2g-\frac{5}{2})\theta_A + \theta_{\mu_1}\right)\left(1+\mathcal{O}\left(\frac{1}{g}\right)\right), \tag{5.4.70}$$

where θ_A and θ_{μ_1} have been defined in (5.1.9). This is indeed the case, as one can see from Fig. 5.7 showing the quotient in the left hand side of (5.4.70) together with the prediction for $2\cos\left((2g-\frac{5}{2})\theta_A + \theta_{\mu_1}\right)$, at two positive values $\lambda = 0.004$ and $\lambda = 3$.

5.4.3 2d Gravity and the Painlevé I Equation

A rather well–known result (see [118] for an excellent review) is that the quartic matrix model has a critical point at

$$\lambda_c = -\frac{1}{48}. \tag{5.4.71}$$

At this critical value of λ, the saddles $\pm x_0$ collide with the two endpoints of the cut $\pm 2\alpha$. One may further use the matrix model near this point in order to define two–dimensional gravity by means of a double–scaling limit. In this specific limit, one takes

$$\lambda \to \lambda_c, \qquad g_s \to 0, \tag{5.4.72}$$

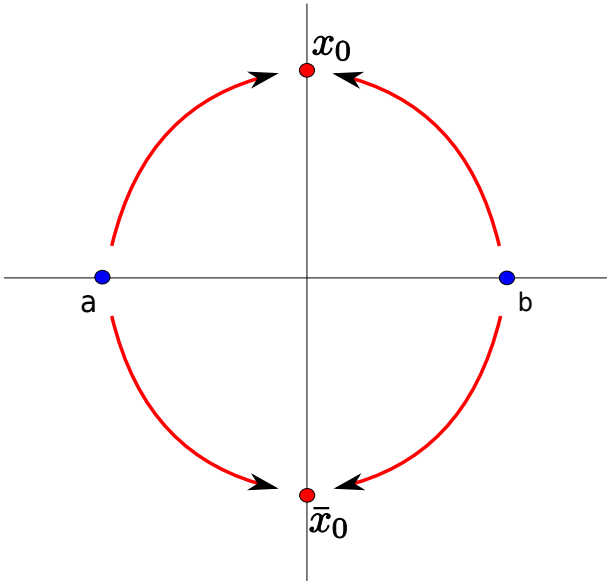

Figure 5.6: This figure shows the instanton effects for the quartic matrix model at *positive* coupling λ. The endpoints of the cut, a and b, are real while the two saddle–points of the effective potential are purely imaginary and complex conjugate to each other. There are two pairs of complex conjugate instantons, corresponding to eigenvalues tunneling from either end of the cut to the saddles x_0 and x_0^*.

in such a way that the variable

$$z = -\frac{1}{\lambda_c}\,(\lambda - \lambda_c)\, g_s^{-4/5} \tag{5.4.73}$$

is kept fixed. In this limit it follows that the total, perturbative free energy of the matrix model becomes the free energy of pure 2d gravity

$$F(g_s, \lambda) \to F_{\rm ds}(z). \tag{5.4.74}$$

Furthermore, in this limit, the pre–string equation of the quartic matrix model (5.4.58) precisely becomes the Painlevé I equation

$$u^2 - \frac{1}{3}u'' = z, \tag{5.4.75}$$

governing the specific heat of the model

$$u(z) = -F''_{\rm ds}(z). \tag{5.4.76}$$

These results may be used to obtain the perturbative expansion of $F_{\rm ds}(z)$, at any given order. It turns out that the free energy obtained in this way is actually doubled, since it gets contributions from the two collisions at $\pm x_0$. This is of course due to the symmetry of the potential, which we have discussed before. In order to remove the doubling it is enough to change the normalization of the quantities appearing above, by

$$z \to 2^{\frac{2}{5}} z, \qquad u \to 2^{\frac{1}{5}} u, \qquad F_{\rm ds} \to 2F_{\rm ds}. \tag{5.4.77}$$

Proceeding in this way one is led to the Painlevé I equation with the normalization

$$u^2 - \frac{1}{6}u'' = z, \tag{5.4.78}$$

while the double–scaled free energy still satisfies (5.4.76). The perturbative expansion of the specific heat has the form

$$u(z) = z^{\frac{1}{2}} \sum_{g=0}^{+\infty} u_g\, z^{-5g/2}, \tag{5.4.79}$$

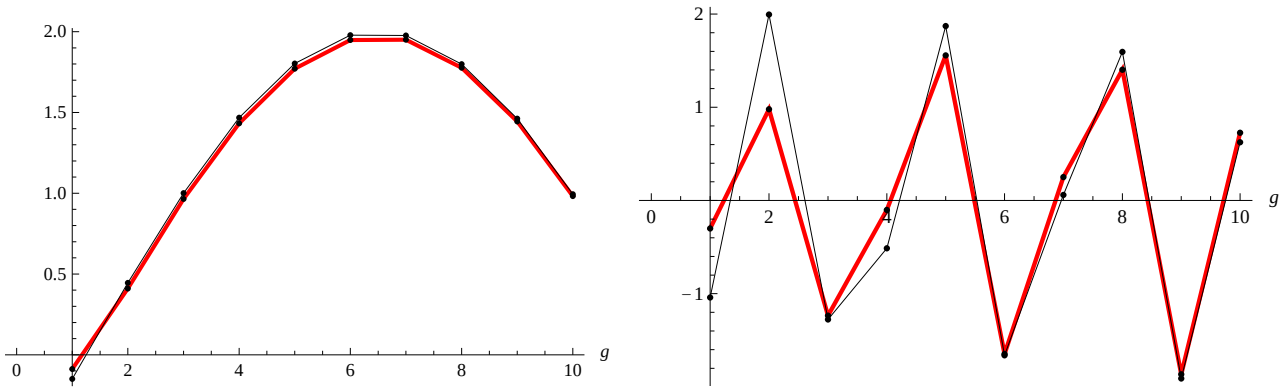

Figure 5.7: The sequence $\pi F_g |A|^{2g-\frac{5}{2}} / \left(|\mu_1|\Gamma(2g-\frac{5}{2})\right)$ for the quartic matrix model, together with the prediction for the leading asymptotics $2\cos\left((2g-\frac{5}{2})\theta_A(\lambda)+\theta_{\mu_1}(\lambda)\right)$ (thin black line), at $\lambda = 0.004$ (left), respectively $\lambda = 3$ (right). At the highest depicted values of g the error is of the order of 2% ($\lambda = 0.004$), respectively 5% ($\lambda = 3$).

so that the Painlevé I equation becomes equivalent to the following difference equation for the coefficients u_g

$$u_g = \frac{25(g-1)^2-1}{48} u_{g-1} - \frac{1}{2}\sum_{\ell=1}^{g-1} u_\ell u_{g-\ell}, \qquad u_0 = 1. \tag{5.4.80}$$

The coefficients a_g, which appear in the perturbative expansion of the double–scaled free energy as

$$F_{\rm ds}(z) = -\frac{4}{15} z^{5/2} - \frac{1}{48}\log z + \sum_{g\geq 2} a_g\, z^{-5(g-1)/2}, \tag{5.4.81}$$

can then be obtained from u_g through the simple relation

$$a_g = -\frac{4}{(5g-5)(5g-3)} u_g. \tag{5.4.82}$$

As a result one finds, for example,

$$F_{\rm ds}(z) = -\frac{4}{15} z^{\frac{5}{2}} - \frac{1}{48}\log z + \frac{7}{5760} z^{-\frac{5}{2}} + \frac{245}{331776} z^{-5} + \cdots. \tag{5.4.83}$$

We are now in a position where we may obtain a prediction for the asymptotics of the coefficients of this series, a_g, by simply evaluating the expressions we obtained for the quartic matrix model near the critical point, and taking into account the change of normalization in (5.4.77). In this way we find

$$\frac{A}{g_s} = \frac{8\sqrt{3}}{5} z^{\frac{5}{4}}. \tag{5.4.84}$$

Moreover, for μ_1 we obtain

$$\sqrt{g_s}\,\mu_1 = \frac{1}{8\cdot 3^{\frac{3}{4}}\sqrt{\pi}} z^{-\frac{5}{8}}, \tag{5.4.85}$$

while at two loops we get the result

$$g_s\,\mu_2 = -\frac{37}{64\sqrt{3}} z^{-\frac{5}{4}}. \tag{5.4.86}$$

Altogether, this means that the one–instanton contribution to the double–scaled free energy, up to two–loop order, is

$$F_{\rm ds}^{(1)} = \frac{\mathrm{i}}{8\cdot 3^{\frac{3}{4}}\sqrt{\pi}} z^{-\frac{5}{8}} \exp\left(-\frac{8\sqrt{3}}{5} z^{\frac{5}{4}}\right)\left\{1 - \frac{37}{64\sqrt{3}} z^{-\frac{5}{4}} + \cdots\right\}. \tag{5.4.87}$$

The result for the one–loop coefficient, μ_1, was first obtained by David in [125] and later re–derived in [126]. We have obtained μ_2 directly from an instanton computation in the matrix model, but we may also verify our result by computing the one–loop instanton expansion directly from the Painlevé I equation. This expansion has been studied in detail in [153], where it has been used to analyze the asymptotics of the perturbative answer. The calculation of this expansion goes as follows. As noticed in [152, 118], the discontinuity of the double–scaled free energy (5.4.87) can be computed by linearizing the string equation (5.4.78) around the perturbative, asymptotic solution. If we denote

$$\epsilon(z) = \mathrm{disc}\, u(z), \qquad F_{\mathrm{ds}}^{(1)} = -\epsilon''(z), \tag{5.4.88}$$

one finds the *linear* and *homogeneous* differential equation

$$\epsilon''(z) - 12 u_0(z)\epsilon(z) = 0, \tag{5.4.89}$$

where

$$u_0(z) = z^{\frac{1}{2}}\left(1 - \frac{1}{48}z^{-\frac{5}{2}} - \frac{49}{4608}z^{-5} - \frac{1225}{55296}z^{-\frac{15}{2}} + \cdots\right). \tag{5.4.90}$$

It is easy to solve (5.4.89) at $z \to \infty$ after "peeling off" the exponential piece,

$$\epsilon(z) = c\, z^{-\frac{1}{8}}\, \exp\left(-\frac{8\sqrt{3}}{5}\, z^{\frac{5}{4}}\right)\left(1 + \sum_{k=1}^{\infty} \epsilon_k z^{-\frac{5k}{4}}\right). \tag{5.4.91}$$

The overall coefficient c cannot be deduced from the differential equation (5.4.89) due to its homogeneity, but the ϵ_k can be easily found in terms of the coefficients of the asymptotic expansion of u_0. One finds, for the very first terms,

$$\epsilon(z) = c\, z^{-\frac{1}{8}}\, \exp\left(-\frac{8\sqrt{3}}{5}\, z^{\frac{5}{4}}\right)\left(1 - \frac{5}{64\sqrt{3}}z^{-\frac{5}{4}} + \frac{75}{8192}z^{-\frac{5}{2}} - \frac{341329}{23592960\sqrt{3}}z^{-\frac{15}{4}} + \cdots\right). \tag{5.4.92}$$

Of course, the coefficient c may still be fixed with the explicit result for the one–loop coefficient μ_1. Assembling all together, one finds the *full* perturbative expansion of the free energy around the one–instanton configuration,

$$F_{\mathrm{ds}}^{(1)} = \frac{1}{8\cdot 3^{\frac{3}{4}}\sqrt{\pi}}\, z^{-\frac{5}{8}}\, \exp\left(-\frac{8\sqrt{3}}{5}\, z^{\frac{5}{4}}\right)\left\{1 - \frac{37}{64\sqrt{3}}\, z^{-\frac{5}{4}} + \frac{6433}{24576}z^{-\frac{5}{2}} - \frac{12741169}{23592960\sqrt{3}}z^{-\frac{15}{4}} + \cdots\right\}. \tag{5.4.93}$$

We can now use (5.4.87), together with (5.1.6), in order to obtain a prediction concerning the large–order behavior of the perturbative coefficients of the double–scaled free energy, as

$$a_g \sim \frac{16\sqrt{30}}{125\,\pi^{\frac{3}{2}}}\left(\frac{25}{192}\right)^g \Gamma\left(2g - \frac{5}{2}\right)\left[1 - \frac{37}{80g} - \frac{3927}{12800g^2} - \frac{3618769}{15360000g^3} + \cdots\right]. \tag{5.4.94}$$

Since one can compute these coefficients up to very large order, by using the Painlevé I equation, we can now perform truly precise tests of some of our proposals. In Fig. 5.8 we show numerical checks for both the one and two–loop predictions, up to genus 400. Indeed both leading and subleading asymptotics of the coefficients a_g clearly agree, to a very high degree of precision, with our prediction (5.4.94). This also leads us to an important point. It is sometimes stated in the literature, *e.g.*, [126, 127], that the one–instanton amplitude (5.4.87) cannot be deduced from the Painlevé I equation. The reason for this assertion is simply that the linearized equation (5.4.89) for ϵ does not allow the calculation of μ_1. But it is clear, in view of the connection between large–order behavior and instanton effects, that there is a more subtle relation between the one–instanton amplitude and the perturbative result. In fact, one could instead have derived

this amplitude from the asymptotics of the coefficients a_g, themselves derived from Painlevé I. It is easy to see that from the difference equation (5.4.80) one may obtain

$$a_g \sim \left(\frac{25}{192}\right)^g (2g)!, \tag{5.4.95}$$

a result which at leading order precisely agrees with (5.4.94). A careful study of the difference equation (5.4.80) beyond (5.4.95) [153] confirms indeed the result (5.4.94) for the asymptotics of a_g, and in particular makes possible to extract the one–instanton amplitude directly from large order. In the next chapter, we will come back to the study of the Painlevé equation and show that the formalism of orthogonal polynomials allows one to compute solutions for arbitrary instanton numbers.

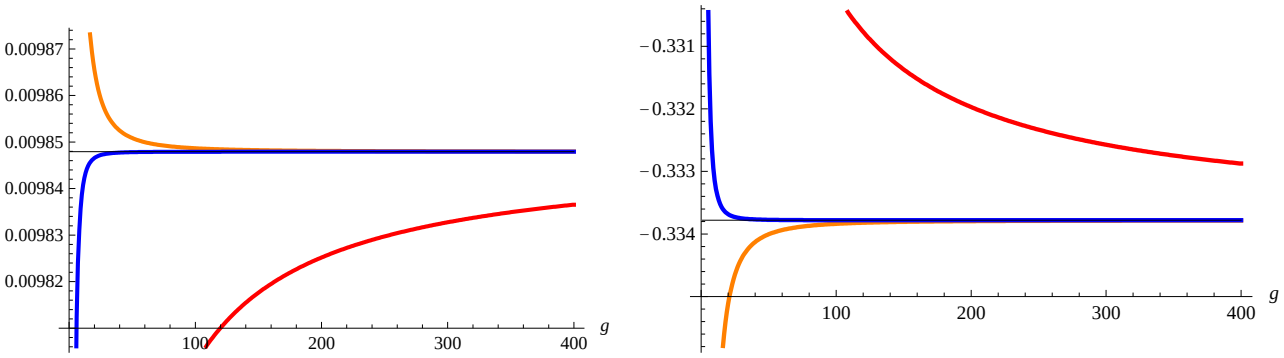

Figure 5.8: The left figure shows the sequence $a_g A^{(2g-5/2)}/\Gamma(2g-5/2)$ for 2d gravity alongside with its Richardson transforms, up to $g = 400$, clearly converging to the one–loop prediction $1/(8 \cdot 3^{3/4}\pi^{3/2}) = 0.009847$. The right figure shows the modified sequence (5.3.51) and its Richardson transforms for a_g, converging towards the two–loop result $-37/(64\sqrt{3}) = -0.33378$, again up to $g = 400$. The error at this genus is of order $10^{-9}\%$.

5.5 Application II: Topological Strings on Local Curves

We now proceed into the realm of topological string theory, beginning with the case of topological strings on local curves. In the previous section we have computed one–instanton effects in one–cut matrix models in terms of data associated to the spectral curve. We can then use the correspondence of [29, 36] to apply our results to topological string theories described by this class of matrix models. The restriction to the one–cut case still leaves a rather general class of CY backgrounds to explore, the so–called local curves. A special limit of the theory of local curves gives the theory of simple Hurwitz numbers studied for example in [151], which will be addressed in the next section.

5.5.1 Topological Strings on Local Curves

Local curves are toric CY manifolds of the form

$$X_p = \mathcal{O}(p-2) \oplus \mathcal{O}(-p) \to \mathbb{P}^1, \quad p \in \mathbb{Z}. \tag{5.5.96}$$

Topological string theory on X_p has received a lot of recent attention (see, *e.g.*, [159] and references therein). As explained in [160], the A–model on X_p has to be defined equivariantly, and the most natural choice (the equivariant CY case) corresponds to the antidiagonal action on the bundle (we refer the reader to [160] for further details). Of more interest to us in the present work is that the free energies at genus g on this geometry, $F_g^{X_p}(t)$, depend on a

single complexified Kähler parameter t, associated to the complexified area of $\mathbb{P}^1$. They can be computed in both the A and B–models.

In the A–model, the total partition function is given by

$$Z_{X_p} = \exp\left(F_{X_p}(g_s,t)\right), \qquad F_{X_p}(g_s,t) = \sum_{g=0}^{+\infty} g_s^{2g-2} F_g^{X_p}(t), \tag{5.5.97}$$

and near $t \to \infty$, $F_g^{X_p}(t)$ has the expansion

$$F_g^{X_p}(t) = \sum_{d=1}^{\infty} N_{g,d}\, \mathrm{e}^{-dt}, \tag{5.5.98}$$

where $N_{g,d}$ are the Gromov–Witten invariants of the CY manifold X_p at genus g and degree d.

The total partition function Z_{X_p} can be computed as a sum over partitions, by making use of the topological vertex formalism as described in [31]. In order to write the explicit resulting formula, we first have to introduce some notation. To begin with, define the q–number $[n]$ as

$$[n] = q^{n/2} - q^{-n/2}, \qquad q = \mathrm{e}^{g_s}. \tag{5.5.99}$$

A representation, R, of $U(\infty)$ is encoded by a Young tableau, labeled by the lengths of its rows $\{l_i\}$. The quantity

$$\ell(R) = \sum_i l_i \tag{5.5.100}$$

is the total number of boxes in the tableau. Another important quantity associated to a given tableau is

$$z_R = \sum_i l_i(l_i - 2i + 1). \tag{5.5.101}$$

We finally introduce the quantity

$$W_R = q^{-z_R/4} \prod_{\square \in R} \frac{1}{[\mathrm{hook}(\square)]}, \tag{5.5.102}$$

with hook($\square$) the hook–length. With all this notation at hand, we may finally write the explicit expression for the topological string partition function on X_p, which is given by

$$Z_{X_p} = \sum_R W_R W_{R^t} q^{(p-1)z_R/2} Q^{\ell(R)}, \quad Q = (-1)^p \mathrm{e}^{-t}, \tag{5.5.103}$$

where R^t denotes the transposed Young tableau (*i.e.*, the tableau where we have exchanged the rows with the columns).

Although (5.5.103) gives an all–genus expression, it is effectively an expansion in powers of Q. In order to obtain an expression for each $F_g^{X_p}(t)$ to all orders in Q, one usually appeals to mirror symmetry and the B–model. However, standard techniques of mirror symmetry do not work well when applied to local curves. The Riemann surface encoding the mirror geometry for local curves was proposed in [29] based on the direct analysis of the sum over partitions presented in [161], and later on some aspects of this mirror construction where confirmed from a more mathematical point of view [162]. The B–model geometry is encoded in the spectral curve

$$y(\lambda) = \frac{2}{\lambda}\left(\tanh^{-1}\left[\frac{\sqrt{(\lambda-a)(\lambda-b)}}{\lambda - \frac{a+b}{2}}\right] - p\tanh^{-1}\left[\frac{\sqrt{(\lambda-a)(\lambda-b)}}{\lambda+\sqrt{ab}}\right]\right), \tag{5.5.104}$$

which has genus zero. Although this curve is not algebraic, it is easy to see that when written in terms of the variables $X = \lambda, Y = \mathrm{e}^y$ one obtains an algebraic equation for the $\mathbb{C}^*$ variables

X, Y, which leads to the mirror CY threefold (5.5.96). The advantage of writing the curve in the nonalgebraic form (5.5.104) is that, as explained in [29, 36], one can apply *verbatim* the standard matrix model technology that we use in this paper. The curve (5.5.104) may also be written in the form (4.1.20), with a moment function $M(\lambda)$ which has various nontrivial zeroes where the spectral curve is singular. The endpoints of the cut, a and b, are given by

$$a = (1-\zeta)^{-p}(1-\zeta^{\frac{1}{2}})^2, \quad b = (1-\zeta)^{-p}(1+\zeta^{\frac{1}{2}})^2, \tag{5.5.105}$$

where ζ is related to Q by the mirror map [161, 162]

$$Q = (1-\zeta)^{-p(p-2)}\zeta. \tag{5.5.106}$$

It was further conjectured in [29] that the free energies $F_g^{X_p}(t)$ can be obtained as the standard genus g free energies of a matrix model with spectral curve (5.5.104). And it was conjectured in [161] that, for $g \geq 2$, these free energies may be written as

$$F_g^{X_p}(t) = \frac{\mathcal{P}_g(\zeta, p)}{(\zeta - \zeta_c)^{5(g-1)}}, \quad \mathcal{P}_g(\zeta, p) = \sum_{i=1}^{5(g-1)} a_{g,i}(p)\, \zeta^i, \tag{5.5.107}$$

where

$$\zeta_c = \frac{1}{(p-1)^2} \tag{5.5.108}$$

is a critical point of the model. In fact, at this point, a zero x_0 of $M(\lambda)$ collides with the endpoint of the cut b, and we are left with a critical theory in the universality class of pure 2d gravity [161]. If one further takes the double–scaling limit,

$$\zeta \to \zeta_c, \quad g_s \to 0, \quad z \text{ fixed}, \tag{5.5.109}$$

where

$$z^{5/2} = g_s^{-2} \frac{(p-1)^8}{4(1-\zeta_c)^3}(\zeta_c - \zeta)^5, \tag{5.5.110}$$

then the total free energy (5.5.97) becomes the free energy of pure 2d gravity.

5.5.2 Instanton Effects and Large–Order Behavior

In [29] the matrix model description, based on the spectral curve (5.5.104), was used to study nonperturbative effects in this topological string theory. The spectral curve (5.5.104) has a nontrivial saddle x_0, which is the solution to

$$M(x_0) = 0. \tag{5.5.111}$$

For the cases $p = 3$ and $p = 4$ the relevant solutions have been determined in [34]; they are given by

$$x_0 = \frac{4ab}{(\sqrt{a} - \sqrt{b})^2}, \qquad p = 3, \tag{5.5.112}$$

and

$$x_0 = \frac{2\sqrt{a}b}{\sqrt{a} - \sqrt{b}}, \qquad p = 4. \tag{5.5.113}$$

In [34] it was argued that this saddle controls the large–order behavior of $F_g^{X_p}(t)$, at any value of t. We now show that this is indeed the case, and that the one and two–loop results $\mu_{1,2}$ computed in terms of the spectral curve (5.5.104) control the subleading large g asymptotics.

The instanton action for an eigenvalue tunneling from b to x_0 has already been computed in [34]; it is given by the rather formidable expression

$$A(Q) = F(x_0) - F(a), \tag{5.5.114}$$

where

$$\begin{aligned} F(x) = &- \log\left(f_1(x)\right)\Big(\log\left(f_1(x)\right) - 2\log\Big(1 + \frac{2f_1(x)}{(\sqrt{a}-\sqrt{b})^2}\Big) + \log\Big(1 + \frac{2f_1(x)}{(\sqrt{a}+\sqrt{b})^2}\Big)\Big) - \\ &- 2\mathrm{Li}_2\Big(-\frac{2f_1(x)}{(\sqrt{a}-\sqrt{b})^2}\Big) - 2\mathrm{Li}_2\Big(-\frac{2f_1(x)}{(\sqrt{a}+\sqrt{b})^2}\Big) - \log\frac{(a-b)^2}{4}\log\, x - \\ &- p\log\left(f_2(x)\right)\Big(\log\left(f_2(x)\right) + 2\log\Big(1 - \frac{f_2(x)}{2\sqrt{ab}}\Big) - \log\Big(1 - \frac{2f_2(x)}{(\sqrt{a}+\sqrt{b})^2}\Big)\Big) - \\ &- 2p\mathrm{Li}_2\Big(-\frac{f_2(x)}{2\sqrt{ab}}\Big) + 2p\mathrm{Li}_2\Big(\frac{2f_2(x)}{(\sqrt{a}+\sqrt{b})^2}\Big) + \frac{p}{2}(\log x)^2 + p\log(\sqrt{a}+\sqrt{b})^2\log\, x, \end{aligned} \tag{5.5.115}$$

and

$$\begin{aligned} f_1(x) &= \sqrt{(x-a)(x-b)} + x - \frac{a+b}{2}, \\ f_2(x) &= \sqrt{(x-a)(x-b)} + x + \sqrt{ab}. \end{aligned} \tag{5.5.116}$$

In these expressions a and b are the endpoints of the cut as usual, given in (5.5.105).

The one and two–loop coefficients are again given by the general expressions (5.2.43) and (5.2.45), as in the previous section. We now compare the analytic results to the large–order behavior of the perturbation series for the case of the local curve X_3 ($p = 3$). The leading and subleading asymptotic behavior of F_g should be given by the same structure found for the quartic matrix model (5.4.69). As explained in section 5.3, we can independently test the predictions for the instanton action, as well as the one and the two–loop results, by applying Richardson transformations to the modified sequences (5.3.48)–(5.3.51). Notice that all these quantities depend on the B–model modulus ζ. For simplicity, we restrict our analysis to the range $0 < \zeta < \zeta_c = \frac{1}{4}$, where the endpoints of the cut, as well as the instanton action, are real. Fig. 5.9 shows the inverse square root of the sequence Q_g in (5.3.48) and its first three Richardson transforms, at two specific values of ζ. The straight line is the prediction for the instanton action, A. As is evident from the plot, and even though we only use data up to genus $g = 8$, the third Richardson transform already falls on the straight line. The mismatch between numerical extrapolation and the prediction is of order 0.02%. Analogously, we may check the one and two–loop results. In Fig. 5.10 and Fig. 5.11 we plot the modified sequences, (5.3.50) and (5.3.51), together with the corresponding Richardson transforms, again at two fixed values of the Kähler modulus. As explained in section 5.3, the predictions for their leading asymptotics are μ_1, respectively μ_2, which are shown in the figures as straight lines. Again, this is confirmed by the Richardson transforms, clearly converging to the prediction from instanton calculus. The error in here is of order 1%.

Similar graphs can be produced at any other point in moduli space. Fig. 5.12 shows the asymptotic value of the instanton action, as approximated by the third Richardson transform, divided by the corresponding analytical prediction, and plotted as a function of the modulus over $0 < \zeta < 1/4$. This quotient is indeed very close to one, as it should be from our discussion. Similarly, in Fig. 5.13 we plot the asymptotic results for μ_1 and μ_2, divided by the corresponding analytic predictions, as functions of ζ. Notice that while the agreement is excellent over most of moduli space, as one approaches $\zeta \sim 0$ the deviation from the predicted value increases. This is again due to the divergence of the instanton action at this particular point of moduli space. Indeed in this region, the Richardson transforms converge too slowly to fall on one line, at low genus $g < 10$. In order to obtain full agreement one would need higher–genus data, which is out of our scope in this paper.

We have performed similar checks of our predictions for the local curve X_4, also obtaining agreement to very high precision, and further strengthening our analytical results.

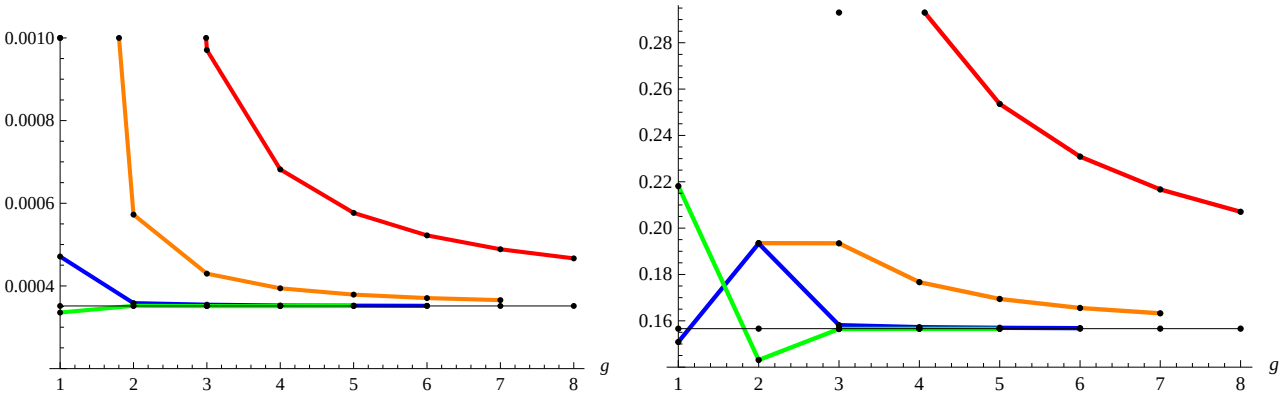

Figure 5.9: The sequence $\sqrt{1/Q_g}$ and the corresponding Richardson transforms for the local curve X_3, at fixed values $\zeta = 0.24$ (left) and $\zeta = 0.15$ (right). The leading asymptotics are predicted to be given by the instanton action $A(\zeta)$, shown as a straight line. The error for the available degree $g = 8$ is 0.014% at $\zeta = 0.24$, respectively 0.025% at $\zeta = 0.15$.

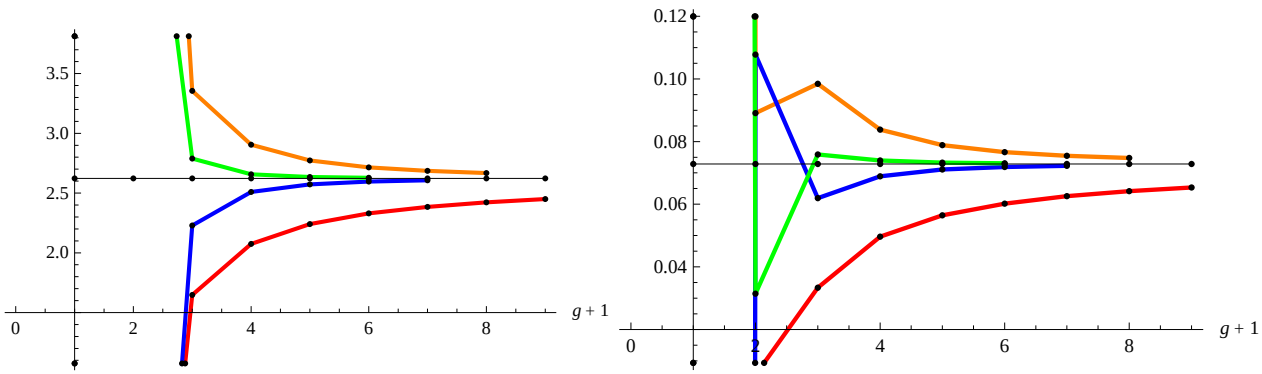

Figure 5.10: The sequence $\pi F_g A^{2g-\frac{5}{2}}/\Gamma(2g-\frac{5}{2})$ and its Richardson transforms for the local curve X_3, at fixed values $\zeta = 0.24$ (left) and $\zeta = 0.15$ (right). The prediction for the asymptotic value is the one–loop result μ_1, shown as a straight line. The error is 0.49% at $\zeta = 0.24$, respectively 0.58% at $\zeta = 0.15$.

5.5.3 Spacetime Interpretation of the Instanton Effects

As we have seen in (5.2.39), the instanton action can be computed as a contour integral from the endpoint of the cut to the saddle x_0. This contour integral measures the potential difference between the cut $\mathcal{C}$ and x_0. When the spectral curve corresponds to a double–scaled matrix model, this instanton action should correspond to the disk amplitude for a D–instanton in noncritical string theory. These D–instanton configurations have been identified in terms of ZZ branes, and it has also been verified that indeed the matrix model computation agrees with the disk amplitude for a ZZ brane [51]. Equivalently, the ZZ disk amplitude can be calculated as the difference between the disk amplitudes for two FZZT branes located, respectively, at the branch cut of the curve and at the pinched point of the curve. It turns out that, for topological string theory on local curves, there is a similar interpretation of the instanton action in terms of D–branes, as well as a spacetime interpretation in terms of domain walls.

The natural branes for the A–model on a toric CY manifold are the Harvey–Lawson branes, first studied in this context in [163]. The mirrors of these branes are just points in the spectral

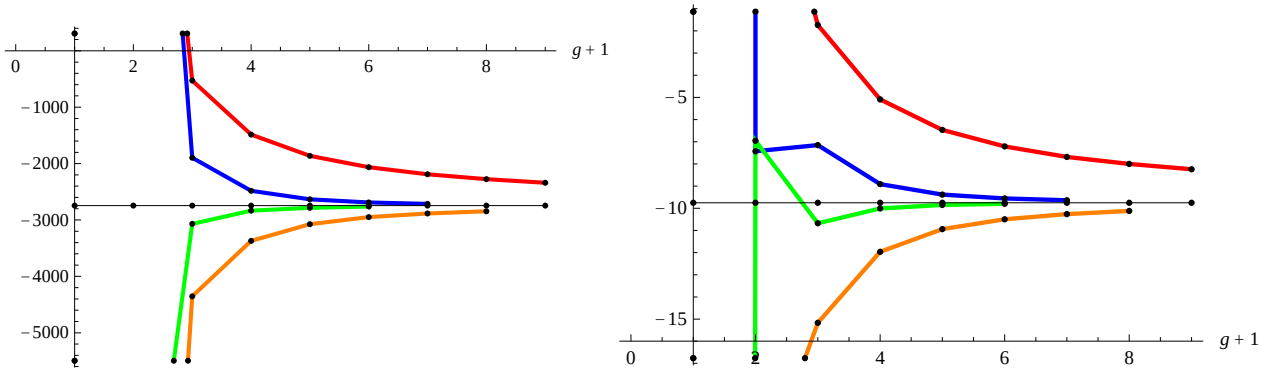

Figure 5.11: The sequence (5.3.51) for the local curve X_3 and its Richardson transforms, at $\zeta = 0.24$ (left) and $\zeta = 0.15$ (right), with leading asymptotics predicted to be given by the two–loop result μ_2. The error is 1.38% at $\zeta = 0.24$, respectively 1.04% at $\zeta = 0.15$.

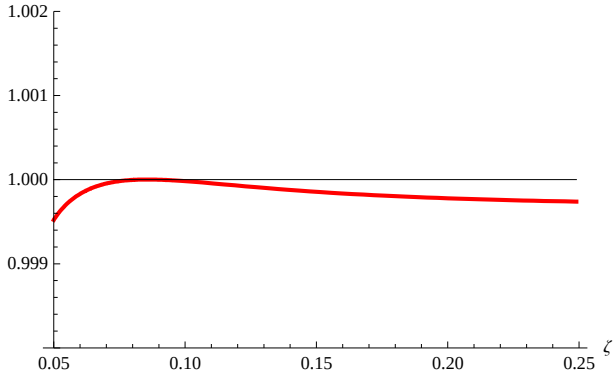

Figure 5.12: The asymptotic value of $\sqrt{1/Q_g}$ for the local curve X_3 as extracted from the third Richardson transform as a function of ζ, divided by the analytic prediction for the instanton action. For $\zeta > 0.05$, the error is always less than 0.03%.

curve of the B–model. Two branes located at points z_0 and z_1 define an interpolating domain wall in the underlying type II theory. The tension of this domain wall is given by the difference of D–brane superpotentials [163]

$$W(z_1) - W(z_0) = \int_{z_0}^{z_1} \mathrm{d}z\, y(z). \tag{5.5.117}$$

When z_0 and z_1 correspond, respectively, to the endpoint of the cut and the saddle x_0, (5.5.117) is exactly the instanton action computed in (5.2.39). The connection between instanton actions in the matrix model and tensions of domain walls was already made in [32] for the backgrounds considered therein. At the same time, (5.5.117) can be regarded as the difference between two disk amplitudes for D–branes located at z_1 and z_0. We then see that the role of FZZT branes in noncritical string theory is played by the Harvey–Lawson branes in topological string theory on local CY threefolds. Indeed, it can be easily seen [34] that, in the case of local curves, the toric branes become FZZT branes near the critical point describing 2d gravity. On the other hand, the saddle x_0 that we have been considering (and which leads to an extremum of the superpotential) gives a topological string analogue of the ZZ brane.

A more invariant way of writing (5.5.117), by taking into account the full six–dimensional geometry of the CY, is

$$A = \int_\Gamma \Omega, \qquad \Gamma = [C_1 - C_0], \tag{5.5.118}$$

where Ω is the holomorphic $(3,0)$ form on the CY, and Γ is a three–cycle interpolating between

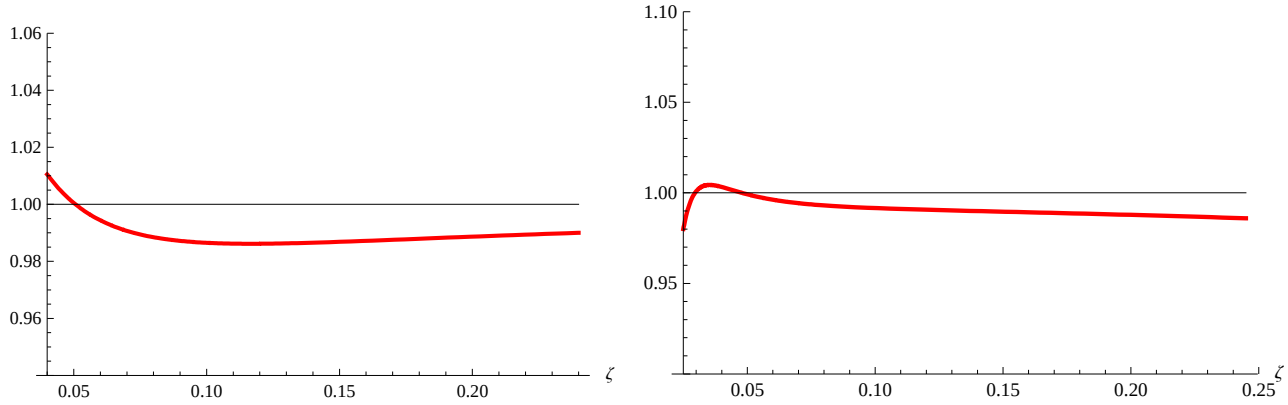

Figure 5.13: The left figure shows μ_1 for the local curve as extracted from the perturbative series using the third Richardson transform of the sequence (5.3.50), divided by the corresponding analytical prediction, and plotted over the range $0 < \zeta < 1/4$. Similarly, the second figure shows the asymptotic result for μ_2 as obtained from the perturbative series using (5.3.51), again divided by the corresponding analytic prediction. The typical error is about 1.5%.

the two–cycles $C_{0,1}$ associated to $z_{0,1}$ in the full geometry. This is indeed the general form for disk amplitudes of B–branes presented in [164].

It is interesting to notice that usually the nonperturbative effects due to B–branes considered in the literature involve the hypermultiplet moduli, since a B–brane supported on a curve will couple to the Kähler form, and not to Ω [28, 49]. This type of D–instanton effects (which in some cases can be computed exactly [165]) cannot however be related to the large–order behavior of the topological string amplitudes, which depend on the vector multiplet moduli. On the other hand, domain walls interpolating between two B–branes *can* couple to Ω and therefore have the right structure to control the large–order behavior of topological string perturbation theory. In this paper we have checked this for a restricted class of toric geometries, but we expect this fact to be true in the more general case, for an appropriate choice of the domain wall.

5.6 Application III: Hurwitz Theory

We finally proceed to our last example, Hurwitz theory.

5.6.1 Hurwitz Theory

Hurwitz theory studies branched covers of Riemann surfaces. Here, we restrict ourselves to the coverings of a sphere $\mathbb{P}^1$ (the "target") by surfaces of genus g (the "worldsheets"). The covering maps will be restricted to have only simple branch points. The number of disconnected coverings of degree d with these topological characteristics is counted by the so–called simple Hurwitz number, which we denote by $H^{\mathbb{P}^1}_{g,d}(1^d)$. It can be computed, in classical Hurwitz theory, in terms of representation theory of the symmetric group:

$$H^{\mathbb{P}^1}_{g,d}(1^d) = \sum_{\ell(R)=d} \left(\frac{d_R}{\ell(R)!}\right)^2 (z_R/2)^{2g-2+2d}. \tag{5.6.119}$$

Here the sum is over Young tableaux R, with a fixed number of boxes $\ell(R)$ equal to the degree d, and d_R is the dimension of R regarded as a representation of the symmetric group S_d. The quantity z_R was defined in (5.5.101).

We can now define the total partition function of Hurwitz theory as a generating functional

for simple Hurwitz numbers,

$$Z^{\mathrm{H}}(t_H, g_H) = \sum_{g\geq 0} g_H^{2g-2} \sum_{d\geq 0} \frac{H^{\mathbb{P}^1}_{g,d}(1^d)}{(2g-2+2d)!} Q^d, \tag{5.6.120}$$

where $Q = \mathrm{e}^{-t_H}$ and g_H can be regarded as formal parameters keeping track of the degree and the genus, respectively. This partition function can be written as

$$Z^{\mathrm{H}}(t_H, g_H) = \sum_R \left(\frac{d_R}{|\ell(R)|!} \right)^2 g_H^{-2\ell(R)} \mathrm{e}^{g_H z_R/2} Q^{\ell(R)}. \tag{5.6.121}$$

The free energy $\log Z^{\mathrm{H}}$ describes *connected*, simple Hurwitz numbers $H^{\mathbb{P}^1}_{g,d}(1^d)^\bullet$,

$$F^{\mathrm{H}} = \log Z^{\mathrm{H}} = \sum_{g\geq 0} g_H^{2g-2} \sum_{d\geq 0} \frac{H^{\mathbb{P}^1}_{g,d}(1^d)^\bullet}{(2g-2+2d)!} Q^d, \tag{5.6.122}$$

and it has the genus expansion

$$F^{\mathrm{H}}(g_H, t_H) = \sum_{g=0}^{\infty} g_H^{2g-2} F^{\mathrm{H}}_g(Q_H). \tag{5.6.123}$$

This theory is in fact a topological string theory in disguise. It can be realized as a special limit of the type–A theory on local curves X_p with Kähler parameter t that we studied in the previous section [161], namely the limit

$$p \to \infty, \qquad t \to \infty, \qquad g_s \to 0, \tag{5.6.124}$$

while the new parameters g_H and t_H, which are defined by

$$g_H = p g_s, \qquad \mathrm{e}^{-t_H} = (-1)^p p^2 \mathrm{e}^{-t}, \tag{5.6.125}$$

are kept fixed. As in the case of the theory on local curves, there is a B–model mirror to this theory. Its natural coordinate χ is related to the A–model coordinate $Q = \mathrm{e}^{-t_H}$ by the mirror map

$$\chi \mathrm{e}^{-\chi} = Q, \tag{5.6.126}$$

which can indeed be understood as an appropriate limit of (5.5.106) for $p \to \infty$ [161]. The inverse mirror map is provided by Lambert's W function [166],

$$\chi = -W(-Q) = \sum_{k=1}^{\infty} \frac{k^{k-1}}{k!} Q^k, \tag{5.6.127}$$

which has convergence radius $Q_c = \mathrm{e}^{-1}$ or $\chi = 1$. The large–radius region corresponds to $Q \to 0$ (and also to $\chi \to 0$). The spectral curve characterizing the B–model is of the form

$$y(h) = 2 \tanh^{-1} \left[2 \frac{\sqrt{(a-h)(b-h)}}{2h-(a+b)} \right] - \sqrt{(a-h)(b-h)}, \tag{5.6.128}$$

where the endpoints of the cut are given by

$$b = \left(1 + \chi^{\frac{1}{2}}\right)^2, \quad a = \left(1 - \chi^{\frac{1}{2}}\right)^2. \tag{5.6.129}$$

The above spectral curve can also be read from the saddle–point description of the sum over partitions (5.6.121) given in [167, 151].

Hurwitz theory has been extensively studied in the mathematical literature, and these studies have unveiled interesting properties. As shown in [168], the higher–genus free energies $F_g^{\rm H}(Q)$, when expressed in terms of the mirror coordinate χ, have a very simple structure, namely

$$\begin{aligned} F_0^{\rm H}(\chi) &= \frac{\chi^3}{6} - \frac{3\chi^2}{4} + \chi, \\ F_1^{\rm H}(\chi) &= -\frac{1}{24}\Big(\log(1-\chi) + \chi\Big), \\ F_g^{\rm H}(\chi) &= \frac{P_g(\chi)}{(1-\chi)^{5(g-1)}}, \quad P_g(\chi) = \sum_{i=2}^{3g-3} c_{g,i}\,\chi^i, \quad g \geq 2. \end{aligned} \tag{5.6.130}$$

Moreover, the polynomials $P_g(\chi)$ have the property

$$P_g(1) = 4^{g-1} a_g, \quad g \geq 2, \tag{5.6.131}$$

where a_g is the genus g free energy of 2d gravity appearing in (5.4.81). Therefore, in the double–scaling limit

$$\chi \to 1, \qquad g_H \to 0, \qquad g_H^{-2}(1-\chi)^5 = 4z^{\frac{5}{2}}, \tag{5.6.132}$$

the total free energy of Hurwitz theory becomes (5.4.81)

$$F^{\rm H}(g_H, t_H) \to F_{\rm ds}(z), \tag{5.6.133}$$

and one recovers 2d gravity at the critical point. This was first pointed out at genus zero in [151] and then established at all genera in [161], using the results of [168].

Another interesting result concerning Hurwitz theory was obtained in [169], where the total free energy was shown to satisfy the Toda equation,

$$\exp\big(F^{\rm H}(g_H, t_H + g_H) + F^{\rm H}(g_H, t_H - g_H) - 2F^{\rm H}(g_H, t_H)\big) = g_H^2 \mathrm{e}^t \partial_{t_H}^2 F^{\rm H}(g_H, t_H). \tag{5.6.134}$$

This equation is the analogue for this model of the pre–string equation (5.4.58) for the quartic matrix model. One can directly derive from (5.6.134) that the double–scaled specific heat satisfies the Painlevé I equation (5.4.78), providing in this way yet another derivation of the result in [161]. We have used the Toda equation to compute Hurwitz amplitudes up to genus 16, and some of these results are presented in appendix B.2.2.

5.6.2 Instanton Effects and Large–Order Behavior

Let us now turn to the computation of the one–instanton quantities. From the curve (5.6.128) we find the moment function,

$$M(h) = \frac{2}{\sqrt{(a-h)(b-h)}} \tanh^{-1}\left[2\frac{\sqrt{(a-h)(b-h)}}{2h-(a+b)}\right] - 1, \tag{5.6.135}$$

where the nontrivial saddle–point is defined by

$$M(h_0) = 0, \tag{5.6.136}$$

or

$$\frac{2}{\sqrt{(a-h_0)(b-h_0)}} \tanh^{-1}\left[2\frac{\sqrt{(a-h_0)(b-h_0)}}{2h_0-(a+b)}\right] = 1. \tag{5.6.137}$$

This equation can be written in a simpler way by defining w as

$$h_0 = 4\sqrt{\chi}\cosh^2\Big(\frac{w}{2}\Big) + (1-\sqrt{\chi})^2. \tag{5.6.138}$$

In terms of these variables, equation (5.6.137) simply reads

$$\frac{w}{\sinh(w)} = \sqrt{\chi}. \tag{5.6.139}$$

Even though we cannot solve analytically for $h_0(\chi)$, we can solve (5.6.137) to find $h_0(\chi)$ near $\chi = 0, 1$ as a power series. Near the critical point $\chi = 1$, it is easy to see that $h_0(\chi)$ has a Taylor series expansions in powers of $\xi = 1 - \chi$

$$h_0(\chi) = 4 + \xi + \frac{4}{5}\xi^2 + \cdots . \tag{5.6.140}$$

Near $\chi = 0$, the power series solution is more complicated. At leading order it is easy to find that

$$w \sim -\frac{1}{2}\log(\chi) + \log(-\log(\chi)), \tag{5.6.141}$$

which yields

$$h_0(\chi) \sim -\log\,\chi + 2\log(-\log\,\chi), \qquad \chi \to 0. \tag{5.6.142}$$

The corrections to the leading asymptotics (5.6.141) can be obtained following a method exposed, for example, in [170]. The full solution can be written as

$$w = \log(-\log(\frac{\sqrt{\chi}}{2})) - \frac{1}{2}\log(\chi) + v, \tag{5.6.143}$$

where v is a power series

$$v = \sum_{j,k,m} c_{jkm}\mu^j\sigma^k\tau^m \tag{5.6.144}$$

in the variables

$$\sigma = \frac{1}{\log(\chi)}, \qquad \tau = \frac{\log(-\log(\chi))}{\log(\chi)}, \qquad \mu = \left(\frac{\chi}{\log(\chi)}\right)^2. \tag{5.6.145}$$

The coefficients c_{jkm} can be explicitly written as

$$\begin{aligned} c_{jkm} = &-\oint \frac{\mathrm{d}z}{2\pi\mathrm{i}} \frac{\mathrm{e}^{(j-1)z} z^{k+1} (-1)^m}{(\mathrm{e}^{-z}-1)^{j+k+m+1}} \frac{(j+k+m)!}{j!k!m!} + \\ &+ \oint \frac{\mathrm{d}z}{2\pi\mathrm{i}} \frac{\mathrm{e}^{jz} z^k (-1)^m}{(\mathrm{e}^{-z}-1)^{j+k+m}} \frac{(j+k+m-1)!}{j!(k-1)!m!}. \end{aligned} \tag{5.6.146}$$

The instanton action

$$A(\chi) = \int_b^{h_0(\chi)} \mathrm{d}h\, y(h) \tag{5.6.147}$$

can now be computed explicitly as a function of h_0 as

$$A(\chi) = (b-a)\left(\gamma\cosh^{-1}(\gamma) - \sqrt{\gamma^2-1}\right) - \frac{(a-b)^2}{8}\left(\gamma\sqrt{\gamma^2-1} - \cosh^{-1}(\gamma)\right), \tag{5.6.148}$$

where

$$\gamma = \frac{1}{b-a}(2h_0(\chi) - a - b). \tag{5.6.149}$$

Using the above results for the behavior of h_0 near $\chi = 0, 1$, we can also find the behavior of the instanton action near these points. At the critical point, one finds

$$\frac{1}{g_H}A(\chi) \to \frac{8\sqrt{3}}{5}z^{5/4} + \cdots, \quad \chi \to 1, \tag{5.6.150}$$

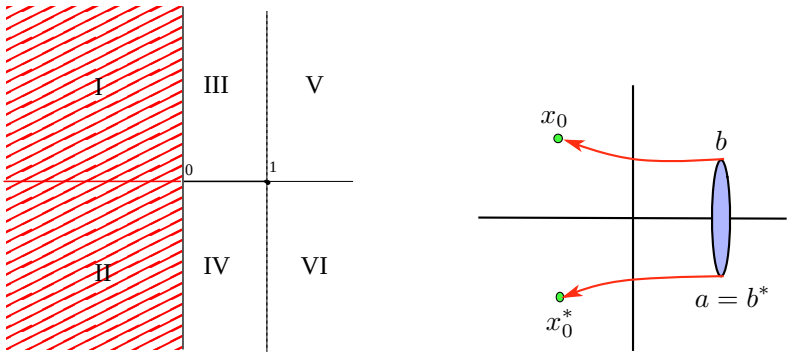

Figure 5.14: The moduli space of Hurwitz theory.

where z is the double–scaled variable introduced in (5.6.132). Of course, this is the expected universal, double–scaled result of (5.4.84). Near $\chi = 0$, we find

$$A(\chi) \sim \frac{1}{2}(\log \chi)^2, \quad \chi \to 0. \tag{5.6.151}$$

We may now compare our predictions with the numerical asymptotics of F_g. The moduli space of χ can be divided into the six segments shown in Fig. 5.14, and we have tested our predictions in each of them. They have the following characteristics:

- The simplest case to study is the real interval $0 < \chi < 1$. Here, there is one single instanton with real action, corresponding to an eigenvalue tunneling from b to the saddle x_0 on the right of the cut, and all F_g are also real.

- As χ moves to the right of $[0, 1]$, beyond the critical point at $\chi = 1$, the only solutions to $M(h) = 0$ are located inside the cut and the instanton action becomes purely imaginary while $\mu_{1,2}$ remain real. The F_g oscillate in sign.

- It turns out that there is no systematic difference between the regions I–VI away from the real axis. The instanton action as well as $\mu_{1,2}$ and of course F_g are generically complex, in spite of which our predictions continue to hold.

- When χ lies on the negative real line, the endpoints of the cut move away from the real axis and become complex conjugate. There are now two saddle–point solutions, x_0 and x_0^*, complex conjugate to each other, and accordingly *two* instanton solutions with conjugate actions, one corresponding to an eigenvalue tunneling from b to x_0 and another from $a = b^*$ to x_0^*, as shown in Fig. 5.14. Therefore the F_g are real, with asymptotics of the form (5.1.10) involving a cosine. Notice that this is very similar to a mechanism for the local curve, first observed in [34].

As before, the one and two–loop coefficients are given by (5.2.43) and (5.2.45), evaluated for the moment function (5.6.135). The saddle–point solution has to be evaluated numerically. The instanton action, as well as μ_1 and μ_2, are well–defined over the whole complex plane of the modulus χ. Fig. 5.15 and Fig. 5.16 show the inverse square root of the sequence Q_g in (5.3.48) and of the corresponding Richardson transforms, alongside with the prediction of instanton calculus for the instanton action, at values of the modulus $\chi = 0.5$, $\chi = 1.5 + \mathrm{i}$, and $\chi = -1 - 0.5\mathrm{i}$. In Fig. 5.17 we compare the sequence $\pi F_g |A|^{2g-5/2}/(\Gamma(2g - \frac{5}{2})|\mu_1|)$ for Hurwitz theory, together with the prediction $2\cos\left(\left(2g - \frac{5}{2}\right)\theta_A + \theta_{\mu_1}\right)$, at $\chi = -0.5$ and $\chi = -3$. Fig. 5.18 and Fig. 5.19 show the modified sequences, (5.3.50) and (5.3.51), with leading asymptotics given by the one and two–loop fluctuations around the one–instanton configuration, together with the analytic prediction. Indeed, the agreement is again quite spectacular.

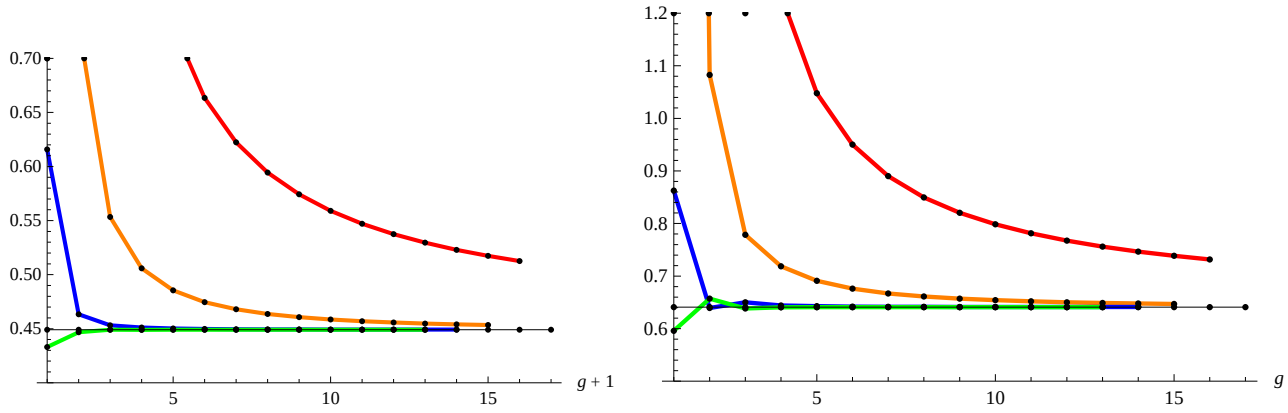

Figure 5.15: The left figure shows the sequence $(\mathrm{Re}(Q_g^{-1}))^{1/2}$ for Hurwitz theory, together with its Richardson transforms. The straight line shows the corresponding prediction $(\mathrm{Re}(A^2))^{1/2}$, at $\chi = 0.5$. On the right, the same for $\chi = 1.5 + \mathrm{i}$. The available degree is $g = 16$, the error is $4 \times 10^{-6}\%$ at $\chi = 0.5$, and $7 \times 10^{-6}\%$ at $\chi = 1.5 + \mathrm{i}$.

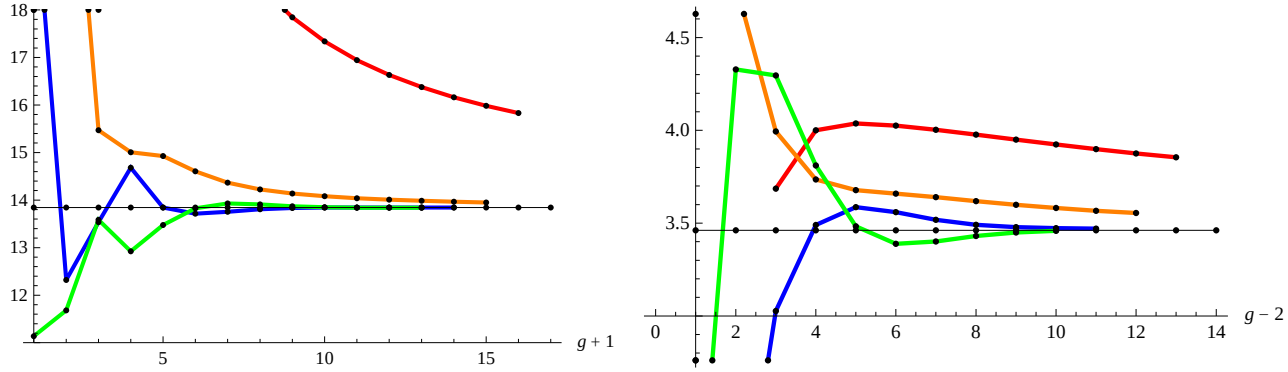

Figure 5.16: On the left, the sequences $(\mathrm{Re}(Q_g^{-1}))^{1/2}$ with its Richardson transforms and the prediction $(\mathrm{Re}(A^2))^{1/2}$, at $\chi = -1 - 0.5\mathrm{i}$ (straight line). On the right, we show the same for the imaginary parts. The errors at $g = 16$ are 0.01% and 0.08%, respectively.

Conclusion

In this chapter we have extended classical results on the connection between instanton effects and the large–order behavior of perturbation theory to general, one–cut matrix models and topological strings. We have tested our one–instanton computation up to two loops in both the standard quartic matrix model off–criticality and in its double–scaled limit, 2d gravity. If correct, the matrix model description of the topological string on toric backgrounds [34, 35] implies that our computation also applies to nonperturbative effects in topological string theory. This is indeed the case, as we have verified testing our predictions with the large–order behavior of the perturbative amplitudes. This is a strong check of the proposal of [34, 35], as the asymptotics of the amplitudes capture information beyond perturbation theory.

From the mathematical point of view, we have presented precise conjectures for the large–order behavior of Hurwitz theory and 2d gravity.

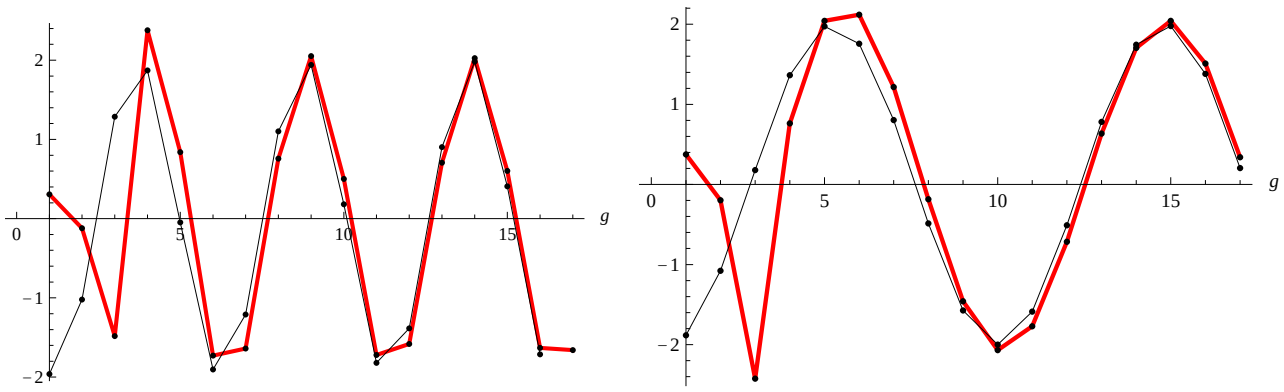

Figure 5.17: The sequence $\pi F_g |A|^{2g-5/2}/(\Gamma(2g-\frac{5}{2})|\mu_1|)$ for Hurwitz theory, together with the prediction $2\cos\left(\left(2g-\frac{5}{2}\right)\theta_A+\theta_{\mu_1}\right)$, at $\chi=-0.5$ (left) and $\chi=-3$ (right). The error at genus 16 is of order 3%.

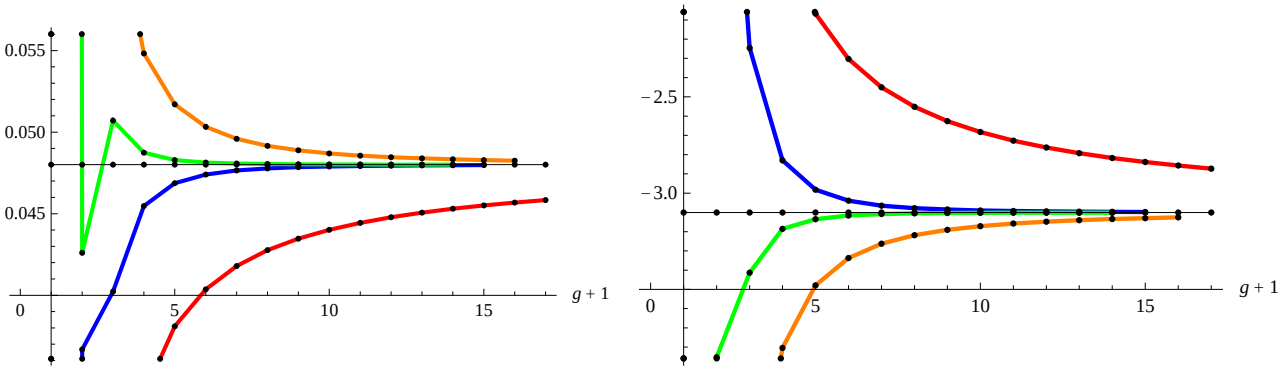

Figure 5.18: The left figure shows $\pi A^{2g-\frac{5}{2}} F_g/\Gamma(2g-\frac{5}{2})$ for Hurwitz theory, and its Richardson transforms, at $\chi=0.5$. The leading asymptotics are predicted by μ_1, shown as a straight line. On the right, we plot the analogous sequence (5.3.51), together with the expected leading asymptotic value μ_2 (straight line). The error at $g=16$ is 0.009% for μ_1, and 0.012% for μ_2.

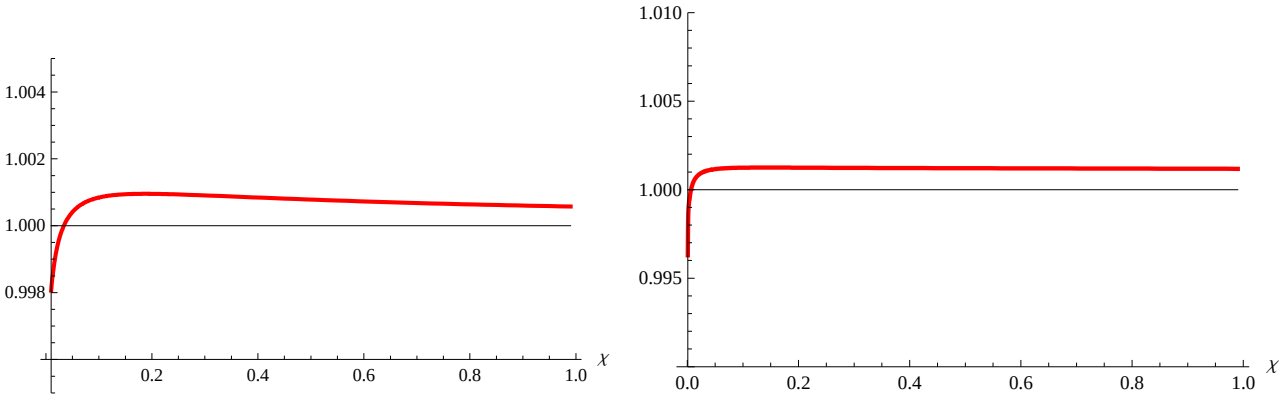

Figure 5.19: The left figure shows μ_1 as a function of χ for Hurwitz theory, as extracted from the perturbative series using the third Richardson transform of the sequence (5.3.50), divided by the corresponding analytical prediction. Similarly, the second figure shows the asymptotic result for μ_2 as obtained from the perturbative series using (5.3.51), again divided by the corresponding analytic prediction. For $\chi>0.01$, the error is of order 0.1%.

Chapter 6

Multi-Instantons and Multi-Cuts

In the last chapter, we have assumed that the eigenvalues are distributed over a single interval $\mathcal{C}$ around a minimum of the potential. However, this is a very special configuration, as the potential may have many extrema and eigenvalues around each of them, i.e. a multi-cut configuration. In this chapter, we will see that this can also be interpreted as a multi-instanton configuration, where many eigenvalues have been moved to the next extremum via instanton transitions. The presented results will appear in a publication with M. Mariño and R. Schiappa [72].

For an n-cut solution, the spectral curve has genus $n-1$. Indeed, the pinched spectral curve that we considered in the one-cut case with one instanton is precisely at the transition point between a one-cut and a two-cut solution, as can also be seen from figures 6.1, 6.2 for a more general potential. Configurations with different filling numbers of the intervals around the extrema of the potential are related by instanton and anti-instanton transitions. Since not only minima, but also maxima of the potential can accommodate eigenvalues, instantons and anti-instantons act with opposite signs, depending on whether the transition moves an eigenvalue from a minimum to a maximum and thus a more stable to a less stable configuration, or the reverse. Hence, there are exponentially suppressed transitions that we refer to as instantons, and exponentially *enhanced* anti-instanton transitions. The full partition sum can always be written down as an infinite Laurent expansion over instanton sectors with respect to a reference configuration, and it can be resummed as a theta function [171, 172]. The choice of the reference configuration is *irrelevant*, as the partition sum does not depend on it [171]. This is related to the problem of quantum background independence in string theory and the holomorphic anomaly equation [173].

For concrete applications, we avoid the subtleties related to enhanced anti-instanton transitions by picking as a reference configuration the most stable one, where all eigenvalues are centered around the absolute minimum of the potential, i.e. a one-cut solution. The general partition function is then a sum over possible filling numbers of this minimum and its neighbouring maximum, that is, two-cut solutions which can equivalently be viewed as multi-instanton configurations with respect to the reference one-cut configuration. The resulting expressions have to be carefully regularized, since the $\frac{1}{N}$ expansion becomes singular as the numbers of eigenvalues in the second cut becomes small compared to N. We obtain in this way explicit, regular results for multi-instanton amplitudes of the one-cut model in terms of the free energies of the two-cut model.

We put these expressions through a number of highly nontrivial tests. They are shown to reproduce the one-instanton formulae that we found in the previous chapter following an entirely different approach. Furthermore, we compute the one- and two instanton amplitudes for the cubic matrix model up to two loops independently using a transseries formalism devised in [174] based on orthogonal polynomials, finding perfect agreement with our general formula. We perform two further checks of the multi-instanton formula in the double-scaling limit at

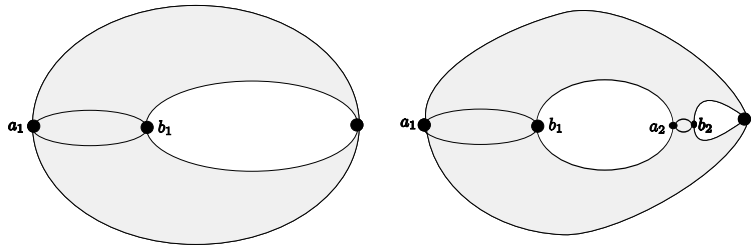

Figure 6.1: Spectral curves corresponding to one-cut respectively two-cut solutions

the critical point, where the cubic matrix model describes two-dimensional gravity. As we have seen in the previous chapter and in the introduction to matrix models in chapter 4, this regime is controlled by the Painlevé I equation. Again using the transseries formalism, this equation can be solved recursively for arbitrary loops and instanton sectors, and we check up to high instanton numbers that the double-scaling limit of the multi-instanton expressions that our master formula yields for the cubic matrix model off criticality reproduces this solution. Based on the connection to multicut models, we conjecture a nontrivial integrality structure of solutions to the Painlevé I equation, namely, the partition sum at fixed order in the coupling constant should be a *polynomial* rather than rational function of the instanton expansion parameter. This is indeed confirmed by the expressions we find.

This chapter is organized as follows. We start with a general review of multicut models in section 6.1, where we also derive some explicit results for two-cut models. In section 6.2, we derive an expression for the ℓ–instanton amplitude of a generic two-cut model. We show that the full partition sum of the two-cut model can be naturally reorganized as an instanton/anti-instanton expansion with respect to an arbitrary reference configuration. We then specialize to the stable reference configuration and derive regular expressions for the ℓ–instanton amplitude in generic one-cut models using the two-cut free energies. We test the result against the low-instanton number amplitudes for the cubic matrix model, computed by the method of orthogonal polynomials. In section 6.3, we test our prediction for the ℓ–instanton amplitude in the double-scaling limit, where we recursively solve the Painlevé I equation for higher instanton sectors using the transseries formalism.

6.1 Review of multicut matrix models

In this chapter we will consider Hermitian matrix models involving one single matrix, but we will extend some of the results of [71] by studying multi-cut configurations. In the following, we will give a brief review of multi-cut matrix models, following [125, 172, 175, 9].

We recall that the one–matrix model partition function is

$$Z_N = \frac{1}{\mathrm{vol}\,[U(N)]} \int \mathrm{d}M\, \exp\left(-\frac{1}{g_s}\mathrm{Tr}\, V(M)\right), \tag{6.1.1}$$

where $V(x)$ is a potential which we will take to be a polynomial. This can be written in terms of eigenvalues as

$$Z_N = \frac{1}{N!} \int \prod_{i=1}^{N} \frac{\mathrm{d}\lambda_i}{2\pi}\, \Delta^2(\lambda)\, \exp\left(-\frac{1}{g_s}\sum_{i=1}^{N} V(\lambda_i)\right) \tag{6.1.2}$$

where $\Delta(\lambda)$ is the Vandermonde determinant. As in the last chapter, we are interested in studying the model at large N but keeping the 't Hooft coupling

$$t = N g_s \tag{6.1.3}$$

fixed. In this limit the model can be described by the density of eigenvalues

$$\rho(\lambda) = \frac{1}{N}\langle \mathrm{Tr}\, \delta(\lambda - M)\rangle. \tag{6.1.4}$$

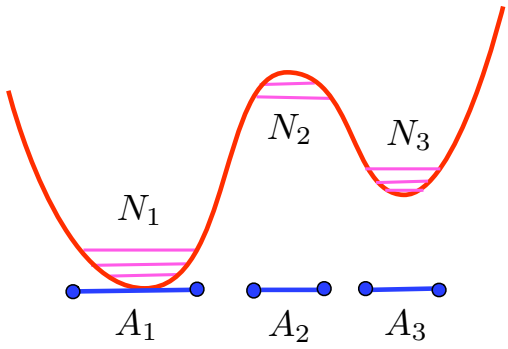

Figure 6.2: An example of a potential leading to a three-cut solution. The N eigenvalues split into three sets, N_I, $I = 1, 2, 3$, and they sit around the extrema of the potential. The support of the density of eigenvalues is the union of the intervals A_I, $I = 1, 2, 3$.

Let us assume that the potential $V(x)$ has s extrema. The most general saddle point of the model will be characterized by a density of eigenvalues supported on a disjoint union of s intervals

$$\mathcal{C} = \bigcup_{I=1}^{s} A_I, \tag{6.1.5}$$

where $A_I = [x_{2I-1}, x_{2I}]$ are the s cuts and $x_1 < x_2 < \cdots < x_{2s}$. If $s > 1$ we call this saddle point a *multi-cut solution* of the Hermitian matrix model. A potential leading to a three-cut solution is depicted in Fig. 6.2. This multicut saddle-point can be described in terms of integration over eigenvalues as follows. In the s-cut configuration described above the N eigenvalues split into s sets of N_I eigenvalues, $I = 1, \cdots, s$. Let us denote each of these s sets by

$$\{\lambda_{k_I}^{(I)}\}_{k_I=1,\cdots,N_I}, \quad I = 1, \cdots, s. \tag{6.1.6}$$

The eigenvalues in the I-th set sit in the interval A_I around the I-th extremum. Along this interval, the effective potential

$$V_{\text{eff}}(\lambda) = V(\lambda) - t \int \mathrm{d}\lambda' \rho(\lambda') \log|\lambda - \lambda'| \tag{6.1.7}$$

is constant. It is possible to choose s integration contours $\mathcal{C}_I$ in the complex plane, $I = 1, \cdots, s$, going to infinity in directions where the integrand decays exponentially, and in such a way that each of them passes through exactly one of the s critical points (see for example [176]). The resulting matrix integral is convergent and can be written as

$$Z(N_1, \cdots, N_s) = \frac{1}{N_1! \cdots N_s!} \int_{\lambda_{k_1}^{(1)} \in \mathcal{C}_1} \cdots \int_{\lambda_{k_s}^{(s)} \in \mathcal{C}_s} \prod_{i=1}^{N} \frac{\mathrm{d}\lambda_i}{2\pi} \Delta^2(\lambda) \mathrm{e}^{-\frac{1}{g_s}\sum_{i=1}^{N} V(\lambda_i)}. \tag{6.1.8}$$

The overall combinatorial factor in this expression, as compared to the one in (6.1.1), is due to the fact that there are

$$\frac{N!}{N_1! \cdots N_s!} \tag{6.1.9}$$

ways to choose the s sets of N_I eigenvalues. Of course, when the integrand is written out in detail, it splits into s sets of eigenvalues which interact among them through the Vandermonde determinant (see for example [177]).

In order to solve for the density of eigenvalues we introduce, as in the one-cut case, the resolvent

$$\omega(z) = \frac{1}{N}\left\langle \mathrm{Tr}\frac{1}{z-M}\right\rangle = \frac{1}{N}\sum_{k=0}^{+\infty}\frac{1}{z^{k+1}}\left\langle \mathrm{Tr}M^k\right\rangle, \tag{6.1.10}$$

which has a standard genus expansion $\omega(z) = \sum_{g=0}^{+\infty} g_s^{2g}\,\omega_g(z)$ with

$$\omega_0(z) = \int_{\mathcal{C}} \mathrm{d}\lambda\,\frac{\rho(\lambda)}{z-\lambda}. \tag{6.1.11}$$

The normalization of the eigenvalue density

$$\int_{\mathcal{C}} \mathrm{d}\lambda\,\rho(\lambda) = 1 \tag{6.1.12}$$

implies that

$$\omega_0(z) \sim \frac{1}{z} \tag{6.1.13}$$

as $z \to +\infty$. Notice that the genus zero resolvent determines the eigenvalue density as

$$\rho(z) = -\frac{1}{2\pi\mathrm{i}}\left(\omega_0(z+\mathrm{i}\epsilon) - \omega_0(z-\mathrm{i}\epsilon)\right). \tag{6.1.14}$$

In (6.1.11), $\mathcal{C}$ denotes a closed contour enclosing the union of intervals. One may compute $\omega_0(z)$ by making use of the large N saddle–point equations of motion of the matrix model,

$$\omega_0(z+\mathrm{i}\epsilon) + \omega_0(z-\mathrm{i}\epsilon) = \frac{1}{t}V'(z) = 2\,\mathsf{P}\int_{\mathcal{C}} \mathrm{d}\lambda\,\frac{\rho(\lambda)}{z-\lambda}. \tag{6.1.15}$$

For a generic multi–cut solution, the large N resolvent is given by

$$\omega_0(z) = \frac{1}{2t}\oint_{\mathcal{C}}\frac{\mathrm{d}w}{2\pi\mathrm{i}}\,\frac{V'(w)}{z-w}\,\sqrt{\frac{\sigma(z)}{\sigma(w)}}, \tag{6.1.16}$$

where we have introduced the notation

$$\sigma(x) = \prod_{k=1}^{2s}(x-x_k). \tag{6.1.17}$$

As in the one-cut case, an equivalent way to describe the large N solution is via the *spectral curve* $y(z)$, which is given by

$$y(z) = V'(z) - 2t\,\omega_0(z) = M(z)\,\sqrt{\sigma(z)} \tag{6.1.18}$$

where

$$M(z) = \oint_{\mathcal{C}_\infty}\frac{\mathrm{d}w}{2\pi\mathrm{i}}\,\frac{V'(w)}{(w-z)\sqrt{\sigma(w)}}, \tag{6.1.19}$$

is the moment function. The moments of this function, which are defined by [175]

$$M_i^{(k)} = \oint_{\mathcal{C}}\frac{\mathrm{d}w}{2\pi\mathrm{i}}\frac{V'(w)}{(w-x_i)^k\sqrt{\sigma(w)}} \tag{6.1.20}$$

can be easily calculated to be

$$M_i^{(k)} = \frac{1}{(k-1)!}\frac{\mathrm{d}^{k-1}}{\mathrm{d}z^{k-1}}M(z)\Big|_{z=x_i} \tag{6.1.21}$$

and will play an important role in the following. We will denote

$$M_i \equiv M_i^{(1)} = M(x_i). \tag{6.1.22}$$

In order to fully determine the large N solution one still needs to specify the endpoints of the s cuts, $\{x_k\}$. The large z asymptotics of the genus zero resolvent immediately yield $s+1$ conditions for these $2s$ unknowns. They are

$$\oint_{\mathcal{C}} \frac{\mathrm{d}w}{2\pi \mathrm{i}} \frac{w^n V'(w)}{\sqrt{\prod_{k=1}^{2s}(w-x_k)}} = 2t\,\delta_{ns}, \tag{6.1.23}$$

for $n = 0, 1, \ldots, s$. In order to fully solve the problem, one still requires $s-1$ extra conditions. These will be fixed in our case by fixing the filling fractions,

$$\epsilon_I \equiv \frac{N_I}{N} = \int_{A_I} \mathrm{d}\lambda\, \rho(\lambda), \qquad I = 1, 2, \ldots, s, \tag{6.1.24}$$

as parameters, or moduli, of the problem under scrutiny. Since $\sum_{I=1}^{s} \epsilon_I = 1$, equation (6.1.24) leads to $s-1$ conditions, as we required. One may also use as moduli the partial 't Hooft couplings $t_I = t\epsilon_I = g_s N_I$, which can be written as

$$t_I = \frac{1}{4\pi \mathrm{i}} \oint_{A^I} \mathrm{d}z\, y(z), \tag{6.1.25}$$

with $\sum_{I=1}^{s} t^I = t$. Notice that in general the saddle point we are considering will be an *unstable* one. This is the generic situation we find in the applications of matrix models to topological string theory [32, 29, 35]. Indeed, as we will see in this chapter, the fact that we consider general unstable saddle-points will allow us to extract multi-instanton amplitudes from multi-cut matrix models.

The free energy of the multi-cut matrix model has a genus expansion of the form

$$F = \log Z = \sum_{g=0}^{\infty} F_g(t_I) g_s^{2g-2}. \tag{6.1.26}$$

The planar free energy $F_0(t_I)$ can be computed from the spectral curve by using the special geometry relation [178]

$$\frac{\partial F_0(t)}{\partial t_I} = \oint_{B_\Lambda^I} y(\lambda)\mathrm{d}\lambda, \qquad I = 1, \cdots, s, \tag{6.1.27}$$

where B_Λ^I is a path which goes from the endpoint of the A_I cycle to the point Λ. This point is then taken to infinity after removing the divergent pieces of the integral.

We will need later on explicit expressions for the derivatives of the endpoints of the cuts, x_j, with respect to the 't Hooft parameters t_j. These are obtained as solutions to a linear system which we now write down. From (6.1.23) we immediately obtain,

$$\sum_{i=1}^{2s} M_i x_i^k \frac{\partial x_i}{\partial t_j} = 4\delta_{ks}, \quad k = 0, \cdots, s. \tag{6.1.28}$$

For fixed j, this gives $s+1$ conditions for $2s$ quantities. The remaining conditions can be obtained from

$$t_k = \frac{1}{2\pi} \int_{x_{2k-1}}^{x_{2k}} \mathrm{d}\lambda\, M(\lambda)\sqrt{\sigma(\lambda)} \tag{6.1.29}$$

by taking derivatives w.r.t. t_j. A similar calculation is done in [175], Appendix A. By deforming the contour away from infinity, we can write the moment function as

$$M(\lambda) = -\oint_{\mathcal{C}\cup\mathcal{C}_\lambda} \frac{\mathrm{d}w}{2\pi\mathrm{i}} \frac{V'(w)}{(w-\lambda)\sqrt{\sigma(w)}}, \tag{6.1.30}$$

where $\mathcal{C}_\lambda$ is a small contour around $w = \lambda$. Therefore, by taking derivatives w.r.t. t_j in (6.1.29) we obtain

$$\delta_{jk} = -\frac{1}{4\pi}\sum_{i=1}^{2s} \frac{\partial x_i}{\partial t_j} \int_{x_{2k-1}}^{x_{2k}} \mathrm{d}\lambda \oint_{\mathcal{C}\cup\mathcal{C}_\lambda} \frac{\mathrm{d}\omega}{2\pi\mathrm{i}} \frac{V'(\omega)}{(\omega-\lambda)} \Big(\frac{1}{\omega - x_i} - \frac{1}{\lambda - x_i}\Big) \frac{\sqrt{\sigma(\lambda)}}{\sqrt{\sigma(\omega)}}, \tag{6.1.31}$$

where the derivative acted on $\sigma(\lambda)$, $\sigma(\omega)$. Since

$$\frac{1}{\omega - x_i} - \frac{1}{\lambda - x_i} = \frac{\lambda - \omega}{(\omega - x_i)(\lambda - x_i)}, \tag{6.1.32}$$

we finally obtain

$$\oint_{\mathcal{C}\cup\mathcal{C}_\lambda} \frac{\mathrm{d}\omega}{2\pi\mathrm{i}} \frac{V'(\omega)}{(\omega-\lambda)} \Big(\frac{1}{\omega - x_i} - \frac{1}{\lambda - x_i}\Big) \frac{\sqrt{\sigma(\lambda)}}{\sqrt{\sigma(\omega)}} = -\frac{\sqrt{\sigma(\lambda)}}{\lambda - x_i} M_i. \tag{6.1.33}$$

Notice that the integrand has no longer a pole at $\omega = \lambda$, hence only the integral around $\mathcal{C}$ contributes. We then end up with the equations

$$\frac{1}{4\pi}\sum_{i=1}^{2s} \frac{\partial x_i}{\partial t_j} M_i \int_{x_{2k-1}}^{x_{2k}} \mathrm{d}\lambda \frac{\sqrt{\sigma(\lambda)}}{\lambda - x_i} = \delta_{jk}, \qquad k = 1, \cdots, s. \tag{6.1.34}$$

If we introduce the integrals [175]

$$K_{i,k} = \int_{x_{2k-1}}^{x_{2k}} \mathrm{d}\lambda \frac{\sqrt{\sigma(\lambda)}}{\lambda - x_i}. \tag{6.1.35}$$

We can write

$$\frac{1}{4\pi}\sum_{i=1}^{2s} M_i K_{i,k} \frac{\partial x_i}{\partial t_j} = \delta_{jk}, \qquad k = 1, \cdots, s. \tag{6.1.36}$$

These equations, together with (6.1.28), determine the derivatives $\partial x_i/\partial t_j$. Other derivatives with respect to the 't Hooft parameters can be also expressed in terms of the derivatives of the branch points. For example, it is easy to find that

$$\frac{\partial M_i}{\partial t_j} = \frac{3}{2} M_i^{(2)} \frac{\partial x_i}{\partial t_j} + \frac{1}{2}\sum_{k\neq i} \frac{M_i - M_k}{x_i - x_k} \frac{\partial x_k}{\partial t_j}. \tag{6.1.37}$$

In the two-cut case, these quantities can be conveniently expressed in terms of elliptic functions, since the spectral curve is elliptic. We define as in [172]

$$\mathcal{K} = \int_{x_1}^{x_2} \frac{\mathrm{d}z}{\sqrt{|\sigma(z)|}} = \frac{2}{\sqrt{(x_1 - x_3)(x_2 - x_4)}} K(k), \quad k^2 = \frac{(x_1 - x_2)(x_3 - x_4)}{(x_1 - x_3)(x_2 - x_4)}, \tag{6.1.38}$$

and introduce the variables

$$t = t_1 + t_2, \qquad s = \frac{1}{2}(t_1 - t_2). \tag{6.1.39}$$

One then finds for the derivatives of the endpoints x_i of the cuts, solving the system of equations (6.1.36)

$$\frac{\partial x_i}{\partial s} = \frac{4\pi}{M_i \mathcal{K}} \frac{1}{\prod_{j\neq i}(x_i - x_j)}. \tag{6.1.40}$$

Another quantity which can be easily computed in the two-cut case in terms of elliptic functions is $F_1(t_1, t_2)$ [175, 177]. It is given by

$$F^{(1)} = -\frac{1}{24}\sum_{i=1}^{4} \ln M_i - \frac{1}{2}\ln K(k) - \frac{1}{12}\sum_{i<j}\ln(x_i - x_j)^2 + \frac{1}{8}\ln(x_1 - x_3)^2 + \frac{1}{8}\ln(x_2 - x_4)^2. \quad (6.1.41)$$

We can now apply the quantities assembled above to compute instanton amplitudes in multicut models.

6.2 Multi-cut solutions as multi-instanton configurations

In this section, we derive expressions for multi-instanton configurations in terms of multi-cut solutions. If one regards (6.1.8) as the matrix integral in a topological sector characterized by the fillings $N_1, \cdots, N_s$, it is natural to consider the general partition function [120, 125, 172, 171]

$$Z = \sum_{N_1+\cdots+N_s=N} \zeta_1^{N_1} \cdots \zeta_s^{N_s} Z(N_1, \cdots, N_s). \quad (6.2.42)$$

The coefficients ζ_k can be regarded as θ parameters which lead to different θ vacua [125]. The sum (6.2.42) can also be regarded as a matrix integral where the N eigenvalues are integrated along the contour

$$\mathcal{C} = \sum_{k=1}^{s} \zeta_k \mathcal{C}_k, \quad (6.2.43)$$

therefore the θ parameters give the relative weight of the different contours $\mathcal{C}_k$ [125, 171].

The different sectors appearing in (6.2.42) can be regarded as instanton sectors of the multicut matrix model. Indeed, let $Z(N_1, \cdots, N_s)$ the partition function in one sector with filling fractions N_I, and $Z(N_1', \cdots, N_d')$ the partition function corresponding to a different choice of filling fractions N_I'. Then we have that

$$\frac{Z(N_1', \cdots, N_d')}{Z(N_1, \cdots, N_d)} \sim \exp\Big[-\frac{1}{g_s}\sum_{I=1}^{s}(N_I - N_I')\frac{\partial F_0(t_I)}{\partial t_I}\Big] \quad (6.2.44)$$

This means that, if we pick a set of filling fractions $(N_1, \cdots, N_s)$ as our reference point, the other sectors can not be seen in g_s perturbation theory. It is then natural to regard them as different *instanton sectors* of the matrix model.

6.2.1 General structure

Notice that, depending on the value of the real part of the exponent appearing in (6.2.44), the sectors with filling fractions $(N_1', \cdots, N_s')$ will be exponentially suppressed or exponentially enhanced with respect to the reference configuration $(N_1, \cdots, N_s)$. Let us consider for example a cubic potential where N_1 eigenvalues sit at the minimum of the potential and N_2 eigenvalues sit at the maximum. The sector with fillings $(N_1 - 1, N_2 + 1)$, which can be regarded as the one-instanton sector, will be more unstable than our reference configuration, and typically it will be exponentially suppressed. However, the anti-instanton sector with fillings $(N_1 + 1, N_2 - 1)$ is more stable and it will be exponentially enhanced. Therefore, in multi-cut matrix models (and in contrast to most field theories) instantons and anti-instantons have actions with opposite signs. As we will see, this leads to some subtleties.

Let us then consider a reference configuration characterized by arbitrary filling fractions N_I, $I = 1, \cdots, s$, and then regard any other set of filling fractions N_I' as instanton configurations. In this case, the determination of the instanton expansion of the partition function amounts to

a Taylor expansion around the configuration with $t_I = g_s N_I$. For simplicity we will write down the formulae in the two-cut case, and refer to [171] for the formal, general expressions. We start from a reference configuration (N_1, N_2) and we write

$$Z = \sum_{\ell=-N_2}^{N_1} \zeta^n Z(N_1 - \ell, N_2 + \ell) = Z^{(0)}(N_1, N_2) \sum_{\ell=-N_2}^{N_1} \zeta^\ell Z^{(\ell)}, \tag{6.2.45}$$

where we denoted $Z^{(0)}(N_1, N_2) = Z(N_1, N_2)$, and

$$Z^{(\ell)} = \frac{Z(N_1 - \ell, N_2 + \ell)}{Z^{(0)}(N_1, N_2)} \tag{6.2.46}$$

Let us now assume that $N_I \neq 0$, $I = 1, 2$. If we recall that $t_I = g_s N_I$, and that

$$Z(N_1, N_2) = \exp\Big[\sum_{g=0}^{\infty} g_s^{2g-2} F_g(t_1, t_2)\Big] \tag{6.2.47}$$

we immediately find

$$Z^{(\ell)} = \zeta^\ell q^{\ell^2/2} \mathrm{e}^{-\ell \frac{A}{g_s}} \Big[1 - g_s \Big(\ell \partial_s F_1 + \frac{\ell^3}{6} \partial_s^3 F_0\Big) + \mathcal{O}(g_s^2)\Big]. \tag{6.2.48}$$

In this equation

$$A(t_I) = \partial_s F_0(t_I), \qquad q = \exp\Big(\partial_s^2 F_0\Big). \tag{6.2.49}$$

A corresponds to the action of an instanton obtained by eigenvalue tunneling. Notice that, due to (6.1.27), we can write A as an integral over the spectral curve,

$$A = \int_{x_2}^{x_3} y(x) \mathrm{d}x. \tag{6.2.50}$$

Since ℓ can be positive or negative, the expansion in (6.2.45) will be a Laurent expansion, in which both positive *and negative* powers of $\xi = \exp(-A/g_s)$ appear. The free energy will be as well a Laurent series in ξ and ξ^{-1}, but each coefficient in this series will be given by an infinite sum of terms. This is the subtlety we were referring to.

6.2.2 Theta function resummation and background independence

It turns out that there is a rather natural way to resum these terms by using theta functions, as has been done in a similar context in [172, 171]. As we mentioned above, in the general case the partition function is a Laurent series in $\xi = \exp(-A/g_s)$ and one has to be careful in order to write the free energy as an instanton expansion, since the coefficient of ξ^ℓ to the free energy is the sum of an infinite number of contributions from the partition function, involving all possible $Z^{(n)}$. Here we point out that one can actually resum this series by rewriting the partition function as a theta series, as in [172, 171].

At large N_1, N_2, one can extend the sum of (6.2.45) from $-\infty$ to ∞, and we obtain

$$Z = Z^{(0)}(t_1, t_2) \sum_{\ell=-\infty}^{\infty} \zeta^\ell q^{\ell^2/2} \xi^\ell \Big[1 - g_s \Big(\ell \partial_s F_1 + \frac{\ell^3}{6} \partial_s^3 F_0\Big) + \mathcal{O}(g_s^2)\Big]. \tag{6.2.51}$$

If we exchange the sum over ℓ with the expansion in g_s, we can write Z in terms of the theta function

$$\vartheta_3(\tau | z) = \sum_{\ell=-\infty}^{\infty} q^{\ell^2/2} z^\ell \tag{6.2.52}$$

where $z = \zeta\xi$, as

$$Z = Z^{(0)}(t_1, t_2)\Big\{\vartheta_3(\tau|z) - g_s\Big(z\partial_z\vartheta_3(\tau|z)\,\partial_s F_1 + \frac{1}{6}(z\partial_z)^3\vartheta_3(\tau|z)\,\partial_s^3 F_0\Big) + \mathcal{O}(g_s^2)\Big\}. \quad (6.2.53)$$

This theta function is well defined due to the fact that τ is indeed the modulus of an elliptic curve, hence $|q| < 1$. We can now use Jacobi's triple identity

$$\vartheta_3(\tau|z) = \prod_{n=1}^{\infty}(1-q^n)\prod_{n=1}^{\infty}(1+zq^{n-1/2})\prod_{n=1}^{\infty}(1+z^{-1}q^{n-1/2}) \quad (6.2.54)$$

to write

$$\log\,\vartheta_3(\tau|z) = \log\phi(q) + \sum_{\ell=1}^{\infty}\frac{(-1)^\ell}{\ell}\frac{z^\ell + z^{-\ell}}{q^{\frac{\ell}{2}} - q^{-\frac{\ell}{2}}} \quad (6.2.55)$$

where

$$\phi(q) = \prod_{n=1}^{\infty}(1-q^n). \quad (6.2.56)$$

The last two terms can also be written in terms of the quantum dilogarithm,

$$\mathrm{Li}_2^q(z) = \sum_{\ell=1}^{\infty}\frac{(-1)^\ell}{\ell}\frac{z^\ell}{q^{\frac{\ell}{2}} - q^{-\frac{\ell}{2}}}. \quad (6.2.57)$$

This reorganization allows us to express the total free energy $F = \log Z$ in terms of an infinite series which has formally the structure of an instanton/anti-instanton expansion,

$$F = F^{(0)}(t_1, t_2) + \log\phi(q) + \sum_{\ell\neq 0}\frac{(-1)^\ell}{\ell(q^{\frac{\ell}{2}} - q^{-\frac{\ell}{2}})}\zeta^\ell \mathrm{e}^{-\ell A/g_s}\Big(1 + \mathcal{O}(g_s)\Big). \quad (6.2.58)$$

It is of course possible to write the g_s corrections in a similar way. Notice that $\log\phi(q)$ gives a contribution to F_1 coming from instanton/anti-instanton interactions in the partition function. It would be interesting to verify that this expansion provides indeed the right instanton expansion of the free energy in the two-cut case when we consider an arbitrary reference configuration, in the same way that we check in the following sections the multi-instanton expansion around the one-cut case.

6.2.3 Stabilizing multi-instantons

One way to avoid the subtleties related to exponentially enhanced transitions is to choose as a reference configuration the most stable one, suppressing in this way anti-instanton configurations. This is the natural choice if we are interested in computing a convergent matrix integral in terms of a perturbative series in g_s plus exponentially small corrections, since every other configuration is exponentially suppressed. Let us consider for example the case in which the potential has a unique minimum (like in Fig. 6.2). If we call A_1 the cut surrounding this minimum, the most stable configuration has filling fractions

$$(N, 0, \cdots, 0) \quad (6.2.59)$$

and it is a one-cut solution of the model. Any other configuration will be exponentially suppressed with respect to this one, and a convergent matrix integral can be computed at large N by considering the partition function $Z(N, 0, \cdots, 0)$ and then adding exponentially suppressed contributions from the other configurations. In this way we compute a multi-cut configuration as a sum of multi-instantons in the one-cut matrix model. This produces in particular general formulae for multi-instanton amplitudes in the one-cut matrix model.

Let us then calculate the partition function in this way, starting from a generic two-cut matrix model. The total partition function is

$$Z = \sum_{\ell=0}^{N} \zeta^{\ell} Z(N-\ell, \ell). \tag{6.2.60}$$

We are interested in the 't Hooft limit in which $N \to \infty$ with $t = g_s N$ fixed, and $\ell \ll N$. In this limit the finite sum in (6.2.60) becomes an infinite sum and we can write

$$Z = Z^{(0)}(t)\Big[1 + \sum_{\ell=1}^{\infty} \zeta^{\ell} \widehat{Z}^{(\ell)}\Big], \tag{6.2.61}$$

where $Z^{(0)}(t) = Z(N, 0)$ is the total partition function of the one-cut matrix model, i.e. the model in which the N eigenvalues sit at the minimum. and

$$Z^{(\ell)} = \frac{Z(t - \ell g_s, \ell g_s)}{Z^{(0)}}. \tag{6.2.62}$$

Like before, we can try to evaluate $Z^{(\ell)}$ by expanding the numerator around $g_s = 0$. There is a subtlety, however, since the free energies $F_g(t_1, t_2)$ are *not* analytic at $t_2 = 0$. To understand the origin of this nonanalyticity, we write

$$F_g(t_1, t_2) = F_g^{\mathrm{G}}(t_2) + \widehat{F}_g(t_1, t_2), \tag{6.2.63}$$

where $F_g^{\mathrm{G}}(t)$ are the genus g free energies of the Gaussian matrix model with 't Hooft parameter t, i.e.

$$F_0^{\mathrm{G}}(t) = \frac{1}{2} t^2 \Big(\log t - \frac{3}{2}\Big), \qquad F_1^{\mathrm{G}}(t) = -\frac{1}{12} \log t, \qquad \cdots \tag{6.2.64}$$

It is easy to see that $\widehat{F}_g(t_1, t_2)$ is *analytic* at $t_2 = 0$, so the lack of analyticity of the matrix model at $t_2 = 0$ is due to $F^{\mathrm{G}}(t_2)$. This issue has been discussed in [55] in a slightly different context: the Gaussian part of the matrix model free energy comes from the measure and it is not analytic when the 't Hooft parameter vanishes. The "regularized" $\widehat{F}_g(t_1, t_2)$ comes from resumming the perturbation theory double-line diagrams with genus g and it is an analytic function.

Physically, the reason for the appearance of this singularity is that in this problem $t_2 = \ell g_s$ and ℓ is small compared to N. Therefore, it is not appropriate to treat the integration over the ℓ eigenvalues from the point of view of the large N expansion. They should be integrated exactly. This argument suggests that in order to regularize the computation we should subtract $F^{\mathrm{G}}(t_2)$ from the total free energy and at the same time we multiply $Z^{(\ell)}$ by the *exact* partition function Z_ℓ^{G} for the Gaussian matrix model with ℓ eigenvalues,

$$Z_\ell^{\mathrm{G}} = \frac{g_s^{\ell^2/2}}{(2\pi)^{\ell/2}} G_2(\ell + 1), \tag{6.2.65}$$

where $G_2(\ell + 1)$ is the Barnes function,

$$G_2(\ell + 1) = \prod_{i=0}^{\ell-1} i!. \tag{6.2.66}$$

The appropriate expression for the partition function around the ℓ-instanton configuration is then

$$Z^{(\ell)} = Z_\ell^{\mathrm{G}} \exp\Big[\sum_{g \geq 0} g_s^{2g-2} (\widehat{F}_g(t - \ell g_s, \ell g_s) - F_g(t))\Big] \tag{6.2.67}$$

We can now expand the exponent appearing in (6.2.67) around $g_s = 0$, since it is analytic, and we obtain, up to two-loops,

$$Z^{(\ell)} = \frac{g_s^{\ell^2/2}}{(2\pi)^{\ell/2}} G_2(\ell+1)\zeta^\ell \hat{q}^{\ell^2/2} \mathrm{e}^{-\ell\widehat{A}/g_s}\left\{1 - g_s\Big(\ell\partial_s\widehat{F}_1(t) + \frac{\ell^3}{6}\partial_s^3\widehat{F}_0(t)\Big) + \mathcal{O}(g_s^2)\right\}. \tag{6.2.68}$$

In this equation

$$\widehat{A}(t) = \partial_s\widehat{F}_0, \qquad \hat{q} = \exp\Big(\partial_s^2\widehat{F}_0\Big). \tag{6.2.69}$$

All the derivatives appearing in (6.2.68) and (6.2.69) are evaluated at $t_2 = 0$, $t_1 = t$.

Expression (6.2.68) is crucial for the rest of this paper. Notice that it is very similar to its counterpart (6.2.48) in the arbitrary unstable configuration, but for the Gaussian prefactor and the fact that $\widehat{F}_g$ is now regularized. Furthermore, notice that it gives a precise prediction for amplitudes corresponding to arbitrary instanton number, with only input besides the instanton action the regularized, two-cut free energies $\widehat{F}_g$. Of course, this simply reflects our philosophy that multi-instanton configurations can be expressed by multi-cut solutions. Another aspect of $Z^{(\ell)}$ is that it is *not* typical of a dilute instanton gas. In a dilute instanton gas one has that, at leading order in the coupling constant,

$$Z^{(\ell)} \approx \frac{1}{\ell!}\left(Z^{(1)}\right)^\ell. \tag{6.2.70}$$

If this was the case here, Z_ℓ would scale like $g_s^{\ell/2}$, but it is clear from (6.2.68) that this is not true: Z_ℓ scales like $g_s^{\ell^2/2}$. It is easy to see that this is due to the presence of the Vandermonde determinant, and this in turn can be easily understood from a simple scaling argument. The ℓ-instanton integral is roughly of the form

$$Z^{(\ell)} \approx \int \prod_{i=1}^{\ell} \mathrm{d}x_i \Delta^2(x_i) \exp\left[-\frac{1}{2g_s}V''_{\text{eff}}(x_0)\sum_{i=1}^{\ell}(x_i - x_0)^2\right]. \tag{6.2.71}$$

If we set $u_i = (x_i - x_0)/g_s^{1/2}$ we see immediately that the measure for the ℓ eigenvalues leads to the factor $g_s^{\ell/2}$ typical of a dilute instanton gas. However, the Vandermonde determinant leads to an extra power of $g_s^{\ell(\ell-1)/2}$. The instanton gas in a matrix model should be rather regarded as a *ultra-diluted* instanton gas, since for small g_s the partition function for ℓ instantons is even more suppressed than in the usual instanton gas. Physically, the ultra-diluteness is of course due to the eigenvalue repulsion.

In particular, we disagree with the analysis of multi-instantons in the one-cut matrix model proposed in section 2 of [126]. In that paper the Vandermonde interaction between the instantons is set to one, and the resulting integral factorized. This cannot be done without jeopardizing the very scaling of Z_ℓ with g_s.

Since we are expanding around the most stable configuration, Z has now a Taylor series in

$$\widehat{\xi} = \mathrm{e}^{-\widehat{A}/g_s}, \tag{6.2.72}$$

and F will be well-defined as a formal series in powers of $\widehat{\xi}$. We can now compute the free energy as

$$F = \log Z = \sum_{\ell=0}^{\infty} \widehat{\xi}^\ell F^{(\ell)}(z, g_s), \tag{6.2.73}$$

where

$$F^{(\ell)}(z, g_s) = F_0^{(\ell)}\left(1 + \sum_n F_n^{(\ell)} g_s^n\right). \tag{6.2.74}$$

This series is appropriately written in terms of "connected" contributions

$$\log\Big(1+\sum_{\ell\geq 1}\zeta^\ell Z^{(\ell)}\Big)=\sum_{\ell\geq 1}\zeta^\ell Z^{(\ell)}_{(c)}, \tag{6.2.75}$$

where

$$Z^{(\ell)}_{(c)}=\sum_{s\geq 1}\frac{(-1)^{s-1}}{s}\sum_{k_1+\cdots+k_s=\ell}Z^{(k_1)}\cdots Z^{(k_s)}=Z^{(\ell)}-\frac{1}{2}\sum_{k=1}^{\ell-1}Z^{(\ell-k)}Z^{(k)}+\cdots. \tag{6.2.76}$$

We then deduce that the ℓ-instanton contribution to the free energy of a one-cut matrix model is given as

$$F^{(\ell)}=\zeta^\ell Z^{(\ell)}_{(c)}. \tag{6.2.77}$$

The explicit expression of $F^{(\ell)}$ at two loops is

$$\begin{aligned}
F^{(1)}&=\frac{g_s^{1/2}}{\sqrt{2\pi}}\zeta\hat{q}^{1/2}\Big\{1-g_s\Big(\partial_s\widehat{F}_1+\frac{1}{6}\partial_s^3\widehat{F}_0\Big)+\mathcal{O}(g_s^2)\Big\},\\
F^{(\ell)}&=\frac{(-1)^{\ell-1}g_s^{\ell/2}}{\ell(2\pi)^{\frac{\ell}{2}}}\zeta^\ell\hat{q}^{\ell/2}\Big\{1-\ell g_s\Big(\partial_s\widehat{F}_1+\frac{1}{6}\partial_s^3\widehat{F}_0-\hat{q}\Big)+\mathcal{O}(g_s^2)\Big\},\qquad \ell\geq 2
\end{aligned} \tag{6.2.78}$$

This gives formulae for the ℓ-instanton free energy, up to two loop order, in an arbitrary one-cut matrix model.

6.2.4 Recovering the one-instanton amplitude from the two-cut solution

We will now test our formulae (6.2.68) and (6.2.78) against other techniques for computing multi-instanton effects. A first, obvious test that equation (6.2.78) has to pass is that at $\ell=1$, it has to reproduce our result for the one-instanton amplitude found in the last chapter, (5.2.45).

The formula (6.2.78) involves the computation of derivatives of two-cut free energies, in the limit in which one of the cuts shrinks down to zero size, i.e. $t_2\to 0$. We will now derive explicit expressions for these derivatives, and in particular we will check that the expression obtained for $F^{(1)}$ agrees with the result of [71]. The limit $t_2\to 0$ corresponds geometrically to a degeneration of the curve in which the A_2 cut shrinks to zero size, i.e. $x_3\to x_4=x_0$. The spectral curve of the two-cut problem becomes

$$y(x)\to M(x)(x-x_0)\sqrt{(x-x_1)(x-x_2)} \tag{6.2.79}$$

Notice that here $M(x)$ is the moment function of the two-cut problem. The moment function of the one-cut problem is then given by

$$M_1(x)=M(x)(x-x_0). \tag{6.2.80}$$

We can now compute the quantities appearing in (6.2.78). First of all, the instanton action is given by

$$\widehat{A}(t)=\lim_{t_2\to 0}\Big(\partial_s F_0(t,t_2)-\partial_{t_2}F_0^{\mathrm{G}}(t_2)\Big). \tag{6.2.81}$$

Both quantities appearing here are regular at $t_2=0$, and from (6.1.27) one immediately finds

$$\widehat{A}=\int_{x_2}^{x_0}M_1(x)\sqrt{(x-x_1)(x-x_2)}\mathrm{d}x, \tag{6.2.82}$$

which is indeed the right formula in the one-cut case.

We next compute

$$\frac{1}{2}\partial_s^2\widehat{F}_0(t,0)=\frac{1}{2}\lim_{t_2\to 0}\Big(\partial_s^2F_0(t,t_2)-\partial_{t_2}^2F_0^{\rm G}(t_2)\Big)=\lim_{x_4\to x_3}\left(\pi{\rm i}\tau-\frac{1}{2}\log\,t_2\right). \tag{6.2.83}$$

In the limit $x_4\to x_3$ the elliptic modulus appearing in (6.1.38) vanishes and both τ and $\log\,t_2$ diverge. In order to calculate this limit, as well as similar ones, we will set

$$\epsilon=x_4-x_3. \tag{6.2.84}$$

As $\epsilon\to 0$ the leading behavior of the elliptic modulus is given by

$$\pi{\rm i}\tau\sim\log\frac{k^2}{16}, \tag{6.2.85}$$

i.e. it diverges as $\log(\epsilon)$. According to our general argument above, this divergence should be removed by subtracting $(\log t_2)/2$. We computed the expansion of t_2 in powers of ϵ. In particular, we find that at leading order $t_2\sim\epsilon^2$, so indeed the cancellation takes place. The subleading order implies

$$\hat{q}^{1/2}=\lim_{\epsilon\to 0}\frac{k^2}{16\sqrt{t_2}}=\frac{x_1-x_2}{4}\frac{1}{\sqrt{M(x_0)[(x_1-x_0)(x_2-x_0)]^{\frac{5}{2}}}}. \tag{6.2.86}$$

where we have set $x_3=x_0$. Since

$$M(x_0)=M_1'(x_0), \tag{6.2.87}$$

(6.2.86) is in complete agreement with the formula obtained in [71] for the one-loop contribution to $F^{(1)}$ (the factor $1/\sqrt{2\pi}$ appearing in the formula of [71] is already included in (6.2.78)).

We now proceed with the calculation of the quantities appearing at two-loops. This is more involved, but leads to a highly nontrivial check of our expressions. We will first calculate $\partial_s^3\widehat{F}_0$. This can be computed, in the full two-cut matrix model, as

$$\partial_s^3F_0=2\pi{\rm i}\frac{\partial\tau}{\partial k^2}\frac{\partial k^2}{\partial s}, \tag{6.2.88}$$

where k^2 is the elliptic modulus defined in (6.1.38). The first factor in the r.h.s can be immediately computed with the identities

$$\begin{aligned}\frac{{\rm d}K}{{\rm d}k^2}&=\frac{1}{2k^2k'^2}(E-k'^2K),\\ \frac{{\rm d}K'}{{\rm d}k^2}&=-\frac{1}{2k^2k'^2}(E'-k^2K'),\end{aligned} \tag{6.2.89}$$

where $E(k)$ is the complete elliptic integral of the second kind (see Appendix C.1), and

$$k'^2=1-k^2,\qquad K'=K(k'),\qquad E'=E(k'). \tag{6.2.90}$$

The second factor is more involved and can be computed from (6.1.40). The result, for a generic two-cut matrix model, is

$$\begin{aligned}\frac{\partial k^2}{\partial s}=&\frac{2\pi\sqrt{(x_4-x_2)(x_3-x_1)}}{K(k)}\frac{1}{(x_1-x_3)^2(x_2-x_4)^2}\frac{1}{M_1\cdots M_4\prod_{i<j}(x_i-x_j)}\\ &\cdot\Big(M_1M_2M_3(x_1-x_2)^2(x_1-x_3)^2(x_2-x_3)^2\\ &+M_1M_2M_4(x_1-x_2)^2(x_1-x_4)^2(x_2-x_4)^2+M_1M_3M_4(x_1-x_3)^2(x_1-x_4)^2(x_3-x_4)^2\\ &+M_2M_3M_4(x_1-x_3)^2(x_1-x_4)^2(x_3-x_4)^2\Big)\end{aligned} \tag{6.2.91}$$

Putting everything together we obtain

$$\begin{aligned}
&\frac{1}{6}\frac{\partial^3 F_0}{\partial s^3} = \\
&\frac{\pi^3\sqrt{(x_4-x_2)(x_3-x_1)}}{6(x_1-x_2)(x_2-x_3)(x_1-x_4)(x_3-x_4)K^3(k)}\frac{1}{M_1\cdots M_4\prod_{i<j}(x_i-x_j)} \\
&\cdot\Big(M_1M_2M_3(x_1-x_2)^2(x_1-x_3)^2(x_2-x_3)^2 \\
&+M_1M_2M_4(x_1-x_2)^2(x_1-x_4)^2(x_2-x_4)^2+M_1M_3M_4(x_1-x_3)^2(x_1-x_4)^2(x_3-x_4)^2 \\
&+M_2M_3M_4(x_1-x_3)^2(x_1-x_4)^2(x_3-x_4)^2\Big)
\end{aligned} \tag{6.2.92}$$

This has a pole of order two in $\epsilon = x_4 - x_3$. The divergent pieces in ϵ^{-2} and ϵ^{-1} should be removed by subtracting $-1/(6t_2)$. Indeed, using again the ϵ–expansion of t_2, we check that this is the case, and we obtain the final limit

$$\begin{aligned}
&\frac{1}{6}\partial_s^3\widehat{F}_0(t,0) = \lim_{\epsilon\to 0}\left(\frac{1}{6}\partial_s^3 F_0(t,t_2)-\frac{1}{6t_2}\right) \\
&=\frac{1}{\sqrt{(x_1-x_0)(x_2-x_0)}}\Bigg\{\frac{8(x_1-x_0)^2}{(x_1-x_2)^2(x_2-x_0)^2M(x_2)}+\frac{8(x_2-x_0)^2}{(x_1-x_2)^2M(x_1)(x_1-x_0)^2} \\
&+\frac{4M'(x_0)^2}{M(x_0)^3}-\frac{3M''(x_0)}{2M(x_0)^2}-\frac{17(x_1+x_2-2x_0)M'(x_0)}{2(x_2-x_0)M(x_0)^2(x_1-x_0)} \\
&+\frac{77x_1^2+118x_2x_1-272x_0x_1+77x_2^2+272x_0^2-272x_2x_0}{8M(x_0)(x_0-x_2)^2(x_1-x_0)^2}\Bigg\}
\end{aligned} \tag{6.2.93}$$

A similar computation can be done in the case of F_1. Explicit formulae for $\partial_s F_1$ in the full two-cut model can be easily obtained with the results collected in the previous section. Again, this is singular as $\epsilon \to 0$, but the following limit turns out to be regular, as expected

$$\begin{aligned}
&\partial_s\widehat{F}_1(t,0) = \lim_{\epsilon\to 0}\left(\partial_s F_1(t,t_2)+\frac{1}{12t_2}\right) \\
&=\frac{1}{\sqrt{(x_1-x_0)(x_2-x_0)}}\Bigg\{\frac{M'(x_0)^2}{6M(x_0)^3}-\frac{(x_1+x_2-2x_0)M'(x_0)}{24(x_1-x_0)(x_2-x_0)M(x_0)^2} \\
&+\frac{19(x_1^2+x_2^2)-22x_2x_1+16x_0(x_0-x_1-x_2)}{96(x_1-x_0)^2(x_0-x_2)^2M(x_0)}-\frac{(3x_1-x_2-2x_0)(x_2-x_0)}{3(x_1-x_2)^2(x_1-x_0)^2M(x_1)} \\
&+\frac{(x_1-x_0)(x_1-3x_2+2x_0)}{3(x_1-x_2)^2(x_2-x_0)^2M(x_2)}-\frac{(x_2-x_0)M'(x_1)}{4(x_1-x_2)(x_1-x_0)M(x_1)^2} \\
&+\frac{(x_1-x_0)M'(x_2)}{4(x_1-x_2)(x_2-x_0)M(x_2)^2}-\frac{M''(x_0)}{8M(x_0)^2}\Bigg\}.
\end{aligned} \tag{6.2.94}$$

One can now easily check that

$$\frac{1}{6}\partial_s^3\widehat{F}_0(t,0)+\partial_s\widehat{F}_1(t,0) \tag{6.2.95}$$

is precisely the two-loop contribution to $F^{(1)}$ (5.2.45) computed in [71] by different means.

6.2.5 Multi-instanton amplitudes from the transseries formalism

An alternative, independent method to derive multi-instanton amplitudes has been put forward in [174]. It is based on the so-called transseries formalism, applied to the solution of the matrix model in terms of orthogonal polynomials.

Transseries formalism

Recall the formalism of orthogonal polynomials $p_n(\lambda)$, explained in detail e.g. in [118]. For a matrix model with potential $V(\lambda)$, the orthogonal polynomials p_n are defined by

$$\int \frac{d\lambda}{2\pi} \mathrm{e}^{-\frac{V(\lambda)}{g_s}} p_n(\lambda) p_m(\lambda) = h_n \delta_{nm}, \qquad n > 0, \tag{6.2.96}$$

where p_n are normalized by requiring that $p_n \sim \lambda^n + \cdots$. It turns out that the partition function (6.1.1) of the matrix model can be expressed in terms of orthogonal polynomials as

$$Z_N = \prod_{i=0}^{N-1} h_i = h_0^N \prod_{i=1}^{N} r_i^{N-i}. \tag{6.2.97}$$

The coefficients

$$r_n = \frac{h_n}{h_{n-1}} \tag{6.2.98}$$

satisfy recursion relations depending on the shape of the potential. They also obviously satisfy

$$r_n = \frac{Z_{n-1} Z_{n+1}}{Z_n^2}. \tag{6.2.99}$$

In the limit $N \to \infty$, $g_s \frac{n}{N}$ becomes a continuous variable that we will call z, and r_n is promoted to a function $R(z, g_s)$, for which we have the multi-instanton transseries ansatz

$$R(z, g_s) = \sum_{\ell=0}^{\infty} C^\ell R^{(\ell)}(z, g_s) \mathrm{e}^{-\ell A(z)/g_s}, \tag{6.2.100}$$

where the ℓ-instanton coefficient can be written as

$$R^{(\ell)}(z, g_s) = R_0^{(\ell)}(z) \left(1 + \sum_{n=1}^{\infty} g_s^n R_n^{(\ell)}(z) \right). \tag{6.2.101}$$

The coefficients $R_n^{(\ell)}(z, g_s)$ can be computed from the so-called pre-string equation, a difference equation which can be derived as the continuum limit of the recursion relations satisfied by the coefficients r_n. For any polynomial potential, the pre-string equation can be written down explicitly [118]. Once (6.2.100) found, we can extract the normalized free energy $\widehat{F}(z, g_s) = \log Z - \log Z_G$ from the continuum limit of (6.2.99), namely

$$\mathrm{e}^{\widehat{F}(z+g_s, g_s) + \widehat{F}(z-g_s, g_s) - 2\widehat{F}(z, g_s)} = \frac{R(z, g_s)}{z}, \tag{6.2.102}$$

or equivalently

$$\widehat{F}(z + g_s, g_s) + \widehat{F}(z - g_s, g_s) - 2\widehat{F}(z, g_s) = \log(\frac{R(z, g_s)}{z}). \tag{6.2.103}$$

This implies for the coefficients $F^{(\ell)}$

$$\mathrm{e}^{-\ell \frac{\widehat{A}(z+g_s)}{g_s}} \widehat{F}^\ell(z + g_s, g_s) + \mathrm{e}^{-\ell \frac{\widehat{A}(z-g_s)}{g_s}} \widehat{F}^\ell(z - g_s, g_s) - 2\mathrm{e}^{-\ell \frac{\widehat{A}(z)}{g_s}} \widehat{F}^\ell(z, g_s) = \mathrm{e}^{-\ell \frac{\widehat{A}(z)}{g_s}} \left[\frac{R^{(\ell)}(z, g_s)}{R^{(0)}(z, g_s)} \right]_c, \tag{6.2.104}$$

where $\left[\frac{R^{(\ell)}(z,g_s)}{R^{(0)}(z,g_s)} \right]_c$ is the connected piece

$$\begin{aligned} \left[\frac{R^{(\ell)}(z, g_s)}{R^{(0)}(z, g_s)} \right]_c &= \sum_{s \geq 1} \frac{(-1)^{s-1}}{s} \sum_{l_1 + \cdots l_s = l} \frac{R^{(\ell_1)}(z, g_s)}{R^{(0)}(z, g_s)} \cdots \frac{R^{(\ell_s)}(z, g_s)}{R^{(0)}(z, g_s)} \\ &= c_{\ell,0}(z) \left(1 + \sum_{n=1}^{\infty} g_s^n c_{\ell,n}(z) \right). \end{aligned} \tag{6.2.105}$$

Plugging (6.2.100),(6.2.101),(6.2.105) in (6.2.104) and expanding in g_s, we obtain the following relations:

$$\begin{aligned}
\widehat{F}_0^{(\ell)}(z) &= \frac{1}{4}c_{\ell,0}(z)\mathrm{csch}^2\Big(\frac{\ell A'(z)}{2}\Big),\\
\widehat{F}_1^{(\ell)}(z) &= c_{\ell,1}(z) + \frac{c'_\ell(z)}{c_\ell(z)}\coth\left(\frac{\ell A'(z)}{2}\right) - \ell A''(z)\left(\frac{\ell}{2}\coth^2\Big(\frac{\ell A'(z)}{2}\Big) + \frac{1}{4}\mathrm{csch}^2\Big(\frac{\ell A'(z)}{2}\Big)\right),\\
\widehat{F}_2^{(\ell)}(z) &= c_{\ell,2} + \frac{c'_{\ell,0}}{c_{\ell,0}}\left[c_{\ell,1}\coth\left(\frac{\ell A'(z)}{2}\right) - \ell A''(z)\left(\frac{\coth\left(\frac{\ell A''(z)}{2}\right)}{2} + \frac{3\cosh\left(\frac{\ell A''(z)}{2}\right)}{2\sinh^3\left(\frac{\ell A''(z)}{2}\right)}\right)\right]\\
&\quad - \ell A''(z)c_{\ell,1}\left[\frac{1}{2} + \frac{3}{4}\mathrm{csch}^2\left(\frac{\ell A''(z)}{2}\right)\right] + c'_{\ell,1}\coth\left(\frac{\ell A''(z)}{2}\right) + \frac{c''_{\ell,0}}{c_{\ell,0}}\left[\frac{\coth^2\left(\frac{\ell A''(z)}{2}\right)}{2} + \frac{\mathrm{csch}^2\left(\frac{\ell A''(z)}{2}\right)}{4}\right]\\
&\quad - \ell A^{(3)}\frac{\coth\left(\frac{\ell A''(z)}{2}\right)}{6}\left(1 + 3\mathrm{csch}^2\left(\frac{\ell A''(z)}{2}\right)\right)\\
&\quad + \ell^2(A''(z))^2\left[\frac{\coth^2\left(\frac{\ell A''(z)}{2}\right)}{8} + \frac{13\mathrm{csch}^2\left(\frac{\ell A''(z)}{2}\right)}{16} + \frac{15\mathrm{csch}^4\left(\frac{\ell A''(z)}{2}\right)}{16}\right].
\end{aligned} \tag{6.2.106}$$

6.2.6 An explicit example: The cubic matrix model

We now use the above transseries formalism to compute the amplitudes $Z^{(\ell)}$ independently for the cubic matrix model *off criticality*, in order to test our results about multi-instantons from section 6.2.3. A similar computation has been performed in [174] for the quartic model.

Consider the cubic matrix model with potential

$$V(M) = -M + \frac{M^3}{3}. \tag{6.2.107}$$

The recursion relation for the coefficients r_n reads [118]

$$r_n\left(\sqrt{1 - r_n - r_{n+1}} + \sqrt{1 - r_n - r_{n-1}}\right) = g_s\frac{n}{N}. \tag{6.2.108}$$

The continuum limit of equation (6.2.108) is

$$R(t, g_s)\left(\sqrt{1 - R(t, g_s) - R(t + g_s, g_s)} + \sqrt{1 - R(t, g_s) - R(t - g_s)}\right) = t. \tag{6.2.109}$$

At lowest order, we find

$$2R_0^{(0)}(t)\sqrt{1 - 2R_0^{(0)}(t)} = t. \tag{6.2.110}$$

It turns out to be convenient to express everything in terms of a new variable $R_{0,0}(t) \equiv r$. Expanding eqn. (6.2.109) and solving recursively, we can compute in this way the coefficients $R_{l,n}(r(t))$. The first few read

$$\begin{aligned}
R_2^{(0)}(t) &= -\frac{(9r - 5)}{32(1 - 3r)^4} \qquad & R_4^{(0)}(t) &= -\frac{3\left(162r^3 + 1017r^2 - 1316r + 385\right)}{2048(3r - 1)^9}\\
R_0^{(1)}(t) &= \frac{\sqrt{r}}{\sqrt[4]{3r - 1}} \qquad & R_1^{(1)}(t) &= \frac{9r^2 - 12r + 8}{192(1 - 3r)^{\frac{5}{2}}}.
\end{aligned} \tag{6.2.111}$$

With these functions at hand, we can compute the free energies using (6.2.106) and compare to our prediction (6.2.78). We find

$$\begin{aligned} F^{(1)} &= -\frac{\sqrt{r}}{4(3r-1)^{\frac{5}{4}}}\left(1 - g_s\frac{8+228r-423r^2}{192r(1-3r)^{\frac{5}{2}}} + \mathcal{O}(g_s^2)\right) \\ F^{(2)} &= -\frac{r}{32(3r-1)^{\frac{5}{2}}}\left(1 + g_s\frac{-8-228r+429r^2}{96r(1-3r)^{\frac{5}{2}}} + \mathcal{O}(g_s^2)\right) \\ F^{(3)} &= -\frac{r^{\frac{3}{2}}}{192(3r-1)^{\frac{15}{4}}}\left(1 + g_s\frac{-8-228r+429r^2}{64r(1-3r)^{\frac{5}{2}}} + \mathcal{O}(g_s^2)\right). \end{aligned} \tag{6.2.112}$$

Indeed, these results show the predicted structure

$$F_0^{(\ell)} = (-1)^{\ell-1}\frac{\left(F_0^{(1)}\right)^\ell}{\ell} \qquad \frac{F_1^{(\ell)}}{\ell} = \text{const.},\ \ell \geq 2. \tag{6.2.113}$$

In order to explicitly verify (6.2.78), we take it as an ansatz for the one-and two instanton expressions $F^{(1)},\ F^{(2)}$ and thereby extract the supposed quantities $\partial_s\widehat{F}_1(t)+\frac{1}{6}\partial_s^3\widehat{F}_0$ and $\hat{q} = \mathrm{e}^{\partial_s^2\widehat{F}_0}$. We find from the above expressions

$$\hat{q} = -\frac{r}{32\,(1-3r)^{\frac{5}{2}}}, \tag{6.2.114}$$

$$\left(\partial_{t_2} - \partial_{t_1}\right)\widehat{F}_1 = \frac{-57r^2+60r-8}{192r(1-3r)^{\frac{5}{2}}} \tag{6.2.115}$$

and

$$\left(\partial_{t_2}^3 - 3\partial_{t_1}\partial_{t_2}^2 + 3\partial_{t_1}^2\partial_{t_2} - \partial_{t_1}^3\right)\widehat{F}_0 = \frac{-183r^2+84r+8}{16r(1-3r)^{\frac{5}{2}}} \tag{6.2.116}$$

which is precisely what one finds from our analytical expressions (6.2.86),(6.2.93) and (6.2.94), specialized to the cubic model. This is a highly non-trivial test of of the formula (6.2.68).

6.3 Multi-instantons in 2d gravity

We can also test the formula (6.2.68) for the multi-instanton expansion against the double scaling limit of the cubic matrix model. Along the way, we will state a prediction about a hidden structure in solutions of the Painlevé I equation that is implicit in the multicut formula, and check it against the loop expansion around higher-instanton solutions of Painlevé I obtained by the transseries formalism.

The critical point of the cubic model is at

$$g_s \to 0, \qquad t \to t_c = \frac{2}{3\sqrt{3}}, \qquad r \to \frac{1}{3}. \tag{6.3.117}$$

At this point, the functions $R^{(\ell)}$ diverge, but the double-scaled variable

$$z^{\frac{5}{4}} = (t_c - t)^{\frac{5}{4}}3^{\frac{5}{8}}g_s^{-1} \tag{6.3.118}$$

is kept finite, and in this limit,

$$u(z) = (3R(z)-1)\,g_s^{-\frac{2}{5}} \tag{6.3.119}$$

satisfies the Painlevé I equation

$$u(z)^2 - \frac{1}{6}u''(z) = z, \tag{6.3.120}$$

as can be deduced from the difference equation (6.2.109).

6.3.1 An all-instanton solution to the Painlevé I equation

In this case, the multi-instanton contributions can be obtained by finding a trans-series solution

$$u(z) = \sum_{\ell \geq 0} \zeta^\ell u^{(\ell)}(z). \tag{6.3.121}$$

to the Painlevé I equation. One obtains a set of recursion equations for the $u^{(\ell)}(z)$ of the form,

$$-\frac{1}{6}(u^{(\ell)})'' + \sum_{k=0}^{\ell} u^{(k)} u^{(\ell-k)} = 0. \tag{6.3.122}$$

We will change variables to

$$z^{-\frac{5}{4}} = \sqrt{3}x. \tag{6.3.123}$$

Each $u^{(\ell)}(x)$ has the structure

$$u^{(\ell)}(x) = u_0^{(\ell)} x^{\frac{\ell}{2}-\frac{2}{5}} \mathrm{e}^{-\ell A/x} \epsilon^{(\ell)}(x), \tag{6.3.124}$$

where

$$A = \frac{8}{5}, \qquad \epsilon^{(\ell)}(x) = 1 + \sum_{k=1}^{\infty} u_k^{(\ell)} x^k. \tag{6.3.125}$$

In (6.3.121) ζ parametrizes the nonperturbative ambiguity. In principle the value of $u_0^{(1)}$ is not fixed by the recursion and it could be absorbed in ζ. However, if we choose ζ to be identical to the nonperturbative ambiguity appearing in the matrix model, then the value of $u_0^{(1)}$ is fixed and will be derived below.

It is convenient to reorganize the series in a different form [148]. We write

$$\begin{aligned} u &= \sum_{n=0}^{\infty} \epsilon_n = \sum_{n=0}^{\infty} x^{n/2-2/5} \mathrm{e}^{-nA/x} \sum_{k=0}^{\infty} u_k^{(n)} x^k \\ &= x^{-\frac{2}{5}} \sum_{n=0}^{\infty} \sum_{k=0}^{\infty} \xi^n u_k^{(n)} x^k \\ &= u_k^{(0)} x^{k-\frac{2}{5}} + u^{\mathrm{np}}(x,\xi), \end{aligned} \tag{6.3.126}$$

where

$$\xi = x^{\frac{1}{2}} \mathrm{e}^{-A/x}, \tag{6.3.127}$$

and we have split u into the zero-instanton solution and the non-perturbative part $u^{np}(x,\xi)$.

This can be plugged into the string equation (6.3.121) and one finds the recursion relation

$$\begin{aligned} u_k^{(n)} =& \frac{3^{\frac{1}{5}}}{2(1-n^2)} \Bigg[\frac{25}{64} \left\{ \left(\frac{n}{2} - \frac{12}{5} + k\right) \left(\frac{n}{2} - \frac{8}{5} + k\right) u_{k-2}^{(n)} + (n-3+2k) n A u_{k-1}^{(n)} \right\} \\ & - \sum_{n'=1}^{n-1} \sum_{k' \geq 0} u_{k-k'}^{(n-n')} u_{k'}^{(n')} - 2 \sum_{k' \geq 0}^{k-1} u_{k'}^{(n)} u_{k-k'}^{(0)} \Bigg]. \end{aligned} \tag{6.3.128}$$

For the leading coefficients $u_0^{(n)}$, $n > 1$, we find the recursion

$$u_0^{(n)} = \frac{3^{\frac{1}{5}}}{2n^2 - 2} \sum_{n'=1}^{n-1} u_0^{(n')} u_0^{(n-n')}, \tag{6.3.129}$$

with explicit solution

$$u_0^{(n)} = \frac{12n}{4^n 3^{\frac{4n+1}{5}}} (u_0^{(1)})^n. \tag{6.3.130}$$

The recursion (6.3.128) easily produces $u(x,\xi)$ to very high orders in both loops and instantons. From the coefficients $u_k^{(n)}$ we can then obtain the free energy. It has the structure

$$F_{\rm ds}(z) = F^{(0)}(z) + F^{\rm np}(z) = \sum_{\ell=0}^{\infty} \zeta^\ell F_{\rm ds}^{(\ell)}(z), \tag{6.3.131}$$

where the $F_{\rm ds}^{(\ell)}$ are functions of x of the form

$$F_{\rm ds}^{(\ell)}(x) = d_\ell x^{\ell/2} {\rm e}^{-\ell A/x}\Big(1 + f_{\ell,1} x + \cdots\Big), \tag{6.3.132}$$

and

$$d_\ell = -\frac{3^{1/5} u_0^{(\ell)}}{12\ell^2}, \qquad f_{\ell,1} = u_1^{(\ell)} - \frac{5}{8} + \frac{1}{8\ell}. \tag{6.3.133}$$

However, the Painlevé I equation can also be analyzed analytically, as it has been done in [148]. One can write

$$u^{\rm np}(x,\xi) = x^{-\frac{2}{5}} \sum_{k=0}^{\infty} x^k f_k(\xi). \tag{6.3.134}$$

The differential equations for $u^{\rm np}$ can then be translated in a series of differential equations for the $f_k(\xi)$, and it turns out that these functions are *rational* [148]. We find for example

$$f_0(\xi) = \frac{12 d_1 \xi}{(1+d_1\xi)^2}, \qquad f_1(\xi) = \frac{-\frac{3}{2} d_1\xi + \frac{35}{2} d_1^2 \xi^2 - 3 d_1^3 \xi^3 - \frac{1}{5} d_1^4 \xi^4}{(1+d_1\xi)^3}. \tag{6.3.135}$$

From $u^{\rm np} = -\partial_z^2 F^{\rm np}$, we find using the transseries ansatz $F^{\rm np}(x,\xi) = \sum_k x^k F_k^{\rm np}(\xi)$

$$\begin{aligned} f_0(\xi) &= -4\ 3^{\frac{4}{5}} \xi \partial_\xi \left(\xi \partial_\xi F_0^{\rm np}(\xi)\right) \\ f_1(\xi) &= -\frac{1}{2} 3^{\frac{4}{5}} \xi \left(4 \partial_\xi F_0^{\rm np}(\xi) + 5 \xi \partial_\xi^2 F_0^{\rm np}(\xi) + 8 \partial_\xi \left(\xi \partial_\xi F_1^{\rm np}(\xi)\right)\right) \end{aligned} \tag{6.3.136}$$

and accordingly

$$F_0^{\rm np}(\xi) = \log\left(1 + d_1 \xi\right), \qquad F_1^{\rm np}(\xi) = -\frac{d_1 \xi (2 d_1 \xi + 111)}{192 (d_1 \xi + 1)}, \tag{6.3.137}$$

and so on.

6.3.2 Comparison with the multicut prediction

We now analyse the predictions the multicut matrix model makes for these solutions of the string equation. The structure (6.2.68) leads, in the double scaling limit, to

$$Z_{\rm ds}^{(\ell)} = \frac{x^{\ell^2/2}}{(2\pi)^{\frac{\ell}{2}}} G_2(\ell+1) \zeta^\ell C^{\ell^2} {\rm e}^{-\ell A/x} \Big[1 - x\Big(\ell \phi_{1,1} + \frac{\ell^3}{6} \phi_{0,3}\Big) + \mathcal{O}(g_s^2)\Big]. \tag{6.3.138}$$

In this equation, C, $\phi_{1,1}$ and $\phi_{0,3}$ are numbers which can be obtained from the double-scaling limit of th quantities $\hat{q}^{1/2}$, $\partial_s \hat{F}_1$ and $\partial_s^3 \hat{F}_0$ that we computed in section 6.2.4. We find

$$C = \frac{-{\rm i}\sqrt{2}}{8\sqrt{3}}, \qquad \phi_{1,1} = \frac{17}{192}, \qquad \phi_{0,3} = \frac{47}{16}. \tag{6.3.139}$$

Notice that

$$\frac{C}{\sqrt{2\pi}} = -\frac{1}{3^{\frac{3}{4}} \cdot 4} S \tag{6.3.140}$$

where

$$S = \mathrm{i}\frac{3^{\frac{1}{4}}}{2\sqrt{\pi}} \tag{6.3.141}$$

is the Stokes parameter for the Painlevé I equation (6.3.121) across the Stokes line $\arg z = 0$. This is precisely what we obtain from comparing the transseries solution at one and two instantons to the ansatz (6.3.138) and solving for the unknowns $C, \phi_{1,1}$ and $\phi_{0,3}$. All higher instanton sectors confirm this structure.

One thing that we can verify with little effort is the value of C. Indeed, we can see that the recursion relations obtained from Painlevé I, together with the structure (6.3.138) coming from the multicut analysis, fix the value of C, and in particular the value of the Stokes parameter. This is not something to be expected, since the Stokes parameter encodes nontrivial information about the differential equation (see for example [179]). Let us see how this works. Looking at $Z_{\mathrm{ds}}^{(1)}$ and comparing (6.3.138) with (6.3.132) and (6.3.133) we find,

$$C = -\sqrt{2\pi}\frac{3^{1/5}}{12}u_0^{(1)}. \tag{6.3.142}$$

Let us now look at $Z_{\mathrm{ds}}^{(2)}$. The string equation gives,

$$Z_{\mathrm{ds}}^{(2)} = \mathrm{e}^{-2A/x}x^2(d_2 f_2 + d_1^2 f_1) + \mathcal{O}(x^3) = -\frac{\left(u_0^{(1)}\right)^2}{4608\cdot 3^{3/5}}\mathrm{e}^{-2A/x}x^2 + \mathcal{O}(x^3). \tag{6.3.143}$$

On the other hand, from (6.3.138) we find that the coefficient of x^2 in $Z_{\mathrm{ds}}^{(2)}$ should be

$$\frac{1}{2\pi}C^4. \tag{6.3.144}$$

Comparing both values and using (6.3.142) we obtain an equation for $\left(u_0^{(1)}\right)^2$ which gives

$$\left(u_0^{(1)}\right)^2 = -\frac{3^{3/5}}{4\pi}. \tag{6.3.145}$$

This determines C, and in turn S, in perfect agreement with the result obtained from the double-scaling limit of the cubic matrix model.

The structure (6.3.138) predicted by the multi-cut analysis of the multi-instanton amplitude is not at all manifest from the analysis we have made of the string equation. By exponentiating the free energies, we find for the total partition function

$$1 + \sum_{\ell\geq 1}\zeta^\ell Z_{\mathrm{ds}}^{(\ell)} = \exp\Big[\sum_{\ell=1}^{\infty}\zeta^\ell F_{\mathrm{ds}}^{(\ell)}\Big], \tag{6.3.146}$$

or, more explicitly,

$$Z_{\mathrm{ds}}^{(\ell)} = \sum_{s\geq 1}\frac{1}{s!}\sum_{\ell_1+\cdots+\ell_s=\ell} F_{\mathrm{ds}}^{(\ell_1)}\cdots F_{\mathrm{ds}}^{(\ell_s)} \tag{6.3.147}$$

Since $F_{\mathrm{ds}}^{(\ell)}$ goes like $x^{\ell/2}$, one expects from (6.3.147) that the $Z_{\mathrm{ds}}^{(\ell)}$ are generically proportional to $x^{\ell/2}$. But (6.3.138) implies that in fact $Z_{\mathrm{ds}}^{(\ell)}$ goes like $x^{\ell^2/2}$. This is because, as we explained above, the instanton gas is ultra-dilute. Hence there must be nontrivial cancellations among the first $\ell(\ell-1)/2$ coefficients of the right-hand side of (6.3.147). We can now check this against the trans-series solution of the string equation.

The first thing one can verify analytically is that the term of order $x^{\ell/2}$ in $Z_{\mathrm{ds}}^{(\ell)}$ vanishes. But this is in fact a consequence of

$$u_0^\ell = \frac{(-1)^{\ell-1}}{n}(u_0^1)^\ell, \tag{6.3.148}$$

which follows from the explicit solution to the recursion (6.3.129).

Furthermore, consider the nonperturbative partition sum

$$Z^{\rm np} = \exp\, F^{\rm np}, \tag{6.3.149}$$

which we write as

$$Z^{\rm np} = \sum_{k\geq 0} x^k Z_k(\xi) = 1 + \sum_{k\geq 0}\sum_{n\geq 1} x^k \xi^n z_{k,n}. \tag{6.3.150}$$

Based on the multicut prediction (6.3.138), we have the conjecture that for each n, the starting power of x is $n^2/2$. But the total power of x in the expression above, for each fixed n, is

$$x^{k+n/2} \tag{6.3.151}$$

Our conjecture says that $z_{k,n}$ must vanish for

$$k + \frac{n}{2} < \frac{n^2}{2} \Rightarrow k < \frac{n(n-1)}{2}. \tag{6.3.152}$$

Therefore, for fixed k, as soon as n is such that the above inequality holds, $z_{k,n}$ vanish. In other words, $z_{k,n}$ is only different from zero for the *finite* number of ns such that

$$\frac{n(n-1)}{2} \leq k. \tag{6.3.153}$$

Let us denote by $n_{\rm m}(k)$ the maximum number satisfying this bound. We have, for example

$$n_{\rm m}(0) = 1, \qquad n_{\rm m}(1) = 2, \qquad n_{\rm m}(2) = 2, \cdots. \tag{6.3.154}$$

We then conclude that

$$Z_k(\xi) = \delta_{k0} + \sum_{n\geq 1} z_{k,n}\xi^n = \delta_{k0} + \sum_{n=1}^{n_{\rm m}(k)} z_{k,n}\xi^n \tag{6.3.155}$$

is a *polynomial* whose degree is $n_{\rm m}(k)$. Since

$$Z_0 = {\rm e}^{F_0} = 1 + d_1\xi \tag{6.3.156}$$

which is indeed a polynomial of degree 1, we confirm the conjecture for $k = 0$. Similarly, we find using the $F^{\rm np}(\xi)$ computed above,

$$\begin{aligned}
Z_1 &= -\frac{1}{192} d_1\xi(2d_1\xi + 111)\\
Z_2 &= \frac{d_1\xi(1048 d_1\xi + 19299)}{24576}\\
Z_3 &= -\frac{d_1\xi\left(160 d_1^2\xi^2 + 11705160 d_1\xi + 114670521\right)}{70778880}\\
Z_4 &= \frac{d_1\xi\left(552320 d_1^2\xi^2 + 12466492352 d_1\xi + 79686828333\right)}{18119393280}\\
Z_5 &= -\frac{d_1\xi\left(331932480 d_1^2\xi^2 + 3646348240864 d_1\xi + 17179325749341\right)}{1159641169920}.
\end{aligned} \tag{6.3.157}$$

The above Z_k are *polynomials* in ξ of the right order $n_m(k)$. Furthermore, one can easily recover from these expansions in ξ at fixed order in g_s the converse expansions in g_s at fixed instanton number and check that they reproduce the form involving the Barnes function (6.2.68).

Conclusion

In this chapter, we have extended some of the results of the previous one to the multi-cut/multi-instanton case. We have found a generic expression for the ℓ–instanton amplitude based on the identification of the higher instanton sectors with multicut solutions with the appropriate filling fractions. We performed several highly nontrivial checks of our general formula. In particular, it is correct for the cubic matrix model and in the double-scaling limit at the critical point. In both these cases, we compute higher-instanton amplitudes independently using a transseries formalism put forward in [174].

Part IV

CONCLUSION

In this thesis, we have shed some light on various aspects of topological string theory. However, much remains yet to be done.

Over the last years, there have been many important new developments concerning the computational accessibility of topological amplitudes. The method of direct integration presented in chapter 2 has contributed to simplifying the task. Furthermore, in a remarkable tour de force the amplitudes have been computed on the quintic up to genus 51 [69]. Yet, the problem of completely solving the topological string even on simple compact Calabi-Yau manifolds remains open. A promising approach might be extending the formalism of [73] to exploit the full diffeomorphism symmetry group to constrain the solution, analogously to the approach that led to the full solution in the open case [180]. Along the way, this should also lead to a better understanding of nonperturbative aspects. It may also well be possible to push further the formalism developed in chapter 2. In section 2.5 we have introduced a set of holomorphic automorphic forms on the Enriques moduli space which might be enough to parametrize the holomorphic ambiguity. Using these forms, the boundary conditions obtained from the field theory and the fiber limits, and some extra information coming for example from Gromov–Witten theory, one might be able to obtain the topological string amplitudes at higher genus.

The results in chapter 2 have in the meantime been applied to the microscopic counting of degrees of freedom for 5d spinning black holes [181], as suggested in [182]. Furthermore, as we have explained in section 4.2, the holomorphic anomaly equations can be rigorously derived within the matrix model. It would therefore be interesting to combine the results of chapter 2 with those of chapters 5 and 6. One main advantage of the matrix model formulation of the B-model is that the full recursive equations for the matrix model amplitudes –even though they imply the holomorphic anomaly equations– are completely determined and don't give rise to any holomorphic ambiguities. Hence, the two approaches combined could provide an efficient, completely determined method to solve the topological string anywhere in moduli space.

From a mathematical point of view, a concrete proof of the generalized integrality conjectures related to Gromov-Witten, Gopakumar-Vafa and Donaldson-Thomas invariants would be desirable, as proofs are generally rare treats in string theory and would put many ideas on firmer ground. Also, proving these conjectures beyond the string motivated cases would probably involve a deeper understanding of the corresponding duality web. A rigorous mathematical framework for computing Gromov-Witten invariants along the fiber of certain K3-fibrations has been established in [62, 183]. With these techniques, one might be able to prove some of the physical predictions made in chapter 3 for Calabi-Yau manifolds of this type.

The matrix model formulation of the B-model and the implications for nonperturbative computations offer many fascinating directions of future research. For instance, one model with a known matrix model description which we have not studied in chapter 5 is topological string theory on the resolved conifold. This theory can be described by a Hermitian matrix model with a potential of the form $(\log x)^2$, which has a global minimum at $x = 1$ and no saddles [184]. In principle, the way to address the large–order behavior in such cases is to deform the model, in order to obtain an unstable potential with a calculable one–instanton amplitude. The original potential is then recovered by analytic continuation [156, 50]. However, we have not found a suitable deformation which allows one to find the large–order behavior for this potential. In fact, we would face the same problems if we were to address the large–order behavior of the perturbation series for the ground–state energy of a $(\log x)^2$ potential in quantum mechanics. This is a situation which, to the best of our knowledge, has also not been addressed in the literature. Furthermore, a more geometric formulation of the instanton contribution computed in this paper, along the lines of the approach in [33], would be desirable. Although our expressions only depend on the form of the spectral curve, in principle they are only suitable for a genus–zero curve written in the form (4.1.20).

The most pressing problem is to extend the large-order analysis in chapter 5 to more complicated topological string models, with multi-cut matrix model descriptions. As we have shown

explicitly in chapter 6, the general multi–cut model with fixed filling fractions can be regarded as a matrix model in a generic, fixed multi–instanton sector, and by studying nearby filling fractions one obtains a general framework to address multi–instanton effects in matrix models. Some aspects of this framework were already discussed in [172], albeit in a different context. These results should now be applied to topological string theory. The effects we computed in chapter 6 should obviously correspond to nonperturbative effects in string theories that have already been found to admit a matrix model description, such as local $\mathbb{P}^2$ or local $\mathbb{P}^1 \times \mathbb{P}^1$, both studied in [34]. In particular, the latter geometry has a special limit where it leads to pure $SU(2)$ Seiberg-Witten theory [88]. It has already been observed in [185] that $SU(2)$ Seiberg-Witten theory should indeed admit a matrix model description. As we have done in the previous chapter, the results of the instanton computation could be compared to the asymptotic behaviour of these theories. This would allow for computation of nonperturbative effects on new and interesting toric backgrounds, such as the case of local $\mathbb{P}^2$, and would also be an important step in further strengthening our understanding of nonperturbative effects in topological string theory. It might even give hints for the future study of these effects in compact backgrounds.

A related aspect is that the topological string models we have studied in chapter 5 are not very conventional, since they correspond to toric diagrams with intersecting lines, and this is reflected in the fact that their spectral curve is pinched. One could smooth out these models by resolving the singularity, obtaining in this way a spectral curve of genus one with two cuts. In the context of noncritical string theory, this process is interpreted as adding ZZ branes to the background [136]. It would be very interesting to see if this leads to some geometric transition from the local curve backgrounds to other topological string backgrounds.

Nonperturbative effects of order e^{-N} can also be found in models defined by sums over partitions, such as two–dimensional Yang–Mills theory [186, 187]. These effects have been used in holographic descriptions of topological string theory [188, 189]. It would be interesting to see if there is any relation between this description and the one we have proposed in terms of matrix models.

Most of all, it would be desirable to promote the matrix-model inspired formalism to a full duality, in the sense of associating not only a spectral curve and a formalism to generate amplitudes, but a well-defined matrix model –including a potential– to a given B-model geometry. It is however not yet clear if such a potential always exists and if it is unique. Furthermore, the nonperturbative effects that we identified in the one-cut case from the traces they leave in the asymptotics of the perturbation series deserve further investigation. Eventually, one should find a full nonperturbative description of the topological string, possibly involving hypermultiplets. This might imply merging our study with the effects investigated by [165]. For the more complicated geometries described by two-cut matrix models, the precise asymptotics and corresponding nonperturbative effects have yet to be identified.

Another puzzling issue related to the multicut models is the interplay between background independence, holomorphic anomaly and modularity. As Witten has observed a long time ago [173], there is a close analogy between background independence and the holomorphic anomaly. In turn, as we have seen in chapter 2, the topological string free energies are modular functions. This structure is again related to the holomorphic anomaly, since modularity or holomorphicity is but a matter of polarization [73]. It would be interesting to check explicitly that our multicut/multiinstanton formalism in the theta-resummation satisfies background independence, and to understand the implications for the modular structure of the amplitudes.

The issue of nonperturbative definitions in terms of gauge theories is obviously central not only in topological strings, but in string theory as a whole. If the AdS-CFT conjecture could be proved, possibly along the lines of [190, 55], one could comfortably take the well-defined holographic gauge theory as a nonperturbative definition of string theory. However, even then a better understanding of the full duality map would still be necessary, and one would need to find holographic descriptions for more general backgrounds.

Summarizing, many aspects of the delicate interplay of topological strings, matrix models and gauge theories clearly remain to be understood. Still, in spite of all these unsolved problems, the topological string has been a source of much challenge, surprise and joy; at least for the author, who personally believes it can yet provide many more hints and clues about the sense in which string theory is a theory of nature.

Appendix A

Heterotic techniques

A.1 Lattice reduction

In [41], Borcherds developed the technique of lattice reduction to compute integrals of the form

$$\Phi_\Gamma = \int_{\mathcal{F}} \frac{d^2\tau}{\tau_2^2} F_M(\tau)\Theta_M(\tau,\gamma_1,\gamma_2;P,\phi), \tag{A.1.1}$$

where M is a lattice of signature (b^+,b^-), $\Theta_M(\tau,\gamma_1,\gamma_2;P,\phi)$ is the generalized Siegel theta function with projection P and polynomial insertion ϕ as defined in appendix C.1 and F_M is a (quasi) modular form of weight $(-\frac{b^-}{2}-m^-,-\frac{b^+}{2}-m^+)$ that can be constructed from a (quasi) modular form F with weights $(\frac{b^+}{2}+m^+-\frac{b^-}{2}-m^-,0)$ as $F_M = {\tau_2}^{\frac{b^+}{2}+m^+}F$. The integral (A.1.1) can be decomposed into a sum over a reduced lattice K of signature (b^+-1,b^--1) and a new integral Φ_K involving K instead of M ([41], Theorem 7.1). Iterating this procedure, on arrives at an integral Φ_{K_f} with a lattice K_f of signature $(b^+-b^-,0)$ respectively $(0,b^--b^+)$ that can in principle be solved using standard methods.
The reduction steps proceed as follows. Choose two vectors z, z' in M with z primitive and $(z,z)=0$, $(z,z')=1$. The reduced lattice is then defined as $K=\frac{M\cap z^\perp}{\mathbb{Z}_z}$. We also define reduced projections $\tilde{P}$ in a natural way:

$$\tilde{P}_\pm(\lambda) = P_\pm(\lambda) - \frac{(P_\pm(\lambda),z_\pm)}{z_\pm^2}z_\pm. \tag{A.1.2}$$

We can then expand the polynomial ϕ in terms of $(\lambda,z_\pm)$ as

$$\phi(P(\lambda)) = \sum_{h^+,h^-} = (\lambda,z_+)^{h^+}(\lambda,z_-)^{h^-}\phi_{h^+,h^-}(\tilde{P}(\lambda)). \tag{A.1.3}$$

The statement of Borcherds' theorem is then that with these conventions, z_+^2 *sufficiently small* and $\tilde{P}_+(\lambda_K)\neq 0$, Φ_M is given by

$$\begin{aligned}
&\frac{\sqrt{2}}{|z_+|}\sum_{h\geq 0}\sum_{h^+,h^-}\frac{h!(-z_+^2/\pi)^h}{(2i)^{h^++h^-}}\binom{h^+}{h}\binom{h^-}{h}\sum_j\sum_{\lambda_K\in K}\frac{(-\Delta)^j(\bar{\phi}_{h^+,h^-})(\tilde{P}(\lambda))}{(8\pi)^j j!}\\
&\cdot\sum_{l,t} q^{l(\lambda_K,(-z'+\frac{z_+}{2z_+^2}+\frac{z_-}{2z_-^2}))}c(\lambda_K^2,t)l^{h^++h^--2h}\left(\frac{l}{2|z_+||\tilde{P}_+(\lambda_K)|}\right)^{h-h^+-h^--j-t+\frac{b^+}{2}+m^+-3/2}\\
&K_{h-h^+-h^--j-t-b^+/2+m^+-3/2}\left(\frac{2\pi l|\tilde{P}_+(\lambda_K)|}{|z_+|}\right).
\end{aligned} \tag{A.1.4}$$

For $\tilde{P}_+(\lambda)=0$, the last two factors have to be replaced by the analytic continuation at $\epsilon=0$ of

$$\left(\frac{\pi l^2}{2z_+^2}\right)^{h-h^+-h^--j-t+b^+/2+m^+-3/2-\epsilon} \Gamma(-h+h^++h^-+j+t-b^+/2-m^++3/2+\epsilon). \quad \text{(A.1.5)}$$

A.2 The antiholomorphic dependence of the heterotic $F^{(g)}$

In this appendix we discuss the antiholomorphic dependence of $F^{(g)}(t,\bar{t})$ in heterotic theories. In section A.2.1, we show how the complicated result of the heterotic computation of the $F^{(g)}$ in the STU-model given in [29] can be simplified, along the lines of [41]. In section A.2.2 we write down the result for $F_E^{(g)}$ on the Enriques Calabi-Yau and derive (2.4.110).

A.2.1 A simple form for $F^{(g)}$ in the STU-model

In [29], an explicit expression for the holomorphic and antiholomorphic dependence of the topological amplitudes in the fiber limit of the STU-model was found. This expression is obtained from a one–loop computation in the dual heterotic theory, given by the integral (2.4.94), which is then performed by using the technique of lattice reduction [41]. One finds that $F^{(g)}=F^{(g)}_{\rm deg}+F^{(g)}_{\rm ndeg}$, where [29]

$$F^{(g)}_{\rm deg}=4\pi^2U_1\delta_{g,1}+\frac{2^{2g-1}\pi^{4g-3}}{T_1^{2g-3}}\sum_{l=0}^{g}c_g(0,l)\frac{l!}{\pi^{l+3}}\left(\frac{T_1}{U_1}\right)^l\zeta(2(2+l-g)), \quad \text{(A.2.6)}$$

$$\begin{aligned}
F^{(g>1)}_{\rm ndeg}&=4\pi^{2g-2}(-1)^{g-1}\sum_{r\neq0}\sum_{l=0}^{g}\sum_{h=0}^{2g-2}\sum_{j=0}^{[g-1-h/2]}\sum_{a=0}^{s}c_g(r^2/2,l)\frac{(2\pi)^l(2g-2)!}{j!h!(2g-h-2j-2)!}\\
&\times\frac{(-1)^{j+h}}{2^{j+a}}\frac{(s+a)!}{a!(s-a)!}(\mathrm{sgn}\,(\mathrm{Re}(r\cdot y))^h\,\frac{1}{(T_1U_1)^l}\,(\mathrm{Re}(r\hat{\cdot}y))^{l-j-a}\,\mathrm{Li}_{3+a+j+l-2g}(\mathrm{e}^{-r\hat{\cdot}y})\\
&+\frac{2\pi^{3g-3}c_g(0,g-1)}{(T_1U_1)^{g-1}}\sum_{s=0}^{g-1}(-1)^s\frac{(2g-2)!}{s!(g-1-s)!}\psi(\frac{1}{2}+s)\\
&+\sum_{\substack{l=0\\ l\neq g-1}}^{g}4^{l+g}\pi^{2g+l-5/2}c_g(0,l)\frac{\zeta(3+2(l-g))}{(T_1U_1)^l}\\
&\times\sum_{s=0}^{g-1}(-1)^s2^{2(s-2g)+5}\frac{(2g-2)!}{(2s)!(g-1-s)!}\Gamma\Big(\frac{3}{2}+s+l-g\Big).
\end{aligned} \quad \text{(A.2.7)}$$

We refer to $F^{(g)}_{\rm deg}$, $F^{(g)}_{\rm ndeg}$ as the degenerate and nondegenerate contributions, respectively. Also, $s:=|2g-2-h-j-l-1/2|-1/2$; $\quad y=(T,U)$, $\quad$ the complex norm is defined as $r^2=2r_1r_2$, and $r\hat{\cdot}y\equiv|\mathrm{Re}(r\cdot y)|+\mathrm{iIm}(r\cdot y)$. The coefficients $c_g(m,l)$ can be obtained from the expansion

$$\frac{E_4E_6}{\eta^{24}}\widehat{\mathcal{P}}_g=\sum_{m\in\mathbb{Q}}\sum_{l\geq0}c_g(m,l)q^m\tau_2^{-l}, \quad \text{(A.2.8)}$$

where $\widehat{\mathcal{P}}_g$ are defined by

$$\left(\frac{2\pi\eta^3\lambda}{\vartheta_1(\lambda|\tau)}\right)^2\mathrm{e}^{-\frac{\pi\lambda^2}{\tau_2}}=\sum_{g=0}^{\infty}(2\pi\lambda)^{2g}\widehat{\mathcal{P}}_g(\tau,\bar{\tau}). \quad \text{(A.2.9)}$$

Note that these $\widehat{\mathcal{P}}_g(\tau,\bar\tau)$ are the modular, almost holomorphic extensions of the $\mathcal{P}_g(\tau)$ defined in (2.4.99), that is, $\widehat{\mathcal{P}}_g$ is obtained from $\mathcal{P}_g$ by replacing $E_2 \to \widehat{E}_2$. The only antiholomorphic dependence in $\widehat{\mathcal{P}}_g$ thus lies in the $\widehat{E}_2(\tau,\bar\tau)$. Using the explicit expressions for $\widehat{\mathcal{P}}_g$ given in [79], one can show that independently of the specific model,

$$c_g(m,l) = \frac{(-1)^l}{l!(4\pi)^l} c_{g-l}(m), \tag{A.2.10}$$

where $c_g(m)$ are defined analogously to (2.4.98), that is

$$\sum_n c_g(n) q^n = \mathcal{P}_g(q) \frac{E_4 E_6}{\eta^{24}}. \tag{A.2.11}$$

In what follows, we will systematically express everything in terms of the coefficients $c_g(m)$.

It turns out that (A.2.7) can be dramatically simplified. We will need the identity:

$$\sum_j (-1)^j \binom{C}{j} \binom{A-2j+C-B-1}{A-2j} = \sum_j (-1)^j \binom{C}{A-j} \binom{B}{j} \tag{A.2.12}$$

This is valid for any $A, B, C \in \mathbb{Z}$, see [41] for a proof. A special case of the above formula is the following. Let C, l and $m^+ - h^+$ be integers such that $0 \le l < C < m^+ - h^+ - l$. Then,

$$\sum_j \frac{(-1)^j (m^+ - h^+ + C - 2j - 1 - l)!}{j!(m^+ - h^+ - 2j)!(C-j)!} = 0.$$

The proof of this statement is easy. Set $B = l, A = m^+ - h^+$ in (A.2.12) to obtain

$$\sum_j (-1)^j \frac{(m^+ - h^+ + C - 2j - 1 - l)! C!}{j!(m^+ - h^+ - 2j)!(C-j)!(C-1-l)!} = \sum_j \binom{C}{m^+ - h^+ - j} \binom{l}{j}. \tag{A.2.13}$$

Since $C > l \ge 0$, any non-vanishing term on the right-hand side must fulfill $m^+ - h^+ - C \le j \le l$, in contradiction with the assumption $C < m^+ - h^+ - l$.

We also have the following three additional nontrivial identities. First of all, let $s := |2g - 2 - h - j - l - 1/2| - 1/2$. Then,

$$\sum_{h=0}^{2g-2} \sum_{j=0}^{C} \frac{(2g-2)!}{2^{2g-2}} \frac{(s+C-j)!(-1)^{C-j}}{l!h!j!(2g-2-h-2j)!(s-C+j)!(C-j)!} \tag{A.2.14}$$

$$= \begin{cases} \binom{2g-3-l}{C} \frac{1}{(l-C)!} & C \le \min(l, 2g-3-l) \\ 0 & \text{otherwise.} \end{cases} \tag{A.2.15}$$

This is valid for any pair of positive integers g, l. The second identity reads,

$$\sum_{s=0}^{g-1} (-1)^s \frac{(2g-2)!}{s!(g-1-s)!} \psi\Big(s + \frac{1}{2}\Big) = -2^{(2g-2)}(g-2)!. \tag{A.2.16}$$

The final identity we will need is

$$\sum_{s=0}^{g-1} (-1)^{l+s} 2^{2(s-2g)+5} \frac{(2g-2)!}{(2s)!(g-1-s)!} \Gamma\Big(\frac{3}{2} + s + l - g\Big) = \frac{(-1)^{g-1}(2g-3-l)!}{(2g-3-2l)!} \sqrt{\pi} 4^{-l}. \tag{A.2.17}$$

which is valid for any $l \in \mathbb{N}, l < g-1$. Making use of (A.2.13) and (A.2.15), we can convert the sums over h, j, a in (A.2.7) into a single one over $C = j + a = \{0, \cdots, l\}$. Then, (A.2.16)

and (A.2.17) can be used to simplify the second respectively third term in (A.2.7). The sum over r can be restricted for all $g \geq 3$ to a sum over r for which $\mathrm{Re}(r \cdot y) < 0$, or equivalently to a sum over positive r and a finite number of boundary cases. At genus 2, however, there is a contribution from $\mathrm{Re}(r \cdot y) > 0$, it reads [29]

$$\frac{c_0(r^2/2)}{16T_1U_1}\mathrm{Li}_3(\mathrm{e}^{-r\cdot y}). \tag{A.2.18}$$

We can then write down a simplified expression for the nondegenerate part of $F^{(g)}$ in the STU model:

$$\begin{aligned} &F^{(g>1)}_{\mathrm{nd,STU}} \\ &= \sum_{l=0}^{g-1}\sum_{C=0}^{\min(l,2g-3-l)}\sum_{r>0}\frac{\binom{2g-l-3}{C}}{(l-C)!2^C}\frac{(-\mathrm{Re}(r\cdot y))^{l-C}}{(2T_1U_1)^l}c_{g-l}(\frac{r^2}{2})\mathrm{Li}_{3-2g+l+C}(\mathrm{e}^{-r\cdot y}) \\ &+ \frac{22}{2^g(g-1)}\frac{1}{(2T_1U_1)^{g-1}} + \sum_{l=0}^{g-2}\frac{c_{g-l}(0)}{l!(4T_1U_1)^l}\zeta(3+2(l-g))\frac{(2g-3-l)!}{(2g-3-2l)!}, \end{aligned} \tag{A.2.19}$$

where we also have used the fact that in the STU model, $c_1(0) = -22$, and we have removed an overall prefactor of $4(2\pi\mathrm{i})^{2g-2}$ to agree with the normalization of the topological string amplitudes.

A.2.2 Application to the Enriques Calabi-Yau

The above expressions have to be adapted slightly for the Enriques Calabi-Yau. We only consider here the geometric reduction suited to the large radius limit. As shown in [79], the polylogarithm is replaced by $\mathrm{Li}_m(x) \to 2^m\mathrm{Li}_m(x^{\frac{1}{2}}) - \mathrm{Li}_m(x)$, and the norm of the reduced lattice is doubled. We also replace the quantity $2T_1U_1$ appearing in the STU-model by $Y = \mathrm{e}^{-K}$ as in (2.4.81), and the coefficients $c_g(m)$ are now defined by (2.4.98). There is a new important simplification: $c_0(r^2)$ and $c_{g>1}(0)$ vanish, and thus there is no contribution from negative r at any genus $g > 1$, since (A.2.18) becomes

$$\frac{c_0(r^2)}{8Y}\left(8\mathrm{Li}_3(\mathrm{e}^{-r\cdot y}) - \mathrm{Li}_3(\mathrm{e}^{-2r\cdot y})\right) = 0. \tag{A.2.20}$$

Furthermore, the degenerate contribution (A.2.6) and the last term in (A.2.7) vanish for all $g > 1$, while $c_1(0) = 4$, and the full $F^{(g)}_E(t,\bar{t})$ for the Enriques reads

$$\begin{aligned} F^{(g>1)}_E(t,\bar{t}) = &\sum_{l=0}^{g-1}\sum_{C=0}^{\min(l,2g-3-l)}\sum_{r>0}\frac{\binom{2g-l-3}{C}}{(l-C)!2^C}\frac{(-2\mathrm{Re}(r\cdot t))^{l-C}}{Y^l}c_{g-l}(r^2) \\ &\cdot\left(2^{3-2g+l+C}\mathrm{Li}_{3-2g+l+C}(\mathrm{e}^{-r\cdot t}) - \mathrm{Li}_{3-2g+l+C}(\mathrm{e}^{-2r\cdot t})\right) - \frac{1}{2^{g-2}(g-1)}\frac{1}{Y^{g-1}}. \end{aligned} \tag{A.2.21}$$

Using

$$\mathrm{Re}(t^a)\partial_{t^a}\mathrm{Li}_n(\mathrm{e}^{-r\cdot t}) = -\mathrm{Re}(r\cdot t)\mathrm{Li}_{n-1}(\mathrm{e}^{-r\cdot t}), \tag{A.2.22}$$

this can be cast into the following recursive form:

$$\begin{aligned} &F^{(g)}_E(t,\bar{t}) \\ &= \sum_{l=0}^{g-1}\sum_{C=0}^{\min(l,2g-3-l)}\frac{(2g-3-l)!}{(2g-3-l-C)!(l-C)!C!2^l}\frac{(t^{a_1}+\bar{t}^{a_1})\cdots(t^{a_{l-C}}+\bar{t}^{a_{l-C}})\partial_{a_1}\cdots\partial_{a_{l-C}}\mathcal{F}^{(g-l)}(t)}{Y^l} \\ &\qquad - \frac{1}{2^{g-2}(g-1)Y^{g-1}}. \end{aligned} \tag{A.2.23}$$

Notice that this exhibits the structure of the antiholomorphic amplitudes written down in [73].

Appendix B

Worldsheet instanton tables and topological amplitudes

B.1 Instanton tables and heterotic-type II duals

Table B.1 lists the dual K3-fibrations for the $\mathbb{Z}_N$-orbifolds defined in table 3.1 [105]. Tables

Type	Group	(n_h, n_v)	CY weights
$\mathbb{Z}_2, 3+8$ WL	$SU(4) \times E_8' \times U(1)^4$	$(167, 15)$	$(1, 1, 12, 16, 18, 20)$
$\mathbb{Z}_2, 2+8$ WL	$SU(3) \times E_8' \times U(1)^4$	$(230, 14)$	$(1, 1, 12, 16, 18)$
$\mathbb{Z}_2, 1+8$ WL	$SU(2) \times E_8' \times U(1)^4$	$(319, 13)$	$(1, 1, 12, 16, 30)$
$\mathbb{Z}_2, 0+8$ WL	$E_8' \times U(1)^4$	$(492, 12)$	$(1, 1, 12, 28, 42)$
$\mathbb{Z}_3, 3+6$ WL	$SU(4) \times E_6' \times U(1)^4$	$(129, 13)$	$(1, 1, 6, 10, 12, 14)$
$\mathbb{Z}_3, 2+6$ WL	$SU(3) \times E_6' \times U(1)^4$	$(168, 12)$	$(1, 1, 6, 10, 12)$
$\mathbb{Z}_3, 1+6$ WL	$SU(2) \times E_6' \times U(1)^4$	$(221, 11)$	$(1, 1, 6, 10, 18)$
$\mathbb{Z}_3, 0+6$ WL	$E_6' \times U(1)^4$	$(322, 10)$	$(1, 1, 6, 16, 24)$
$\mathbb{Z}_4, 3+4$ WL	$SU(4) \times SO(8)' \times U(1)^4$	$(123, 11)$	$(1, 1, 4, 8, 10, 12)$
$\mathbb{Z}_4, 2+4$ WL	$SU(3) \times SO(8)' \times U(1)^4$	$(154, 10)$	$(1, 1, 4, 8, 10)$
$\mathbb{Z}_4, 1+4$ WL	$SU(2) \times SO(8)' \times U(1)^4$	$(195, 9)$	$(1, 1, 4, 8, 14)$
$\mathbb{Z}_4, 0+4$ WL	$SO(8)' \times U(1)^4$	$(272, 8)$	$(1, 1, 4, 12, 18)$
$\mathbb{Z}_6, 3+0$ WL	$SU(4) \times E_6' \times U(1)^4$	$(139, 7)$	$(1, 1, 2, 6, 8, 10)$
$\mathbb{Z}_6, 2+0$ WL	$SU(3) \times E_6' \times U(1)^4$	$(162, 6)$	$(1, 1, 2, 6, 8)$
$\mathbb{Z}_6, 1+0$ WL	$SU(2) \times E_6' \times U(1)^4$	$(191, 5)$	$(1, 1, 2, 6, 10)$
$\mathbb{Z}_6, 0+0$ WL	$E_6' \times U(1)^4$	$(244, 4)$	$(1, 1, 2, 8, 12)$

Table B.1: The chains of heterotic-type II duals studied in [105]

B.2–B.15 give instanton numbers at $g = 0, \cdots 4$ for the $\mathbb{Z}_{2,3,4,6}$ orbifolds defined in table 3.1.

g	$\frac{p^2}{2} = -1$	0	1	2	3	4	5	6
0	-2	960	56808	1364480	20920140	240357888	2244734960	17884219392
1	0	4	-1908	-119360	-3077460	-50495040	-617959240	-6118785792
2	0	0	-6	2848	185694	5045376	87240260	1122823296
3	0	0	0	8	-3780	-255792	-7276660	-131766240
4	0	0	0	0	-10	4704	329630	9782592

Table B.2: $\mathbb{Z}_2$, 8 Wilson lines, dual to $X^{1,1,12,28,42}$

g	$\frac{p^2}{2}=-1$	$-\frac{1}{4}$	0	$\frac{3}{4}$	1	$\frac{7}{4}$	2	$\frac{11}{4}$	3	$\frac{15}{4}$
0	-2	176	612	12672	30240	320976	661696	5031040	9509328	58372272
1	0	0	4	-352	-1212	-26400	-64136	-719392	-1509700	-12091776
2	0	0	0	0	-6	528	1804	40832	100422	1173600
3	0	0	0	0	0	0	8	-704	-2388	-55968
4	0	0	0	0	0	0	0	0	-10	880

Table B.3: $\mathbb{Z}_2$, 8+1 Wilson lines, dual to $X^{1,1,12,16,30}$

g	$\frac{p^2}{2}=-1$	$-\frac{1}{3}$	0	$\frac{2}{3}$	1	$\frac{5}{3}$	2	$\frac{8}{3}$	3	$\frac{11}{3}$
0	-2	90	432	5904	18252	142146	365600	2144016	4936140	24107760
1	0	0	4	-180	-852	-12348	-39080	-320436	-844140	-5189400
2	0	0	0	0	-6	270	1264	19152	61578	524952
3	0	0	0	0	0	0	8	-360	-1668	-26316
4	0	0	0	0	0	0	0	0	-10	450

Table B.4: $\mathbb{Z}_2$, 8+2 Wilson lines, dual to $X^{1,1,12,16,30}$

g	$\frac{p^2}{2}=-1$	$-\frac{1}{2}$	$-\frac{3}{8}$	0	$\frac{1}{2}$	$\frac{5}{8}$	1	$\frac{3}{2}$	$\frac{13}{8}$	2	$\frac{5}{2}$
0	-2	28	64	304	2144	3392	11412	52144	75136	211040	781312
1	0	0	0	4	-56	-128	-596	-4456	-7168	-24632	-117376
2	0	0	0	0	0	0	-6	84	192	880	6880
3	0	0	0	0	0	0	0	0	0	8	-112

Table B.5: $\mathbb{Z}_2$, 8+3 Wilson lines, dual to $X^{1,1,12,16,18}$

g	$\frac{p^2}{2}=-1$	$-\frac{3}{5}$	$-\frac{2}{5}$	0	$\frac{2}{5}$	$\frac{3}{5}$	1	$\frac{7}{5}$	$\frac{8}{5}$	2	$\frac{12}{5}$
0	-2	14	52	200	1020	2158	7068	23916	43080	122840	347376
1	0	0	0	4	-28	-104	-388	-2124	-4628	-15320	-54064
2	0	0	0	0	0	0	-6	42	156	568	3284
3	0	0	0	0	0	0	0	0	0	8	-56

Table B.6: $\mathbb{Z}_2$, 8+4 Wilson lines, dual to $X^{1,1,12,16,18,20}$

g	$\frac{p^2}{2}=-1$	$-\frac{1}{2}$	$-\frac{3}{8}$	0	$\frac{1}{2}$	$\frac{5}{8}$	1	$\frac{3}{2}$	$\frac{13}{8}$	2
0	-2	8	24	264	9104	17272	86292	634464	1009936	3647120
1	0	0	0	4	-16	-48	-516	-18256	-34688	-174152
2	0	0	0	0	0	0	-6	72	760	27440
3	0	0	0	0	0	0	0	0	0	8

Table B.7: $\mathbb{Z}_6$, 3 Wilson lines, dual to $X^{1,1,2,6,8,10}$

g	$\frac{p^2}{2}=-1$	0	1	2	3	4	5	6
0	-2	624	54792	1609088	28265184	360251424	3659578208	31296575232
1	0	4	-1236	-113312	-3551892	-66631944	-903741184	-9729986112
2	0	0	-6	1840	174270	5731824	113066144	1610777952
3	0	0	0	8	-2436	-237648	-8154292	-168125136
4	0	0	0	0	-10	3024	303422	10826544

Table B.8: $\mathbb{Z}_3$, 6 Wilson lines, dual to $X^{1,1,6,16,24}$

g	$\frac{p^2}{2}=-1$	$-\frac{1}{4}$	0	$\frac{3}{4}$	1	$\frac{7}{4}$	2	$\frac{11}{4}$	3
0	-2	104	420	11856	30240	373464	801472	6750016	13138500
1	0	0	4	-208	-828	-24336	-62984	-818896	-1787716
2	0	0	0	0	-6	312	1228	37232	97350
3	0	0	0	0	0	0	8	-416	-1620

Table B.9: $\mathbb{Z}_3$, 6+1 Wilson lines, dual to $X^{1,1,6,10,18}$

g	$\frac{p^2}{2}=-1$	$-\frac{1}{3}$	0	$\frac{2}{3}$	1	$\frac{5}{3}$	2	$\frac{8}{3}$	3
0	-2	54	312	5616	18900	167778	454688	2914704	6972912
1	0	0	4	-108	-612	-11556	-39656	-369684	-1025244
2	0	0	0	0	-6	162	904	17712	61602
3	0	0	0	0	0	0	8	-216	-1188

Table B.10: $\mathbb{Z}_3$, 6+2 Wilson lines, dual to $X^{1,1,6,10,12}$

g	$\frac{p^2}{2}=-1$	$-\frac{1}{2}$	$-\frac{3}{8}$	0	$\frac{1}{2}$	$\frac{5}{8}$	1	$\frac{3}{2}$	$\frac{13}{8}$	2	$\frac{5}{2}$
0	-2	16	40	232	2024	3320	12228	61600	90592	269456	1065784
1	0	0	0	4	-32	-80	-452	-4144	-6880	-25832	-135472
2	0	0	0	0	0	0	-6	48	120	664	6328
3	0	0	0	0	0	0	0	0	0	8	-64

Table B.11: $\mathbb{Z}_3$, 6+3 Wilson lines, dual to $X^{1,1,6,10,12}$

g	$\frac{p^2}{2}=-1$	0	1	2	3	4	5
0	-2	528	90036	3679520	80559180	1212246784	14073864648
1	0	4	-1044	-183224	-7903452	-183923136	-2938551600
2	0	0	-6	1552	278466	12502704	304651808
3	0	0	0	8	-2052	-375744	-17481820
4	0	0	0	0	-10	2544	475034

Table B.12: $\mathbb{Z}_4$, 4 Wilson lines, dual to $X^{1,1,4,12,18}$

g	$\frac{p^2}{2}=-1$	$-\frac{1}{4}$	0	$\frac{3}{4}$	1	$\frac{7}{4}$	2	$\frac{11}{4}$	3
0	-2	80	372	18432	52428	832848	1908808	18982912	38738880
1	0	0	4	-160	-732	-37344	-107072	-1776928	-4135132
2	0	0	0	0	-6	240	1084	56576	163146
3	0	0	0	0	0	0	8	-320	-1428

Table B.13: $\mathbb{Z}_4$, 4+1 Wilson lines, dual to $X^{1,1,4,8,14}$

g	$\frac{p^2}{2}=-1$	$-\frac{1}{3}$	0	$\frac{2}{3}$	1	$\frac{5}{3}$	2	$\frac{8}{3}$	3
0	-2	42	288	8928	34488	381894	1127168	8355360	21263796
1	0	0	4	-84	-564	-18108	-70688	-817692	-2463540
2	0	0	0	0	-6	126	832	27456	107982
3	0	0	0	0	0	0	8	-168	-1092

Table B.14: $\mathbb{Z}_4$, 4+2 Wilson lines, dual to $X^{1,1,4,8,10}$

g	$\frac{p^2}{2}=-1$	$-\frac{1}{2}$	$-\frac{3}{8}$	0	$\frac{1}{2}$	$\frac{5}{8}$	1	$\frac{3}{2}$	$\frac{13}{8}$	2	$\frac{5}{2}$
0	-2	12	32	224	3136	5536	23392	139688	213248	694400	3063424
1	0	0	0	4	-24	-64	-436	-6344	-11264	-48112	-298288
2	0	0	0	0	0	0	-6	36	96	640	9600
3	0	0	0	0	0	0	0	0	0	8	-48

Table B.15: $\mathbb{Z}_4$, 4+3 Wilson lines, dual to $X^{1,1,4,8,10,12}$

B.2 Explicit Higher–Genus Formulae

In this appendix we present some explicit expressions for free energies at high genera, in both the quartic matrix model and Hurwitz theory. This is just a partial list of our results, as most formulae quickly become too intricate to put in print. In spite of this, we hope these explicit expressions may be of future interest (and, as far as we know, have never been computed before).

B.2.1 Quartic Matrix Model

As we have reviewed in section 4, an algorithm for computing free energies in the quartic matrix model was put forward in [132], and we have applied it up to genus $g = 10$. Here, we present a partial list of our final results. In [132], the quartic free energies were computed up to genus two, with the result (here $t = 1$)

$$F_0(\alpha^2) = -\frac{1}{2}\log\left(\alpha^2\right) - \frac{1}{24}\left(1-\alpha^2\right)\left(9-\alpha^2\right), \tag{B.2.1}$$

$$F_1(\alpha^2) = \frac{1}{12}\log\left(2-\alpha^2\right), \tag{B.2.2}$$

$$F_2(\alpha^2) = \frac{1}{6!}\frac{\left(1-\alpha^2\right)^3}{\left(2-\alpha^2\right)^5}\left(82+21\alpha^2-3\alpha^4\right). \tag{B.2.3}$$

It was further conjectured that, for genus $g \geq 2$, the general structure of the free energies should be of the form

$$F_g(\alpha^2) = \frac{\left(1-\alpha^2\right)^{2g-1}}{\left(2-\alpha^2\right)^{5(g-1)}}\,\mathcal{P}_g(\alpha^2), \tag{B.2.4}$$

with $\mathcal{P}_g(\alpha^2)$ a polynomial in α^2 such that

$$\mathcal{P}_g(\alpha^2=1) = \frac{1}{2\cdot 6^{2g-1}}\,\frac{(4g-3)!}{g!(g-1)!}. \tag{B.2.5}$$

Using the exact same procedure as in [132], we have extended the analysis up to genus ten, verifying both conjectures above. In particular, we have obtained at genus three

$$\mathcal{P}_3(\alpha^2) = -\frac{1}{9072}\left(17260+\alpha^2\left(-32704+9\alpha^2\left(-325+95\alpha^2-15\alpha^4+\alpha^6\right)\right)\right), \tag{B.2.6}$$

which can be explicitly compared to another genus three calculation performed in [191, 192], with both results in complete agreement. At genus four, we obtained

$$\begin{aligned}\mathcal{P}_4(\alpha^2) &= -\frac{1}{38880}\left(-1421392+\alpha^2\left(12438536+\alpha^2\left(-13719796+27\alpha^2\left(-15694+\right.\right.\right.\right.\\ &\left.\left.\left.\left.+5810\alpha^2-1456\alpha^4+238\alpha^6-23\alpha^8+\alpha^{10}\right)\right)\right)\right),\end{aligned} \tag{B.2.7}$$

and at genus five

$$\begin{aligned}\mathcal{P}_5(\alpha^2) &= -\frac{1}{85536}\left(-383964880+\alpha^2\left(-1573981616+\alpha^2\left(7592114712+\right.\right.\right.\\ &+\alpha^2\left(-6114807776+81\alpha^2\left(-781725+326811\alpha^2-101961\alpha^4+23535\alpha^6+\right.\right.\\ &\left.\left.\left.\left.-3915\alpha^8+445\alpha^{10}-31\alpha^{12}+\alpha^{14}\right)\right)\right)\right).\end{aligned} \tag{B.2.8}$$

Finally, at genus six the free energy follows from the polynomial

$$\begin{aligned}\mathcal{P}_6(\alpha^2) &= -\frac{1}{79606800}\left(139728961867968+\alpha^2\left(-369974786833952+\right.\right.\\ &+\alpha^2\left(-955888270184512+3\alpha^2\left(1037832523698416+\alpha^2\left(-662581722466844+\right.\right.\right.\\ &+55971\alpha^2\left(-39761282+17910398\alpha^2-6371112\alpha^4+1787698\alpha^6-392007\alpha^8+\right.\\ &\left.\left.\left.\left.\left.+65901\alpha^{10}-8214\alpha^{12}+716\alpha^{14}-39\alpha^{16}+\alpha^{18}\right)\right)\right)\right)\right).\end{aligned} \tag{B.2.9}$$

Although we have extended this calculation up to genus ten, the expressions quickly get too messy and little illuminating, therefore we do not display any further polynomials. Our results further allow us to conclude that the polynomial $\mathcal{P}_g(\alpha^2)$ is of order $3g-4$ in α^2. One final consistency check concerns the case of $\alpha^2=2$, corresponding to the critical point of the quartic model. In this situation it must be the case that

$$\mathcal{P}_g(\alpha^2=2)=(-1)^g\,2^{5(g-1)}\,a_g, \tag{B.2.10}$$

where a_g are the coefficients appearing in the expansion of the double–scaled free energy (obtained from Painlevé I in the 1/3 normalization; see section 4 for details). Again, our results pass the test.

B.2.2 Hurwitz Theory

If we expand (5.6.134) in g_H, and use that [151, 161]

$$\frac{\partial^2 F_0^{\mathrm{H}}}{\partial t_H^2}=\chi=\sum_{k=1}^{\infty}\frac{k^{k-1}}{k!}\mathrm{e}^{-t_H k}, \tag{B.2.11}$$

we obtain the recursion relation

$$F_g^{\mathrm{H}}(\mathrm{e}^{-t_H})=\frac{\chi}{1-\chi}\exp\left(\sum_{l\geq 1}^{g-1}g_H^{2l}\partial_{t_H}^2F_l^{\mathrm{H}}(\mathrm{e}^{-t_H})+2\sum_{k\geq 2}\sum_{l\geq 0}^{g-1}\frac{1}{2k!}\partial_{t_H}^{2k}F_l^{\mathrm{H}}(\mathrm{e}^{-t_H})g_H^{2k+2l-2}\right)\Bigg|_{g_H^{2g}}, \tag{B.2.12}$$

where we keep the coefficient of g_H^{2g} in the right hand side. If we combine this recursion with the general form of Hurwitz numbers (5.6.130), we can obtain explicit expressions for the polynomials appearing in (5.6.130) up to high genus. The first few are,

$$P_2(\chi)=\frac{\chi^3}{240}+\frac{\chi^2}{1440}, \tag{B.2.13}$$

$$P_3(\chi)=\frac{\chi^6}{1008}+\frac{53\chi^5}{10080}+\frac{1741\chi^4}{362880}+\frac{137\chi^3}{181440}+\frac{\chi^2}{80640}, \tag{B.2.14}$$

$$P_4(\chi) = \frac{\chi^9}{1440} + \frac{6079\chi^8}{604800} + \frac{42419\chi^7}{1209600} + \frac{87739\chi^6}{2177280} + \frac{280603\chi^5}{17418240} + \frac{109\chi^4}{53760} + \frac{1291\chi^3}{21772800} + \frac{\chi^2}{7257600}, \tag{B.2.15}$$

$$\begin{aligned} P_5(\chi) \quad = \quad & \frac{\chi^{12}}{1056} + \frac{17387\chi^{11}}{665280} + \frac{67289\chi^{10}}{345600} + \frac{44696593\chi^9}{79833600} + \frac{193701347\chi^8}{273715200} + \frac{37315313\chi^7}{91238400} + \\ & + \frac{8679559\chi^6}{82114560} + \frac{2295119\chi^5}{205286400} + \frac{1525901\chi^4}{3832012800} + \frac{23\chi^3}{7603200} + \frac{\chi^2}{958003200}. \end{aligned} \tag{B.2.16}$$

Appendix C

Mathematical Background

C.1 Theta functions and modular forms

Properties

In our conventions, the theta functions are defined as follows:

$$\vartheta[^a_b](v|\tau) = \sum_{n\in Z} q^{\frac{1}{2}(n-a)^2} e^{2\pi i(v-b)(n-a)} \tag{C.1.1}$$

where a, b are rational numbers and $q = e^{2\pi i\tau}$. They show the following periodicity properties:

$$\begin{aligned} &\vartheta[^{a+1}_{\ b}](v|\tau) = \vartheta[^a_b](v|\tau), \qquad \vartheta[_{b+1}^{\ a}](v|\tau) = e^{2i\pi a}\vartheta[^a_b](v|\tau) \\ &\vartheta[^{-a}_{-b}](v|\tau) = \vartheta[^a_b](-v|\tau), \qquad \vartheta[^a_b](-v|\tau) = e^{4i\pi ab}\vartheta[^a_b](v|\tau) \qquad (a,b\in\frac{1}{2}\mathbb{Z}) \end{aligned} \tag{C.1.2}$$

We use a modified Jacobi/Erderlyi notation where $\vartheta_1 = \vartheta[^{1/2}_{1/2}]$, $\vartheta_2 = \vartheta[^{1/2}_0]$, $\vartheta_3 = \vartheta[^0_0]$, $\vartheta_4 = \vartheta[^0_{1/2}]$.

Under modular transformations, the theta functions transform according to

$$\begin{aligned} \vartheta[^a_b](v|\tau+1) &= e^{-i\pi a(a-1)}\ \vartheta[_{a+b-1/2}^{\ a}](v|\tau) \\ \vartheta[^a_b]\left(\frac{v}{\tau}|-\frac{1}{\tau}\right) &= \sqrt{-i\tau}\ e^{2i\pi ab+i\pi\frac{v^2}{\tau}}\ \vartheta[_{-a}^{\ b}](v|\tau) \end{aligned} \tag{C.1.3}$$

The Dedekind η-function of weight $\frac{1}{2}$ is related to the v-derivative of ϑ_1:

$$\eta(\tau) = q^{\frac{1}{24}}\prod_{n=1}^{\infty}(1-q^n), \tag{C.1.4}$$

$$\frac{\partial}{\partial v}\vartheta_1(v)|_{v=0} \equiv \vartheta_1' = 2\pi\eta^3(\tau). \tag{C.1.5}$$

We can always set the variable v to zero by changing the shifts (a, b) appropriately:

$$\vartheta[^a_b]\left(v+\epsilon_1\tau+\epsilon_2|\tau\right) = e^{-i\pi\tau\epsilon_1^2-i\pi\epsilon_1(2v-b)-2i\pi\epsilon_1\epsilon_2}\ \vartheta[^{a-\epsilon_1}_{b-\epsilon_2}](v|\tau)\,. \tag{C.1.6}$$

In our conventions, we will systematically use shifts rather than the variable v. We also note the following identities

$$\vartheta_2(0|\tau)\vartheta_3(0|\tau)\vartheta_4(0|\tau) = 2\ \eta^3\,, \tag{C.1.7}$$

$$\vartheta_2^4(v|\tau) - \vartheta_1^4(v|\tau) = \vartheta_3^4(v|\tau) - \vartheta_4^4(v|\tau)\,, \tag{C.1.8}$$

We have the following identities for the derivatives of ϑ-functions

$$\partial_\tau(\frac{\vartheta_2}{\eta}) = \frac{i\pi}{12\eta}\left(\vartheta_3^4 + \vartheta_4^4\right) \tag{C.1.9}$$

$$\partial_\tau(\frac{\vartheta_3}{\eta}) = \frac{i\pi}{12\eta}\left(\vartheta_2^4 - \vartheta_4^4\right) \tag{C.1.10}$$

$$\partial_\tau(\frac{\vartheta_4}{\eta}) = \frac{i\pi}{12\eta}\left(-\vartheta_2^4 - \vartheta_3^4\right) \tag{C.1.11}$$

Note that the above is valid for all rational values of a,b,h,g. The case $h, g \in \{0, 1/2\}$can be seen as a special case, relevant for $\mathbb{Z}_2$-orbifolds, while $h, g \in \{0, 1/n, \cdots (n-1)/n\}$ arise in the $\mathbb{Z}_n$-case (see, e.g., [193] or [194]).
We also use the short-hand notation

$$\vartheta[^a_b](\tau) := \vartheta[^a_b](0|\tau) \tag{C.1.12}$$

as well as

$$\vartheta[^a_b](m\cdot) := \vartheta[^a_b](0|m\tau) \tag{C.1.13}$$

The following formulae for doubling the τ–modulus hold:

$$\begin{aligned}
\vartheta_2^2(2\tau) &= \frac{1}{2}\left(\vartheta_3^2(\tau) - \vartheta_4^2(\tau)\right) \\
\vartheta_3^2(2\tau) &= \frac{1}{2}\left(\vartheta_3^2(\tau) + \vartheta_4^2(\tau)\right) \\
\vartheta_4^2(2\tau) &= \vartheta_3(\tau)\vartheta_4(\tau).
\end{aligned} \tag{C.1.14}$$

Eisenstein series

The Eisenstein series E_{2n} are defined as

$$E_{2n} = 1 - \frac{4n}{B_{2n}}\sum_{k\geq 1}\frac{k^{2n-1}q^k}{1-q^k}. \tag{C.1.15}$$

E_{2n} with $n > 1$ are holomorphic modular forms of weight $2n$. The Eisenstein series E_2 is often called quasi–modular since under modular transformations, it transforms with a shift

$$E_2(-\frac{1}{\tau}) = \tau^2\left(E_2(\tau) + \frac{6}{\pi \mathrm{i}\tau}\right). \tag{C.1.16}$$

Adding a term that compensates this shift yields the modular, but only "almost holomorphic" form of weight two $\widehat{E}_2$

$$\widehat{E}_2 = E_2 - \frac{3}{\pi\tau_2}. \tag{C.1.17}$$

The ring of almost holomorphic modular forms is generated by $\widehat{E}_2$ and the next two Eisenstein series

$$\begin{aligned}
E_4 &= 1 + 240\sum_{k\geq 1}\frac{k^3q^k}{1-q^k} = \frac{1}{2}\left(\vartheta_2^8 + \vartheta_3^8 + \vartheta_4^8\right) \\
E_6 &= 1 - 504\sum_{k\geq 1}\frac{k^5q^k}{1-q^k} = \frac{1}{2}\left(\vartheta_2^4 + \vartheta_3^4\right)\left(\vartheta_3^4 + \vartheta_4^4\right)\left(\vartheta_4^4 - \vartheta_2^4\right).
\end{aligned} \tag{C.1.18}$$

For derivatives of Eisenstein series, we have

$$q\frac{d}{dq}\log\,\eta=\frac{1}{24}E_2(\tau) \tag{C.1.19}$$

and the Ramanujan identities

$$\begin{aligned} q\frac{d}{dq}\;E_2(q)=&\frac{1}{12}(E_2^2(q)-E_4(q)),\\ q\frac{d}{dq}\;E_4(q)=&\frac{1}{3}(E_2(q)E_4(q)-E_6(q)),\\ q\frac{d}{dq}\;E_6(q)=&\frac{1}{2}(E_2(q)E_6(q)-E_4^2(q)). \end{aligned} \tag{C.1.20}$$

Lie algebra lattice sums

Any shifted lattice sum over E_8 can be written in terms of theta functions as

$$\sum_{p\in\Gamma_{E_8}+a\gamma} q^{\frac{p^2}{2}}\mathrm{e}^{2\pi\mathrm{i}bp\cdot\gamma}=\sum_{\alpha,\beta}\prod_{i=1}^{8}\vartheta[^{\alpha+a\gamma_i}_{\beta+b\gamma_i}]\mathrm{e}^{-\pi\mathrm{i}\sum_i\gamma_i\beta a} \tag{C.1.21}$$

In particular,

$$E_4=\frac{1}{2}\sum_{p\in\Gamma_{E_8}} q^{\frac{p^2}{2}} \tag{C.1.22}$$

and E_6 is related to the E_8 lattice shifted by any modular invariant embedding γ

$$E_6=\sum_{(a,b)\neq(0,0)}\frac{c(a,b)}{2\vartheta[^{\frac12+a}_{\frac12+b}]\vartheta[^{\frac12-a}_{\frac12-b}]}\sum_{p\in\Gamma_{E_8}+a\gamma} q^{\frac{p^2}{2}}\mathrm{e}^{2\pi\mathrm{i}bp\cdot\gamma}, \tag{C.1.23}$$

with $c(a,b)$ as defined in section 3.2.
An obvious generalization of (C.1.21) is the modified Siegel-Narain Theta function over a general shifted lattice Γ of signature (b^+,b^-) with an insertion of $(p_R)^{2g-2}$

$$\Theta^g_\Gamma(\tau,\gamma,a,b)=\sum_{p\in\Gamma+a\gamma}(p_R)^{2g-2}q^{\frac{|p_L|^2}{2}}\bar q^{\frac{|p_R|^2}{2}}\mathrm{e}^{2\pi\mathrm{i}b\gamma\cdot p}. \tag{C.1.24}$$

We also use the notation

$$\Theta_\Gamma(\tau,\gamma_1,\gamma_2;P,\phi)=\sum_{p\in\Gamma+\gamma_1}\exp(-\frac{\Delta}{8\pi\tau_2})\phi(P(p))q^{\frac{|p_L|^2}{2}}\bar q^{\frac{|p_R|^2}{2}}\mathrm{e}^{2\pi\mathrm{i}\gamma_2\cdot p}, \tag{C.1.25}$$

where γ_1,γ_2 are shifts, P is an isometry from $\Gamma\times\mathbb{R}$ to $\mathbb{R}^{b^+,b^-}$, ϕ is a polynomial on $\mathbb{R}^{b^+,b^-}$ of degree m^+ in the first b^+ variables and of degree m^- in the others, and Δ is the Euclidean Laplacian on $\mathbb{R}^{b^+,b^-}$. The isometry P defines projections on $\mathbb{R}^+,\mathbb{R}^-$ written as $P_+(p)=p_R,\quad P_-(p)=p_L$. We will here only consider cases where the shifts are proportional, $\gamma_1=a\gamma\sim\gamma_2=b\gamma$.

Elliptic Identities

We use the following conventions for the elliptic integrals of the first, second and third kind:

$$F(\varphi,k)=\int_0^\varphi\frac{\mathrm{d}t}{\sqrt{1-k\sin^2(t)}},\qquad F(\frac{\pi}{2},k)\equiv K(k), \tag{C.1.26}$$

$$E(\varphi,k)=\int_0^{\varphi}\sqrt{1-k\sin^2(t)}\mathrm{dt},\qquad E(\frac{\pi}{2},k)\equiv E(k), \tag{C.1.27}$$

$$\Pi(n,\varphi,k)=\int_0^{\varphi}\frac{\mathrm{dt}}{(1-n\sin^2(t))\sqrt{1-k\sin^2(t)}},\qquad \Pi(n,\frac{\pi}{2},k)\equiv\Pi(n,k). \tag{C.1.28}$$

A key relation is due to Legendre;

$$E(k)k(1-k)+E(1-k)K(k)-K(k)k(1-k)=\frac{\pi}{2}. \tag{C.1.29}$$

Furthermore, we have the following elliptic identities for the "circular" case $k<n<1$ [195]:

$$\Pi(n,k)=K(k)+\frac{\pi}{2}\delta(n,k)\left(1-\Lambda_0(\epsilon(n,k),k)\right), \tag{C.1.30}$$

where

$$\delta(n,k)=\sqrt{\frac{n}{(1-n)(n-k)}},\qquad \epsilon(n,k)=\frac{1-n}{1-k}, \tag{C.1.31}$$

and Λ_0 is Heuman's Lambda-function

$$\Lambda_0=\frac{2}{\pi}\left\{K(k)E(\epsilon(n,k),1-k)-\left(K(k)-E(k)\right)F(\epsilon(n,k),1-k)\right\}. \tag{C.1.32}$$

Furthermore, if $(1-k)\frac{n_1}{1-n_1}\frac{n_2}{1-n_2}=1$ [195],

$$F(n_1,k)+F(n_2,k)=K(k),\qquad E(n_1,k)+E(n_2,k)=E(k)+\sqrt{n_1n_2}k. \tag{C.1.33}$$

Theta functions and Eisenstein series can be expressed in terms of elliptic functions as follows:

$$\begin{aligned}
\vartheta_2^4&=-\frac{4}{\pi^2}kK(k)^2\\
\vartheta_3^4&=-\frac{4}{\pi^2}K(k)^2\\
\vartheta_4^4&=-\frac{4}{\pi^2}(1-k)K(k)^2\\
E_2(q)&=\frac{4}{\pi^2}\left(3K(k)E(k)+(k-2)K(k)^2\right)\\
E_4(q)&=\frac{16}{\pi^4}\left(k^2-k+1\right)K(k)^4\\
E_6(q)&=-\frac{64}{\pi^6}(k+1)(k-2)(k-\frac{1}{2})K(k)^6,
\end{aligned} \tag{C.1.34}$$

where

$$k=\frac{\vartheta_2^4}{\vartheta_3^4}. \tag{C.1.35}$$

C.2 Cohomology and characteristic classes

In this section, we summarize some basic concepts of differential and algebraic topology used throughout this thesis. For more details and further reading, see the classic book [196].

Cohomology

Let M be a differentiable manifold, and $\Omega^p(M)$ the space of p-forms on M. Then the ordinary exterior derivative of forms d, defined by

$$df:=\frac{\partial f}{\partial x^i}dx^i,\qquad d(\omega\wedge\rho):=d\omega\wedge\rho)+(-1)^{|\omega|}\omega\wedge d\rho, \tag{C.2.36}$$

is a map from $\Omega^p(M)$ to Ω^{p+1} inducing the complex

$$0 \xrightarrow{d} \Omega^0 \xrightarrow{d} \Omega^1 \to \cdots \to \Omega^n \xrightarrow{d} 0. \tag{C.2.37}$$

Let $Z^p(M) \subset \Omega^p(M)$ denote the subspace of closed p-forms. Since $d^2 = 0$, $d\Omega^{p-1}(M) \subset Z^p(M)$. The de Rham cohomology groups of M are defined by

$$H^p_{DR}(M) = \frac{Z^p(M)}{d\Omega^{p-1}(M)} = \frac{\text{Ker } d}{\text{Im } d}|_{\Omega^p}. \tag{C.2.38}$$

If M is a complex manifold, the complex structure induces a split of the tangent spaces at each point as

$$T^*_{\mathbb{C},z}(M) = T^*_z(M) \oplus \bar{T}^*_z(M) \tag{C.2.39}$$

and we can define

$$\Omega^{p,q}(M) = \{\phi \in \Omega^{p+q}(M) : \phi(z) \in \wedge^p T^*_z(M) \otimes \wedge^q \bar{T}^*_z(M) \forall z \in M\}. \tag{C.2.40}$$

Similarly, the operator d breaks up into two parts, $d = \partial + \bar{\partial}$. Denoting the space of $\bar{\partial}$–closed forms as $Z^{p,q}_{\bar{\partial}}(M)$, we can define the *Dolbeault cohomology* as

$$H^{p,q}_{\bar{\partial}}(M) = \frac{Z^{p,q}_{\bar{\partial}}(M)}{\bar{\partial}\Omega^{p,q-1}(M)}. \tag{C.2.41}$$

The Dolbeault theorem says that for any complex manifold M

$$H^q(M, \Omega^p) \cong H^{p,q}_{\bar{\partial}}(M). \tag{C.2.42}$$

We also have the following famous lemma:

Lemma (Poincaré).

Every closed form on $\mathbb{R}^n$ is exact.

This fact simply means that the de Rham cohomology groups on reasonable real manifolds are locally trivial. There is also a $\bar{\partial}$–Poincaré lemma for the Dolbeault cohomology, stating that the same is true for $\bar{\partial}$–closed forms on environments in $\mathbb{C}^n$. Another central fact is the following

Theorem (de Rham).

Let M be a real C^∞ manifold. Then, the de Rham cohomology is isomorphic to the singular homology, in fact, the cohomology groups $H^*(M)$ and the (singular) homology groups $H_*(M)$ are –as notation and naming suggest– dual vector spaces.

To put it otherwise, there is a direct correspondence between closed modulo exact forms and cycles modulo boundaries. This is also encoded in Stokes' theorem: given a real manifold M, a p-form A and a $(p+1)$–chain N, recall that Stokes theorem states

$$\int_N dA = \int_{\partial N} A. \tag{C.2.43}$$

This induces a map from $H^p(M)$ to $H_{d-p}(M)$, associating to each closed p-form A a $(d-p)$–cycle N with the property

$$\int_M A \wedge B = \int_N B \quad \forall B \in Z^{d-p}(M). \tag{C.2.44}$$

Poincaré duality states that this map is an isomorphism.

Definition.

The *Betti number* b_n of a manifold M is the dimension of the n-th de Rham cohomology $H^n(M)$. For complex manifolds, the *Hodge number* $h^{p,q}$ gives the dimension of the Dolbeault cohomology $H^{p,q}(M)$, and we have

$$b_n = \sum_{p+q=n} h^{p,q}. \tag{C.2.45}$$

If M is Kähler, complex conjugation and Poincaré duality imply

$$h^{p,q} = h^{n-q,n-p} = h^{q,p}. \tag{C.2.46}$$

Characteristic classes

Consider a bundle E with fibre F and structure group G over a base space M. The *characteristic classes* of E encode the non-triviality of E, i.e. "how much" E differs from the trivial bundle $F \times M$. They are subsets of the cohomology classes of M. By extension, we call the characteristic class of a manifold the characteristic class of its tangent bundle. For us, the most relevant characteristic classes are the Chern classes, defined as follows.

Let $F = dA + A \wedge A$ be the curvature of the connection A on E. The total Chern class $c(E)$ is then defined as

$$\begin{aligned} c(E) &= \det\left(1 + \frac{\mathrm{i}F}{2\pi}\right) = 1 + \frac{\mathrm{i}}{2\pi}\mathrm{Tr}F + \cdots \\ &= 1 + c_1(E) + \cdots \in H^0(M,\mathbb{R}) \oplus H^2(M,\mathbb{R}) \oplus \cdots . \end{aligned} \tag{C.2.47}$$

A Calabi-Yau manifold is defined as a Kähler manifold with $c_1 = 0$. The theorem conjectured by Calabi and proved by Yau (1977) states that any compact Kähler n-fold with $c_1 = 0$ admits a metric of $SU(n)$ holonomy. Such a metric can be shown to allow for a covariantly constant spinor field and is therefore necessarily Ricci flat.

C.3 Toric Geometry, local Calabi Yau manifolds and mirror symmetry

Many of the backgrounds considered in this thesis are *local* Calabi-Yau's. We now briefly review the main ideas about this class of geometries, focusing on the toric case and following the approach of [31]. For more details, see [31, 197, 198]. Recall that the tautological line bundle J over the projective space $\mathbb{P}^n$ is the obvious bundle where the fiber over a point in $\mathbb{P}^n$ is just the corresponding line in $\mathbb{C}^{n+1}$. Maps from this fiber to $\mathbb{C}$ are sections of its dual line bundle $H = \mathrm{Hom}(J, \mathbb{C})$. More general line bundles can be generated as direct products of these two basic ones, and we get the bundles $\mathcal{O}(d) = H^{\otimes d}$ and $\mathcal{O}(-d) = J^{\otimes d}$.

Now consider a Riemann surface, holomorphically embedded in a Calabi-Yau manifold X. The holomorphic tangent bundle of X at Σ_g can be decomposed as the direct sum of the tangent bundle of Σ_g and its component normal to Σ_g

$$TX|_{\Sigma_g} = T\Sigma_g \oplus N_{\Sigma_g}. \tag{C.3.48}$$

The normal bundle N_{Σ_g} is a holomorphic rank two complex bundle, and its first Chern class precisely cancels the one of $T\Sigma_g$ due to the Calabi-Yau condition, thus

$$c_1(N_{\Sigma_g}) = 2g - 2. \tag{C.3.49}$$

Locally, X can then be described as the total space of the normal bundle over Σ, and we obtain the noncompact, local Calabi-Yau threefold

$$N \to \Sigma_g. \tag{C.3.50}$$

A general lemma (for a proof, see [196], p.516) says that any holomorphic line bundle over $\mathbb{P}^1$ is decomposable into a direct sum of line bundles, therefore, local Calabi-Yau's with the two-sphere as a base can *always* be written as

$$\mathcal{O}(p-2) \oplus \mathcal{O}(-p) \to \mathbb{P}^1. \tag{C.3.51}$$

The special case where $p = 1$ is our old friend, the resolved conifold.

As explained in [199, 163, 143, 31], many local Calabi-Yaus admit a toric construction as patches of $\mathbb{C}^3$ glued together. In terms of toric geometry, this procedure can be described as

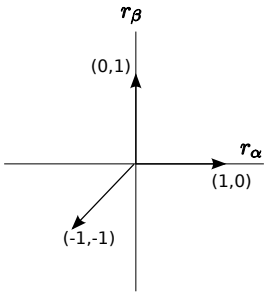

Figure C.1: a patch of $\mathbb{C}^3$

follows. We want to describe a Calabi-Yau threefold as a $T^2 \times \mathbb{R}$ fibration over a base $\mathbb{R}^3$. The geometry of this fibration is completely determined by its degeneration loci where one or several cycles shrink to zero, and these can be represented by a planar graph in a subspace of $\mathbb{R}^3$. Each edge v points to a vector $(p, q) \in \mathbb{Z}$, which labels the cycle degenerating along this edge, fulfilling $pr_\alpha + qr_\beta = \text{const.}$. The Calabi-Yau condition can be translated to

$$\sum_i v_i = 0, \tag{C.3.52}$$

smoothness is ensured by demanding

$$|v_i \wedge v_j| = 1, \tag{C.3.53}$$

and $\mathbb{C}^3$-patches correspond to trivalent vertices. Let us see explicitly how $\mathbb{C}^3$ patches are constructed. We introduce the moment map

$$\begin{aligned} \rho : \mathbb{C}^3 &\to \mathbb{R}^3 \\ (z_1, z_2, z_3) \to (r_\alpha, r_\beta, r_\gamma) &= (|z_1|^2 - |z_3|^2, |z_2|^2 - |z_3|^2, \mathrm{Im}(z_1 z_2 z_3)). \end{aligned} \tag{C.3.54}$$

The fibers are then generated by the r_ι via the Poisson brackets $\partial_\epsilon z = \{\epsilon \cdot r, z_i\}$ with respect to the standard symplectic form $\omega = \mathrm{i} \sum_i dz_i \wedge d\bar{z}_i$ on $\mathbb{C}^3$. With our choice of basis, r_γ generates the line $\mathbb{R}$ and the $\mathbb{T}^2$-fiber is generated by the circle actions

$$\mathrm{e}^{\mathrm{i}\alpha r_\alpha + \mathrm{i}\beta r_\beta} : (z_1, z_2, z_3) \to (\mathrm{e}^{\mathrm{i}\alpha} z_1, \mathrm{e}^{\mathrm{i}\beta} z_2, \mathrm{e}^{-\mathrm{i}(\alpha+\beta)} z_3). \tag{C.3.55}$$

Labeling the cycles generated by r_α, r_β by $(0, 1)$ respectively $(1, 0)$, the degeneration loci of this fibration in the r_ι-base can be graphically represented as shown in Fig. C.1. More complicated geometries can be represented gluing different $\mathbb{C}^3$–patches together.

Generally, the geometry that we want to describe by a toric diagram is given by a set of k D-term constraint equations

$$\sum_i Q_i^A |z_i|^2 = t^A, \quad A = 1, \cdots, k, \tag{C.3.56}$$

where Q_i^A are integral charges summing to zero, and the toric manifold is obtained after dividing out the toric symmetry group[1]

$$G : z_i \to \mathrm{e}^{\mathrm{i} Q_i^A \epsilon_A} z_i. \tag{C.3.57}$$

Each $\mathbb{C}^3$–patch is naturally described by a different set of three coordinates among $z_1, \cdots z_{N+3}$. Let us illustrate this procedure of constructing a toric diagram from a given geometry with the standard example of $\mathcal{O}(-3) \to \mathbb{P}^2$. This geometry is described as a hypersurface in $\mathbb{C}^4$ by the constraint equation

$$|z_1|^2 + |z_2|^2 + |z_3|^2 - 3|z_0|^2 = t. \tag{C.3.58}$$

[1] see [31] for a physical interpretation of this construction

The coordinates are labeled such that $z_1, \cdots z_3$ parameterize the $\mathbb{P}^2$–base and z_0 the $\mathbb{C}$–fiber. There are three patches labeled by $z_i \neq 0$ for $i = 1, \cdots 3$, since the base is not allowed to shrink completely. Each of them locally looks like $\mathbb{C}^3$, since z_i can be chosen to ensure the constraint (C.3.58) and the remaining three coordinates are unconstrained. In the patch $z_3 \neq 0$, we can choose the same Hamiltonians as above,

$$\begin{aligned} r_\alpha &= |z_1|^2 - |z_0|^2 \\ r_\beta &= |z_2|^2 - |z_0|^2, \end{aligned} \tag{C.3.59}$$

and the degeneration loci are again as shown in Fig. C.1. However, in the patch where the constrained coordinate is e.g. z_1, we have to replace z_1 in r_α and write $r_\alpha = t + 2|z_0|^2 - |z_2|^2 - |z_3|^2$. Accordingly, the $\mathbb{T}^2$ is on this patch generated by

$$\mathrm{e}^{\mathrm{i}\alpha r_\alpha + \mathrm{i}\beta r_\beta} : (z_1, z_2, z_3) \to (\mathrm{e}^{\mathrm{i}(2\alpha-\beta)} z_0, \mathrm{e}^{-\mathrm{i}(\alpha-\beta)} z_2, \mathrm{e}^{-\mathrm{i}\alpha} z_3), \tag{C.3.60}$$

and one can read off that the degenerating cycles are a $(2, -1)$, a $(-1, 1)$ and a $(-1, 0)$–cycle, corresponding to $r_\alpha + r_\beta = \text{const.}$, $r_\alpha + 2r_\beta = \text{const.}$, and $r_\alpha = 0$. Hence, the $\mathbb{C}^3$–patch looks like the lower right corner of Fig. C.2. The full picture shown is obtained after adding the third patch and gluing the three patches together, connecting parallel edges.

Now we need to add branes in order to obtain the full, open string picture. In this thesis, we consider Harvey-Lawson-branes wrapping special Lagrangian submanifolds [200, 163, 143]. They are specified by their location on the edges of the toric diagram, and therefore have topology $\mathbb{C} \times S^1$, since one circle is degenerate. In the toric diagram, they appear as lines. What does

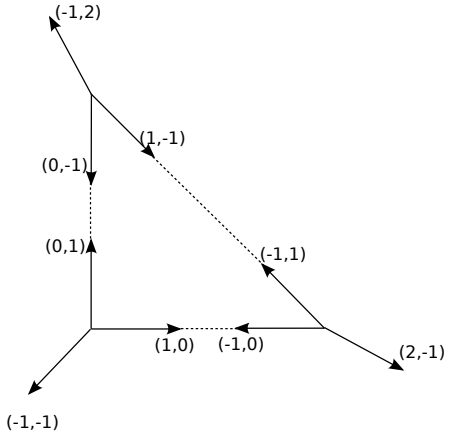

Figure C.2: The toric diagram of $\mathcal{O}(-3) \to \mathbb{P}^2$

the mirror of a toric Calabi-Yau manifold with branes look like? It turns out that the effect of mirror symmetry is thickening the lines in the diagram such that one obtains a Riemann surface. The B-model geometry is then a fibration over this surface. It is obtained from the mirror of the D-term constraint, reading

$$Q_1^a y_1 + \cdots Q_{k+3}^a y_{k+3} = -\tilde{t}^a, \tag{C.3.61}$$

where y_i are the $\mathbb{C}^*$-fields dual to z_i, and $\tilde{t}^a = t^a + \mathrm{i}\theta^a$ is the complexified Kähler parameter. Here, θ^a are the θ-angles of the gauge group $U(1)^a$. The corresponding mirror geometry is then

$$xz = \mathrm{e}^{y_1(u,v,t)} + \cdots + \mathrm{e}^{y_{k+3}(u,v,t)} \equiv \Sigma_t(U, V). \tag{C.3.62}$$

where $U = \mathrm{e}^u, V = \mathrm{e}^v$ are variables in $\mathbb{C}^*$ parametrizing the solutions $\{y_i(U, V)\}$ to (C.3.61), and $\Sigma_t(U, V) = 0$ describes a family of Riemann surfaces, parameterized by t. A-branes wrapping

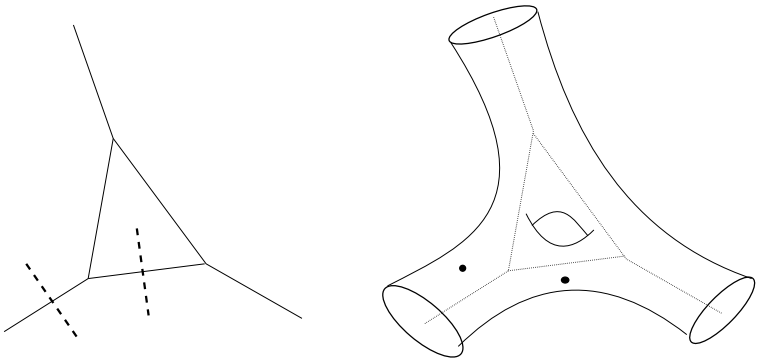

Figure C.3: The local $\mathbb{P}^2$-geometry with A-branes and its mirror with B-branes appearing as points

special Lagrangian submanifolds map to B-branes on holomorphic submanifolds in the mirror geometry. These submanifolds are defined by $x = 0$ in the above geometry, thus, they are parameterized by z and can occur at any point on the Riemann surface. Accordingly, their moduli space is parametrized by (u, v) satisfying $\Sigma(u, v) = 0$. This mirror picture is illustrated in Fig. C.3. The mirror curve is thus visualized as a thickened version of the one-dimensional toric diagram. In particular, this regularizes the geometry, as branes can now move smoothly from positions at the outer edges to positions on the inner edges without any singularities. This regularization effect is due to A-model world-sheet instantons "absorbed" in the geometry. Note also that the mirror curve is punctured and therefore *non-compact*.

Bibliography

[1] Frederik Denef. "Les Houches Lectures on Constructing String Vacua". 2008, 0803.1194.

[2] Kenneth Intriligator and Nathan Seiberg. "Lectures on Supersymmetry Breaking". *Class. Quant. Grav.*, 24:S741–S772, 2007, hep-ph/0702069.

[3] Dieter Lust, Stephan Stieberger, and Tomasz R. Taylor. "The LHC String Hunter's Companion". 2008, 0807.3333.

[4] Juan Martin Maldacena. "The large N limit of superconformal field theories and supergravity". *Adv. Theor. Math. Phys.*, 2:231–252, 1998, hep-th/9711200.

[5] Gerard 't Hooft. "A planar diagram theory for strong interactions". *Nucl. Phys.*, B72:461, 1974.

[6] Edward Witten. "Topological Sigma Models". *Commun. Math. Phys.*, 118:411, 1988.

[7] Edward Witten. "On the structure of the topological phase of two-dimensional gravity". *Nucl. Phys.*, B340:281–332, 1990.

[8] M. Bershadsky, S. Cecotti, H. Ooguri, and C. Vafa. "Holomorphic anomalies in topological field theories". *Nucl. Phys.*, B405:279–304, 1993, hep-th/9302103.

[9] Marcos Mariño. "Les Houches lectures on matrix models and topological strings". 2004, hep-th/0410165.

[10] Marcel Vonk. "A mini-course on topological strings". 2005, hep-th/0504147.

[11] Andrew Neitzke and Cumrun Vafa. "Topological strings and their physical applications". 2004, hep-th/0410178.

[12] K. Hori et al. *"Mirror symmetry"*. American Mathematical Society, 2003. Providence, USA: AMS (2003) 929 p.

[13] J. Polchinski. *String Theory*, volume II. "Cambridge University Press", 2005.

[14] Katrin Becker, Melanie Becker, and John H. Schwarz. *"String Theory and M-theory"*. Cambridge University Press, 2007.

[15] Elias Kiritsis. Introduction to superstring theory, 1997, hep-th/9709062.

[16] Edward Witten. "Mirror manifolds and Topological Field theory". 1991, hep-th/9112056.

[17] Robbert Dijkgraaf, Herman L. Verlinde, and Erik P. Verlinde. "Notes on topological string theory and 2-D quantum gravity". 1990. Based on lectures given at Spring School on Strings and Quantum Gravity, Trieste, Italy, Apr 24 - May 2, 1990 and at Cargese Workshop on Random Surfaces, Quantum Gravity and Strings, Cargese, France, May 28 - Jun 1, 1990.

[18] Ignatios Antoniadis, E. Gava, K. S. Narain, and T. R. Taylor. "Topological amplitudes in string theory". *Nucl. Phys.*, B413:162–184, 1994, hep-th/9307158.

[19] M. Bershadsky, S. Cecotti, H. Ooguri, and C. Vafa. "Kodaira-Spencer theory of gravity and exact results for quantum string amplitudes". *Commun. Math. Phys.*, 165:311–428, 1994, hep-th/9309140.

[20] Ignatios Antoniadis, E. Gava, K. S. Narain, and T. R. Taylor. "N=2 type II heterotic duality and higher derivative F terms". *Nucl. Phys.*, B455:109–130, 1995, hep-th/9507115.

[21] B. de Wit, P. G. Lauwers, and Antoine Van Proeyen. "Lagrangians of N=2 Supergravity - Matter Systems". *Nucl. Phys.*, B255:569, 1985.

[22] Andrew Strominger. "Massless black holes and conifolds in string theory". *Nucl. Phys.*, B451:96–108, 1995, hep-th/9504090.

[23] Rajesh Gopakumar and Cumrun Vafa. "M-theory and topological strings. I". 1998, hep-th/9809187.

[24] Rajesh Gopakumar and Cumrun Vafa. "M-theory and topological strings. II". 1998, hep-th/9812127.

[25] A. Okounkov D. Maulik, N. Nekrasov and R. Pandharipande. "Gromov-Witten theory and Donaldson-Thomas theory, I and II"". math.AG/0312059 and math.AG/0406092.

[26] Edward Witten. "Chern-Simons gauge theory as a string theory". *Prog. Math.*, 133:637–678, 1995, hep-th/9207094.

[27] Rajesh Gopakumar and Cumrun Vafa. "On the gauge theory/geometry correspondence". *Adv. Theor. Math. Phys.*, 3:1415–1443, 1999, hep-th/9811131.

[28] Nikita Nekrasov, Hirosi Ooguri, and Cumrun Vafa. "S-duality and topological strings". *JHEP*, 10:009, 2004, hep-th/0403167.

[29] Marcos Mariño and Gregory W. Moore. "Counting higher genus curves in a Calabi-Yau manifold". *Nucl. Phys.*, B543:592–614, 1999, hep-th/9808131.

[30] Mina Aganagic, Marcos Mariño, and Cumrun Vafa. "All loop topological string amplitudes from Chern-Simons theory". *Commun. Math. Phys.*, 247:467–512, 2004, hep-th/0206164.

[31] Mina Aganagic, Albrecht Klemm, Marcos Mariño, and Cumrun Vafa. "The topological vertex". *Commun. Math. Phys.*, 254:425–478, 2005, hep-th/0305132.

[32] Robbert Dijkgraaf and Cumrun Vafa. "Matrix models, topological strings, and supersymmetric gauge theories". *Nucl. Phys.*, B644:3–20, 2002, hep-th/0206255.

[33] Bertrand Eynard and Nicolas Orantin. "Invariants of algebraic curves and topological expansion". 2007, math-ph/0702045.

[34] Marcos Mariño. "Open string amplitudes and large order behavior in topological string theory". *JHEP*, 03:060, 2008, hep-th/0612127.

[35] Vincent Bouchard, Albrecht Klemm, Marcos Mariño, and Sara Pasquetti. "Remodeling the B-model". 2007, 0709.1453.

[36] Vincent Bouchard, Albrecht Klemm, Marcos Mariño, and Sara Pasquetti. "Topological open strings on orbifolds". 2008, 0807.0597.

[37] C. M. Hull and P. K. Townsend. "Unity of superstring dualities". *Nucl. Phys.*, B438:109–137, 1995, hep-th/9410167.

[38] Paul S. Aspinwall. "K3 surfaces and string duality". 1996, hep-th/9611137.

[39] Sergio Ferrara, Jeffrey A. Harvey, Andrew Strominger, and Cumrun Vafa. "Second quantized mirror symmetry". *Phys. Lett.*, B361:59–65, 1995, hep-th/9505162.

[40] S. Kachru and C. Vafa. "Exact results for N = 2 compactifications of heterotic strings". *Nucl. Phys. Proc. Suppl.*, 46:210–224, 1996.

[41] Richard E. Borcherds. Automorphic forms with singularities on grassmannians. *Inventiones mathematicae*, 132:491, 1998.

[42] Thomas W. Grimm, Albrecht Klemm, Marcos Mariño, and Marlene Weiss. "Direct integration of the topological string". 2007, hep-th/0702187.

[43] Marlene Weiss. "Topological Amplitudes in Heterotic Strings with Wilson Lines". *JHEP*, 08:024, 2007, 0705.3112.

[44] Jeffrey A. Harvey and Gregory W. Moore. "Algebras, BPS States, and Strings". *Nucl. Phys.*, B463:315–368, 1996, hep-th/9510182.

[45] Jan Ambjorn, L. Chekhov, C. F. Kristjansen, and Yu. Makeenko. "Matrix model calculations beyond the spherical limit". *Nucl. Phys.*, B404:127–172, 1993, hep-th/9302014.

[46] Sidney Coleman. *"Aspects of Symmetry"*. Cambridge University Press, 1985.

[47] R. Rajaraman. *"Solitons and Instantons"*. North-Holland Publishing Company, 1987.

[48] Stephen H. Shenker. "The Strength of nonperturbative effects in string theory". 1990. Presented at the Cargese Workshop on Random Surfaces, Quantum Gravity and Strings, Cargese, France, May 28 - Jun 1, 1990.

[49] Nikita Nekrasov. "A la recherche de la M-Theorie perdue. Z theory: Chasing M/F theory". 2004, hep-th/0412021.

[50] J. Zinn-Justin. *"Quantum Field Theory and Critical Phenomena"*. Oxford University Press, 2002.

[51] Sergei Yu. Alexandrov, Vladimir A. Kazakov, and David Kutasov. "Non-perturbative effects in matrix models and D-branes". *JHEP*, 09:057, 2003, hep-th/0306177.

[52] Hirosi Ooguri, Andrew Strominger, and Cumrun Vafa. "Black hole attractors and the topological string". *Phys. Rev.*, D70:106007, 2004, hep-th/0405146.

[53] Boris Pioline. "Lectures on on black holes, topological strings and quantum attractors". *Class. Quant. Grav.*, 23:S981, 2006, hep-th/0607227.

[54] H. Jockers and W. Lerche. "Matrix Factorizations, D-Branes and their Deformations". *Nucl. Phys. Proc. Suppl.*, 171:196–214, 2007, 0708.0157.

[55] Hirosi Ooguri and Cumrun Vafa. "Worldsheet derivation of a large N duality". *Nucl. Phys.*, B641:3–34, 2002, hep-th/0205297.

[56] W.B.R. Lickorish. *"An introduction to knot theory"*. Springer, 1997.

[57] Weimin Chen and Yongbin Ruan. "Orbifold Gromov-Witten Theory". 2001.

[58] Jim Bryan and Tom Graber. "The Crepant Resolution Conjecture". 2006.

[59] Yongbin Ruan. "Cohomology ring of crepant resolutions of orbifolds". 2001.

[60] Maxim Kontsevich. Enumeration of rational curves via Torus actions. 1994, hep-th/9405035.

[61] Andreas Gathmann. "Topological recursion relations and Gromov-Witten invariants in higher genus". 2003.

[62] D. Maulik and R. Pandharipande. "A topological view of Gromov-Witten theory". 2004, math/0412503.

[63] D. Maulik and R. Pandharipande. "New calculations in Gromov-Witten theory". 2006, math/0601395.

[64] Aleksey Zinger. "The Reduced Genus-One Gromov-Witten Invariants of Calabi-Yau Hypersurfaces". 2007.

[65] R. Pandharipande, J. Solomon, and J. Walcher. "Disk enumeration on the quintic 3-fold". 2006.

[66] Johannes Walcher. "Opening mirror symmetry on the quintic". *Commun. Math. Phys.*, 276:671–689, 2007, hep-th/0605162.

[67] Hans Jockers and Masoud Soroush. "Effective superpotentials for compact D5-brane Calabi-Yau geometries". 2008, 0808.0761.

[68] Duiliu-Emanuel Diaconescu and Bogdan Florea. "Large N duality for compact Calabi-Yau threefolds". *Adv. Theor. Math. Phys.*, 9:31–128, 2005, hep-th/0302076.

[69] Min-xin Huang, Albrecht Klemm, and Seth Quackenbush. "Topological String Theory on Compact Calabi-Yau: Modularity and Boundary Conditions". 2006, hep-th/0612125.

[70] Kai Behrend and Jim Bryan. "Super-rigid Donaldson-Thomas invariants". 2006.

[71] Marcos Mariño, Ricardo Schiappa, and Marlene Weiss. "Nonperturbative Effects and the Large-Order Behavior of Matrix Models and Topological Strings". 2007, 0711.1954.

[72] Marcos Mariño, Ricardo Schiappa, and Marlene Weiss. "Multi-cuts and Multi-instantons", to be published. 2008, 0709.??

[73] Mina Aganagic, Vincent Bouchard, and Albrecht Klemm. "Topological Strings and (Almost) Modular Forms". *Commun. Math. Phys.*, 277:771–819, 2008, hep-th/0607100.

[74] Satoshi Yamaguchi and Shing-Tung Yau. "Topological string partition functions as polynomials". *JHEP*, 07:047, 2004, hep-th/0406078.

[75] S. Hosono, M. H. Saito, and A. Takahashi. "Holomorphic anomaly equation and BPS state counting of rational elliptic surface". *Adv. Theor. Math. Phys.*, 3:177–208, 1999, hep-th/9901151.

[76] Shinobu Hosono. "Counting BPS states via holomorphic anomaly equations". 2002, hep-th/0206206.

[77] J. A. Minahan, D. Nemeschansky, and N. P. Warner. "Instanton expansions for mass deformed N = 4 super Yang- Mills theories". *Nucl. Phys.*, B528:109–132, 1998, hep-th/9710146.

[78] J. A. Minahan, D. Nemeschansky, and N. P. Warner. "Partition functions for BPS states of the non-critical E(8) string". *Adv. Theor. Math. Phys.*, 1:167–183, 1998, hep-th/9707149.

[79] Albrecht Klemm and Marcos Mariño. "Counting BPS states on the Enriques Calabi-Yau". *Commun. Math. Phys.*, 280:27–76, 2008, hep-th/0512227.

[80] Nikita A. Nekrasov. "Seiberg-Witten prepotential from instanton counting". *Adv. Theor. Math. Phys.*, 7:831–864, 2004, hep-th/0206161.

[81] Philip Candelas and Xenia de la Ossa. "Moduli space of Calabi-Yau manifolds". *Nucl. Phys.*, B355:455–481, 1991.

[82] L. Andrianopoli et al. "N = 2 supergravity and N = 2 super Yang-Mills theory on general scalar manifolds: Symplectic covariance, gaugings and the momentum map". *J. Geom. Phys.*, 23:111–189, 1997, hep-th/9605032.

[83] Ben Craps, Frederik Roose, Walter Troost, and Antoine Van Proeyen. "What is special Kaehler geometry?". *Nucl. Phys.*, B503:565–613, 1997, hep-th/9703082.

[84] Daniel S. Freed. "Special Kaehler manifolds". *Commun. Math. Phys.*, 203:31–52, 1999, hep-th/9712042.

[85] G. Tian. "Smoothness of the universal deformation space of compact Calabi–Yau manifolds and its Petersson–Weil metric, in S.–T. Yau (ed.), *Mathematical aspects of string theory*". page 629, 1987.

[86] A. N. Todorov. "The Weil-Petersson geometry of the moduli space of $SU(n \geq 3)$ (Calabi–Yau) manifolds I". *Commun. Math. Phys.*, 126:325, 1989.

[87] N. Seiberg and Edward Witten. "Electric - magnetic duality, monopole condensation, and confinement in N=2 supersymmetric Yang-Mills theory". *Nucl. Phys.*, B426:19–52, 1994, hep-th/9407087.

[88] Sheldon H. Katz, Albrecht Klemm, and Cumrun Vafa. "Geometric engineering of quantum field theories". *Nucl. Phys.*, B497:173–195, 1997, hep-th/9609239.

[89] Min-xin Huang and Albrecht Klemm. "Holomorphic anomaly in gauge theories and matrix models". *JHEP*, 09:054, 2007, hep-th/0605195.

[90] Cumrun Vafa. "A Stringy test of the fate of the conifold". *Nucl. Phys.*, B447:252–260, 1995, hep-th/9505023.

[91] Jeffrey A. Harvey and Gregory W. Moore. "Exact gravitational threshold correction in the FHSV model". *Phys. Rev.*, D57:2329–2336, 1998, hep-th/9611176.

[92] Mans Henningson and Gregory W. Moore. "Threshold corrections in K(3) x T(2) heterotic string compactifications". *Nucl. Phys.*, B482:187–212, 1996, hep-th/9608145.

[93] R. E. Borcherds. "The moduli space of Enriques surfaces and the fake monster Lie superalgebra". *Topology*, 35:699, 1996.

[94] Reinhold W. Gebert. "Introduction to vertex algebras, Borcherds algebras, and the Monster Lie algebra". *Int. J. Mod. Phys.*, A8:5441–5504, 1993, hep-th/9308151.

[95] Robbert Dijkgraaf. unpublished. 1998.

[96] Toshiya Kawai and Kota Yoshioka. "String partition functions and infinite products". *Adv. Theor. Math. Phys.*, 4:397–485, 2000, hep-th/0002169.

[97] A. Klemm, M. Kreuzer, E. Riegler, and E. Scheidegger. "Topological string amplitudes, complete intersection Calabi-Yau spaces and threshold corrections". *JHEP*, 05:023, 2005, hep-th/0410018.

[98] Gabriel Lopes Cardoso, Dieter Lust, and Thomas Mohaupt. "Threshold corrections and symmetry enhancement in string compactifications". *Nucl. Phys.*, B450:115–173, 1995, hep-th/9412209.

[99] R.E. Borcherds. "Automorphic forms in $O_{s+2,2}(\mathbb{R})$ and infinite products". *Inv. Math.*, 120:161, 1995.

[100] Nikita Nekrasov and Andrei Okounkov. "Seiberg-Witten theory and random partitions". 2003, hep-th/0306238.

[101] Ugo Bruzzo, Francesco Fucito, Jose F. Morales, and Alessandro Tanzini. "Multi-instanton calculus and equivariant cohomology". *JHEP*, 05:054, 2003, hep-th/0211108.

[102] Shamit Kachru, Albrecht Klemm, Wolfgang Lerche, Peter Mayr, and Cumrun Vafa. "Nonperturbative results on the point particle limit of N=2 heterotic string compactifications". *Nucl. Phys.*, B459:537–558, 1996, hep-th/9508155.

[103] Nicholas Dorey, Valentin V. Khoze, and Michael P. Mattis. "Multi-instanton calculus in N = 2 supersymmetric gauge theory. II: Coupling to matter". *Phys. Rev.*, D54:7832–7848, 1996, hep-th/9607202.

[104] Nicholas Dorey, Valentin V. Khoze, and Michael P. Mattis. "On N = 2 supersymmetric QCD with 4 flavors". *Nucl. Phys.*, B492:607–622, 1997, hep-th/9611016.

[105] G. Aldazabal, A. Font, Luis E. Ibanez, and F. Quevedo. "Chains of N=2, D=4 heterotic/type II duals". *Nucl. Phys.*, B461:85–100, 1996, hep-th/9510093.

[106] Anna Ceresole, R. D'Auria, S. Ferrara, and Antoine Van Proeyen. "Duality transformations in supersymmetric Yang-Mills theories coupled to supergravity". *Nucl. Phys.*, B444:92–124, 1995, hep-th/9502072.

[107] Bernard de Wit, Vadim Kaplunovsky, Jan Louis, and Dieter Lust. "Perturbative couplings of vector multiplets in N=2 heterotic string vacua"". *Nucl. Phys.*, B451:53–95, 1995, hep-th/9504006.

[108] P. Mayr and S. Stieberger. "Moduli dependence of one loop gauge couplings in (0,2) compactifications". *Phys. Lett.*, B355:107–116, 1995, hep-th/9504129.

[109] Gabriel Lopes Cardoso, Gottfried Curio, and Dieter Lust. "Perturbative couplings and modular forms in N = 2 string models with a Wilson line". *Nucl. Phys.*, B491:147–183, 1997, hep-th/9608154.

[110] Per Berglund, Sheldon H. Katz, Albrecht Klemm, and Peter Mayr. "New Higgs transitions between dual N = 2 string models". *Nucl. Phys.*, B483:209–228, 1997, hep-th/9605154.

[111] S. Stieberger. "(0,2) heterotic gauge couplings and their M-theory origin". *Nucl. Phys.*, B541:109–144, 1999, hep-th/9807124.

[112] Brian R. Greene, David R. Morrison, and Andrew Strominger. "Black hole condensation and the unification of string vacua". *Nucl. Phys.*, B451:109–120, 1995, hep-th/9504145.

[113] Jose F. Morales and Marco Serone. "Higher derivative F-terms in N = 2 strings". *Nucl. Phys.*, B481:389–402, 1996, hep-th/9607193.

[114] W. Lerche, B. E. W. Nilsson, A. N. Schellekens, and N. P. Warner. "Anomaly cancelling terms from the elliptic genus". *Nucl. Phys.*, B299:91, 1988.

[115] Wolfgang Lerche. "Elliptic index and superstring effective actions". *Nucl. Phys.*, B308:102, 1988.

[116] Edward Witten. "Instantons, the Quark Model, and the 1/N Expansion". *Nucl. Phys.*, B149:285, 1979.

[117] (ed.) Le Guillou, J. C. and (ed.) Zinn-Justin, Jean. "Large order behavior of perturbation theory". Amsterdam, Netherlands: North-Holland (1990) 580 p. (Current physics - sources and comments.

[118] P. Di Francesco, Paul H. Ginsparg, and Jean Zinn-Justin. "2-D Gravity and random matrices". *Phys. Rept.*, 254:1–133, 1995, hep-th/9306153.

[119] Paul H. Ginsparg and Jean Zinn-Justin. "Large order behavior of nonperturbative gravity". *Phys. Lett.*, B255:189–196, 1991.

[120] Francois David. "Phases of the large N matrix model and nonperturbative effects in 2-d gravity". *Nucl. Phys.*, B348:507–524, 1991.

[121] Francois David. "Nonperturbative effects in two-dimensional quantum gravity". Lectures given at 8th Jerusalem Winter School for Theoretical Physics, Two-Dimensional Gravity and Random Surfaces, Jerusalem, Israel, Dec 27 - Jan 4, 1991.

[122] Emil J. Martinec. "The annular report on non-critical string theory". 2003, hep-th/0305148.

[123] Igor R. Klebanov, Juan Martin Maldacena, and Nathan Seiberg. "D-brane decay in two-dimensional string theory". *JHEP*, 07:045, 2003, hep-th/0305159.

[124] Alexander B. Zamolodchikov and Alexei B. Zamolodchikov. "Liouville field theory on a pseudosphere". 2001, hep-th/0101152.

[125] Francois David. "Nonperturbative effects in matrix models and vacua of two- dimensional gravity". *Phys. Lett.*, B302:403–410, 1993, hep-th/9212106.

[126] Masanori Hanada et al. "Loops versus matrices: The nonperturbative aspects of noncritical string". *Prog. Theor. Phys.*, 112:131–181, 2004, hep-th/0405076.

[127] Nobuyuki Ishibashi and Atsushi Yamaguchi. "On the chemical potential of D-instantons in c = 0 noncritical string theory". *JHEP*, 06:082, 2005, hep-th/0503199.

[128] E. Brezin, C. Itzykson, G. Parisi, and J. B. Zuber. "Planar Diagrams". *Commun. Math. Phys.*, 59:35, 1978.

[129] Fröhlich, Jürg. "The Statistical Mechanics of Surfaces". in: Springer Lecture Notes in Physics, vol.216, 31-57 (1985); L. Garrido (ed.); Proceedings Sitges Conference, June 1984.

[130] Milan Krbalek and Petr Seba. The statistical properties of the city transport in cuernavaca (mexico) and random matrix ensembles. *Journal of Physics A: Mathematical and General*, 33(26):L229–L234, 2000.

[131] V. Plerou, P. Gopikrishnan, B. Rosenow, L. A. N. Amaral, T. Guhr, and H. E. Stanley. A random matrix approach to cross-correlations in financial data. 2001.

[132] D. Bessis, C. Itzykson, and J. B. Zuber. "Quantum field theory techniques in graphical enumeration". *Adv. Appl. Math.*, 1:109–157, 1980.

[133] B. Eynard. "Topological expansion for the 1-hermitian matrix model correlation functions". *JHEP*, 11:031, 2004, hep-th/0407261.

[134] L. Chekhov and B. Eynard. "Hermitean matrix model free energy: Feynman graph technique for all genera". *JHEP*, 03:014, 2006, hep-th/0504116.

[135] Jan Ambjorn, J. Jurkiewicz, and Yu. M. Makeenko. "Multiloop correlators for two-dimensional quantum gravity". *Phys. Lett.*, B251:517–524, 1990.

[136] Nathan Seiberg and David Shih. "Branes, rings and matrix models in minimal (super)string theory". *JHEP*, 02:021, 2004, hep-th/0312170.

[137] F. Cachazo, Kenneth A. Intriligator, and Cumrun Vafa. "A large N duality via a geometric transition". *Nucl. Phys.*, B603:3–41, 2001, hep-th/0103067.

[138] Jose D. Edelstein, Kyungho Oh, and Radu Tatar. "Orientifold, geometric transition and large N duality for SO/Sp gauge theories". *JHEP*, 05:009, 2001, hep-th/0104037.

[139] Keshav Dasgupta, Kyungho Oh, and Radu Tatar. "Geometric transition, large N dualities and MQCD dynamics". *Nucl. Phys.*, B610:331–346, 2001, hep-th/0105066.

[140] F. Cachazo, B. Fiol, K. A. Intriligator, S. Katz, and C. Vafa. "A geometric unification of dualities". *Nucl. Phys.*, B628:3–78, 2002, hep-th/0110028.

[141] Robbert Dijkgraaf and Cumrun Vafa. "On geometry and matrix models". *Nucl. Phys.*, B644:21–39, 2002, hep-th/0207106.

[142] Robbert Dijkgraaf and Cumrun Vafa. "A perturbative window into non-perturbative physics". 2002, hep-th/0208048.

[143] Mina Aganagic, Albrecht Klemm, and Cumrun Vafa. "Disk instantons, mirror symmetry and the duality web". *Z. Naturforsch.*, A57:1–28, 2002, hep-th/0105045.

[144] Bertrand Eynard, Marcos Mariño, and Nicolas Orantin. "Holomorphic anomaly and matrix models". *JHEP*, 06:058, 2007, hep-th/0702110.

[145] Jean Zinn-Justin. "Perturbation Series At Large Orders in Quantum Mechanics and Field Theories: Application to the problem of Resummation". *Phys. Rept.*, 70:109, 1981.

[146] Gerald V. Dunne. "Perturbative - nonperturbative connection in quantum mechanics and field theory". 2002, hep-th/0207046.

[147] John C. Collins and Davison E. Soper. "Large Order Expansion in Perturbation Theory". *Ann. Phys.*, 112:209–234, 1978.

[148] Jr. Callan, Curtis G. and Sidney R. Coleman. "The Fate of the False Vacuum. 2. First Quantum Corrections". *Phys. Rev.*, D16:1762–1768, 1977.

[149] Carl M. Bender and T. T. Wu. "Anharmonic oscillator. 2: A Study of perturbation theory in large order". *Phys. Rev.*, D7:1620–1636, 1973.

[150] B. Simon. "Large Orders and Summability of Eigenvalue Perturbation Theory: A Mathematical Overview". *Int. J. Quant. Chem.*, 21:3, 1982.

[151] Ivan K. Kostov, Matthias Staudacher, and Thomas Wynter. "Complex matrix models and statistics of branched coverings of 2D surfaces". *Commun. Math. Phys.*, 191:283–298, 1998, hep-th/9703189.

[152] B. Eynard and Jean Zinn-Justin. "Large order behavior of 2-D gravity coupled to d ¡ 1 matter". *Phys. Lett.*, B302:396–402, 1993, hep-th/9301004.

[153] N. Joshi and A.V. Kitaev. "On Boutroux's Tritronquée Solutions of the First Painlevé Equation"". *Stud. Appl. Math.*, 107:253, 2001.

[154] S. Hikami and E. Brezin. "Large-Order Behavior of the 1/N-Expansion in Zero- dimensions and One-dimensions". *J. Phys.*, A12:759–770, 1979.

[155] L. N. Lipatov. "Divergence of Perturbation Series and Pseudoparticles". *JETP Lett.*, 25:104–107, 1977.

[156] E. Brezin, J. C. Le Guillou, and Jean Zinn-Justin. "Perturbation Theory at Large Order. 2. Role of the Vacuum Instability". *Phys. Rev.*, D15:1558–1564, 1977.

[157] Robert de Mello Koch, Antal Jevicki, and Joao P. Rodrigues. "Instantons in c = 0 CSFT". *JHEP*, 04:011, 2005, hep-th/0412319.

[158] C.M. Bender and S. Orszag. *"Advanced Mathematical Methods for Scientists and Engineers"*. Springer–Verlag, New York, 1999.

[159] Mina Aganagic, Hirosi Ooguri, Natalia Saulina, and Cumrun Vafa. "Black holes, q-deformed 2d Yang-Mills, and non- perturbative topological strings". *Nucl. Phys.*, B715:304–348, 2005, hep-th/0411280.

[160] Jim Bryan and Rahul Pandharipande. "The local Gromov-Witten theory of curves". 2004, math/0411037.

[161] Nicola Caporaso, Luca Griguolo, Marcos Mariño, Sara Pasquetti, and Domenico Seminara. "Phase transitions, double-scaling limit, and topological strings". *Phys. Rev.*, D75:046004, 2007, hep-th/0606120.

[162] Brian Forbes and Masao Jinzenji. "Local mirror symmetry of curves: Yukawa couplings and genus 1". 2006, math/0609016.

[163] Mina Aganagic and Cumrun Vafa. "Mirror symmetry, D-branes and counting holomorphic discs". 2000, hep-th/0012041.

[164] David R. Morrison and Johannes Walcher. "D-branes and Normal Functions". 2007, 0709.4028.

[165] Daniel Robles-Llana, Martin Rocek, Frank Saueressig, Ulrich Theis, and Stefan Vandoren. "Nonperturbative corrections to 4D string theory effective actions from SL(2,Z) duality and supersymmetry"". *Phys. Rev. Lett.*, 98:211602, 2007, hep-th/0612027.

[166] D.E.G. Hare D.J. Jeffrey R.M. Corless, G.H. Gonnet and D.E. Knuth. "On the Lambert *W* Function". *Adv. Comput. Math.*, 5:329, 1996.

[167] Michael J. Crescimanno and Washington Taylor. "Large N phases of chiral QCD in two-dimensions". *Nucl. Phys.*, B437:3–24, 1995, hep-th/9408115.

[168] D.M. Jackson I.P. Goulden and R. Vakil. "The Gromov–Witten Potential of a Point, Hurwitz Numbers, and Hodge Integrals". *Proc. Lond. Math. Soc.*, 83:563, 2001, arXiv:math/9910004.

[169] R. Pandharipande. "The Toda Equation and the Gromov–Witten Theory of the Riemann Sphere". *Lett. Math. Phys.*, 53:59, 2000, arXiv:math/9912166 [math.AG].

[170] N.G. De Bruijn. *"Asymptotic Methods in Analysis"*. North–Holland, Amsterdam, 1958.

[171] Bertrand Eynard. Large N expansion of convergent matrix integrals, holomorphic anomalies, and background independence. 2008, 0802.1788.

[172] Gabrielle Bonnet, Francois David, and Bertrand Eynard. "Breakdown of universality in multi-cut matrix models". *J. Phys.*, A33:6739–6768, 2000, cond-mat/0003324.

[173] Edward Witten. "Quantum background independence in string theory". 1993, hep-th/9306122.

[174] Marcos Mariño. "Nonperturbative effects and nonperturbative definitions in matrix models and topological strings". 2008, 0805.3033.

[175] G. Akemann. "Higher genus correlators for the Hermitian matrix model with multiple cuts". *Nucl. Phys.*, B482:403–430, 1996, hep-th/9606004.

[176] Giovanni Felder and Roman Riser. "Holomorphic matrix integrals". *Nucl. Phys.*, B691:251–258, 2004, hep-th/0401191.

[177] Albrecht Klemm, Marcos Mariño, and Stefan Theisen. "Gravitational corrections in supersymmetric gauge theory and matrix models". *JHEP*, 03:051, 2003, hep-th/0211216.

[178] L. Chekhov, A. Marshakov, A. Mironov, and D. Vasiliev. "Complex geometry of matrix models". 2005, hep-th/0506075.

[179] A. S. Fokas, A. R. Its, and A. V. Kitaev. "Discrete Painleve equations and their appearance in quantum gravity". *Commun. Math. Phys.*, 142:313–344, 1991.

[180] Mina Aganagic, Robbert Dijkgraaf, Albrecht Klemm, Marcos Mariño, and Cumrun Vafa. "Topological strings and integrable hierarchies". *Commun. Math. Phys.*, 261:451–516, 2006, hep-th/0312085.

[181] Min-xin Huang, Albrecht Klemm, Marcos Marino, and Alireza Tavanfar. Black Holes and Large Order Quantum Geometry. 2007, 0704.2440.

[182] Sheldon H. Katz, Albrecht Klemm, and Cumrun Vafa. "M-theory, topological strings and spinning black holes". *Adv. Theor. Math. Phys.*, 3:1445–1537, 1999, hep-th/9910181.

[183] D. Maulik and R. Pandharipande. "Gromov-Witten theory and Noether-Lefschetz theory"". arXiv:0705.1653v1.

[184] Mina Aganagic, Albrecht Klemm, Marcos Marino, and Cumrun Vafa. "Matrix model as a mirror of Chern-Simons theory"". *JHEP*, 02:010, 2004, hep-th/0211098.

[185] Gaetano Bertoldi and Nick Dorey. "Non-critical superstrings from four-dimensional gauge theory". *JHEP*, 11:001, 2005, hep-th/0507075.

[186] Simone Lelli, Michele Maggiore, and Anna Rissone. "Perturbative and non-perturbative aspects of the two- dimensional string / Yang-Mills correspondence". *Nucl. Phys.*, B656:37–62, 2003, hep-th/0211054.

[187] Robert de Mello Koch, Antal Jevicki, and Sanjaye Ramgoolam. "On exponential corrections to the 1/N expansion in two- dimensional Yang Mills theory". *JHEP*, 08:077, 2005, hep-th/0504115.

[188] Robbert Dijkgraaf, Rajesh Gopakumar, Hirosi Ooguri, and Cumrun Vafa. "Baby universes in string theory". *Phys. Rev.*, D73:066002, 2006, hep-th/0504221.

[189] Mina Aganagic, Hirosi Ooguri, and Takuya Okuda. "Quantum entanglement of baby universes". *Nucl. Phys.*, B778:36–68, 2007, hep-th/0612067.

[190] Berkovits, Ooguri, and Vafa. On the world-sheet derivation of large-n dualities for the superstring.

[191] Hiroshi Shirokura. "Generating functions in two-dimensional quantum gravity". *Nucl. Phys.*, B462:99–140, 1996, hep-th/9506103.

[192] Hiroshi Shirokura. "Exact solution of 1-matrix model". 1996, hep-th/9603038.

[193] D. Mumford. *"Tata lectures on Theta"*, volume I,II, and III. Birkhaeuser, 1983.

[194] Luis Alvarez-Gaume, Gregory W. Moore, and Cumrun Vafa. Theta functions, modular invariance, and strings. *Commun. Math. Phys.*, 106:1–40, 1986.

[195] I. Stegun M. Abramowitz. *Handbook of mathematical functions with formulas, graphs, and mathematical tables*. National Bureau of Standards, Applied Mathematics Series, 1972.

[196] P. Griffiths and J. Harris. "Principles of Algebraic Geometry". 1994.

[197] M. Mariño. "Chern-Simons theory, matrix models, and topological strings". Oxford, UK: Clarendon (2005) 197 p.

[198] Paul S. Aspinwall, Brian R. Greene, and David R. Morrison. "Calabi-Yau moduli space, mirror manifolds and spacetime topology change in string theory". *Nucl. Phys.*, B416:414–480, 1994, hep-th/9309097.

[199] Naichung Conan Leung and Cumrun Vafa. "Branes and toric geometry". *Adv. Theor. Math. Phys.*, 2:91–118, 1998, hep-th/9711013.

[200] R. Harvey and Jr. Lawson, H. B. "Calibrated geometries". *Acta Math.*, 148:47, 1982.

Curriculum Vitæ

Personal Data

- **Name:** Marlene Weiß
- **Date of Birth:** 18.08.1980
- **Place of Birth:** Berlin, Germany
- **Nationality:** German

Education

- 04/2005-09/2008: Ph.D. student at CERN and ETH Zurich, advisors M. Mariño (CERN) and J. Fröhlich (ETH Zurich)
- 04/2004-08/2004: Master thesis at EPF Lausanne, "The structure of the energy-momentum tensor in a five-dimensional brane world", Advisors M. Shaposhnikov (EPF Lausanne), J. Fröhlich (ETH Zürich)
- 10/1999-08/2004: ETH Zürich, Master in theoretical physics (Diplom)
- 10/2001-07/2002: Université Pierre et Marie Curie, Paris 6 (Erasmus exchange program)
- 08/1992-06/1999: High School, Rückert-Gymnasium, Berlin, Germany
- 08/1996-07/1997: High School, 桐蔭高等学校, Hita, Japan

Awards and Grants

- 05/2006-04/2007 Marie Curie EST-Fellowship, CERN
- 2004 Polyà book award for master's degree in theoretical physics (ETH Zurich)

Publications

- M. Marino, R. Schiappa and M. Weiss, "Multi-Instantons and Multi-Cuts", to appear
- M. Marino, R. Schiappa and M. Weiss, "Nonperturbative Effects and the Large-Order Behavior of Matrix Models and Topological Strings", arXiv:0711.1954[hep-th]
- M. Weiss, "Topological Amplitudes in Heterotic Strings with Wilson Lines, arXiv:0705.3112[hep-th], JHEP 0708:024
- T. Grimm, A. Klemm, M. Marino and M. Weiss, "Direct Integration of the Topological String", arXiv:hep-th/0702187, JHEP 0708:058